Universiteit
Leiden
The Netherlands

Tail regeneration in the Tokay Gecko (Gekko gecko)

Nurhidayat, L.

Citation
Nurhidayat, L. (2025, January 9). *Tail regeneration in the Tokay Gecko (Gekko gecko)*. Retrieved from https://hdl.handle.net/1887/4175313

Version:	Publisher's Version
License:	Licence agreement concerning inclusion of doctoral thesis in the Institutional Repository of the University of Leiden
Downloaded from:	https://hdl.handle.net/1887/4175313

Note: To cite this publication please use the final published version (if applicable).

Tail Regeneration in the Tokay Gecko (*Gekko gecko*)

LUTHFI NURHIDAYAT

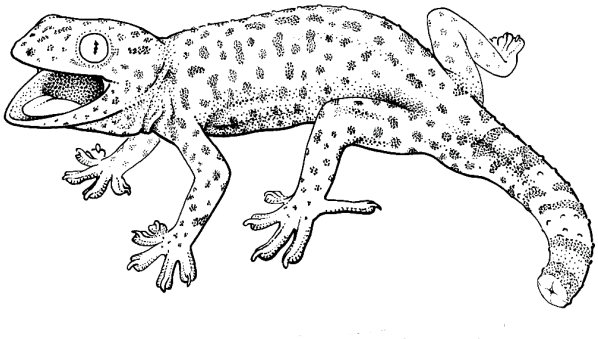

Printing: Ipskamp Printing (www.ipskampprinting.nl)
Tail Regeneration in the Tokay Gecko (*Gekko gecko*).
Luthfi Nurhidayat.
PhD. Thesis, Institute of Biology Leiden (IBL), University of Leiden, The Netherlands
Layout by Luthfi Nurhidayat.

Tail Regeneration in the Tokay Gecko (*Gekko gecko*)

Proefschrift

ter verkrijging van

de graad van doctor aan de Universiteit Leiden,

op gezag van rector magnificus prof.dr.ir. H. Bijl,

volgens besluit van het college voor promoties

te verdedigen op donderdag 9 januari 2025

klokke 13:00 uur

door

Luthfi Nurhidayat

geboren te Sragen, Indonesia

in 1987

Promotores:
Prof. dr. M. K. Richardson
Prof. dr. H. P. Spaink

Promotiecommissie:
Prof. dr. A.H. Meijer
Prof. dr. M. Drukker
Prof. dr. F. Verbeek
Prof. dr. J. Bakkers (Utrecht University Medical Center)
Dr. V. Benes (European Molecular Biology Laboratory, Heidelberg, Germany)
Dr. A. Hamidy (Museum Zoologicum Bogorienses, Indonesia)

Table of Contents

Chapter 1. General Introduction and Thesis Outline

Abstract

Regeneration is the ability of an organism to grow a new tissue or organ that can act as a functional replacement for lost or damaged tissue. Invertebrates, such as *Hydra* sp. and Planarians, show a remarkable regenerative capacity. Regeneration in the vertebrates is more limited, but some taxa (zebrafish, salamanders, frogs, and lizards) show impressive regeneration capacity. Lizards (Scincidae, Gekkonidae, Lacertidae) are common animal models in regeneration studies and are able to fully regrow their tail after accidental amputation or self-amputation (autotomy). Tail regeneration in lizards includes formation of a multipotent cell mass (blastema)and its differentiation into a regenerated tail which shows small differences from the original tail. Regeneration has some similarities with embryonic development, but these similarities are not well understood. The aim of this thesis is to make a comprehensive characterization of the cellular and molecular mechanisms underlying tail development and regeneration in the tokay gecko (*Gekko gecko*). We used histology, bulk transcriptomics, single-cell sequencing, *in situ* hybridization and genome sequencing. We compare multiple stages of tail regeneration with the embryonic tail bud. This will provide insight into shared and unique gene regulatory pathways involved in both regeneration and normal development. The studies reported here, together with other research on lizard tail regeneration, have potential applications in regenerative medicine.

Regeneration

Regeneration is the ability of an organism to restore damaged or lost tissue, without the production of scar tissue, and with the newly formed tissue able to function the same as the original tissue (Pirotte et al., 2016; Poss, 2010). Regeneration goes beyond wound healing or repair, in which the lost tissue is simply covered over by epithelium or replaced by scar tissue. Regeneration can take place at various level of biological organization, from a cell to a whole body, and can be induced by a wide-variety of events in the animal's lifecycle (Bely and Nyberg, 2010). It always involves cell proliferation and differentiation after injury (Ricci and Srivastava, 2018; Tanaka and Reddien, 2011). Therefore, it relies on a population of stem cells (Ricci and Srivastava, 2018; Tanaka and Reddien, 2011). The availability of stem cells in different species may explain the widely differing regenerative capacity in different animals.

Regeneration biology has the potential for translational applications in human regenerative medicine. This is a field that offers potential for treatments of traumatic injuries, heart disease, degenerative diseases, cancers and other diseases for which treatment options are limited (Ahmed et al., 2014; Oviedo and Beane, 2010). One example of a translational application is in the treatment of degenerative bone and cartilage diseases such as osteoarthritis. This disease is suffered by about 10% of people over 60 years of age (Tiku and Sabaawy, 2015).

Cartilage is an important connective tissue mostly found in the ear, nose, and joints, and it can be damaged due to injury, such as the common sporting injuries, or by diseases. Human cartilage lacks self-healing capacity and so, much attention has been given recently to potential regenerative therapies (Zhang et al., 2016). In this context, it is interesting to note that lizards are able to regenerate a cartilage tube in their tail. This makes them an interesting animal model for engineering cartilage tissue for osteoarthritis treatment (Lozito and Tuan, 2016). In the more distant future, it may even be possible to replace a whole limb using regenerative biology (Gilbert et al., 2015).

Evolutionary aspects of regeneration

Regeneration is important as a one of the survival strategies used by animals to deal with injuries (Bely and Nyberg, 2010; Gurtner et al., 2008). Furthermore, regeneration is used routinely by animals such as the cnidarian *Hydra* sp. and planarians such as *Schmidtea mediterranea* and *Dugesia japonica*. These animals show a remarkable regenerative capacity, not only at the tissue level but also at the whole-body level (Ivankovic et al., 2019; Vogg et al., 2019). The regenerative capacity in both *Hydra* and planarians is supported by an abundant stem cell population.

Hydra possess three variant stem cells populations to deal with body-loss. They are two kinds of unipotent epithelial stem cells, the epidermal (eESCs) and gastrodermal (gESCs) stem cells; and one type of multipotent interstitial stem cell (ISC) (Vogg et al., 2019). These three stem cell populations each have specialized roles in proliferation and differentiation to generate new tissues or organs. By contrast, planarians have numerous adult stem cells scattered all over the body, corresponding to a single stem-cell type called a neoblast (Ivankovic et al., 2019; Ricci and Srivastava, 2018; Wagner et al., 2011). Neoblasts play an important role in whole body regeneration (Ivankovic et al., 2019; Sánchez Alvarado, 2006; Wagner et al., 2011).

Regeneration in the vertebrates is more limited compared to that of the invertebrates described above. In humans and mice, for example, the capacity for true regeneration is limited to the fingertips, provided (in humans) that the nail bed is preserved (Gang and Lenghi, 1982; Muneoka and Dawson, 2021; Narayanan, 2015; Tang et al., 2014). The liver in humans and other mammals can restore lost parts, but there are some researchers who describe this as physiological size regulation rather than true regeneration (Michalopoulos, 2007; Wang et al., 2019). Other vertebrates, however, show impressive regeneration capacity. These include teleosts such as the zebrafish (*Danio rerio*), lissamphibia such as salamanders (Urodela), Squamata such as lizards (Li et al., 2015). Those animals are commonly used as models for regeneration studies as they can provide insights not available from mammals which have such limited regeneration capacities (Kurup and Ramachandran, 2011; Song et al., 2010).

Tail autotomy and regeneration in lizards

Lizards (including Scincidae, Gekkonidae, Lacertidae, Eublepharidae) are able to shed part of their own tail to help them distract, and escape from, a predator (Bae et al., 2014). This shedding of the tail is called autotomy and is followed by regeneration of the tail. The autotomized tail will continue to twitch for up to 30 minutes due to the event of anaerobic metabolism (Dial and Fitzpatrick, 1983; Higham and Russell, 2010). This will divert the attention of predator, giving the lizard a chance to escape (Daniels, 1983). Autotomy is observed in the majority of lizard families with the exception of only the Chamaeleonidae and Varanidae (Bateman and Fleming, 2009; Higham et al., 2013b). Only lizards that show autotomy show tail regeneration. Many researchers have found that tail autotomy and regeneration make lizards a useful model for studying tissue regeneration (Alibardi, 2010; Bely and Nyberg, 2010; Hill et al., 2012; Lozito and Tuan, 2015; Russell et al., 2015).

Autotomy is a useful anti-predatory strategy that may help the lizard escape. However, there are many fitness costs associated with autotomy, resulting in a trade-off. For example, the normal lizard tail stores more than half of the body's valuable

storage fat (Congdon et al., 1974; Russell et al., 2015). Therefore, autotomy of the tail means the loss of stored energy. However, at least some lizards may return to the place where they lost their tail and eat the autotomized tail as compensation (Sanggaard et al., 2012). Furthermore, loss of the tail temporarily comprises locomotor performance of the lizard (Bateman and Fleming, 2009). Another fitness cost is that lizards who have shed their tail lose social status in their colony (Fox and McCoy, 2000) and may show decreased courtship and mating success (Boozalis et al., 2012; Martin and Salvador, 1993).

Tail autotomy also causes a decrease of somatic growth and reproductive output, leading to a smaller home range and less access to females for males (Fox and McCoy, 2000; Simou et al., 2008). For these reasons, loss of the tail can be maladaptive because the tail has significant functions (Sanggaard et al., 2012; Sheppard and Bellairs, 1972).

Two types of autotomy

Intravertebral autotomy

Intravertebral autotomy is found in most lizard species and involves the presence of preformed breaks (fracture planes) in the postpygal vertebrae. These anatomical modifications of the vertebrae are found mainly in lizard tails (Gilbert et al., 2013; McLean and Vickaryous, 2011). In the tokay gecko (*Gekko gecko*) the fracture planes are situated posterior to the transverse processes of each postpygal vertebra (Rumping and Jayne, 1996).

Fracture planes are effectively pre-existing planes of weakness formed by connective tissue (Cox, 1969; Delorme et al., 2012; Kusumi and Fisher, 2012; Pratt, 1920). Other supporting structures playing important roles in autotomy are the interdigitation arrangement of tail muscles (Sanggaard et al., 2012) and modified structure of the spinal cord and caudal vasculature (Bellairs and Bryant, 1985; Gilbert et al., 2013). Although fracture planes do not extend into the neural canal, in the Italian Wall Lizard (*Podarcis sicula*), the spinal cord at the level of each fracture plane is thinner than in the non-autotomous region (Alibardi, 2009). Another feature plane in lizards is that the caudal artery thickens around each preformed break, this thickening resembling the structure of a sphincter. The caudal veins are equipped with valves situated just in front of each fracture plane (Bellairs and Bryant, 2001). This system of vascular sphincters and valves prevents excessive blood loss after tail amputation (Gilbert et al., 2013; Sanggaard et al., 2012), as does the rapid clotting response post-autotomy (Fernando et al., 2011; Mescher et al., 2015).

Intervertebral autotomy

Intervertebral autotomy involves intervertebral planes as the site of autotomy (Bateman and Fleming, 2009). In this type of autotomy, there are no pre-existing fracture planes

or other obvious modifications in the normal tail (Bateman and Fleming, 2009). It occurs in fewer species (most agamids and some of iguanids) (Sanggaard et al., 2012).

Tail regeneration processes

The ability of some lizards to regrow their tail following tail autotomy or amputation is known as tail regeneration (Hutchins et al., 2016). The following account applies intra- and intervertebral autotomy. Tail regeneration involves the formation of a blastema, which is a mass of progenitor cells. In the lizards that have been studies, these cells are produced by the dedifferentiation of mature cells at the wound site (Alibardi, 2019; Alibardi and Lovicu, 2010; Daniels et al., 2003). These progenitor cells play an important role in regeneration (Alibardi, 2015). They proliferate and re-differentiate to form new tissues to replace the lost or damaged ones (Bruce, 2007; Narayanan, 2015). Tail regeneration can be divided into four phases (timing is given in parentheses and indicates days post amputation or dpa):

Phase 1. Wound healing (0–10 dpa)

The wound healing phase is initiated by the formation of a highly proliferative wound epithelium within hours of amputation (Echeverri et al., 2001), and the degradation of the stump bone by osteoclasts (Fernando et al., 2011). The wound site will be covered by the wound epithelium, a stratified squamous epithelium with a prominent apical thickening (epithelial cap) that forms within days of autotomy. Without the wound epithelium, regeneration will not take place, suggesting an important role for the epithelium in regeneration (Gilbert et al., 2015). In the wound healing phase of the anole lizard (*Anolis carolinensis*), osteoclasts appear at 2 dpa at the autotomy plane, producing a focal area of bone dissolution. By 4 dpa, a large number of osteoclasts are concentrated in the area between the last remaining caudal vertebra and the newly-formed wound epithelium. This vertebra is extensively degraded, producing a population of chondrocytes destined for the cartilage tube. The chondrocytes are initially flat in shape, and in contact with the bone (Alibardi, 2015; Cox, 1969; Lozito and Tuan, 2015). The osteoclasts then disappear two or three days after the completion of wound healing process (Cox, 1969).

Phase 2. Blastema formation (10–15 dpa)

During regeneration in lizards with intravertebral autotomy, numerous mesenchymal calls are produced in the autotomy plane from the existing dermis, muscle myoseptum, periosteum of the vertebra, adipose tissue and bone marrow. These cells may be the source of the regeneration blastema (Alibardi, 2010; Bellairs and Bryant, 2001) and are believed to re-differentiate into the same cell lineage that they arose from. It is thought that all injured tissues of the tail stump contribute to the formation of the blastema, although the contribution of each tissue is unclear (Alibardi, 2009). As the blastema is

forming, there is a focal degeneration of the spinal cord which leaves only its ependymal lining remaining as a tube-like structure, the so-called ependymal tube. When the blastema has formed underneath the wound epithelium, the ependymal tube grows in the center of the blastema and acts as a guide for the regeneration process (Alibardi, 2009; Alibardi and Miolo, 1990; Gilbert et al., 2015; Shieh and Cheng, 2015).

Phase 3. Tail growth and differentiation (15–25 dpa)

The regenerating tail does not usually elongate during wound healing (phase 1, above) and blastema formation (phase 2 above); however, it will grow rapidly several weeks later (Bellairs and Bryant, 2001). A population of blastemal cells around the ependymal tube forms a pre-cartilaginous aggregation. The cells in this aggregation rapidly differentiate a tissue resembling hyaline cartilage, except that it has little intercellular matrix. This cartilage tissue then quickly grows to surround the newly-formed ependymal tube. By doing so, the two tissues together form the so-called cartilage tube. The cartilage tube isolates the ependymal tube from other tissues, with the exception of blood vessels which reach the ependymal tube through foramina in the tube wall.

Pre-muscular condensations, originating from clusters of myoblasts, are formed surrounding the cartilage tube (Alibardi, 2009). These myoblasts will differentiate into myotubes (Simpson and Cox, 1967). Connective tissue will subsequently develop between the forming muscle bundles and the cartilage tube. It consists of a heterogeneous population of cells consisting of fibroblasts, melanocytes, nerve fibers and small adipocytes in The adipocytes increase in size a few days later as they accumulate lipids. Cell proliferation, mostly in the axial tissues, determines the rate of tail growth (Alibardi, 2009). The end result is a regenerated tail with an axial skeleton in the form of a hyaline cartilage tube instead of segmented caudal vertebrae.

Phase 4. Tail maturation (25-60 dpa)

Tail maturation is reached when the tail epidermis becomes completely covered with keratinized, pigmented scales (Alibardi, 2010). These scales are smaller than the original scales on the tail, and are arranged in a simpler scalation pattern (Alibardi, 2009). This stage is usually reached at 25–60 dpa (Fisher et al., 2012; McLean and Vickaryous, 2011). In the tail maturation phase, differentiation continues in the more distal part of the regenerated tail. A small remnant of blastemal cells is still found beneath the wound epithelium at the tip of the new tail. Overall, tail regeneration in lizards yields a new tail which shows small differences from the original tail, namely: (1) the axial skeleton of the regenerated tail is replaced by a cartilage tube, which also resulting on no true tendons in the muscle; (2) the spinal cord in the regenerated tail is formed only from meninges and the ependymal cells lining the central canal; and (3) the size and pattern of scales covering the regenerated tail is different (Higham et al., 2013a).

We will now consider the embryonic development of the tail, because the pathways of adult regeneration are often compared with those in embryonic development (at least in some amphibians: (Gerber et al., 2018; Muneoka and Bryant, 1982).

Embryonic development of the tail

The embryonic development of the tail is a useful reference for understanding tail regeneration because both processes involve the production of patterned tissues from precursor cells. A comparison of normal embryonic tail development with adult tail regeneration may provide insight into shared regulatory pathways involved in both processes; or into pathways unique to one process. In this thesis, we are particularly interested in examining these issues in the tokay gecko.

The vertebrates tail develops from an embryonic structure called the tailbud which consists of mesenchymal cells covered by an ectodermal cap (Griffith et al., 1992). The tailbud continues the morphogenesis of axial structures (neural tube, somites etc.), a process that took place earlier in the head and trunk (Aires et al., 2018; Beck, 2015; Griffith et al., 1992; Handrigan, 2003). Tail bud development involves secondary neurulation and somite formation by the tailbud mesenchyme (Beck, 2015; Handrigan, 2003). This is unique since tailbud mesenchyme give rise to both ectodermal and mesodermal tissue. Secondary neurulation in the tailbud is started by mesenchymal cell condensation to form a solid cord which subsequently undergoes hollow neural tube formation (Beck, 2015; Griffith et al., 1992; Handrigan, 2003). Meanwhile, somite formation in the tailbud involves similar mechanism to that of trunk somites and develop from caudal pre-somitic mesoderm (PSM) cells (Beck, 2015; Handrigan, 2003).

Tailbud development involves a genetic network including *gdf11*, *lin28*, and paralog 13 hox genes, especially *hoxc13* (Aires et al., 2019). The somites develop from the tailbud mesenchyme under the influence of cyclical expression of the *hes7* gene (a segmentation gene) which is high in regions expressing high canonical *wnt* and FGF signaling but low in regions expressing retinoic acid (Beck, 2015; Cunningham et al., 2011; Goto et al., 2017; Handrigan, 2003; Takada et al., 1994).

Somite-formation and BMP-signaling in the mouse and chicken tailbud requires induction by the ventral ectodermal ridge (VER). The VER is ridge-like, midline thickening on the ventral aspect of the tail bud. In anurans, by contrast, induction is by the ventral blastopore lip (Beck, 2015). Secondary neurulation seems to depend on different genetic pathways in different species. For example, zebrafish secondary neurulation depends on canonical wnt signaling repression; in anurans it relies on *notch/wnt* signaling; and in mice, *tbx6* exerts negative regulation (Beck, 2015). Regulation of *notch* signalling by *lfng* along the neural tube is conserved in all vertebrates, but in mammals and birds there

are *hes*-binding regulatory mechanisms that allow *lfng* cycles within the PSM (Beck, 2015). Other transcription factors and signaling molecules needed for normal tail development include: *T* (*brachyury*) (Herrmann et al., 1990), *tbx6* (Chapman and Papaioannou, 1998), *cdx4* (van Nes et al., 2006), *cyp26a1* (Abu-Abed et al., 2001; Sakai et al., 2001) .

The tokay gecko

In this thesis, we use the tokay gecko (*Gekko gecko*) as a model species. This lizard tokay gecko is a member of the Suborder Lacertilia, Family Gekkonidae whose members are found from South Asia to Southeast Asia (Das, 2015). There are two subspecies of tokay gecko, namely: *G. g. gecko* (Linnaeus, 1758) and *G. g. azhari* (Mertens, 1955). The first is the common tokay gecko found in Southeast Asia, China and India, and the latter is endemic to Bangladesh (Rösler, 2001; Rösler, 2005). The tokay gecko inhabits tropical rain forest; some individuals have entered human habitation and live, and sometimes breed, in houses (Kongbuntad et al., 2016). The tokay gecko feeds mainly on insects (Aowphol et al., 2006).

The Indonesian tokay gecko population exhibits low genetic diversity despite geographic barriers (Kadafi et al., 2024). This contrasts with the higher genetic diversity observed in tokay geckos from mainland Southeast Asia, which suggests biogeographical separation and ecological barriers have played a role. The reduced genetic diversity of the Indonesian tokay gecko population may be attributed to anthropogenic influences their adaptation to human environments (Kadafi et al., 2024).

The total body length (TL; snout to tip of tail) of the tokay gecko is around 35 cm and the snout-vent length (SVL) is around 18.5 cm (Cobos and Higham, 2022); it is the second largest living geckos after the New Caledonian gecko (*Rhacodactylus leachianus*) (Kongbuntad et al., 2016). The head of the tokay gecko is large and there is a distinct neck region. The eyes are protruding and large with vertical pupils and a yellow iris, while the ears appear as two small holes on each side of the head. The limbs are well-developed and the digits are equipped on their volar surface with toe pads (setae) enabling them to adhere to, and move fast on, vertical surfaces such as trees, cliffs and walls (Henkel and Schmidt, 1995). The skin is covered by granular scales interspersed with subconical tubercles. The coloration of the dorsal skin is bluish-grey with red or orange spots, while the ventral part is cream-colored, with or without grey or pink spots. The male is usually brighter in color and slightly larger than the female (Das, 2015). For details of the histology of the normal and regenerating tail, see Chapter 2.

Single-cell sequencing

Single-cell sequencing (sc-seq) is a tool to obtain individual cell genome or transcriptome profiles. It is therefore a powerful technology to uncover cellular responses, cell population diversity and, cellular evolutionary connections (Dey et al., 2014; Haque et al., 2017; Tang et al., 2019). This technique eliminates the problem of bulk mRNA sequencing, namely that the tissue sample is homogenized from all of the cells, meaning that all unique, single-cell information is lost (Tang et al., 2019; Wang and Navin, 2015). Bulk transcriptomics remains useful however, because of its much lower cost. Among its applications, single-cell mRNA sequencing (sc-mRNA seq) is able to reveal the heterogeneity of tumor cell populations, providing accurate new diagnostic and treatment options (Lim et al., 2020; Tang et al., 2019).

The sc-mRNA seq workflow starts with the isolation of single cells in suspension by enzyme disaggregation of the tissue. This is followed by mRNA extraction, amplification, library preparation, next-generation sequencing, and, finally, bioinformatical analysis (AlJanahi et al., 2018; Haque et al., 2017). Various protocols and platforms are available and can be applied depending on the type of sample, number of cells required, and transcripts capture per cell (AlJanahi et al., 2018; Dey et al., 2014; Haque et al., 2017; Tang et al., 2019; Wang and Navin, 2015). A typical run might sequence, per sample, 5,000 cells to a depth of 25k transcripts per cell; but the parameters can be varied, and the technology is rapidly advancing.

Sc-mRNA seq is a very promising method for understanding molecular programs within cells during regeneration. For instance, it has already uncovered the role of phagocytic cell populations during lizard tail regeneration (Londono et al., 2020). It has also shown that phagocytes induce the activation of fibroblast genes during lizard blastema formation in response to Hedgehog signaling (Vonk et al., 2023). In addition, sc-mRNA seq has also elucidated the cellular heterogeneity and lineage restriction during mouse digit tip regeneration (Johnson et al., 2020). Finally, Gerber et al. (Gerber et al., 2018) revealed the significant role of connective tissue cells during axolotl limb regeneration using sc-mRNA seq. Those authors were able to explain how connective tissue cells form a patterned limb skeleton which serves as a guide for the other limb tissues. In this thesis, I use sc-mRNA seq on both the embryonic tail and adult regenerated tail to identify the shared and distinctive cell populations associated with tail regeneration.

Aims and outline of the thesis

This thesis investigates the genes and cell populations involved in tail regeneration in the adult tokay gecko (*G. gecko*) and compare them with those in normal embryonic tail

development. Several studies have given rise to the hypothesis that developmental genes are reactivated during tail regeneration. We will test this hypothesis by making a detailed comparison between adult tail regeneration and embryonic tail development.

One possibility is that different genetic programs initiate embryonic tail development and adult tail regeneration. This possibility will be addressed as follows. (1) We will characterize the histological structure of the regenerating tail. (2) We will perform bulk transcriptomic analysis on multiple stages of regenerating tail of tokay gecko and compared the results with the bulk transcriptome of the embryonic tail. This will hopefully reveal a molecular signature for each stage of tail regeneration, as well as revealing differences with embryonic tail development. (3) We will perform sc-mRNA seq of the adult regenerating tail blastema, and the embryonic tailbud, to identify cell populations, their gene expression profiles, and their differentiation direction probability. (4) Once critical candidate genes have been identified, we will study their expression in depth using *in situ* hybridization on tissue sections. (5) Finally, because of the potential of the tokay gecko as a model in regeneration research, we will sequence, assemble, and annotate the genome of this species.

In **Chapter 2,** We establish a foundation for this thesis using paraffin histology to describe the tissue structure of seven stages of the adult tokay gecko regenerating tail.

In **Chapter 3,** We sequence and analyze the bulk transcriptome of the regenerating tail of the tokay gecko and identify a molecular signature of each stage of regeneration. I also compare the transcriptome profile of the regenerating tail with that of the embryonic tail.

In **Chapter 4,** We describe the single-cell mRNA sequencing analysis of regeneration blastema cells and embryonic tail cells. I identify cell populations, their gene expression patterns, and their differentiation direction probability.

In **Chapter 5,** We examine the candidate genes identified with bulk transcriptomics and single-cell mRNA sequencing by means of *in situ* hybridization on tissue sections. This permits a spatial and temporal analysis of gene expression during tail regeneration and allows me to make predictions about their roles in tail regeneration.

In **Chapter 6,** We describe sequencing, assembly and annotation the genome of the tokay gecko. This genome provides a crucial resource for this emerging model species.

Finally**,** in **Chapter 7,** We provide a summary of the thesis, including our new findings on tail regeneration pathways in the tokay gecko. We also summarize how tail regeneration

compares with tail development. We also consider the potentials for translating my findings to regenerative medicine.

References

Abu-Abed, S., Dollé, P., Metzger, D., Beckett, B., Chambon, P. and Petkovich, M. (2001). The retinoic acid-metabolizing enzyme, CYP26A1, is essential for normal hindbrain patterning, vertebral identity, and development of posterior structures. *Genes and Development* **15**.

Ahmed, N., Iu, J., Brown, C. E., Taylor, D. W. and Kandel, R. A. (2014). Serum- and growth-factor-free three-dimensional culture system supports cartilage tissue formation by promoting collagen synthesis via sox9– col2a1 interaction. *Tissue Engineering Part A* **20**, 2224-2233.

Aires, R., de Lemos, L., Nóvoa, A., Jurberg, A. D., Mascrez, B., Duboule, D. and Mallo, M. (2019). Tail bud progenitor activity relies on a network comprising gdf11, lin28, and hox13 genes. *Developmental Cell* **48**, 383-395.e388.

Aires, R., Dias, A. and Mallo, M. (2018). Deconstructing the molecular mechanisms shaping the vertebrate body plan. *Current Opinion in Cell Biology* **55**, 81-86.

Alibardi, L. (2009). *Morphological and Cellular Aspects of Tail and Limb Regeneration in Lizards*. Berlin: Springer-Verlag.

Alibardi, L. (2010). Morphological and cellular aspects of tail and limb regeneration in lizards. A model system with implications for tissue regeneration in mammals. *Advances in anatomy, embryology, and cell biology* **207**, iii, v-x, 1-109.

---- (2015). Original and regenerating lizard tail cartilage contain putative resident stem / progenitor cells. *Micron* **78**, 10-18.

---- (2019). Stimulation of regenerative blastema formation in lizards as a model to analyze limb regeneration in amniotes. *Histology and Histopathology* **34**, 1111-1120.

Alibardi, L. and Lovicu, F. J. (2010). Immunolocalization of FGF1 and FGF2 in the regenerating tail of the lizard Lampropholis guichenoti: Implications for FGFs as trophic factors in lizard tail regeneration. *Acta Histochemica* **112**, 459-473.

Alibardi, L. and Miolo, V. (1990). Fine observation on nerves colonizing the regenerating tail of the lizard Podarcis sicula. *Histology and Histopathology* **5**, 387-396.

AlJanahi, A. A., Danielsen, M. and Dunbar, C. E. (2018). An Introduction to the Analysis of Single-Cell RNA-Sequencing Data. *Molecular Therapy - Methods and Clinical Development* **10**, 189-196.

Aowphol, A., Thirakhupt, K., Nabhitabhata, J. and Voris, H. K. (2006). Foraging ecology of the Tokay gecko,

Gekko gecko in a residential area in Thailand. *Amphibia-Reptilia* **27**, 491-503.

Bae, K. S., Kim, S. Y., Park, S. Y., Jeong, A. J., Lee, H. H., Lee, J., Cho, Y. S., Leem, S. H., Kang, T. H., Bae, K. H., et al. (2014). Identification of lactoferrin as a human dedifferentiation factor through the studies of reptile tissue regeneration mechanisms. *Journal of Microbiology and Biotechnology* **24**, 869-878.

Bateman, P. W. and Fleming, P. A. (2009). To cut a long tail short: A review of lizard caudal autotomy studies carried out over the last 20 years. *Journal of Zoology* **277**, 1-14.

Beck, C. W. (2015). Development of the vertebrate tailbud. *Wiley Interdisciplinary Reviews: Developmental Biology* **4**, 33-44.

Bellairs, A. A. and Bryant, S. V. (2001). *Biology of Reptilia*. Brisbane: John Willey and Sons.

Bellairs, A. D. and Bryant, S. V. (1985). Autotomy and Regeneration in Reptiles. (ed. C. G. A. F. Billet), pp. 303-410. New York: John Wiley & Sons, Inc.

Bely, A. E. and Nyberg, K. G. (2010). Evolution of animal regeneration: re-emergence of a field. *Trends in Ecology and Evolution* **25**, 161-170.

Boozalis, T. S., LaSalle, L. T. and Davis, J. R. (2012). Morphological and biochemical analyses of original and regenerated lizard tails reveal variation in protein and lipid composition. *Comparative Biochemistry and Physiology - A Molecular and Integrative Physiology* **161**, 77-82.

Bruce, M. C. (2007). *Principles of Regenerative Biology, 1st Edition | Bruce Carlson | ISBN 9780123694393* (1st edn): Academic Press.

Chapman, D. L. and Papaioannou, V. E. (1998). Three neural tubes in mouse embryos with mutations in T-box gene Tbx6. *Nature* **391**.

Cobos, A. J. and Higham, T. E. (2022). Growing up in a rough world: scaling of frictional adhesion and morphology of the Tokay gecko (Gekko gecko). *Beilstein J Nanotechnol* **13**, 1292-1302.

Congdon, J. D., Vitt, L. J. and King, W. W. (1974). Geckos: adaptive significance and energetics of tail autotomy. *Science (New York, N.Y.)* **184**, 1379-1380.

Cox, P. G. (1969). Some aspects of tail regeneration in the lizard, Anolis carolinensis. *Journal of Experimental Zoology* **171**, 127-149.

Cunningham, T. J., Zhao, X. and Duester, G. (2011). Uncoupling of retinoic acid signaling from tailbud development before termination of body axis extension. *Genesis* **49**, 776-783.

Daniels, C. B. (1983). Running: an escape strategy enhanced by autotomy. *Herpetologica* **39**, 162-165.

Daniels, C. B., Lewis, B. C., Tsopelas, C., Munns, S. L., Baldwin, M. E., Stacker, S. A., Achen, M. G., Chatterton, B. E. and Cooter, R. D. (2003). Regenerating lizard tails: A new model for investigating lymphangiogenesis.

Das, I. (2015). A field guide to the reptiles of South-East Asia. pp. 375-375.

Delorme, S. L., Lungu, I. M. and Vickaryous, M. K. (2012). Scar-Free Wound Healing and Regeneration Following Tail Loss in the Leopard Gecko, Eublepharis macularius. *Anatomical Record* **295**, 1575-1595.

Dey, S. S., Kester, L., Spanjaard, B., Bienko, M., Van Oudenaarden, A., Gupta, R. K., Kuznicki, J., Fabre, P. J., Leleu, M., Mascrez, B., et al. (2014). Concurrent single-cell RNA and targeted DNA sequencing on an automated platform for comeasurement of genomic and transcriptomic signatures. *Nature Methods* **65**, 82-91.

Dial, B. E. and Fitzpatrick, L. C. (1983). Lizard Tail Autotomy: Function and Energetics of Postautotomy Tail Movement in Scincella lateralis. *Science (New York, N.Y.)* **219**, 391-393.

Echeverri, K., Clarke, J. D. and Tanaka, E. M. (2001). In vivo imaging indicates muscle fiber dedifferentiation is a major contributor to the regenerating tail blastema. *Developmental biology* **236**, 151-164.

Fernando, W. A., Leininger, E., Simkin, J., Li, N., Malcom, C. A., Sathyamoorthi, S., Han, M. and Muneoka, K. (2011). Wound healing and blastema formation in regenerating digit tips of adult mice. *Developmental Biology* **350**, 301-310.

Fisher, R. E., Geiger, L. A., Stroik, L. K., Hutchins, E. D., George, R. M., Denardo, D. F., Kusumi, K., Rawls, J. A. and Wilson-Rawls, J. (2012). A histological comparison of the original and regenerated tail in the green anole, Anolis carolinensis. *Anatomical record (Hoboken, N.J. : 2007)* **295**, 1609-1619.

Fox, S. F. and McCoy, J. K. (2000). The effects of tail loss on survival, growth, reproduction, and sex ratio of offspring in the lizard Uta stansburiana in the field. *Oecologia* **122**, 327-334.

Gang, R. K. and Lenghi, M. (1982). Conservative management of guillotine amputations of finger tips - Another application of zinc oxide tape. *Chirurgia Plastica* **7**, 75-81.

Gerber, T., Murawala, P., Knapp, D., Masselink, W., Schuez, M., Hermann, S., Gac-Santel, M., Nowoshilow, S., Kageyama, J., Khattak, S., et al. (2018). Single-cell analysis uncovers convergence of cell identities during axolotl limb regeneration. *Science* **362**.

Gilbert, E. A. B., Delorme, S. L. and Vickaryous, M. K. (2015). The regeneration blastema of lizards: an amniote model for the study of appendage replacement. *Regeneration* **2**, 45-53.

Gilbert, E. A. B., Payne, S. L. and Vickaryous, M. K. (2013). The anatomy and histology of caudal autotomy and regeneration in lizards. *Physiological and Biochemical Zoology* **86**, 631-644.

Goto, H., Kimmey, S. C., Row, R. H., Matus, D. Q. and Martin, B. L. (2017). FGF and canonical Wnt signaling cooperate to induce paraxial mesoderm from tailbud neuromesodermal progenitors through regulation of a two-step epithelial to mesenchymal transition. *Development (Cambridge)* **144**, 1412-1421.

Griffith, C. M., Wiley, M. J. and Sanders, E. J. (1992). The vertebrate tail bud: three germ layers from one tissue. *Anatomy and Embryology* **185**, 101-113.

Gurtner, G. C., Werner, S., Barrandon, Y. and Longaker, M. T. (2008). Wound repair and regeneration. *Nature* **453**, 314-321.

Handrigan, G. R. (2003). Concordia discors: Duality in the origin of the vertebrate tail. *Journal of Anatomy* **202**, 255-267.

Haque, A., Engel, J., Teichmann, S. A. and Lönnberg, T. (2017). A practical guide to single-cell RNA-sequencing for biomedical research and clinical applications. *Genome Medicine* **9**, 1-12.

Henkel, F.-W. and Schmidt, W. (1995). *Geckoes : biology, husbandry, and reproduction* (English edn). Malabar, Fla.: Krieger Pub.

Herrmann, B. G., Labeit, S., Poustka, A., King, T. R. and Lehrach, H. (1990). Cloning of the T gene required in mesoderm formation in the mouse. *Nature* **343**.

Higham, T. E., Lipsett, K. R., Syme, D. A. and Russell, A. P. (2013a). Controlled chaos: three-dimensional kinematics, fiber histochemistry, and muscle contractile dynamics of autotomized lizard tails. *Physiological and Biochemical Zoology* **86**, 611-630.

Higham, T. E. and Russell, A. P. (2010). Flip, flop and fly: modulated motor control and highly variable movement patterns of autotomized gecko tails. *Biology letters* **6**, 70-73.

Higham, T. E., Russell, A. P. and Zani, P. a. (2013b). Integrative biology of tail autotomy in lizards. *Physiological and biochemical zoology* **86**, 603-610.

Hill, C., Jain, A., Takemoto, H., Silver, M. D., Nagesh, S. V. S., Ionita, C. N., Bednarek, D. R. and Rudin, S. (2012). A histological comparison of the original and regenerated tail in the green anole, Anolis carolinensis. *Anat Rec (Hoboken)* **295**, 1609-1619.

Hutchins, E. D., Eckalbar, W. L., Wolter, J. M., Mangone, M. and Kusumi, K. (2016). Differential expression of conserved and novel microRNAs during tail regeneration in the lizard Anolis carolinensis. *BMC Genomics* **17**, 339-339.

Ivankovic, M., Haneckova, R., Thommen, A., Grohme, M. A., Vila-Farré, M., Werner, S. and Rink, J. C. (2019). Model systems for regeneration: Planarians. *Development (Cambridge)* **146**, 0-1.

Johnson, G. L., Masias, E. J. and Lehoczky, J. A. (2020). Cellular heterogeneity and lineage restriction during mouse digit tip regeneration at single-cell resolution. *Developmental Cell* **52**, 525-540.e525.

Kadafi, A. M., Fauzi, M. A., Ardiantoro, A., Zakky, Q., Nugraha, F. A. D., Priambodo, B., Fahmi, M., Munir, M., , Riyanto, A. and Hamidy, A. (2024). Low genetic diversity of the Indonesian Tokay Gecko (Gekko gecko) (Reptilia: Gekkonidae): Introduce or Native? *Jurnal Biologi Indonesia* **20**, 63-75.

Kongbuntad, W., Tantrawatpan, C., Pilap, W., Jongsomchai, K., Chanaboon, T., Laotongsan, P., Petney, T. N. and Saijuntha, W. (2016). Genetic diversity of the red-spotted tokay

gecko (Gekko gecko Linnaeus, 1758) (Squamata: Gekkonidae) in Southeast Asia determined with multilocus enzyme electrophoresis. *Journal of Asia-Pacific Biodiversity* **9**, 63-68.

Kurup, A. and Ramachandran, A. V. (2011). Exogenous NGF favors initiation of lizard tail regeneration while EGF and TGF- β truncate regenerative growth and commit to precocious muscle and cartilage differentiation. *journal of Developmental Biology and Tissue Engineering* **3**, 1-10.

Kusumi, K. and Fisher, R. E. (2012). Special Issue: Studying mechanisms of regeneration in amphibian and reptilian vertebrate models. **295**, 1529-1531.

Li, Q., Yang, H. and Zhong, T. P. (2015). Regeneration across metazoan phylogeny: lessons from model organisms. *Journal of genetics and genomics = Yi chuan xue bao* **42**, 57-70.

Lim, B., Lin, Y. and Navin, N. (2020). Advancing cancer research and medicine with single-cell genomics. *Cancer Cell* **37**, 456-470.

Londono, R., Tighe, S., Milnes, B., DeMoya, C., Quijano, L. M., Hudnall, M. L., Nguyen, J., Tran, E., Badylak, S. and Lozito, T. P. (2020). Single cell sequencing analysis of lizard phagocytic cell populations and their role in tail regeneration. *Journal of Immunology and Regenerative Medicine* **8**, 100029-100029.

Lozito, T. P. and Tuan, R. S. (2015). Lizard tail regeneration: Regulation of two distinct cartilage regions by Indian hedgehog. *Developmental Biology* **399**, 249-262.

---- (2016). Lizard tail skeletal regeneration combines aspects of fracture healing and blastema-based regeneration. *Development* **143**, 2946-2957.

Martin, J. and Salvador, A. (1993). Tail loss reduces mating success in the Iberian rock-lizard, Lacerta monticola. *Behavioral Ecology and Sociobiology* **32**, 185-189.

McLean, K. E. and Vickaryous, M. K. (2011). A novel amniote model of epimorphic regeneration: the leopard gecko, Eublepharis macularius. *BMC Developmental Biology* **11**, 50-50.

Mescher, A. L., Neff, A. W. and King, M. W. (2015). Inflammation and immunity in organ regeneration. *Developmental and Comparative Immunology*.

Michalopoulos, G. K. (2007). Liver regeneration. *Journal of Cellular Physiology* **213**, 286-300.

Muneoka, K. and Bryant, S. V. (1982). Evidence that patterning mechanisms in developing and regenerating limbs are the same. *Nature* **298**, 369-371.

Muneoka, K. and Dawson, L. A. (2021). Evolution of epimorphosis in mammals. *J Exp Zool B Mol Dev Evol* **336**, 165-179.

Narayanan, A. (2015). Biochips & Tissue Chips The Initiation and Progression of Tail Regeneration in Northern House Gecko Hemidactylus Flaviviridis at Role of Fibroblast Growth Factor 2. *Biochip & Tissue Chip* **5**, 1-7.

Oviedo, N. J. and Beane, W. S. (2010). Regeneration : The Origin of Cancer or a Possible Cure ? **20**, 617-627.

Pirotte, N., Leynen, N., Artois, T. and Smeets, K. (2016). Do you have the nerves to regenerate? The importance of neural signalling in the regeneration process. *Developmental Biology* **409**, 4-15.

Poss, K. D. (2010). Advances in understanding tissue regenerative capacity and mechanisms in animals. *Nature Reviews Genetics* **11**, 710-722.

Pratt, C. W. M. (1920). The Plane of Farcture of the Caudal Vertebrae of Certain Lacertilians.

Ricci, L. and Srivastava, M. (2018). Wound-induced cell proliferation during animal regeneration. *Wiley Interdisciplinary Reviews: Developmental Biology* **7**, 1-17.

Rösler, H. (2001). Studien am Tokeh: 1. Gekko gecko azhari Mertens, 1955 (Sauria: Gekkonidae). *Gekkota* **3**, 33-46.

Rösler, H. (2005). Studien am Tokeh: 2. Intraspezifische Variation der südostasiatischen Populationen von Gekko gecko (Linnaeus, 1758)(Sauria: Gekkonidae). *Gekkota* **5**, 65-149.

Rumping, J. M. and Jayne, B. C. (1996). Muscle activity in autotomized tails of a lizard (Gekko gecko): a naturally occurring spinal preparation. *Journal of comparative physiology. A, Sensory, neural, and behavioral physiology* **179**, 525-538.

Russell, A. P., Lynn, S. E., Powell, G. L. and Cottle, A. (2015). The regenerated tail of juvenile leopard geckos (Gekkota: Eublepharidae: Eublepharis macularius) preferentially stores more fat than the original. *Zoology* **118**, 183-191.

Sakai, Y., Meno, C., Fujii, H., Nishino, J., Shiratori, H., Saijoh, Y., Rossant, J. and Hamada, H. (2001). The retinoic acid-inactivating enzyme CYP26 is essential for establishing an uneven distribution of retinoic acid along the anterio-posterior axis within the mouse embryo. *Genes and Development* **15**.

Sánchez Alvarado, A. (2006). Planarian regeneration: Its end is its beginning. *Cell* **124**, 241-245.

Sanggaard, K. W., Danielsen, C. C., Wogensen, L., Vinding, M. S., Rydtoft, L. M., Mortensen, M. B., Karring, H., Nielsen, N. C., Wang, T., Thøgersen, I. B. and Enghild, J. J. (2012). Unique structural features facilitate lizard tail autotomy. *PLoS ONE* **7**.

Sheppard, L. and Bellairs, A. A. (1972). The mechanism of autotomy in Lacerta. *British Journal of Herpetology* **4**, 276-286.

Shieh, S.-j. and Cheng, T.-c. (2015). Regeneration and repair of human digits and limbs : fact and fiction. 149-168.

Simou, C., Pafilis, P., Skella, A., Kourkouli, A. and Valakos, E. D. (2008). Physiology of Original and Regenerated Tails in Aegean Wall Lizard (Podarcis erhardii). 504-509.

Simpson, S. B. and Cox, P. G. (1967). Vertebrate regeneration system: Culture in vitro. *Science* **157**, 1330-1332.

Song, F., Li, B. and Stocum, D. L. (2010). Amphibians as research models for regenerative medicine. *Organogenesis* **6**, 141-150.

Takada, S., Stark, K. L., Shea, M. J., Vassileva, G., McMahon, J. A. and McMahon, A. P. (1994). Wnt-3a regulates somite and tailbud formation in the mouse embryo. *Genes and Development* **8**.

Tanaka, E. and Reddien, P. W. (2011). The cellular basis for animal regeneration Sources of new cells in animal regeneration. *Dev Cell* **21**, 172-185.

Tang, J. B., Elliot, D., Adani, R., Saint-Cyr, M. and Stang, F. (2014). Repair and reconstruction of thumb and finger tip injuries: A global view. *Clinics in Plastic Surgery* **41**, 325-359.

Tang, X., Huang, Y., Lei, J., Luo, H. and Zhu, X. (2019). The single-cell sequencing: New developments and medical applications. *Cell and Bioscience* **9**, 1-9.

Tiku, M. L. and Sabaawy, H. E. (2015). Cartilage regeneration for treatment of osteoarthritis: a paradigm for nonsurgical intervention. *Therapeutic advances in musculoskeletal disease* **7**, 76-87.

van Nes, J., de Graaff, W., Lebrin, F., Gerhard, M., Beck, F. and Deschamps, J. (2006). The Cdx4 mutation affects axial development and reveals an essential role of Cdx genes in the ontogenesis of the placental labyrinth in mice. *Development* **133**.

Vogg, M. C., Galliot, B. and Tsiairis, C. D. (2019). Model systems for regeneration: Hydra. *Development (Cambridge)* **146**.

Vonk, A. C., Zhao, X., Pan, Z., Hudnall, M. L., Oakes, C. G., Lopez, G. A., Hasel-Kolossa, S. C., Kuncz, A. W. C., Sengelmann, S. B., Gamble, D. J. and Lozito, T. P. (2023). Single-cell analysis of lizard blastema fibroblasts reveals phagocyte-dependent activation of Hedgehog-responsive chondrogenesis. *Nat Commun* **14**, 4489.

Wagner, D. E., Wang, I. E. and Reddien, P. W. (2011). Clonogenic neoblasts are pluripotent adult stem cells that underlie planarian regeneration. *Science* **332**, 811-816.

Wang, S., Zhang, C., Hasson, D., Desai, A., SenBanerjee, S., Magnani, E., Ukomadu, C., Lujambio, A., Bernstein, E. and Sadler, K. C. (2019). Epigenetic compensation promotes liver regeneration. *Developmental Cell* **50**, 43-56.e46.

Wang, Y. and Navin, N. E. (2015). Advances and Applications of Single-Cell Sequencing Technologies.

Zhang, C., Cai, Y. z. and Lin, X. j. (2016). One-step cartilage repair technique as a next generation of cell therapy for cartilage defects: biological characteristics, preclinical application, surgical techniques, and clinical developments. *Arthroscopy - Journal of Arthroscopic and Related Surgery* **32**, 1444-1450.

Chapter 2. Descriptive Analysis of Tail Regeneration in The Tokay Gecko

Abstract

Lizards, including the tokay gecko, possess the remarkable ability to regenerate their tails following autotomy. Understanding the histological structure of the regenerating tail is a fundamental starting point for this thesis and for future research on tail regeneration. It provides crucial insights into the specific cellular and tissue structures involved in the regenerative process, including the blastema and the various regenerating tissues such as muscle, bone, nerves, and blood vessels. We studied seven stages of tail regeneration in the tokay gecko: 4, 8, 16, 20, 24, 28, and 49 days post-autotomy using paraffin histology. The tails were sagittally sectioned and stained with hematoxylin eosin-alcian blue and periodic acid Schiff-alcian blue. In the wound healing phase (4 and 8 dpa), the regenerating tail displayed formation of a wound epithelium and the presence of erythrocytes and leukocytes, at the autotomy site. The blastema formation phase (stages 16 and 20 dpa) was characterized by the formation of undifferentiated blastema tissues. Stages 24 and 28 dpa marked the tissue differentiation phase, characterized by formation of the cartilage tube and segmented skeletal muscles. Finally, the tail maturation phase (stage 49 dpa), exhibiting mature epidermis, skeletal muscles, cartilage tube, and adipose tissue. Interestingly, we saw no evidence of a distal, undifferentiated growth zone. Instead, the distal tissue showed an abundance of blood vessels.

Introduction

Autotomy, or self-amputation of body parts, is a common and effective self-defense mechanism to distract predators. Lizards are an example of animals in which autotomy is possible. It typically occurs in response to predation attempts, allows the lizard to escape (Clause and Capaldi, 2006; Fleming and Bateman, 2012). The autotomy process occurs spontaneously, and there are no visible signs of damage at the site of tail loss, even though the tail is composed of tissues with varying consistencies. Lizards can perform autotomy because they have pre-existing, transversely oriented fracture planes (autotomy planes) in the tail (Delorme et al., 2012; Pratt, 1946). Each fracture plane contains fibroblast-rich connective tissue that connects the dermis to the intermuscular, inter-adipose, and vertebral bone tissue (Bellairs and Bryant, 1985). If autotomy occurs outside the fracture plane, regeneration will be hindered, and may even cease completely (Delorme et al., 2012; Pratt, 1946) .

Lizards have the ability to regenerate their tails after autotomy (Alibardi, 2015; Simpson, 1970). The main differences between the original tail and the regenerated tail lie in the vertebral structure and the spinal cord. Regenerated tails are primarily supported by a longitudinal tube-shaped structure composed of cartilage which replaces the series of vertebrae seen in the original tail (Alibardi, 2014; Gilbert et al., 2013; Lozito and Tuan, 2015). In regenerated tails, the spinal cord is replaced by an ependymal tube lining the cartilage tube, and consisting of ependymal cells, glial cells, and nerve fibers without neuronal cell bodies (Gilbert and Vickaryous, 2018). The ependymal tube consists of cells that originated in the central canal of the original spinal cord (Gilbert and Vickaryous, 2018).

The regeneration of the tail can be divided into four phases (Alibardi, 2010; Lozito and Tuan, 2016): wound healing, blastema formation, differentiation and maturation. In the wound healing phase, stump tissue is broken down and mesenchymal stem cells accumulate underneath the wound epidermis (Lozito and Tuan, 2017). Eventually, the wound is re-epithelialized, forming a thickened epithelium known as the wound epithelium or wound epidermis (Alibardi, 2019). Ependymal cells are organized into the ependymal tube, which is regenerated from the spinal cord. Afterwards, the aggregation of cells, released during the breakdown of the stump tissues, proliferates, and swell beneath the wound epithelium forming the blastema. Blastema formation is followed by rapid tail growth, and the blastema begins to differentiate into tissues including muscle and cartilage (Lozito and Tuan, 2017). A cartilage tube in the regenerated tail takes the place of the vertebrae in the original tail. This tube may originate from stem cells in the intervertebral cartilage (Londono et al., 2017) and almost completely encloses the ependyma. During the elongation phase, the cartilage tube grows, and

muscles elongate and thicken. Lastly, in the maturation phase the regenerated tail reaches maximum length and the tissue is completely differentiated (Alibardi, 2014).

Understanding the histological structure of the regenerating tail is crucial for further research on tail regeneration (Alibardi, 2010; Alibardi, 2014). Histological analysis provides crucial insights into the specific cellular and tissue structures involved in the regenerative process, including the blastema and various regenerating tissues such as muscle, bone, nerves, and blood vessels (Alibardi, 2014; Gilbert et al., 2013; Lozito and Tuan, 2016). Moreover, it allows for the observation of temporal and spatial dynamics during regeneration, revealing how different cell types interact and contribute to tissue renewal (Gilbert et al., 2013; McLean and Vickaryous, 2011). By characterizing the different cell types present, researchers can better understand their roles in regeneration, from stem/progenitor cells to immune cells and differentiated tissues (Alibardi, 2010; Jacyniak et al., 2017). Additionally, histological study facilitates the assessment of tissue quality and functionality, enabling comparisons between regenerated and uninjured tissues (Alibardi, 2010). Considering these factors, this chapter aims to characterize the histological structure of seven stages of tail regeneration in the tokay gecko. This will establish a foundation for the further studies of tokay gecko tail regeneration in the following chapters of this thesis.

Materials and methods

Ethics statement

The tokay gecko (*Gekko gecko*) is listed as 'least concern' in the International Union for Conservation of Nature *Red List* (IUCN, https://www.iucnredlist.org/species/195309/2378260) and also listed in Appendix II in the Convention on International Trade in Endangered Species of Wild Fauna and Flora (CITES; https://cites.org/eng/taxonomy/term/3919). In Indonesia, the tokay gecko is not a protected species. All animals were collected in Yogyakarta, Indonesia under a license issued by the Ministry of Environment and Forestry, the Republic of Indonesia (permit number SK.83/KSDAE/SET/KSA.2/5/2021 signed on 7 May 2021) and a recommendation letter issued by The Indonesian Institute of Sciences (Lembaga Ilmu Pengetahuan Indonesia/LIPI; Recommendation Number: B- 2158 /IV/KS.01.04/3/2021 signed on 19 March 2021). The transport of samples from Indonesia to the Netherlands was conducted under CITES permit numbers 05717/IV/SATS-LN/2021 and 09160/IV/SATS-LN/2022 issued by the Ministry of Environment and Forestry, the Republic of Indonesia.

All experimental and surgical procedures needed for samples collection were done at Faculty of Biology, Universitas Gadjah Mada, Yogyakarta, Indonesia with the approval from The Ethical Committee of the Integrated Laboratory for Research and

Testing (Laboratorium Penelitian dan Pengujian Terpadu/LPPT) Universitas Gadjah Mada (Ethical Clearance number: 00014/04/LPPT/IV/2021 signed on 30 April 2021).

Experimentation and sample collection

Twenty-one adult tokay geckos were anaesthetized with intramuscular ketamine injection (50–75 mg/Kg body weight) administered in the thigh prior to the autotomy procedure. Autotomy was performed by gently restraining the gecko manually, while leaving the tail accessible. Using the thumb and index finger, a firm pinch was applied to the required autotomous region (every segment after the 5th caudal vertebra) of the tail causing the gecko to spontaneously shed its tail. The wound was painted with Betadine® iodine antiseptic solution but no dressing was applied. After the autotomy procedure was performed, the geckos were allowed to regenerate a new tail. The geckos were distributed into experimental groups based on the number of days post-autotomy, each consisting of three geckos. After ketamine-anesthesia, the tails of geckos in each group were re-autotomized 2 cm cranially from the previous autotomy site at 4, 8, 16, 20, 24, 28, and 49 days post-autotomy (dpa). The regenerated tail samples were washed and further handled in phosphate-buffered saline (PBS, 4 °C) and subsequently fixed with cold 4% paraformaldehyde (pFA) in PBS.

Histology

The regenerating tail blastema samples were rinsed in RNAse-free PBS and fixed in cold 4% pFA in PBS. The fixed samples were then decalcified by soaking them in Osteosoft® (Sigma-Aldrich) for 3–5 days. The decalcified samples were then dehydrated with a graded concentration series of ethanols (70%, 80%, 90%, 100%) for 2 × 30 min each. The samples were cleared 3 x 1 h (Neo-Clear®, Merck-Millipore). They were infiltrated 2 × 1 h molten paraffin (62 °C) and 1 × 8–18 h. The samples we finally embedded with fresh molten paraffin and solidified at room temperature. Longitudinal sections (6-8 µm thickness) were cut using a microtome. Prior to staining, the sections were deparaffinized with xylene (3 × 5 min) followed by rehydration through graded ethanols (90%, 80%, 70% for 1 min each) and demi-water (2 × 1 min).

For hematoxylin, eosin and alcian blue (HE-AB) staining, the sections were stained in 1% alcian blue 8GX in 2.5% acetic acid for 10–15 min, then washed under running tap water (5 min). Alcian blue gives a blue stain to the acidic polysaccharides and glycosaminoglycans in the extracellular matrix of hyaline cartilage. Next, the sections were stained with Mayer's hematoxylin and eosin according to standard protocols (Bancroft, 2008).

Periodic acid Schiff and alcian blue (PAS-AB) staining was started by staining the sections with alcian blue (10–15 min), 1% alcian blue (8GX) in 2.5% acetic acid and washed under running tap water (5 min). The sections were then treated with 1%

periodic acid (5 min) and washed with demi-water. Next, the sections were stained with Schiff's reagent (10min) and washed in running tap water (5 min). To stain the nuclei, the sections were subsequently stained with hematoxylin (1 min) and washed in running tap water (5 min).

After the staining steps, the sections were washed in demi-water (1 min) and dehydrated with graded ethanols (70%, 80%, 90% for 1 min each and 100% 3 × 1min) followed by xylene (3 × 5 min). Finally, the sections were coverslipped using Eukitt® (Sigma-Aldrich; St. Louis, USA) and left overnight at 37 °C.

Results

Macroscopic appearance

Tail regeneration in the tokay gecko began with the formation of a scab, which appeared 4–8 days post-autotomy (dpa) regenerating tail (Figure 2-1B–C). This scab started to disappear at 12 dpa (Figure 2-1D), and by 16 dpa, it had completely disappeared, and the blastema became dome-shaped (Figure 2-1E). Subsequently, this dome-shaped structure elongated and cone-like (Figure 2-1F–H). The scalation (pattern of scales) of the regenerating tail first began to become visible at 28 dpa, at which stage the scales had a uniform brownish-gray pigment (Figure 2-1H). At 58 dpa, the multiple dark patches of pigment were visible (Figure 2-1K)and by 12 weeks post-autotomy (wpa) the pigmentation pattern of the regenerated tail was quite similar to the original tail (Figure 2-1L). However, despite the similarities in color and scale patterns, the regenerated tail could still be distinguished from the original tail by the absence of the 'segments' that mark the skin of the original tail (Figure 2-1L). These segments presumably represent the site of the fracture planes because autotomy always happens in this location (Luthfi Nurhidayat, unpublished observations).

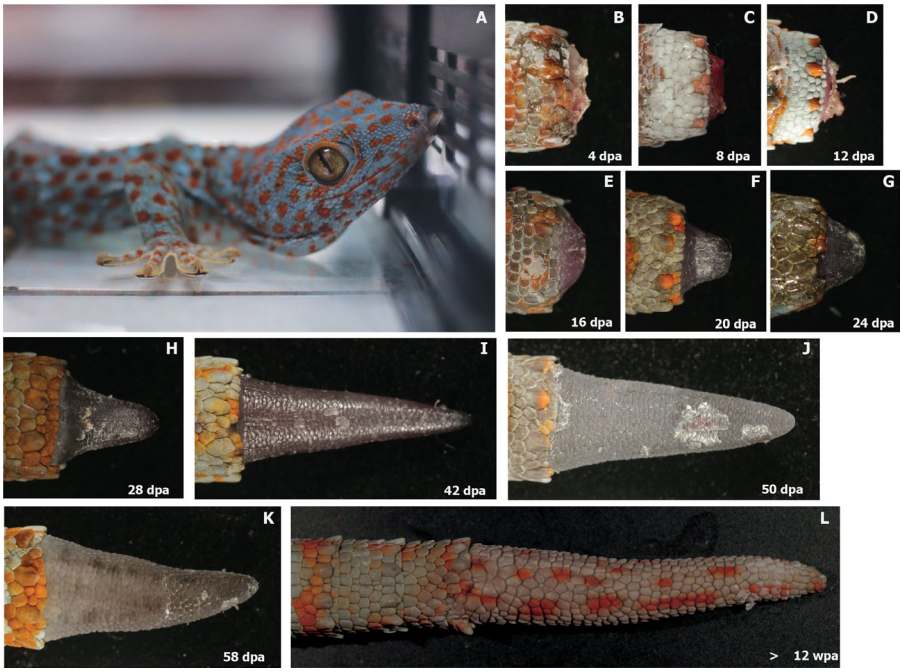

Figure 2-1. **Macroscopic appearance of tail regeneration in the tokay gecko (*Gekko gecko*)**. (A) tokay gecko morphology. (B, C) Regenerating tail undergo wound healing phase marked by scab formation. (D) The scab started to exfoliate. (E – H) The regenerating tail appears in dome-shaped and grows elongated as the progression of the regeneration stages. (I , J) the regenerating tail shows clear scales pattern. (K) Pigmentation patterns start to visible in the regenerating tail. (L) The pigmentation pattern of the regenerating tail is similar with that of the original tail but can still be distinguishable. Note that the original tail looks morphologically segmented.

Wound healing phase

Histology confirms that the wound healing phase involves the formation of a scab covering the wound or autotomy site (Figure 2-2 – Figure 2-5). At 4 dpa, a thinner layer of epithelial cells begins to form under the scab, covering the tissues in the tail stump (Figure 2-2 A). This wound epithelium shows a reduction in its number layers, from multiple layers near the tail stump epidermis (Figure 2-2B) to 1–2 layers of cells in the middle area of the wound site (Figure 2-2D). Notably, populations of blood cells, including both erythrocytes and leukocytes, were observed, particularly in the central region of the wound site (Figure 2-2C). At this stage, thin connective tissue started to form under the wound epithelium. This connective tissue has a matrix with acidic and neutral mucin (Figure 2-3).

At 8 dpa, the scab was still present (Figure 2-4A). The wound epithelium comprised multiple layers of epithelial cells but remained thinner than the normal

epidermis of the tail stump (Figure 2-4B, D). Notably, there was tissue starting to form between the epidermis and the tail stump tissues (Figure 2-4D). This tissue which we envisage as a 'pre-blastema', displayed a heterogeneous composition, consisting of connective tissue, blood vessels, and various cell populations that cannot be characterized using histology. The connective tissue in this area also has a matrix with acidic and neutral mucin scattered through the area (Figure 2-5). Moreover, red blood cells (erythrocytes) and white blood cells (leukocytes) were still noticeable in multiple regions, particularly within the central area of the wound site (Figure 2-4C). We also found that this central area has not been covered by wound epithelium and is still connected to the scab (Figure 2-4C). We did not find any histological evidence of a structure (such as condensed, undifferentiated mesenchyme) resembling an apical growth zone.

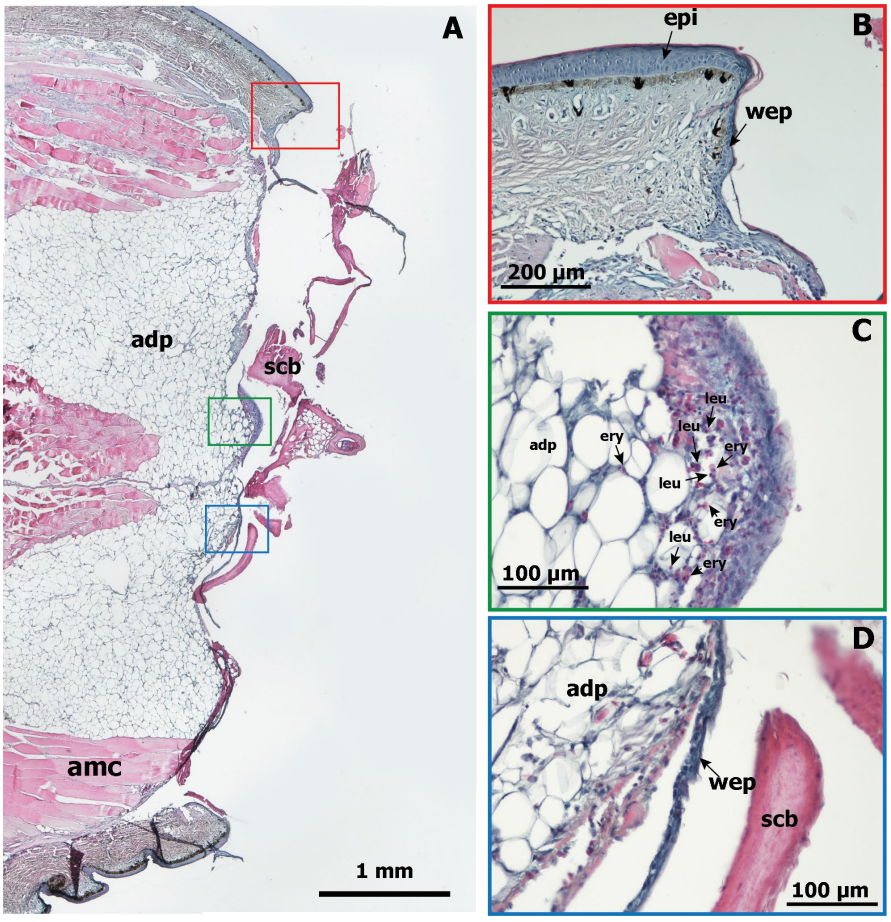

Figure 2-2. **Scab and wound epithelium formations in the wound site of the 4 dpa regenerating tail of the tokay gecko**. (A) Sagittal section of 4 dpa regenerating tail of the tokay gecko showed the scab covering the wound site. (B) Epithelium transition from epidermis to wound epithelium. (C) Blood cell populations (erythrocytes and leukocytes) in the central area of the wound sites. (D) Thin layer of wound epithelial is formed under the scab. Hematoxylin-Eosin Alcian Blue Staining. *Key:* adp, adipose tissue; amc, adult muscle cells; ery, erythrocytes; epi, epidermis; leu, leukocytes; scb, scabs; wep, wound epithelium.

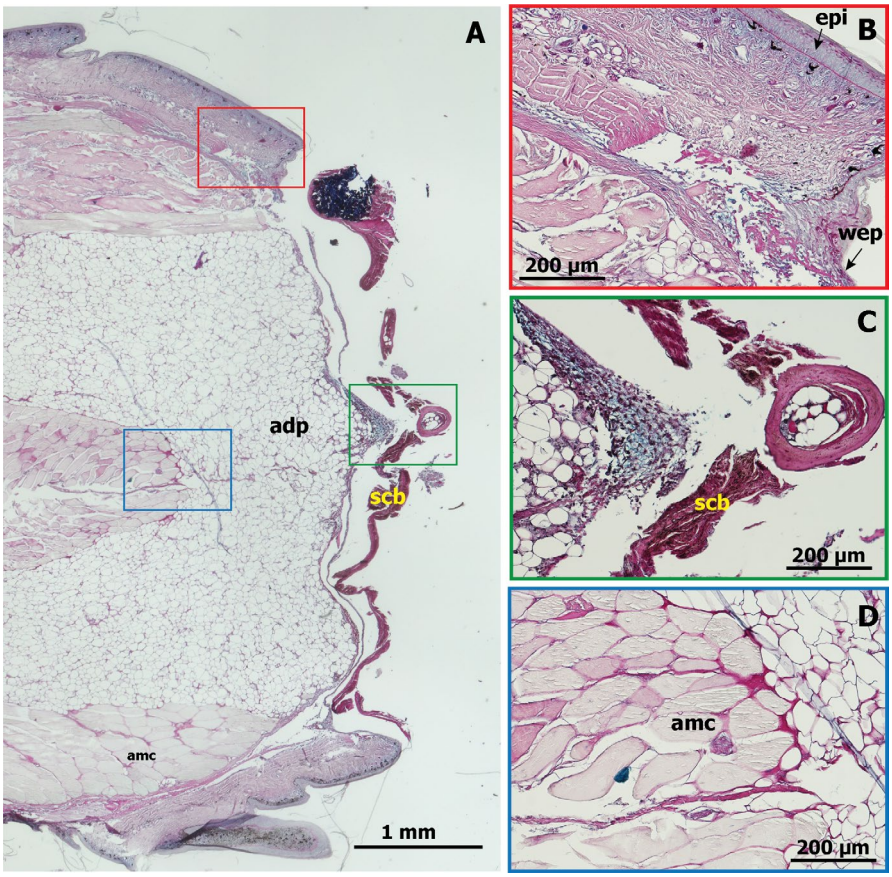

Figure 2-3. **Distribution of neutral mucin (red) and acidic mucin (blue) in the 4 dpa regenerating tail of the tokay gecko**. (A) The original tail tissue generally contains neutral mucin. (B) the subepidermal tissue of original tail is dominated by neutral mucin while the tissue under wound epithelium contains both neutral and acidic mucin. (C) The neutral mucin and acidic mucin are both visible in the central area of the wound site. (D) The adult muscle tissue in the original tail, especially muscle fascia, dominated by neutral mucin. Periodic acid-Schiff alcian blue staining. *Key:* adp, adipose tissue; amc, adult muscle cells; epi, epidermis; scb, scabs; wep, wound epithelium.

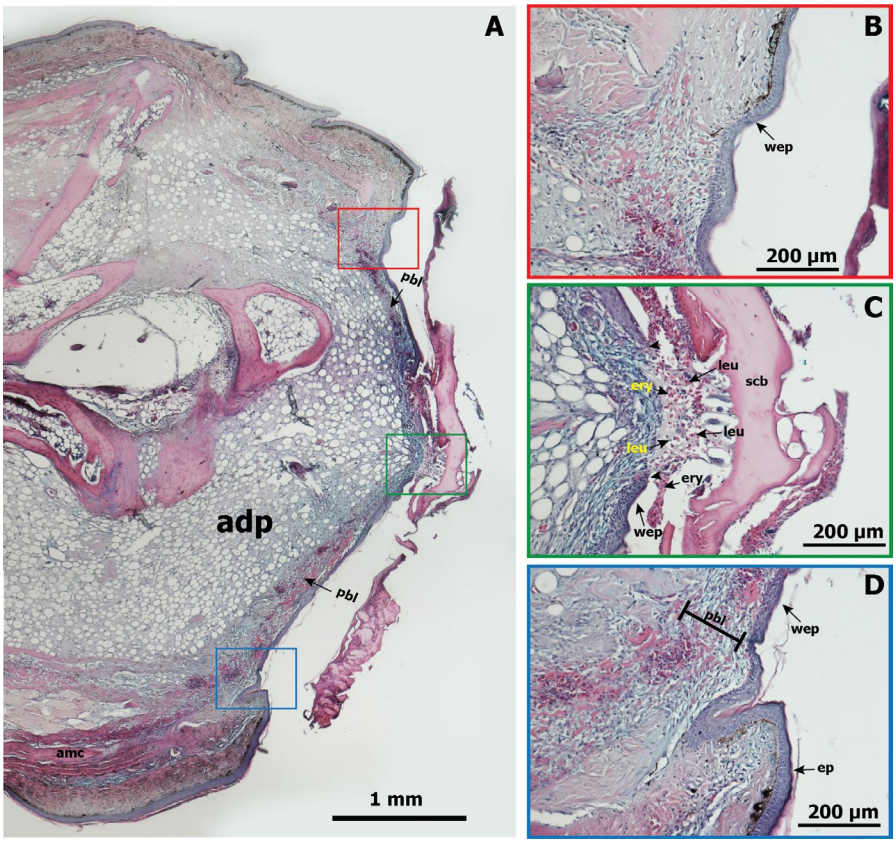

Figure 2-4. **Pre-blastema tissue start to infiltrate equally in the area between the wound epithelium and the tail stump tissues at 8 dpa regenerating tail of the tokay gecko.** (A) The pre-blastema tissue infiltrate from the periphery to the central area of the wound site. (B) The wound epithelium is now multilayered. (C) Blood cell populations (erythrocytes and leukocytes) are still prominent in the central area of the wound sites. Note that this central area has not been covered by wound epithelium. (D) The pre-blastema tissue looks heterogenous. Hematoxylin eosin alcian blue staining. *Key:* adp, adipose tissue; amc, adult muscle cells; ery, erythrocytes; epi, epidermis; leu, leukocytes; pbl, pre-blastema; scb, scabs; wep, wound epithelium.

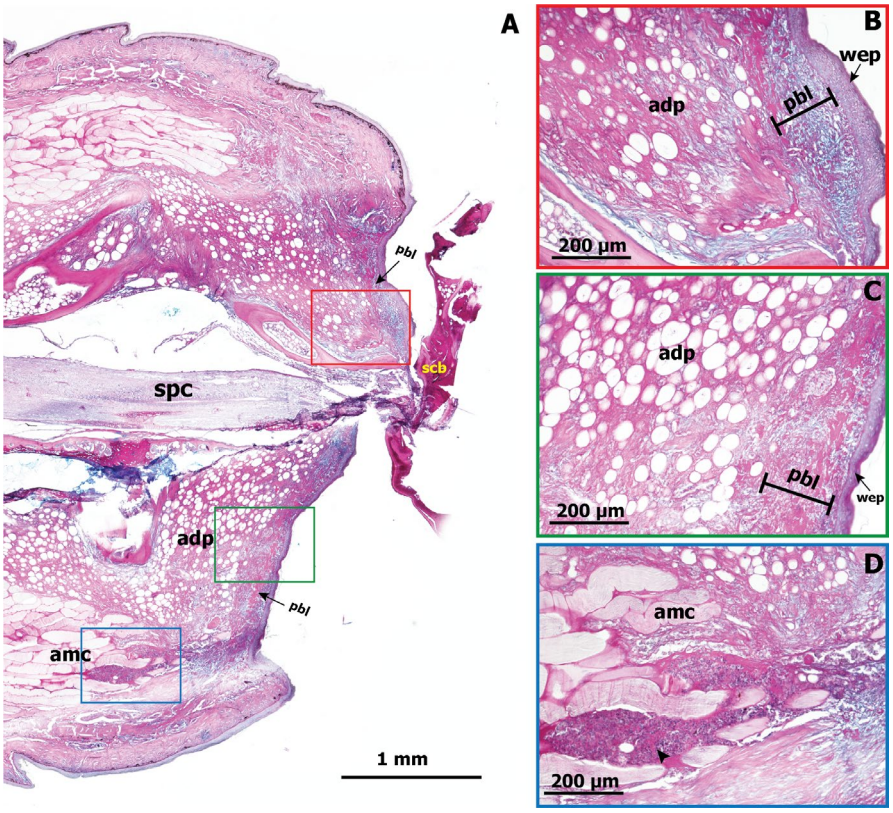

Figure 2-5. **Distribution of neutral mucin (red) and acidic mucin (blue) in the 8 dpa regenerating tail of the tokay gecko**. (A) The pre-blastema tissue matrix shows acidic and neutral mucin. (B,C) The scattered distribution of acidic and neutral mucin in the dorsal (B) and ventral (C) parts of pre-blastema tissue. (D) the adult muscle tissue is dominated by neutral mucin. Periodic acid-Schiff alcian blue staining. *Key:* adp, adipose tissue; amc, adult muscle cells; pbl, pre-blastema; scb, scabs; spc, spinal cord; wep, wound epithelium.

Blastema formation phase

The blastema formation phase can be distinguished at **16 dpa**. At this time, the regenerating tail consists of cells and tissues in the early stages of differentiation (Figure 2-6A) as well as connective tissue. The early differentiating cells included dorsal and ventral clusters aggregates of myoblast-like cells (Figure 2-6B). We still could not evidence of any mesenchymal cells organized into a growth zone in the distal part of blastema. Instead, this distal region consisted mainly of connective tissues containing many blood vessels (Figure 2-6C). The wound epithelium at this stage already showed a mature epidermal structure similar to the epidermis of the tail stump but was weakly keratinized and unpigmented (Figure 2-6D). In addition, nerve fibers can be seen at this stage, possibly originating from the dorsal root ganglia in the uninjured tail.

We found that blastema tissue had atypical distribution of acidic mucin and neutral mucin (Figure 2-7A). Acidic mucin dominated the dorsal and ventral areas of the regenerating tail (Figure 2-7B, D), while neutral mucin was concentrated in the central area (Figure 2-7C). Moreover, we also found that the connective tissue of the uninjured tail muscle extends into the regenerating tail showing the similar characteristics with neutral mucinous connective tissue (Figure 2-6A, Figure 2-7A, D).

At **20 dpa** the regenerating tail showed a similar structure to that of 16 dpa (Figure 2-8). The main differences that can be observed at 20 dpa are that the myoblast population is more clearly visible and cartilage condensation begins to occur in the central area of the tail (Figure 2-8A & D). Moreover, pre-cartilage condensations are visible in the proximal part of the tail (Figure 2-8B). The blood vessels also appear to be more concentrated in the distal part of the regenerating tail at this stage (Figure 2-8C).

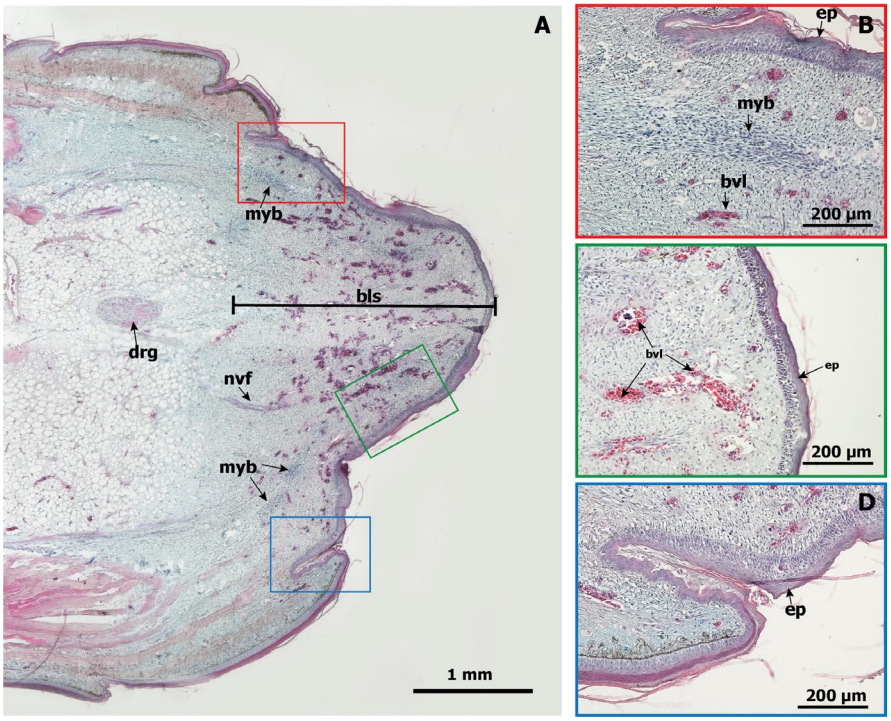

Figure 2-6. **The blastema consist of heterogenous tissue structure at 16 dpa regenerating tail of the tokay gecko**. (A) the heterogenous tissues structure within the blastema, including myoblast, nerve fibers, and blood vessels. (B) the myoblasts aggregate in the dorsal area. (C) The distal region of blastema consisted mainly of connective tissues and blood vessels. (D) The wound epithelium has transformed into more mature epidermal structure, but without pigmentation. Hematoxylin eosin alcian blue staining. *Key*: bls, blastema; bvl, blood vessel; drg, dorsal root ganglia; ep, epidermis; myb, myoblast; nvf, nerve fiber.

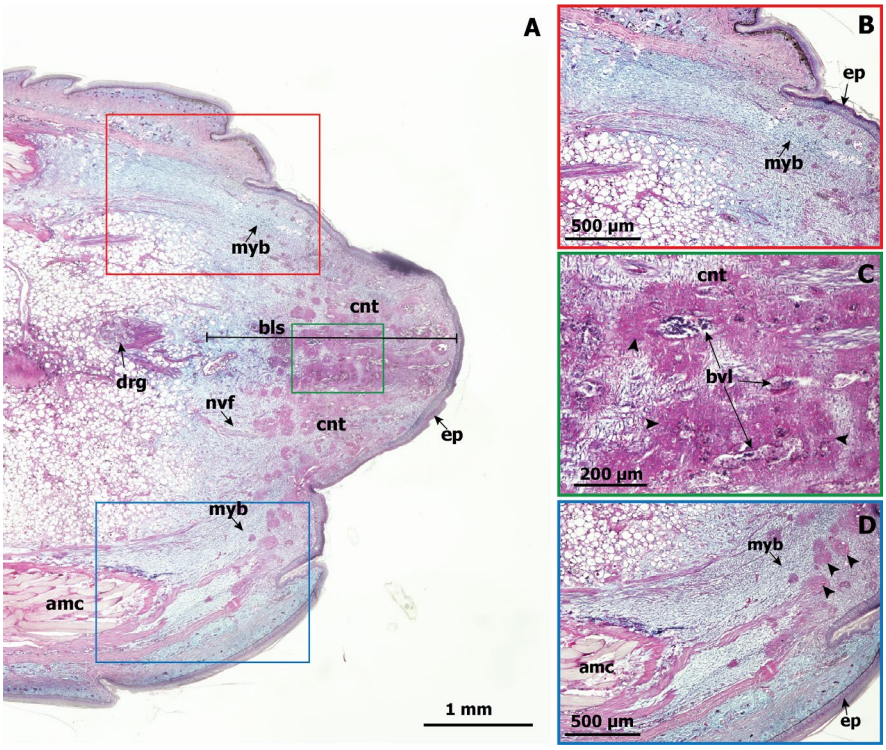

Figure 2-7. **Atypical distribution of neutral mucin (red) and acidic mucin (blue) in the regeneration blastema of the tokay gecko at 16 dpa.** (A) An overview of the mucin distribution in the regeneration blastema. (B,D) Acidic mucin dominates the dorsal (B) and ventral (D) areas of the regeneration blastema. (C) Neutral mucin is concentrated in the central area of the regeneration blastema. Periodic acid-Schiff alcian blue staining. *Key:* amc, adult muscle cells; bls, blastema; bvl, blood vessel; cnt, connective tissue; drg, dorsal root ganglia; ep, epidermis; myb, myoblast; nvf, nerve fiber.

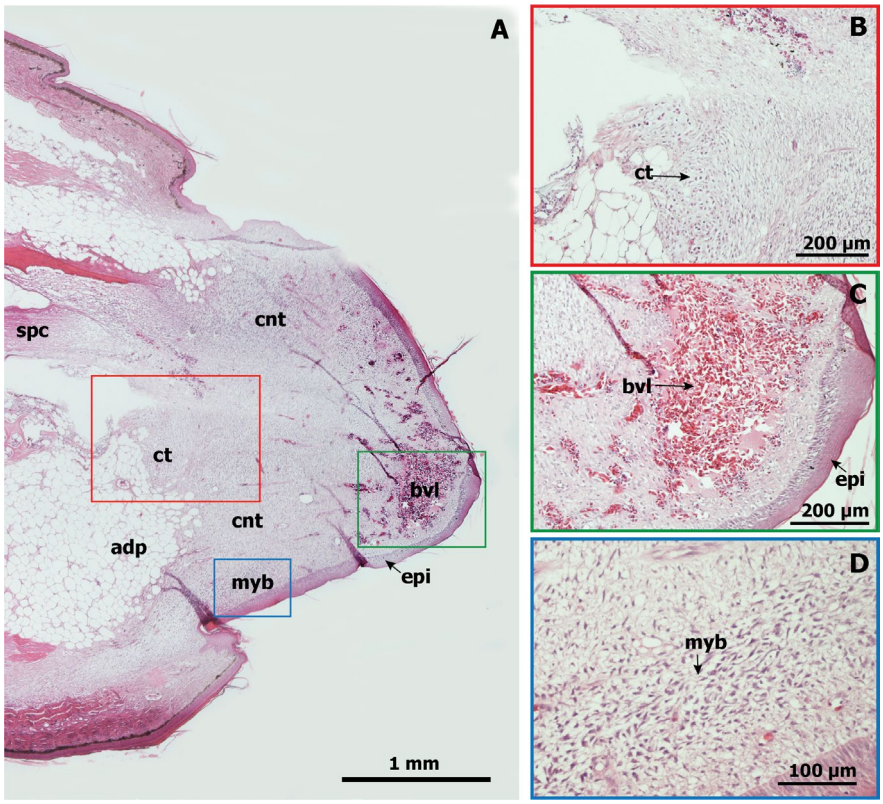

Figure 2-8. **The regeneration blastema of the tokay gecko at 20 dpa is quite similar with that of 16 dpa.** (A) the heterogenous tissues structure within the blastema, including myoblast, nerve fibers, and blood vessels. (B) pre-cartilage condensations are visible in the proximal part of the tail. (C) The blood vessels are more concentrated in the distal region of the blastema. (D) the myoblasts aggregate in the ventral area. Hematoxylin Eosin Staining. *Key:* adp, adipose tissue; amc, adult muscle cells; bls, blastema; bvl, blood vessel; cnt, connective tissue; ct, cartilage tube; ep, epidermis; myb, myoblast; nvf, nerve fiber; spc, spinal cord.

Tissue differentiation phase

The tissue differentiation phase becomes apparent at **24 dpa** in the regenerating tail (Figure 2-9). At this stage, the cartilage tube is distinctly visible from the proximal to distal parts of the regenerating tail (Figure 2-9A). Notably, the proximal segment of the cartilage tube is attached to the vertebra in the uninjured tail (Figure 2-9B), exhibits a more mature chondrification compared to the distal part. Concurrently, the regenerating muscle displays well-defined myotubes and myosepta, indicating muscle segmentation (Figure 2-9C). Although the former wound epidermis has developed into an epidermis that is thickened basally, has increased pigmentation, but no distinguishable dermis layer yet (Figure 2-9C). Additionally, blood vessels remain prominently scattered throughout the regenerating tail, with larger vessels observable

in the ventral region, likely originating from the ventral aorta of the tail stump (Figure 2-9).

We found more evenly distributed mucin in the connective tissue of the regenerating tail at this stage, predominantly comprising neutral mucin (Figure 2-10). However, the cartilage tube is characterized by acid mucin, distinguishing it from neighboring connective tissue (Figure 2-10B&D). Furthermore, muscle tissue also exhibits acid mucin (Figure 2-10C).

By **28 dpa**, signs of ongoing tissue differentiation persist (Figure 2-11). Myotubes were lengthened, and myosepta shortened, compared to the 24 dpa regenerating tail (Figure 2-11B). Epidermal pigmentation intensifies further (Figure 2-11D). Overall, the structural composition of the 28 dpa regenerating tail is similar with that observed at 24 dpa (Figure 2-12).

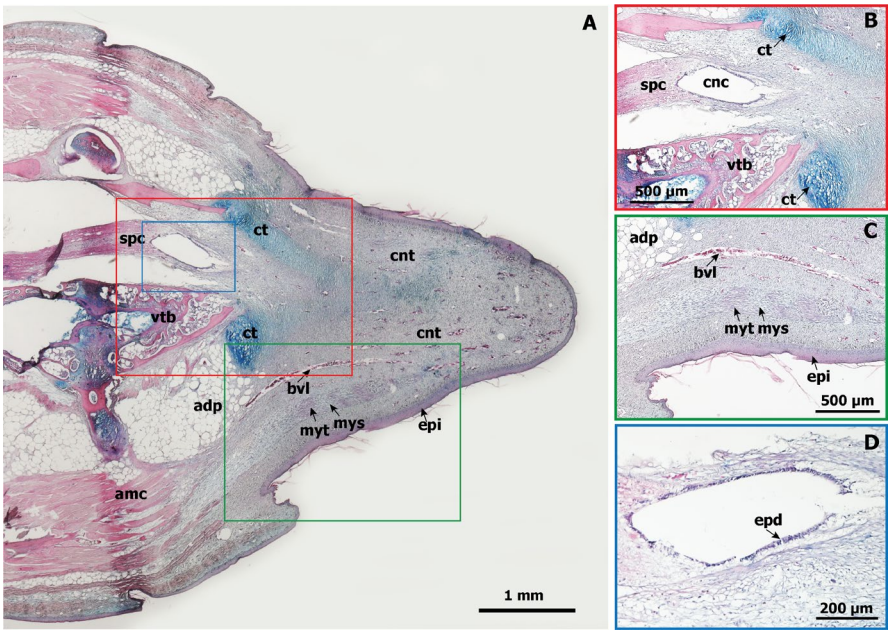

Figure 2-9. **The tissue differentiation become evidence at 24 dpa regenerating tail of the tokay gecko.** (A) the cartilage tube and muscles structure is distinctly visible in the regenerating tail. (B) The attachment of the proximal part of cartilage tube with the vertebra of uninjured tail. (C) Skeletal muscle segmentation can be clearly observed in the regenerating tail. (D) The central canal of spinal cord consisted of ependymal cell layer. Hematoxylin Eosin Alcian Blue Staining. *Key:* adp, adipose tissue; amc, adult muscle cells; bvl, blood vessel; ct, cartilage tube; cnc, canalis centralis; cnt, connective tissue; ep, epidermis; epd, ependymal cells; mys, myoseptum; myt, myotubes; spc, spinal cord; vtb, vertebra.

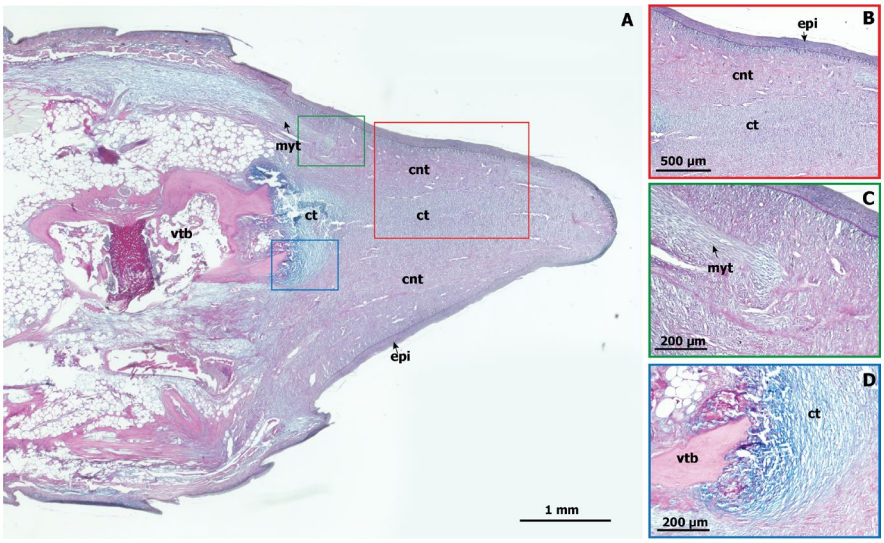

Figure 2-10. **The mucin in the connective tissue of the regenerating tail at 24 dpa is more distributed.** (A) An overview of the mucin distribution in the regenerating tail. (B, D) The cartilage tube is characterized by acid mucin (blue) and can be distinguished from the neighboring connective tissue containing neutral mucin (red). (C) muscle tissue demonstrates acid mucin. Periodic acid-Schiff alcian blue staining. *Key:* bvl, blood vessel; ct, cartilage tube; cnt, connective tissue; ep, epidermis; mys, myoseptum; myt, myotubes; spc, spinal cord; vtb, vertebra.

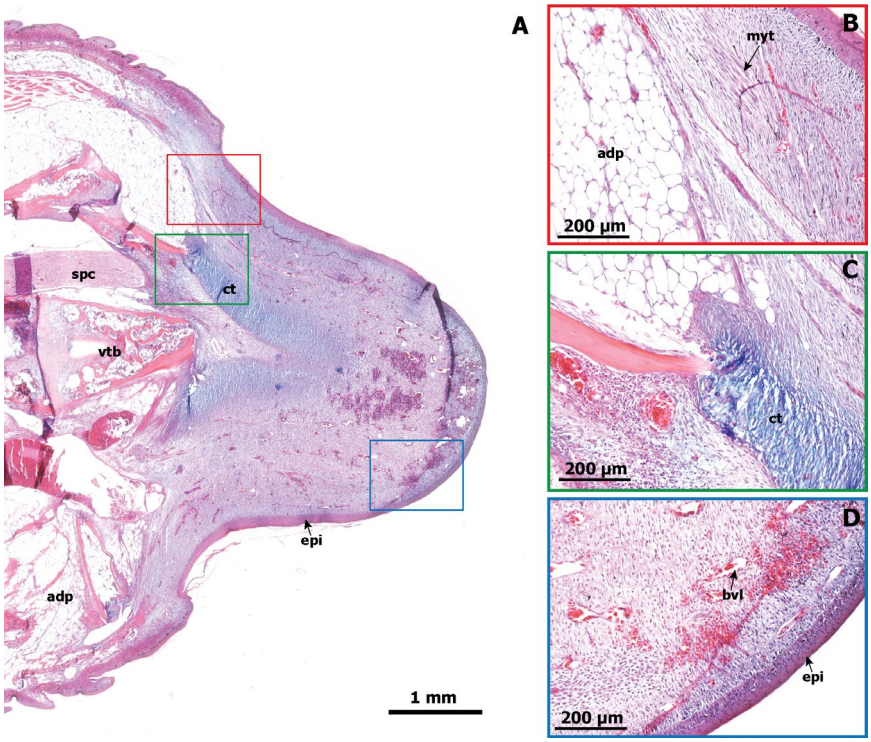

Figure 2-11. **Tissue differentiation is advancing at 28 dpa regenerating tail of the tokay gecko**. (A) The tissue structures of the regenerating tail, such as epidermis, cartilage tube, and skeletal muscle, are more advanced compared to that of 24 dpa. (B) the myotubes are lengthened. (C) The cartilage tube shows clear chondrocytes and extracellular matrix arrangement. (D) the epidermal pigmentation is more visible. Hematoxylin Eosin Alcian Blue Staining. *Key:* adp, adipose tissue; bvl, blood vessel; ct, cartilage tube; ep, epidermis; myt, myotubes; spc, spinal cord; vtb, vertebra.

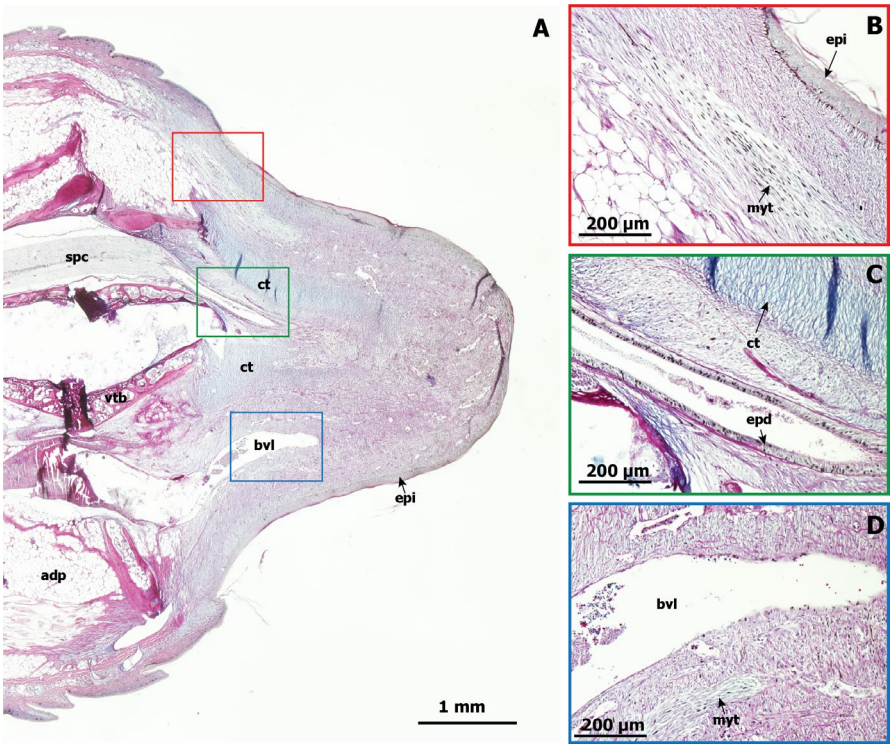

Figure 2-12. **The mucin distribution in 28 dpa regenerating tail is quite similar with that of 24 dpa regenerating tail.** (A) The regenerating tail tissue contain mostly neutral mucin (red), specifically the connective tissue, except the cartilage tube. (B) the neutral mucin start to be identified in the muscle but not as strong as the surrounding connective tissue. (C) Acidic mucin (blue) is still prominent in the cartilage tube. (D) A big blood vessel originating from the ventral aorta of the tail stump is visible in the ventral part of regenerating tail. Periodic acid-Schiff alcian blue staining. Key: adp, adipose tissue; bvl, blood vessel; ct, cartilage tube; cnt, connective tissue; ep, epidermis; epd, ependymal cells; mys, myoseptum; myt, myotubes; spc, spinal cord; vtb, vertebra.

Tail maturation phase

The tail maturation phase becomes evident at **49 dpa** in the regenerating tail and is characterized by a structure that increasingly resembles the original tail (Figure 2-13A). Skin maturation is identified by the development of scales in the epidermis and the distinct presence of the dermis layer (Figure 2-13C). In the regenerating tail muscles, longer myofiber structures and shorter myosepta indicate the maturation of muscle tissue (Figure 2-13C). Additionally, the cartilage tube exhibits a mature hyaline cartilage structure, with a clear arrangement of chondroblasts and chondrocytes (Figure 2-13D). The presence of adipose tissue between the muscles and cartilage tube further indicates the maturity of the tail at this stage (Figure 2-13C).

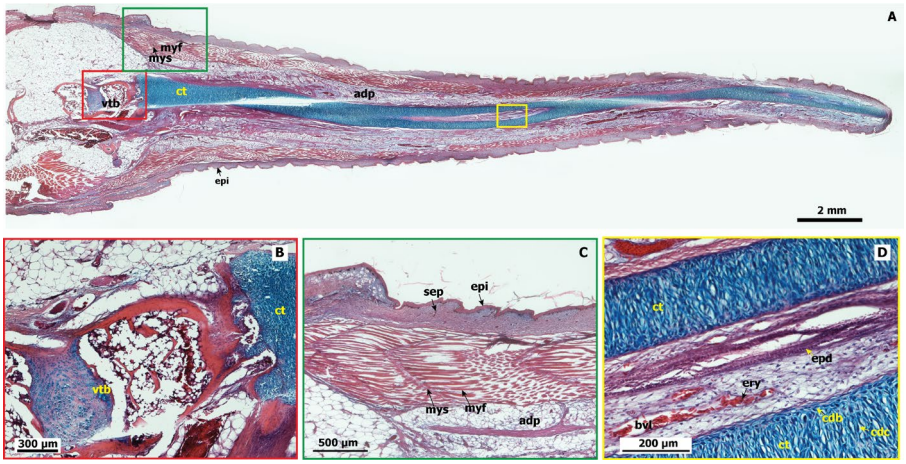

Figure 2-13. **The tissue structures of 49 dpa regenerating tail increasingly resembles the tissue structure in the original tail.** (A) an overview of the mature tissue structure of the regenerating tail indicated by the visible scale development in the skin and adipose tissue underneath the muscle tissue. (B) The attachment of the proximal part of cartilage tube with the vertebra of uninjured tail. (C) mature structure of muscle indicated by longer myofiber with shorter myosepta. The presence of sub-epidermal tissue (dermis) also indicates the maturation of the skin. (D) the clear arrangement of chondroblasts and chondrocytes in the cartilage tube implies the maturation of the hyaline cartilage structure. Hematoxylin Eosin Alcian Blue Staining. *Key:* adp, adipose tissue; bvl, blood vessel; cdb, chondroblast; cdc, chondrocytes; ct, cartilage tube; cnt, connective tissue; ep, epidermis; epd, ependymal cells; ery, erythrocytes; mys, myoseptum; myf, myofibers; sep, sub-epidermal tissue (dermis); vtb, vertebra.

Discussion

The tokay gecko is one of many lizard species showing caudal autotomy, whereby it can shed its tail to distract the attention of predators in order to escape (Rumping and Jayne, 1996). Generally, tail regeneration in this Gecko shows similarities to that in other lizards, such as the green anole, *Anolis carolinensis* (Cox, 1969), and the leopard gecko, *Eublepharis macularius* (McLean and Vickaryous, 2011).

In the tokay gecko, the wound healing phase starts with the formation of a scab at 4–8 days post-autotomy (dpa), which gradually disappears by 16 dpa. This scab serves as a temporary barrier protecting the wound site while the wound epithelium forms underneath. In axolotl and zebrafish regeneration, the formation of the scab is accompanied by the migration of epithelial cells and the recruitment of blood cells to the injury site, and these two processes facilitate tissue repair (Mescher et al., 2015). Moreover, the formation of the wound epidermis is crucial for subsequent regenerative processes, providing a protective barrier and a source of signaling molecules that promote regeneration (Mescher et al., 2015).

Tail regeneration in other lizards that show autotomy, including the green anole (Cox, 1969), the Common Wall Lizard, *Podarcis muralis* (Alibardi and Toni, 2005) and leopard gecko (McLean and Vickaryous, 2011), also shows scab formation followed by re-epithelialization. This re-epithelialization creates a conducive environment for blastema formation (Alibardi, 2010). The timeframe of the wound healing phase in the tokay gecko (4–8 d) is comparable with that in other lizards, namely: 5–7 d in the leopard gecko (McLean and Vickaryous, 2011), 7–9 d in the green anole (Cox, 1969), and 5-7 d in the Common Wall Lizard (Alibardi and Toni, 2005).

The presence of a thin layer of connective tissue under the wound epithelium, that stains for mucins, is consistent with the remodeling of the extracellular matrix during the wound healing phase. This matrix remodeling is essential for providing structural support and facilitating cell migration during tissue repair (Olczyk et al., 2014; Provenzano et al., 2005). One of the common early features of regeneration in the tokay gecko and other lizards is the inflammatory response. This can be seen from the presence of blood cells (including erythrocytes and leukocytes), both inside and outside blood vessel lumina, at the wound site. The recruitment of immune cells, especially macrophages, to the wound site plays a essential role regeneration by modulating the regenerative environment, promoting tissue repair and preventing infection (Godwin and Rosenthal, 2014; Londono et al., 2020; Mescher et al., 2015).

As we have shown in this chapter, blastema formation in the tokay gecko begins around 16 dpa, marked by a dome-shaped structure that undergoes elongation and differentiation. Blastema formation is a critical regenerative phase observed across multiple vertebrates. In the axolotl (*Ambystoma mexicanum*), for example, the blastema comprises dedifferentiated cells that proliferate and eventually differentiate into various tissues, guided by complex signaling pathways (Kragl et al., 2009).

However, the blastema in the regenerating tail of the tokay gecko is heterogeneous, even when there was only pre-blastema tissue underneath the wound epithelium at 8 dpa (This chapter). Another striking feature of the tokay gecko blastema is its rich vascularization at blastema formation stages, particularly in the distal part of the blastema. (Hutchins et al., 2014) also noted the rich vascularization of the tail regeneration blastema in the green anole lizard and contrasted this with the largely avascular regeneration blastema of the axolotl and zebrafish. In Chapter 3, we will show that this pre-blastema tissue expressed markers for connective tissue and muscle lineages. Therefore, this pre-blastema is heterogeneous, and the fact that it contains connective tissue, makes it unlike the typical progress zone of the limb or other developmental fields. Studies on the green anole and leopard gecko have also shown that the blastema contains a heterogeneous population of cells, including progenitors for cartilage, muscle, and epidermis (Londono et al., 2017; Lozito and Tuan, 2017; McLean and Vickaryous, 2011).

The distribution of acidic and neutral mucin within the blastema tissue indicates dynamic extracellular matrix (ECM) remodeling during blastema formation. In the tokay gecko, the distribution of acidic and neutral mucins within the blastema indicates the presence of a complex ECM that supports diverse cellular functions. Acidic mucins may facilitate cell proliferation and migration, while neutral mucins provide structural support and contribute to ECM stability (Godwin et al., 2014). Hyaluronic acid, a critical component of the extracellular matrix (ECM), plays a key role in tissue regeneration and wound healing, with high molecular weight HA showing anti-inflammatory properties and low molecular weight HA being proinflammatory (Litwiniuk et al., 2016). HA contributes to regeneration blastema formation in zebrafish (Ouyang et al., 2017) and lizards (Alibardi, 2018).

The tissue differentiation phase in the tokay gecko tail, marked by the formation of a cartilage tube, well-defined muscle structures, blood vessel development, and increased epidermal pigmentation, parallels similar phases in other regenerating species. The presence of well-defined myotubes and myosepta in the tokay gecko regenerating tail indicates successful muscle differentiation, essential for restoring tail functionality. Studies in green anole and leopard gecko reveal similar stages of differentiation, with cartilage and muscle tissues becoming distinct by 14–21 dpa (Cox, 1969; McLean and Vickaryous, 2011). However, the green anole and leopard gecko demonstrate a faster timeline for differentiation, likely due to differences in species-specific regenerative capacities.

The role of blood vessels in supporting tissue differentiation is highlighted by studies on zebrafish caudal fin regeneration (Bayliss et al., 2006) and axolotl tail regeneration (Ritenour and Dickie, 2017), where angiogenesis is critical for supplying nutrients and oxygen to the regenerating tissues, promoting cell survival and differentiation. The balanced distribution of mucins in the connective tissue of the regenerating tail of the tokay gecko further underscores the importance of the extracellular matrix in giving structural support and assisting cell signaling during regeneration (Godwin et al., 2014).

The maturation phase in the regenerating tokay gecko tail becomes evident at 49 dpa, it exhibits morphological similarities to the original tail, especially in the pattern of scales and skin pigment. These observations are consistent with previous studies on the green anole (Fisher et al., 2012) and leopard gecko (McLean and Vickaryous, 2011) that also regenerate producing similar scaling and pigmentation patterns as the original tail. In all three species, the boundary between the original and regenerated tail is visible because the scalation and pigment patterns are not identical with the original.

The tail maturation phase in the tokay gecko is characterized by the development of scales, mature muscle fibers, and well-defined cartilage tissue (in the cartilage tube).

The histological appearance of these tissues closely resembles those of the original tail, indicating the successful regeneration of complex tissue architectures. In both the tokay gecko and the green anole, although the maturation of the regenerated tail involves the formation of scales and pigmentation patterns similar to the original, the distinctive segmentation marks of the original tail (this Chapter and (Ritzman et al., 2012) are lacking in the regenerated tail (Lozito and Tuan, 2016; Lozito and Tuan, 2017). The presence of adipose tissue in the tokay gecko regenerated tail indicates the restoration of a fully functional and integrated tissue environment. Adipose tissue is a common structure in the tail of autotomous lizards suggesting the importance of the fat layer for autotomy (Sheppard and Bellairs, 1972).

In summary, we have shown in this chapter that the process of tail regeneration in the tokay gecko involves a series of well-defined phases that mirror those observed in other lizards, even though with species-specific variations in timing and complexity.

References

Alibardi, L. (2010). Morphological and cellular aspects of tail and limb regeneration in lizards. A model system with implications for tissue regeneration in mammals. *Advances in anatomy, embryology, and cell biology* **207**, iii, v-x, 1-109.

---- (2014). Histochemical, Biochemical and Cell Biological aspects of tail regeneration in lizard, an amniote model for studies on tissue regeneration. *Progress in Histochemistry and Cytochemistry* **48**, 143-244.

---- (2015). Original and regenerating lizard tail cartilage contain putative resident stem / progenitor cells. *Micron* **78**, 10-18.

---- (2018). Hyaluronate likely contributes to the immunesuppression of the regenerating tail blastema in lizards: Implications for organ regeneration in amniotes. *Acta Zoologica* **99**, 321-330.

---- (2019). Stimulation of regenerative blastema formation in lizards as a model to analyze limb regeneration in amniotes. *Histology and Histopathology* **34**, 1111-1120.

Alibardi, L. and Toni, M. (2005). Wound keratins in the regenerating epidermis of lizard suggest that the wound reaction is similar in the tail and limb. *Journal of Experimental Zoology Part A: Comparative Experimental Biology* **303A**, 845-860.

Bancroft, J. D. G., M. (2008). *Theory and Practice of Histological Techniques*. London: Churchill Livingstone.

Bayliss, P. E., Bellavance, K. L., Whitehead, G. G., Abrams, J. M., Aegerter, S., Robbins, H. S., Cowan, D. B., Keating, M. T., O'Reilly, T., Wood, J. M., et al. (2006). Chemical modulation of receptor signaling inhibits regenerative angiogenesis in adult zebrafish. *Nat Chem Biol* **2**, 265-273.

Bellairs, A. D. and Bryant, S. V. (1985). Autotomy and Regeneration in Reptiles. (ed. C. G. A. F. Billet), pp. 303-410. New York: John Wiley & Sons, Inc.

Clause, A. R. and Capaldi, E. A. (2006). Caudal Autotomy and Regeneration in Lizards. *Journal of experimental zoology* **305A**, 965-973.

Cox, P. G. (1969). Some aspects of tail regeneration in the lizard, Anolis carolinensis. I. A description based on histology and autoradiography. *Journal of Experimental Zoology* **171**, 127-149.

Delorme, S. L., Lungu, I. M. and Vickaryous, M. K. (2012). Scar-Free Wound Healing and Regeneration Following Tail Loss in the Leopard Gecko, Eublepharis macularius. *Anatomical Record* **295**, 1575-1595.

Fisher, R. E., Geiger, L. A., Stroik, L. K., Hutchins, E. D., George, R. M., Denardo, D. F., Kusumi, K., Rawls, J. A. and Wilson-Rawls, J. (2012). A histological comparison of the original and regenerated tail in the green anole, Anolis carolinensis. *Anatomical record (Hoboken, N.J. : 2007)* **295**, 1609-1619.

Fleming, P. A. and Bateman, P. W. (2012). Autotomy, Tail Regeneration and Jumping ability in Cape Dwarf Geckos (Lygodactylus capensis) (Gekkonidae). *African Zoology* **47**, 55-59.

Gilbert, E. A. B., Payne, S. L. and Vickaryous, M. K. (2013). The anatomy and histology of caudal autotomy and regeneration in lizards. *Physiological and Biochemical Zoology* **86**, 631-644.

Gilbert, E. A. B. and Vickaryous, M. K. (2018). Neural stem/progenitor cells are activated during tail regeneration in the leopard gecko (Eublepharis macularius). *Journal of Comparative Neurology* **526**, 285-309.

Godwin, J., Kuraitis, D. and Rosenthal, N. (2014). Extracellular matrix considerations for scar-free repair and regeneration: Insights from regenerative diversity among vertebrates. *The International Journal of Biochemistry & Cell Biology* **56**, 47-55.

Godwin, J. W. and Rosenthal, N. (2014). Scar-free wound healing and regeneration in amphibians: Immunological influences on regenerative success. *Differentiation* **87**, 66-75.

Hutchins, E. D., Markov, G. J., Eckalbar, W. L., George, R. M., King, J. M., Tokuyama, M. A., Geiger, L. A., Emmert, N., Ammar, M. J., Allen, A. N., et al. (2014). Transcriptomic Analysis of Tail Regeneration in the Lizard Anolis carolinensis Reveals Activation of Conserved Vertebrate Developmental and Repair Mechanisms. *PLOS ONE* **9**, e105004.

Jacyniak, K., McDonald, R. P. and Vickaryous, M. K. (2017). Tail regeneration and other phenomena of wound healing and tissue restoration in lizards. *The Journal of Experimental Biology* **220**, 2858-2869.

Kragl, M., Knapp, D., Nacu, E., Khattak, S., Maden, M., Epperlein, H. H. and Tanaka, E. M. (2009). Cells keep a memory of their tissue origin during axolotl limb regeneration. *Nature* **460**, 60-65.

Litwiniuk, M., Krejner, A., Speyrer, M. S., Gauto, A. R. and Grzela, T. (2016). Hyaluronic Acid in Inflammation and Tissue Regeneration. *Wounds : a compendium of clinical research and practice* **28 3**, 78-88.

Londono, R., Tighe, S., Milnes, B., DeMoya, C., Quijano, L. M., Hudnall, M. L., Nguyen, J., Tran, E., Badylak, S. and Lozito, T. P. (2020). Single cell sequencing analysis of lizard phagocytic cell populations and their role in tail regeneration. *Journal of Immunology and Regenerative Medicine* **8**, 100029-100029.

Londono, R., Wenzhong, W., Wang, B., Tuan, R. S. and Lozito, T. P. (2017). Cartilage and Muscle Cell Fate and Origins during Lizard Tail Regeneration. *Frontiers in Bioengineering and Biotechnology* **5**, 1-9.

Lozito, T. P. and Tuan, R. S. (2015). Lizard tail regeneration: Regulation of two distinct cartilage regions by Indian hedgehog. *Developmental Biology* **399**, 249-262.

---- (2016). Lizard tail skeletal regeneration combines aspects of fracture healing and blastema-based regeneration. *Development* **143**, 2946-2957.

---- (2017). Lizard tail regeneration as an instructive model of enhanced healing capabilities in an adult amniote. *Connective Tissue Research* **58**, 145-154.

McLean, K. E. and Vickaryous, M. K. (2011). A novel amniote model of epimorphic regeneration: the leopard gecko, Eublepharis macularius. *BMC Developmental Biology* **11**, 50-50.

Mescher, A. L., Neff, A. W. and King, M. W. (2015). Inflammation and immunity in organ regeneration. *Developmental and Comparative Immunology*.

Olczyk, P., Mencner, Ł. and Komosinska-Vassev, K. (2014). The Role of the Extracellular Matrix Components in Cutaneous Wound Healing. *BioMed Research International* **2014**, 747584.

Ouyang, X., Panetta, N. J., Talbott, M. D., Payumo, A. Y., Halluin, C., Longaker, M. T. and Chen, J. K. (2017). Hyaluronic acid synthesis is required for zebrafish tail fin regeneration. *PLoS One* **12**, e0171898.

Pratt, C. W. (1946). The plane of fracture of the caudal vertebrae of certain lacertilians. *Journal of anatomy* **80**, 184-188.

Provenzano, P. P., Alejandro-Osorio, A. L., Valhmu, W. B., Jensen, K. T. and Vanderby, R. (2005). Intrinsic fibroblast-mediated remodeling of damaged collagenous matrices in vivo. *Matrix Biology* **23**, 543-555.

Ritenour, A. M. and Dickie, R. (2017). Inhibition of Vascular Endothelial Growth Factor Receptor Decreases Regenerative Angiogenesis in Axolotls. *Anat Rec (Hoboken)* **300**, 2273-2280.

Ritzman, T. B., Stroik, L. K., Julik, E., Hutchins, E. D., Lasku, E., Denardo, D. F., Wilson-Rawls, J., Rawls, J. A., Kusumi, K. and Fisher, R. E. (2012). The gross anatomy of the original and regenerated tail in the green anole (Anolis carolinensis). *Anat Rec (Hoboken)* **295**, 1596-1608.

Rumping, J. M. and Jayne, B. C. (1996). Muscle activity in autotomized tails of a lizard (Gekko gecko): a naturally occurring spinal preparation. *Journal of comparative physiology. A, Sensory, neural, and behavioral physiology* **179**, 525-538.

Sheppard, L. and Bellairs, A. A. (1972). The mechanism of autotomy in Lacerta. *British Journal of Herpetology* **4**, 276-286.

Simpson, S. B. (1970). Studies on regeneration of the lizard's tail. *Integrative and Comparative Biology* **10**, 157-165.

Chapter 3. Transcriptomic Study of Tail Regeneration in The Tokay Gecko

Luthfi Nurhidayat[1,2], Vladimir Benes[3], Herman P. Spaink[1], Michael K. Richardson[1]

1. Institute of Biology Leiden, Leiden University, Sylvius Laboratory, Sylviusweg 72, 2333 BE, Leiden, The Netherlands.
2. Faculty of Biology, Universitas Gadjah Mada, Jalan Teknika Selatan Sekip Utara, 55281, Yogyakarta, Indonesia
3. Genomics Core Facility, European Molecular Biology Laboratory Heidelberg, Meyerhofstraße 1, 69117 Heidelberg, Germany

---

This chapter is part of: Nurhidayat, L., Benes, V., Blom, S., Gomes, I., Firdausi, N., de Bakker, M.A.G., Spaink, H.P., Richardson. M.K. Tokay gecko tail regeneration involves temporally collinear expression of HOXC genes and early expression of satellite cell markers. *BMC Biology*. Under revision. (2024).

Abstract

Regeneration is the replacement of missing or lost tissue with a functional copy. It is an important survival strategy used by animals to deal with injuries. Some lizards are well-known for the phenomenon of tail autotomy — the spontaneous shedding of part of the tail when the animal is attacked by a predator — followed by regeneration of the missing piece of the tail. Transcriptomic comparisons of multiple stages of tail regeneration stages are needed to give more a comprehensive picture of tail regeneration in this species. In addition, comparing tail regeneration in an adult lizard with the process of normal tail development is also important to determine whether adult regeneration involves the same mechanisms as embryonic tail development. We have performed mRNA sequencing (bulk transcriptomics) at 0, 4, 8, 16, 20, 28 days post autotomy (dpa) in the tokay gecko (a lizard) and compared the results with one stage of tail development in the embryonic tailbud of the same species. We found a distinctive molecular signature at each stage of tail regeneration. The early-regeneration (0–8 dpa) transcriptome was dominated by immune-related genes and genes associated with wound epithelium formation and bone remodeling. The blastema formation phase involves mass up-regulation of genes associated with developmental pathways. Finally, the 28 dpa transcriptome is characterized by maturation and functional development of skeletal muscle. The transcriptome profile of the regenerating adult tail is quite different from that of the embryonic tailbud.

Introduction

Regeneration is the replacement of missing or lost tissue with a functional copy. It is important as a one of the survival strategies used by animals to deal with injuries (Bely and Nyberg, 2010; Gurtner et al., 2008). Regeneration is seen at various levels of biological organization, ranging from the cell (as in muscle cell and hepatocytes) to the whole body (as in Hydra and Planaria), and can take place at different stages of the animal's development (Bely and Nyberg, 2010). In all species, regeneration always involves a particular programmed cell-proliferation and differentiation after the injury (Ricci and Srivastava, 2018; Tanaka and Reddien, 2011).

Regeneration typically requires a significant population of stem cells (Ricci and Srivastava, 2018; Tanaka and Reddien, 2011). Species differences in the availability of stem cells might partly explain the diverse range of regenerative capacity in different species. Regenerative capacity in different species is also influenced by factors such as the characteristics of stem cells, potentials for dedifferentiation and transdifferentiation, the expression of genes associated with regeneration, the presence of epigenetic regulators, and immune system responses (Zhao et al., 2016).

Comparing regeneration in different species is not only interesting to fundamental biology, but it may also one day have translation applications in regenerative medicine and tissue engineering (Daponte et al., 2021; Stocum, 2006; Zhao et al., 2016). Regenerative medicine involves the application of regeneration science to the treatment of disease, and aims to develop treatments for traumatic injuries, heart disease, degenerative diseases, cancers and others diseases for which treatment options are limited (Ahmed et al., 2014; Oviedo and Beane, 2009).

One group of model species commonly used in regeneration studies are the lizards (Lacertilia) a group of cold-blooded 'reptiles'. This group includes the geckos (Gekkonidae). Lizards are well-known for the phenomenon of tail autotomy whereby the tail breaks off at pre-existing fracture planes when grabbed by a predator. This presumably distracts the predator because the broken-off tail fragment remains twitching for some time (Bae et al., 2014). Autotomy ability in lizards is generally accompanied by the ability to regenerate the missing tail piece.

Tail regeneration in lizards results in the development of a new, complex structure (the replacement tail) from a group of proliferating cells on the tail stump called the blastema. It is blastema formation and differentiation, among other things, that make the lizard a useful model for studying tissue regeneration (Bely and Nyberg, 2010; Hill et al., 2012; Lozito and Tuan, 2015; Russell et al., 2015).

Transcriptomic studies have been done on tail regeneration in lizards including the Common Wall Lizard, *Podarcis muralis* (Vitulo et al., 2017), the green anole, *Anolis*

carolinensis (Hutchins et al., 2014), and the Common House Gecko *Hemidactylus frenatus* (Nagumantri et al., 2021) (nomenclature from Pubmed Taxonomy, www.ncbi.nlm.nih.gov/taxonomy/). However, there is still a need for transcriptomic comparisons of more extensive series of tail regeneration stages (this Chapter). In addition, we have compared tail regeneration in an adult lizard with the process of normal tail development.

Materials and methods

Ethics statement

The tokay gecko (*Gekko gecko*) is listed as 'least concern' in the International Union for Conservation of Nature *Red List* (IUCN, https://www.iucnredlist.org/species/195309/2378260) and also listed in Appendix II in the Convention on International Trade in Endangered Species of Wild Fauna and Flora (CITES; https://cites.org/eng/taxonomy/term/3919). In Indonesia, the tokay gecko is not a protected species. All animals were collected in Yogyakarta, Indonesia under a license issued by the Ministry of Environment and Forestry, the Republic of Indonesia (permit number SK.83/KSDAE/SET/KSA.2/5/2021 signed on 7 May 2021) and a recommendation letter issued by The Indonesian Institute of Sciences (Lembaga Ilmu Pengetahuan Indonesia/LIPI; Recommendation Number: B- 2158 /IV/KS.01.04/3/2021 signed on 19 March 2021). The transport of samples from Indonesia to the Netherlands was conducted under CITES permit numbers 05717/IV/SATS-LN/2021 and 09160/IV/SATS-LN/2022 issued by the Ministry of Environment and Forestry, the Republic of Indonesia.

All experimental and surgical procedures needed for sample collection were done at the Faculty of Biology, Universitas Gadjah Mada, Yogyakarta, Indonesia with the approval from The Ethical Committee of the Integrated Laboratory for Research and Testing (Laboratorium Penelitian dan Pengujian Terpadu/LPPT) Universitas Gadjah Mada (Ethical Clearance number: 00014/04/LPPT/IV/2021 signed on 30 April 2021). Tail autotomy was performed under ketamine anesthesia.

Animal collection and maintenance

Thirty-nine adult tokay geckos were captured in the vicinity of the Faculty of Biology, Universitas Gadjah Mada, Yogyakarta, Indonesia. They were acclimatized for two weeks, two males with one female, in a stainless-steel terrarium and fed various species of live crickets and sometimes cockroaches, twice a day. They were maintained at ambient temperature and sprayed once a day with water. The geckos were also basked under natural sunlight once every two days for 1 h in the period 09:00–11:00. Twenty-one were used for the harvesting of regeneration blastemas under anesthesia. Of these, three were euthanized for the harvesting of internal organs. The remaining 18 geckos were bred to produce eggs for embryo sampling.

Experimentation and sample collection

Regenerated tail samples

Twenty-one adult tokay geckos were anaesthetized with intramuscular ketamine injection (50–75 mg/Kg body weight) administered in the thigh prior to the autotomy procedure. Autotomy was performed by gently restraining the gecko manually, while leaving the tail accessible. Using the thumb and index finger, a firm pinch was applied to the required autotomous region (every segment after the 5th caudal vertebra) of the tail causing the gecko to spontaneously shed its tail. The wound was painted with Betadine® iodine antiseptic solution but no dressing was applied. After the autotomy procedure was performed, the geckos were allowed to regenerate a new tail. The geckos were distributed into experimental groups based on the number of days post-autotomy, each consisting of three geckos. After ketamine-anesthesia, the tails of geckos in each group were re-autotomized 2 cm cranially from the previous autotomy site at 0, 4, 8, 16, 20, 28 days post-autotomy (dpa). The regenerated tail samples were washed and further handled in phosphate-buffered saline (PBS, 4 °C) and subsequently fixed with cold RNA*later*® stabilization solution (Invitrogen).

Embryo samples

Eighteen adult tokay geckos were grouped and bred as described above. The terraria were checked daily for the presence of gecko eggs. The eggs were left in the terrarium for the required number of days of incubation at ambient temperature. The embryos were harvested into cold PBS and subsequently fixed with RNA*later*® (4 °C).

Organ samples

Three adult tokay gecko were euthanized by an overdose of intramuscular ketamine (150 mg/Kg body weight, intramuscular injection). The geckos were then dissected to harvest internal organs, namely: pancreas, liver, brain, heart, skeletal muscle, whole skin, kidneys and lungs. These eight organ samples were cut up in cold PBS and placed in RNA*later*® (4 °C).

RNA isolation and cleaning

The samples were taken from RNA*later*® solution with sterile forceps and rinsed with sterile PBS. They were then put in 1.5 mL Eppendorf tubes together with 1 mL Trizol and two steel balls (⌀ 4 mm). The tubes were then shaken with a TissueLyser II (Qiagen) at 30/s for 1–2 min. The resulting tissue homogenates were triturated with a hypodermic needle (21G = 0.8mm) attached to a 1 mL syringe until no tissue clumps were visible. The homogenates were then incubated for 30 min and subsequently centrifuged for 10 min at 12,000 RCF (relative centrifugal force).

The supernatants were transferred into new tubes and 0.2 mL of chloroform added to each. The mixture in the tubes were incubated for 2 to 3 min after 11 s of vigorous hand shaking and then centrifuged for 15 min at 16,000 RCF. The colorless aqueous phase of each mixture was transferred to a fresh tube, and 0.7 mL of propan-2-ol (isopropyl alcohol, isopropanol) added to each tube. After leaving for 10 min at room temperature, the samples were centrifuged at 16,000 RCF for 15 min. The supernatants were discarded, and the RNA pellet washed with 1 mL of 75% ethanol. The pellet with 75% ethanol was centrifuged again for 5 min at 7,500 RCF. The supernatants were discarded, and the RNA pellets allowed to dry for 5–10 min. The dry RNA pellets were dissolved in 50 µL of RNase-free water and incubated at 55° C for 10 min. The total RNA of each sample was then cleaned with Qiagen RNeasy Mini Kit (Cat. No. 74104) according to the manufacturer's protocols.

Library preparation and transcriptome sequencing

The library preparation and transcriptome sequencing were done by the European Molecular Biology Laboratory (EMBL) Heidelberg, Germany with in-house protocols. The sequencing platform used was Illumina NextSeq 2000 with a read length of 2×100 bp.

Transcriptome data analysis

Transcriptome data analysis was carried out within the computing resources of the Academic Leiden Interdisciplinary Cluster Environment (ALICE) provided by Leiden University. The transcriptomic analysis workflow is shown in Figure 3-1.

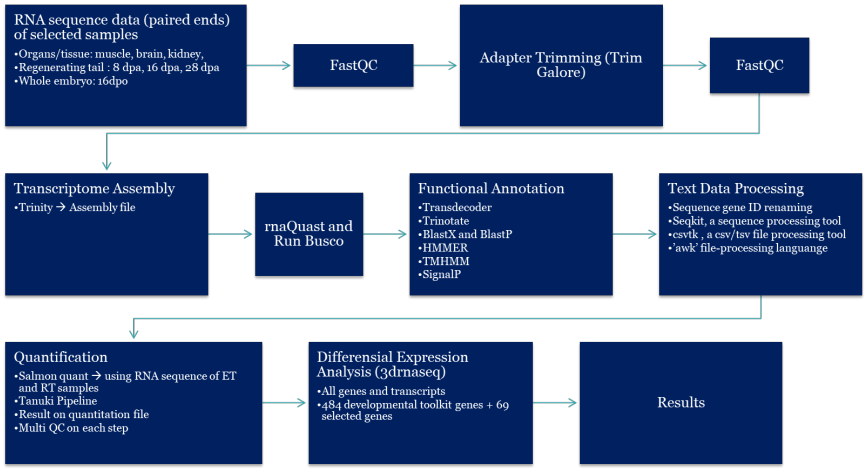

Figure 3-1. **Transcriptomic analysis workflow for analyzing tail regeneration in the tokay gecko adult tail and the embryonic tailbud**. *Key*: ET, embryonic tailbud; QC, quality control; RT, regenerating adult tail.

The sequencing data (paired-end reads, fastq files) were examined with FastQC (https://github.com/s-andrews/FastQC) to check the sequence quality. The sequence adapters were subsequently cut using Trim Galore (https://github.com/FelixKrueger/TrimGalore) before transcriptome assembly. Later on, the transcriptome assembly was done using Trinity RNA-Seq *de novo* assembler (Grabherr et al., 2011; Haas et al., 2013). Finally, the transcriptome assembly results were then evaluated using rnaQUAST (Bushmanova et al., 2016) with the *Gekko japonicus* genome as a reference, and BUSCO (Manni et al., 2021a; Manni et al., 2021b), and FastQC.

Functional annotation was initiated by predicting coding region within the Trinity assembly result using Transdecoder (https://github.com/TransDecoder/TransDecoder). The predicted protein fasta files were then search against databases (NCBI, pFAM, Swissprot) using the Trinotate functional annotation pipeline (Bryant et al., 2017). The tools made use of NCBI Blast+, HMMER (Potter et al., 2018), TMHMM (Krogh et al., 2001), and SignalP (Almagro Armenteros et al., 2019). After functional annotation was completed, the transcripts of both regenerated and embryonic tail samples were quantified using Salmon 1.6.0 (Patro et al., 2017) with Tanuki pipeline (https://github.com/RxLoutre/tanuki.git). The quantification files were then analyzed with differential expression analysis with 3DRNAseq (Guo et al., 2021) using limma (R package) pipeline for differential expression comparison (Ritchie et al., 2015). Differential gene/transcript expression analyses were conducted using $\log_2$ fold change (L_2FC) calculations based on contrasted experimental groups. Statistical significance of expression changes was assessed through t-tests, with p-values adjusted via the Benjamini-Hochberg method to account for multiple testing and control the false discovery rate (FDR). Genes/transcripts were considered significantly differentially expressed in a contrast group if they met the criteria of adjusted p-value < 0.01 and $L_2FC \geq 1$. Furthermore, Gene Ontology and Kegg Pathways were analyzed using Gene Set Enrichment Analysis (Subramanian et al., 2005) with clusterProfiler 4.0 (Wu et al., 2021). Some interesting pathways were visualized based on the transcriptome data using Pathvisio (Kutmon et al., 2015).

Results

For quality control, see Figure S 3-1.

A distinctive molecular signature at each stage of tail regeneration

We conducted mRNA-seq of the regenerating tail at different stages, namely 0, 4, 8, 16, 20, 28 days post autotomy (dpa; *N*=3 per stage; Figure 3-2). Filtering of low-expressed transcripts [counts per million (CPM) cut-off = 1 and minimum samples to CPM cut-off = 9] resulted in 34,472 expressed transcripts from 12,190 expressed genes.

Differential gene expression analysis was performed by comparing each stage with the previous adjacent stage (for example, stage 4 with stage 0, stage 8 with stage 4 and so on). The stagewise pattern of differentially expressed genes is shown in Figure 3-3A , Figure 3-3C, and Figure 3-5A.

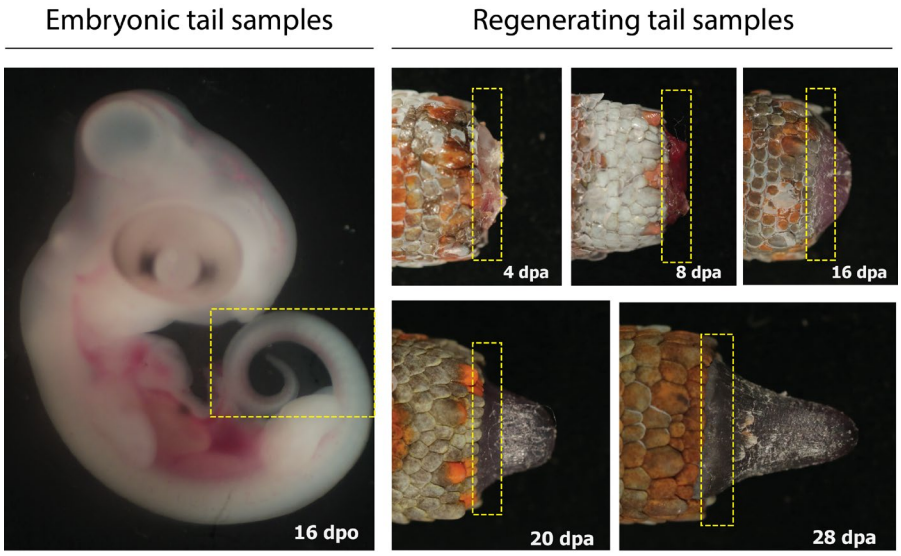

Figure 3-2. **Gecko samples used for transcriptome analysis** (indicated by boxed areas)

As can be seen, the most dramatic change in the transcriptome is seen at the beginning of regeneration, between 0 and 4 dpa. The next major change is at the blastema formation stage, between 8 and 16 dpa. Of these stages, the 0–4 dpa regenerating tail has relatively more uniquely regulated genes, namely 1,241/2,565 (Figure 3-3C). This compares with only 355/1,462 uniquely genes in the 8–16 dpa regenerating tail. At the other stages (4–8 dpa, and the stages after 16 dpa) the number of uniquely regulated genes is much less (Figure 3-3C).

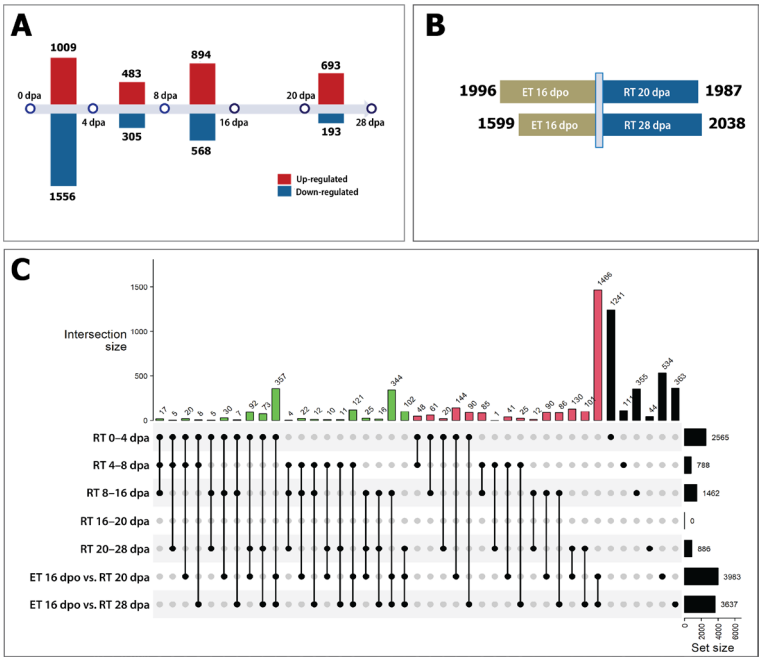

Figure 3-3. **Transcriptome analysis shows a distinctive gene expression profile at each stage of regenerating tail and embryonic tail.** (A) Number of up- and down-regulated genes during tail regeneration stages. Differential gene expression analysis by stage-wise comparison. Three biological replicates each stage. Significant differential expression (DE) genes with adjusted p-value < 0.01 and L2FC≥1. (B) Number of genes regulated in regenerating tail *vs.* embryonic tail. Three biological replicates each stage. Significant differential expression (DE) genes with adjusted p-value < 0.01 and L2FC≥1. ET, embryonic tail; RT, regenerating tail. (C) UpSet of cross-state showing the comparison between different stages of regeneration and tail development. ET, embryonic tail; RT, regenerating tail.

We characterized gene ontology (GO), with a focus on biological processes, and analyzed KEGG pathways using gene set enrichment analysis (GSEA) of all genes expressed at each stage (Figure 3-4). Immune system-related GO terms are enriched at 4 dpa, while muscle activity-related and muscle development-related GO terms are depleted (Figure 3-4A). Bone remodeling-related and epidermis development-related GO terms are also enriched at this stage. In the 8 dpa regenerating tail, only collagen fibril organization and cartilage development are enriched, while epidermis development is depleted.

At 16 dpa, many developmental processes-related GO terms are enriched (e.g. pattern specification process, embryonic morphogenesis, *Wnt* Signaling pathway, cell fate specification, response to BMP, somite development.). By contrast, immune system-related GO terms are depleted. At 20 dpa, muscle development-related GO are becoming enriched together with extracellular matrix organization, while the

developmental-processes-related GO terms are maintained. Finally, at 28 dpa, the muscle-activity-related and muscle development-related GO terms, that were suppressed at 4 dpa, are now enriched.

The KEGG pathway analysis gives a similar pattern to the GO enrichment analysis (Figure 3-4B). Thus, immune system-related pathways are enriched at 4 dpa, as are osteoclast differentiation, TNF signaling pathways, pathways in cancer and steroid biosynthesis. The enrichment of pathways in cancer at this early stage draw our attention so we made a pathway visualization based on our data (Figure S 3-3). It showed some pathways that initiate proliferation are upregulated, such as PI3K-AKT, MAPK, and cell cycle pathways, sustain angiogenesis such as VEGF and HIF-1 signaling, and evading apoptosis potentially via apoptosis inhibitor upregulation.

At 8 dpa, some immune system-related pathways, such as NFκB and IL-17 signaling pathways, together with cancer pathway and TNF signaling pathway are depleted in the regenerating tail. The only two enriched KEGG pathways at this stage are complement and coagulation cascades and ECM receptor interaction. At 16 dpa, pathways related to stem cells and cancer development are enriched, together with melanogenesis and axon guidance, while immune-system-related pathways are depleted. Later on, only cardiac muscle contraction pathway that is enriched in 20 dpa of regenerated tail while maintaining pathways that are enriched in the previous stage. Finally, the further downregulation of immune-system-related pathways is still happening in the 28 dpa regenerating tail.

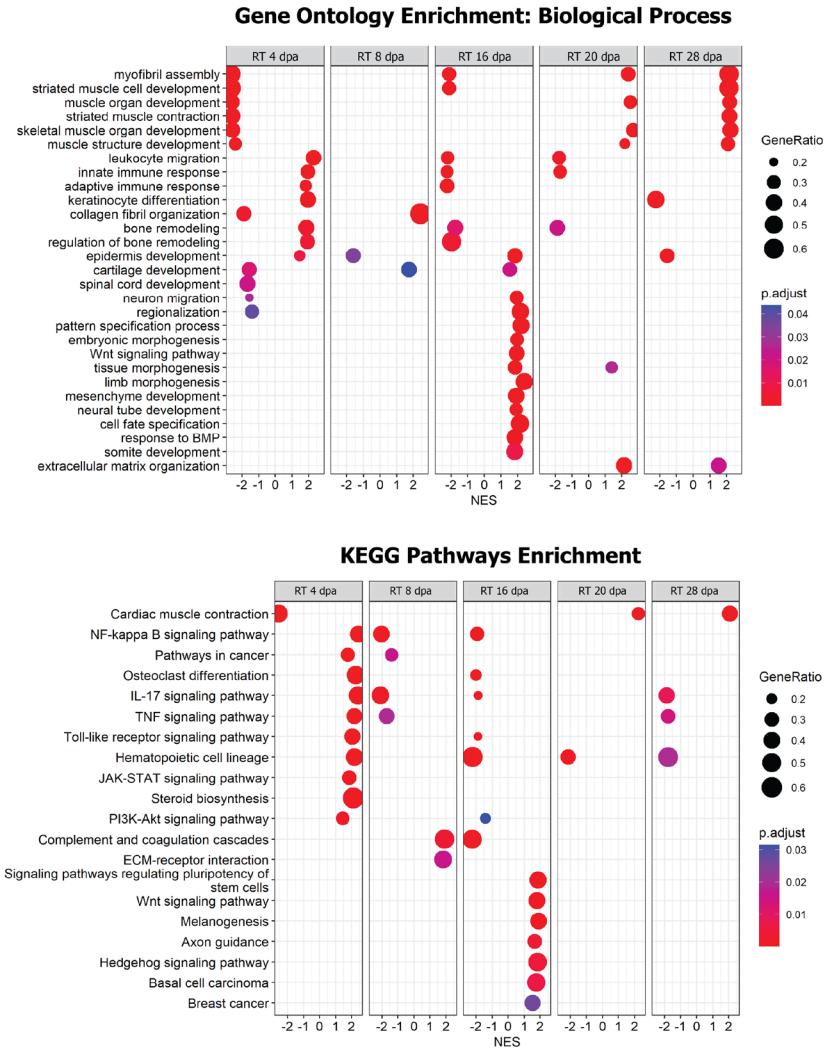

Figure 3-4. **Gene Set Enrichment Analysis reveals biological processes and pathways enriched across stages of tail regeneration**. (A) Biological processes enrichment at different stages of tail regeneration. ET, embryonic tail; RT, regenerating tail. (B) Pathway enrichment at different stages of tail regeneration. RT, regenerating tail. Note that each stage of regeneration has its own signature pathway enrichment.

The regenerating adult tail has a different transcriptomic profile to the embryonic tail

In order to determine whether adult regeneration involves the same mechanisms as embryonic tail development, we performed mRNA-seq on the embryonic tail (*N*=3) at 16 days post oviposition (dpo; Figure 3-2; stage based on (Noro et al., 2009). The heatmap of differentially expressed genes (whose differential expression was

statistically significant) shows that the embryonic tail has a different expression profile from the regenerating adult tail (Figure 3-5A). Notably, genes in clusters 6 and 9 of the heatmap (Figure 3-5A) are strongly expressed in the embryonic tail but not in any stages of the adult regenerating tail.

We then looked at the so-called developmental toolkit genes (developmental patterning genes). These genes encode transcription factors, signaling molecules, transmembrane receptors and other proteins that play a crucial role in embryonic pattern formation. They constitute 484 genes according to (Binda et al., 2024). We found 236/484 of these developmental patterning genes among the significant differentially expressed genes in all comparisons (Figure 3-5B; see for example clusters 3 and 5 of the heatmap in Figure 3-5B).

Then, to focus only on comparable stages of histogenesis, we compared the embryonic tail transcriptome with that of 20 and 28 dpa regenerating tails only. We chose this narrower comparison because the embryonic tail and regenerating tail at these stages all show early stages of tissue differentiation. The comparison generated 3,983 genes that are differentially expressed in embryonic tail *vs.* regenerating tail at 20 dpa (Figure 3-3B). At least 1,996 of these genes are significantly enriched in the 16 dpo embryonic tail whereas 1,987 genes are significantly enriched in the 20 dpa regenerated tail. A similar outcome is also seen in the comparison of the embryonic tail with the 28 dpa regenerating tail. Thus, in that comparison, there are 3,637 genes that are significantly different in expression, of which 1,599 genes are significantly enriched in the embryonic tail, and 2,038 genes that are significantly enriched in the 28 dpo regenerating tail (Figure 3-3B). These two comparisons share 1,446 differentially expressed genes (Figure 3-3C). Of these, 534 genes are uniquely regulated in the embryonic tail *vs.* the 20 dpa regenerating tail, and 363 are in the embryonic tail *vs.* the 28 dpa regenerating tail (Figure 3-3C). In summary, these data show major differences between embryonic tail and regenerating adult tail transcriptomes.

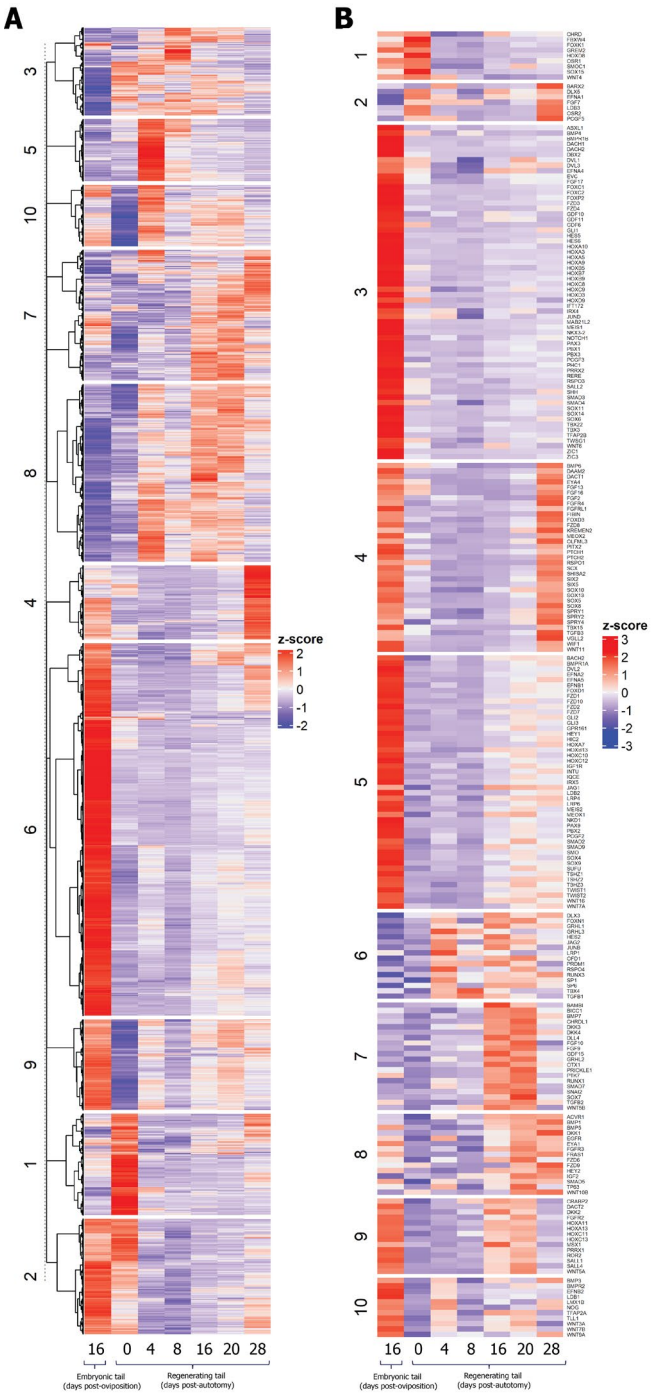

Figure 3-5. **Heatmaps showing the different transcriptome profiles of regenerating and embryonic tails in the tokay gecko**. 6,817 significant differentially expressed genes of whole transcriptome (A) and 236 significant differentially expressed genes of toolkit genes only (B) in embryonic and regenerating tails of the tokay gecko. Significant differential expression (DE) genes with adjusted p-value <0.01 and $L_2FC \geq 1$.

We also characterized gene ontology (GO) and KEGG pathways using gene set enrichment analysis (GSEA) for both comparisons of the embryonic tail and the adult regenerating tail (Figure 3-6). For GO enrichment analysis, both comparisons have a similar result whereby the embryonic tail is dominated by developmental process-related GO terms, while the adult regenerating tails, of both stages, are dominated by immune system-related GO terms and epidermis development-related GO terms (Figure 3-6A). Major differences in GO terms included, in the embryonic tail *vs.* 20 dpa regenerating tail, a comparable enrichment for genes associated with spinal cord development, anterior/posterior pattern specification, and embryonic pattern specification. By contrast, the same GO terms are dominant in the embryonic tail when compared with the 28 dpa regenerating tail. Some GO terms related to tissue morphogenesis or axonogenesis are equally enriched in embryonic tail *versus* 28 dpa regenerating tail. By contrast, these same GO terms are dominant in the embryonic tail if compared to the 20 dpa regenerating tail. Moreover, muscle structure development-related, and extracellular matrix organization GO terms, are dominant in the 28 dpa regenerating tail compared to the embryonic tail.

The KEGG pathway analysis gives a similar pattern to the GO enrichment analysis. Thus, the embryonic tail is relatively enriched in developmental process-related pathways while the regenerating tail is enriched in immune system-related pathways (Figure 3-6B). The term pathways in cancer is dominant in the 20 dpa regenerating tail *vs.* the embryonic tail (Figure 3-6B). Finally, the term signaling pathways regulating pluripotency of stem cells is dominant in the embryonic tail *vs.* the 20 dpa regenerating tail comparison, while this term is equally enriched in embryonic tail *vs.* 28 dpa regenerating tail (Figure 3-6B).

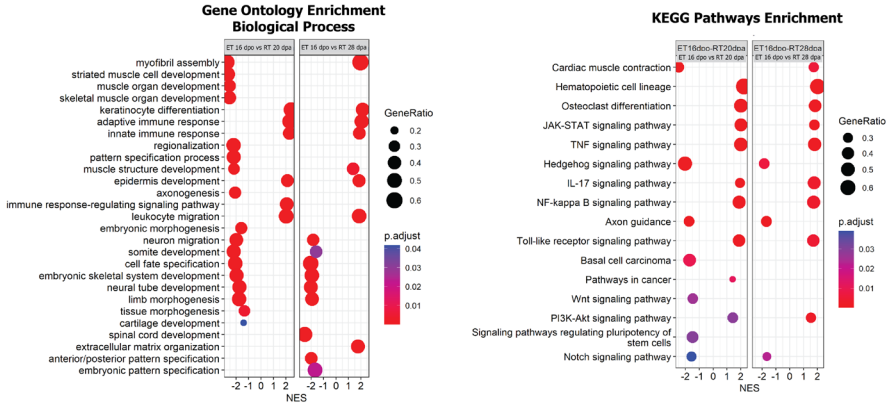

Figure 3-6. **Gene Set Enrichment Analysis reveals biological processes and pathways enriched in regenerating tail and embryonic tail comparison.** (A) Biological process enrichment in regenerating tail vs. embryonic tail. ET, embryonic tail; (B) Pathway enrichment in regenerating tail *vs.* embryonic tail.

In-depth expression profiling on organogenesis related genes

We further explored the expression profile of genes involved in selected tissues in the regenerating tail to see how gene expression in tail regeneration compares with that in tail development in the embryo.

One of the sets of genes we are interested in comparing between regeneration and development are the HOX genes, a family of transcription factors that play a key role in embryonic axial patterning (Di-Poi et al., 2010; Holzman et al., 2018; Kawanishi et al., 2003; McGinnis and Krumlauf, 1992; Spitz et al., 2001; van den Akker et al., 2001) and, potentially, in adult tissue regeneration (Gersch et al., 2005; Rux and Wellik, 2017). Because the tail is an axial structure, we analyzed the expression profile of HOX genes in the transcriptomes of regeneration blastemas and, for comparison, the embryonic tail. Genes from all HOX clusters were expressed in the embryonic tail (Figure 3-7). However, using a stage-wise comparison among regenerating tail blastemas the only HOX genes that were statistically significantly upregulated at any stage were *hoxa5*, *hoxa13*, *hoxb9*, *hoxb13* and *hoxc13* (Figure 3-7). Even though there was minimal evidence in the bulk transcriptomes of any statistically significant upregulation of hox genes during regeneration (Figure S 3-2), visual inspection of the graphs (Figure 3-7) appeared to show that the posterior HOXC genes *hoxc10*–13 might be enriched in the regenerating tail.

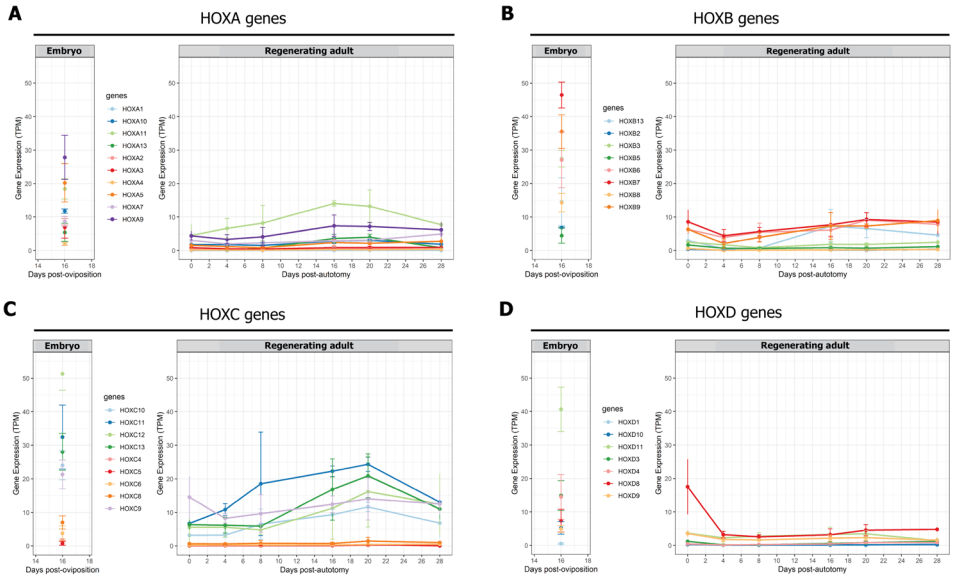

Figure 3-7. **HOXC genes are more active than the other HOX genes clusters during tail regeneration in the gecko**. (A) Expression profile of HOXA genes in the embryonic tail (left) and during adult tail regeneration (right). (B) Expression profile of HOXB genes in the embryonic tail (left) and during adult tail regeneration (right). (C) Expression profile of HOXC genes in the embryonic tail (left) and during adult tail regeneration (right). (D) Expression profile of HOXD genes in the embryonic tail (left) and during adult tail regeneration (right). Note that HOX transcript abundances in the embryonic tails are generally higher than that of the regenerating tails.

The axial skeleton of the normal tail of the gecko is made up of segmentally arranged vertebrae (Chapter 2). In the regenerating gecko tail, however, the vertebrae are replaced by a continuous, unsegmented 'cartilage tube' (Chapter 2; (Lozito and Tuan, 2015)). Therefore, we also examine the typical chondrogenesis-related genes *shh*, *sox9*, *wnt5a*, *wnt3*, *bmp1* and *bmp3* to test the hypothesis that genes associated with chondrogenesis in the development of vertebrae in the embryo, are not expressed in the regenerating tail. We also include *pax1* since it mediates the notochordal signal required for differentiation of the ventral part of the vertebrae (Koseki et al., 1993).

Our transcriptome data show that, in general, the chondrogenesis-related genes had low transcript abundance in the early regenerating tail compared to the embryonic tail (Figure 3-8). Exceptions were *wnt3a* and *bmp3* which had expression levels during early regeneration comparable to the embryonic tail. At later stages of adult tail regeneration, only *wnt5a* and *bmp1* showed equal or higher transcript abundance than the embryonic tail. *Pax1*, a gene critical for the development of the ventral vertebrae in the embryo, has a very low level of expression at all stages.

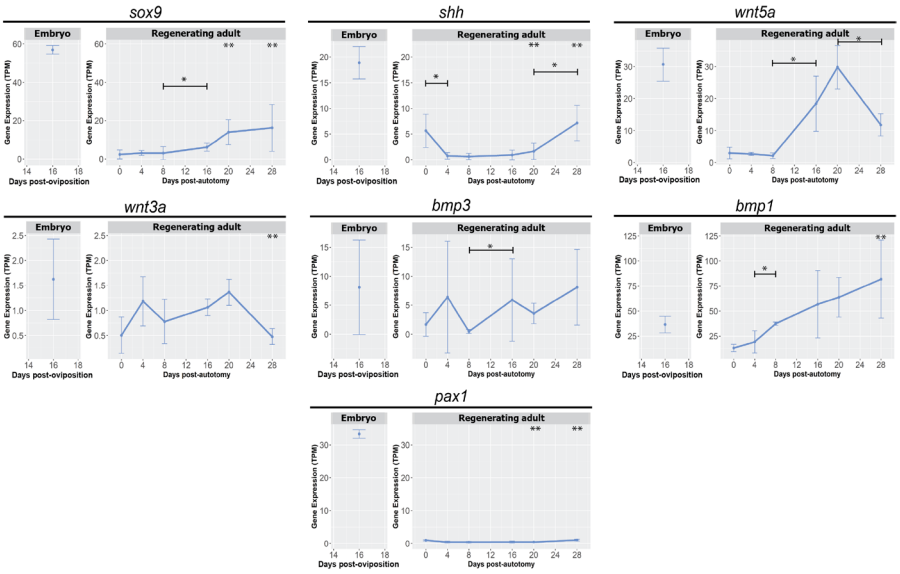

Figure 3-8. **Expression profiles of chondrogenesis genes in the embryonic tail (left) and during adult tail regeneration (right)**. One asterisk (*) shows significant differential expression in stage-wise comparison. Two asterisk (**) shows significant differential expression compared to embryonic tail 16 dpo. Significant differential expression (DE) genes with adjusted p-value < 0.01 and $L_2FC \geq 1$.

The skeletal muscles of the regenerating tail are formed segmentally, as a longitudinal series of myomeres separated by fibro-connective tissue myosepta. We wanted to examine whether muscle development in the regenerating tail resembles the development of axial muscles in the embryo. To do this, we looked at the transcript profiles of genes related to muscle development, namely: *pax3*, *pax7*, *myod1*, *myog*, *ckm*, and *tnc*. Furthermore, we hypothesized that the segmentation of the regenerating muscles was based on the activity of genes that are normally involved in embryonic somite segmentation. To test this hypothesis, we looked at the expression of *lfng* and *hes7*, because they are known to be involved in somite segmentation (Bessho et al., 2001; Chen et al., 2005; Kageyama et al., 2012; Okubo et al., 2012) . We also looked at paralogs of *hes7*, namely *hes1*, *hes2*, *hes5*, and *hes6* to see if they have acquired a function in regeneration (by neofunctionalization).

If we examine Figure 3-9A, we can see that *pax3* were significantly upregulated at 20 dpa. *Pax7*, *myod1*, *myog* and *ckm* all showed a significant increase in transcript abundance at stage 20–28 dpa. At 28 dpa, *myog*, *ckm*, and *myod1* were all significantly upregulated. All of the somite segmentation genes (Figure 3-9) except *hes2* showed higher expression in the embryo tail than in the regenerating tail. The other major finding was that *lfng* was significantly upregulated at 28 dpa.

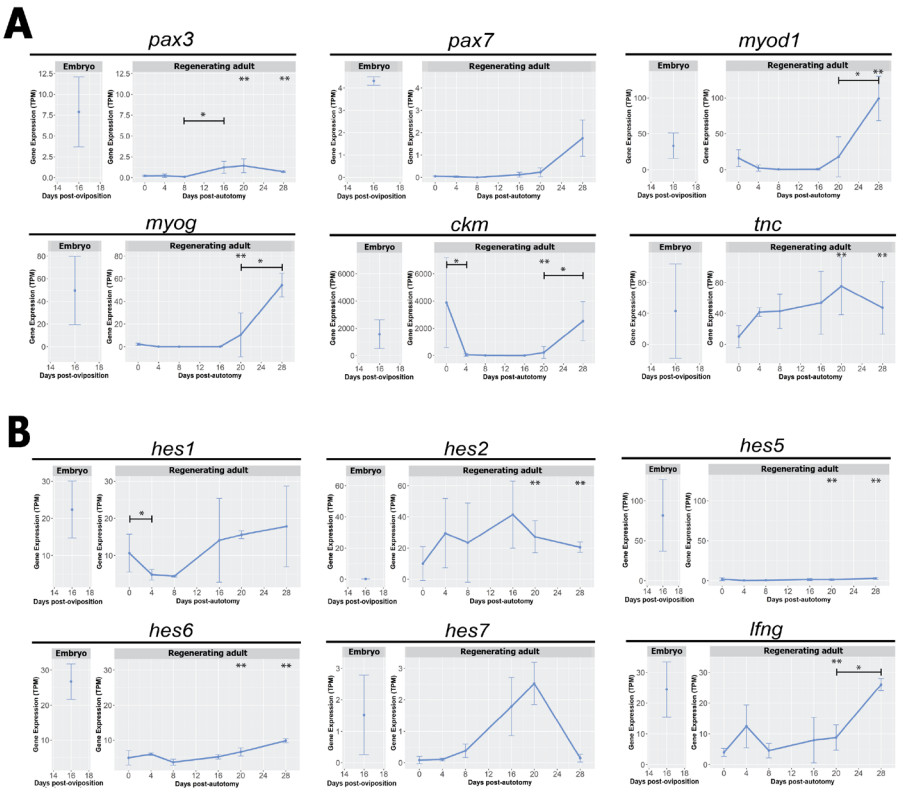

Figure 3-9. Expression profiles of myogenesis genes (A) and somite segmentation genes (B) in the embryonic tail (left) and during adult tail regeneration (right). One asterisk (*) shows significant differential expression in stage-wise comparison. Two asterisk (**) shows significant differential expression compared to embryonic tail 16 dpo. Significant differential expression (DE) genes with adjusted p-value < 0.01 and $L_2FC \geq 1$.

We also examined the transcript abundance of these axonogenesis-related genes in the transcriptomes. *Gap43* and *sema3a* showed statistically significant downregulation when compared to the embryonic tail transcriptome. *Gap43* was significantly downregulated between 0 and 4 dpa and its expression is significantly lower in the adult regenerating tail than in the embryo tail. *Sema3a* expression was significantly lower in the regenerating tail at all stages, than in the embryonic tail (Figure 3-10). Visual inspection of the graphs indicates that all of them, except *nefh,* had much lower expression in the regenerating tail than in the embryonic tail (Figure 3-10).

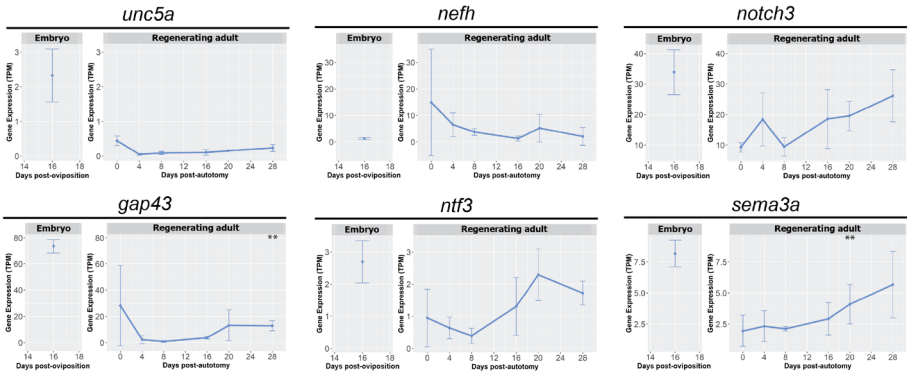

Figure 3-10. **Expression profile of axonogenesis genes in the embryonic tail (left) and during adult tail regeneration (right)**. One asterisk (*) shows significant differential expression in stage-wise comparison. Two asterisk (**) shows significant differential expression compared to embryonic tail 16 dpo. Significant differential expression (DE) genes with adjusted p-value < 0.01 and $L_2FC \geq 1$.

Discussion

Our analysis of mRNA-seq data from regenerating tails at different stages revealed a unique molecular signature in each stage of gecko tail regeneration which we have summarized graphically in (Figure 3-11). We found a much higher number of differentially-expressed genes at the initial stage (0–8 dpa) of tail regeneration compared to what is seen in tail regeneration in the Common Wall Gecko (*Hemidactylus frenatus*) (Nagumantri et al., 2021).

The early-regeneration transcriptome was dominated by immune-related genes and genes associated with wound epithelium formation and bone remodeling. During the early stages of regeneration, immune-related genes play a vital role in both protecting against infection and initiating blastema formation (Londono et al., 2020; Tsai et al., 2019; Vitulo et al., 2017). Additionally, platelets in blood clots release chemokines that aid in recruiting inflammatory cells like neutrophils and macrophages to wound sites (Darby et al., 2014). Macrophages are known to have an important role in the regeneration of many species, for instance, salamanders , zebrafish (Laplace-Builhé et al., 2021), and lizards (Vonk et al., 2023), and spiny mouse (Simkin et al., 2017). Macrophages contribute significantly to tissue regeneration by clearing debris from the wound site by phagocytosis, and by facilitating the shift from inflammation to regeneration. They are able to change their phenotype, which is essential for tissue remodeling and functional recovery (Wynn and Vannella, 2016). Thus, macrophages have functionality for potential guidance and modulation to shift from inflammation to regeneration (Mescher et al., 2015; Oishi and Manabe, 2018; Wynn and Vannella, 2016).

Our data also indicate the enrichment of NF-kappa B signaling and JAK-STAT signaling pathways at this early stage. Both pathways are known for their involvement in inflammatory responses (Hu et al., 2021; Liu et al., 2017). However, they also have some roles in tissue regeneration. NF-kappa B signaling has a role in bone regeneration (Mishra et al., 2020), while JAK-STAT signaling has a role in muscle regeneration (Price et al., 2014; Tierney et al., 2014). This indicates that the initial immune response is likely essential for triggering the regenerative cascade in tokay gecko tails.

Another group of genes enriched in the early stages (4–8 dpa) are the bone remodeling genes. These genes are essential for bone regeneration (Dimitriou et al., 2011; Dirckx et al., 2013), which in the case of tokay gecko tail regeneration is the cartilage tube formation. Epidermis development-related genes are also enriched at this stage, which is consistent with the formation of the wound epidermis, a critical structure for successful regeneration (Alibardi, 2012). The wound epidermis forms early after amputation and provides signals to underlying cells to start the regeneration process. Specifically, the wound epidermis produces factors including FGFs that stimulate blastema formation and outgrowth (Alibardi, 2012).

In addition, we found that cancer pathways are enriched in this stage. These cancer-related pathways might indicate the high proliferative capacity and avoidance of apoptosis that characterize the regeneration blastema (Figure S 3-3). Other workers have suggested similarities between the blastema and cancers (Alibardi, 2022; Oviedo and Beane, 2009). Further investigation into the relationship between regeneration and cancer-related processes could yield valuable insights, as both involve rapid cell division and tissue growth, despite being regulated through distinct mechanisms. It might also shed light on how animals capable of body-axis regeneration like zebrafish, salamander, and lizards evolved the ability to regenerate complex structures while avoiding the cancer-like uncontrolled growth (Alibardi, 2019; Greco et al., 2023; Oviedo and Beane, 2009; Sarig and Tzahor, 2017).

Contrasting with the early inflammatory and proliferative phase, we observed a shift towards more developmental and patterning processes during the blastema formation stage (16-20 dpa). The blastema, a mass of proliferating progenitor cells, is the key structure that drives regenerative outgrowth. The regeneration blastema in the tokay gecko tail is much larger than the blastema in the regenerating zebrafish caudal fin (Pfefferli and Jazwinska, 2015) and the regenerating axolotl limb (Gerber et al., 2018; Kragl et al., 2009). We find that the onset of blastema formation involves mass up-regulation of genes associated with developmental pathways, and down-regulation of immune-related genes. Because of this transcriptomic profile, we believe that 16–20 dpa is the dominant phase of pattern formation.

For example, genes in the WNT signaling pathway are enriched at this stage. This pathway is not only involved in developmental patterning (Komiya and Habas, 2008) but is also essential for tissue regeneration by maintaining stem/progenitor cell fate and coordinating regenerative outgrowth (Clevers et al., 2014; Wang et al., 2007). In the regenerating lizard tail, Wnt signaling pathways are crucial for blastema formation by promoting cell proliferation and regulating proximo-distal patterning (Alibardi, 2020).

Pathway visualizations of our data suggest that Wnt signaling pathways in the regeneration tail are more involved in regulating tissue patterning and remodeling processes, rather than primarily inducing pluripotency (Figure S 3-4, Figure S 3-5). This modelling predicts that the blastema in the tokay gecko is not the result of any kind of dedifferentiation. Instead, it arises from lineage-specific progenitor cells originating from diverse tissues surrounding the wound site, which coordinate to regenerate the complex structure in a regulated manner (discussed also by (Clevers et al., 2014). This is further supported by the enrichment of muscle activity-related and muscle development gene ontology terms during the blastema formation stage, indicating that muscle differentiation and reorganization occur concurrently with the patterning processes.

We also found that Hedgehog signaling pathways were enriched in these stages (pathway visualization in Figure S 3-6). Hedgehog signaling is critical for many developmental processes in vertebrates (Varjosalo and Taipale, 2008). This pathway, in response to BMP signaling, is essential in initiating chondrogenesis in the regenerating lizard tail (Lozito and Tuan, 2015; Lozito and Tuan, 2016; Vonk et al., 2023). Hedgehog signaling is also known to interact with Wnt and Notch signaling to pattern vertebrate body axes and somites (Lewis et al., 2009). Thus, the simultaneous activation of Wnt, Notch, and Hedgehog pathways in the regenerating tokay gecko tail suggests the redeployment of a complex network of conserved developmental regulators to repattern the lost structure (Hikasa and Sokol, 2013).

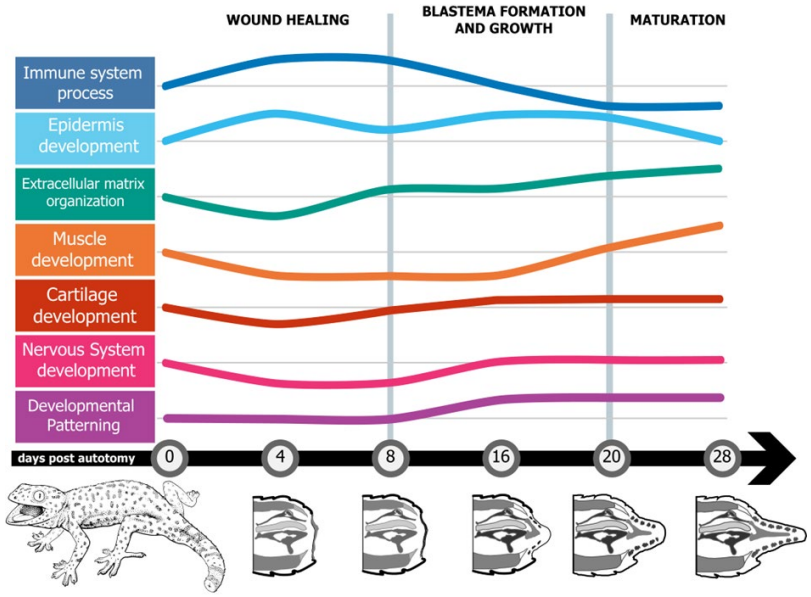

Figure 3-11. **Schematic overview of biological process enrichment in the transcriptome at selected stages of tail regeneration.** The height of each line represents (schematically) the relative enrichment or the process. The greyscale drawings at the bottom represent the histological structure of the regenerating tail at that stage.

Tail regeneration of a lizard involves the development of different tissues or organs, including skeletal muscle, cartilage tube, skin, nerve fibers and others (Di-Poi et al., 2010; Holzman et al., 2018; Kawanishi et al., 2003; McGinnis and Krumlauf, 1992; Spitz et al., 2001; van den Akker et al., 2001). Organ development involves a highly regulated process governed by specific gene regulatory networks (GRNs) and signaling pathways (Zaret, 2002). These pathways ensure proper cell differentiation, tissue formation, and organogenesis through precise control of gene expression. Some other vertebrates such as salamanders and zebrafish are known to reactivate embryonic patterning mechanisms in the blastema during regeneration (Gerber et al., 2018; Pfefferli and Jazwinska, 2015; Randal Voss et al., 2018; Thummel et al., 2007; Wouter et al., 2024).

Interestingly, we find that the gene expression profile of the regenerating tail does not fully recapitulate that of embryonic tail development. When we compared the transcriptome of the adult regenerating tail and the embryonic tail, we found that the regenerating tail shares a limited subset of differentially expressed genes and pathways with the embryonic tail. The regenerating tail is dominated in its early stages by the upregulation of immune system genes, while the embryonic tail is dominated by classical developmental regulatory genes (Figure 3-12).

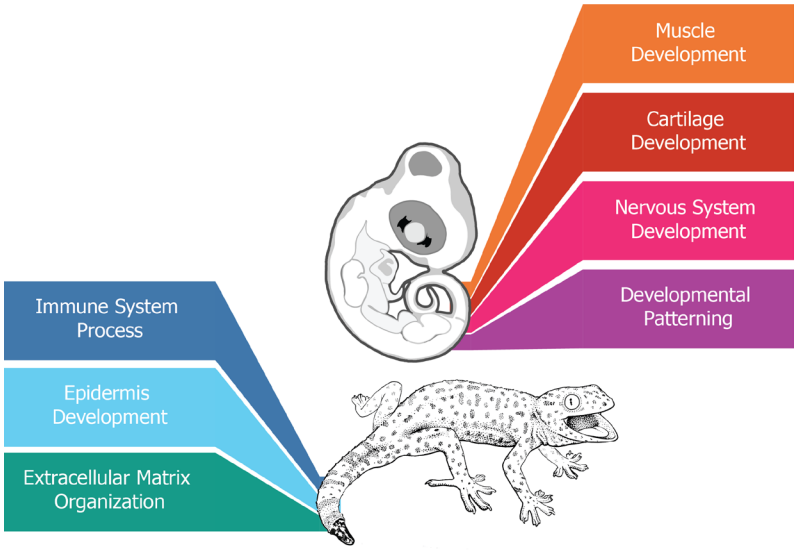

Figure 3-12. **Tail regeneration is not simply a recapitulation of embryonic development.** Schematic illustration highlighting the major differences in the dominant pathways in the regenerating tail vs. the embryonic tail.

The regenerated lizard tail is a functional replica of the original but shows some anatomical differences (Di-Poi et al., 2010; Holzman et al., 2018; Kawanishi et al., 2003; McGinnis and Krumlauf, 1992; Spitz et al., 2001; van den Akker et al., 2001). For instance, the axial skeleton of the normal tail of the gecko is made up of segmentally arranged vertebrae. In the regenerating gecko tail, however, the vertebrae are replaced by a continuous, unsegmented 'cartilage tube' (Lozito and Tuan, 2015). The other major difference is in the nervous system which in the regenerating tail only has the ependymal tube and nerve innervation instead of a complete spinal cord and nerve extensions characteristic of the original tail (Alibardi, 2014; McLean and Vickaryous, 2011). These anatomical differences indicate that the regeneration process only partially recapitulates the embryonic development of the tail and likely relies on distinct mechanisms to reform the lost structures.

Our histological analysis in Chapter 2 revealed that the regeneration blastema in the tokay gecko tail lacks a distinct apical growth zone that might function as a developmental field. As we will show in Chapter 5, the expression profile of the pre-blastema is more consistent with a heterogeneous mix of connective tissue and cells of the muscle lineage. These differences between the gecko blastema and, say, an embryonic tailbud or an axolotl regeneration blastema, may explain why the gene expression profile of the regenerating tokay gecko tail does not fully recapitulate that of embryonic tail development. In contrast, during axolotl limb regeneration, an apical growth zone forms within the blastema, and this growth zone exhibits gene expression

patterns similar to embryonic limb development (Bryant et al., 2002; Gardiner et al., 1995; Gerber et al., 2018; Kragl et al., 2009; McCusker et al., 2015; Muneoka and Bryant, 1982; Muneoka and Bryant, 1984). Similarly, the blastema in zebrafish tail regeneration retains similarities with the embryonic tail bud (Pfefferli and Jazwinska, 2015). Consequently, both axolotl limb and zebrafish tail regeneration are able to reform structures closely resembling the original limb and tail, respectively, through major reactivation of embryonic developmental programs.

In summary, our data demonstrate that the regenerating tail of the tokay gecko does not completely recapitulate the embryonic tail development program. Instead, it activates a limited set of developmental pathways, such as Wnt and Hedgehog, along with genes involved in cell proliferation, immune response, and tissue remodeling to reform only some of the lost structures, and some of those structures (including the scales) are anatomically distinct from those of the original tail. In Chapter 5, we will further discuss the spatial and tissue-specific expression of these organogenesis related genes.

References

Ahmed, N., Iu, J., Brown, C. E., Taylor, D. W. and Kandel, R. A. (2014). Serum- and growth-factor-free three-dimensional culture system supports cartilage tissue formation by promoting collagen synthesis via sox9– col2a1 interaction. *Tissue Engineering Part A* **20**, 2224-2233.

Alibardi, L. (2012). Observations on FGF immunoreactivity in the regenerating tail blastema, and in the limb and tail scars of lizard suggest that FGFs are required for regeneration. *Belgian Journal of Zoology* **142**, 23-38.

---- (2014). Histochemical, Biochemical and Cell Biological aspects of tail regeneration in lizard, an amniote model for studies on tissue regeneration. *Progress in Histochemistry and Cytochemistry* **48**, 143-244.

Alibardi, L. (2019). Review: The Regenerating Tail Blastema of Lizards as a Model to Study Organ Regeneration and Tumor Growth Regulation in Amniotes. *Anat Rec (Hoboken)* **302**, 1469-1490.

Alibardi, L. (2020). Immunolocalization of Wnts in the lizard blastema supports a key role of these signaling proteins for tail regeneration. *Journal of Morphology* **281**, 68-80.

---- (2022). The regenerating tail of lizard transits through a tumour-like stage represented by the regenerative blastema. *Acta Zoologica* **104**, 489-496.

Almagro Armenteros, J. J., Tsirigos, K. D., Sønderby, C. K., Petersen, T. N., Winther, O., Brunak, S., von Heijne, G. and Nielsen, H. (2019). SignalP 5.0 improves signal peptide predictions using deep neural networks. *Nature Biotechnology* **37**, 420-423.

Bae, K. S., Kim, S. Y., Park, S. Y., Jeong, A. J., Lee, H. H., Lee, J., Cho, Y. S., Leem, S. H., Kang, T. H., Bae, K. H., et al. (2014). Identification of lactoferrin as a human dedifferentiation factor through the studies of reptile tissue regeneration mechanisms. *Journal of Microbiology and Biotechnology* **24**, 869-878.

Bely, A. E. and Nyberg, K. G. (2010). Evolution of animal regeneration: re-emergence of a field. *Trends in Ecology and Evolution* **25**, 161-170.

Bessho, Y., Sakata, R., Komatsu, S., Shiota, K., Yamada, S. and Kageyama, R. (2001). Dynamic expression and essential functions of Hes7 in somite segmentation. *Genes Dev* **15**, 2642-2647.

Binda, A. H. J., Kerkkamp, H. M. I., Liem, M., Nurhidayat, L., Xie, B., Elias, K. A., Vonk, F. J. and Richardson, M. K. (2024). What Exactly is the 'Genetic Toolkit' Of Developmental Patterning Genes? *bioRxiv*.

Bryant, D. M., Johnson, K., DiTommaso, T., Tickle, T., Couger, M. B., Payzin-Dogru, D., Lee, T. J., Leigh, N. D., Kuo, T. H., Davis, F. G., et al. (2017). A Tissue-Mapped Axolotl De Novo Transcriptome Enables Identification of Limb Regeneration Factors. *Cell Rep* **18**, 762-776.

Bryant, S. V., Endo, T. and Gardiner, D. M. (2002). Vertebrate limb regeneration and the origin of limb stem cells. *International Journal of Developmental Biology* **46**, 887-896.

Bushmanova, E., Antipov, D., Lapidus, A., Suvorov, V. and Prjibelski, A. D. (2016). rnaQUAST: a quality assessment tool for de novo transcriptome assemblies. *Bioinformatics* **32**, 2210-2212.

Chen, J., Kang, L. and Zhang, N. (2005). Negative feedback loop formed by Lunatic fringe and Hes7 controls their oscillatory expression during somitogenesis. *genesis* **43**, 196-204.

Clevers, H., Loh, K. M. and Nusse, R. (2014). An integral program for tissue renewal and regeneration: Wnt signaling and stem cell control. *Science* **346**, 1248012.

Daponte, V., Tylzanowski, P. and Forlino, A. (2021). Appendage Regeneration in Vertebrates: What Makes This Possible? *Cells* **10**.

Darby, I. A., Laverdet, B., Bonte, F. and Desmouliere, A. (2014). Fibroblasts and myofibroblasts in wound healing. *Clin Cosmet Investig Dermatol* **7**, 301-311.

Di-Poi, N., Montoya-Burgos, J. I., Miller, H., Pourquie, O., Milinkovitch, M. C. and Duboule, D. (2010). Changes in Hox genes' structure and function during the evolution of the squamate body plan. *Nature* **464**, 99-103.

Dimitriou, R., Jones, E., McGonagle, D. and Giannoudis, P. V. (2011). Bone regeneration: current concepts and future directions. *BMC Medicine* **9**, 66.

Dirckx, N., Van Hul, M. and Maes, C. (2013). Osteoblast recruitment to sites of bone formation in skeletal development, homeostasis, and regeneration. *Birth defects research. Part C, Embryo today : reviews* **99**, 170-191.

Gardiner, D. M., Blumberg, B., Komine, Y. and Bryant, S. V. (1995). Regulation of HoxA expression in developing and regenerating axolotl limbs. *Development* **121**, 1731-1741.

Gerber, T., Murawala, P., Knapp, D., Masselink, W., Schuez, M., Hermann, S., Gac-Santel, M., Nowoshilow, S., Kageyama, J., Khattak, S., et al. (2018). Single-cell analysis uncovers convergence of cell identities during axolotl limb regeneration. *Science* **362**.

Gersch, R. P., Lombardo, F., McGovern, S. C. and Hadjiargyrou, M. (2005). Reactivation of Hox gene expression during bone regeneration. *Journal of Orthopaedic Research* **23**, 882-890.

Grabherr, M. G., Haas, B. J., Yassour, M., Levin, J. Z., Thompson, D. A., Amit, I., Adiconis, X., Fan, L., Raychowdhury, R., Zeng, Q., et al. (2011). Full-length transcriptome assembly from RNA-Seq data without a reference genome. *Nature Biotechnology* **29**, 644-652.

Greco, N., Onisto, M. and Alibardi, L. (2023). Protein extracts from regenerating lizard tail show an inhibitory effect on human cancer cells cultivated in-vitro. *Ann Anat* **250**, 152115.

Guo, W., Tzioutziou, N. A., Stephen, G., Milne, I., Calixto, C. P., Waugh, R., Brown, J. W. S. and Zhang, R. (2021). 3D RNA-seq: a powerful and flexible tool for rapid and accurate differential expression and alternative splicing analysis of RNA-seq data for biologists. *RNA Biology* **18**, 1574-1587.

Gurtner, G. C., Werner, S., Barrandon, Y. and Longaker, M. T. (2008). Wound repair and regeneration. *Nature* **453**, 314-321.

Haas, B. J., Papanicolaou, A., Yassour, M., Grabherr, M., Blood, P. D., Bowden, J., Couger, M. B., Eccles, D., Li, B., Lieber, M., et al. (2013). De novo transcript sequence reconstruction from RNA-seq using the Trinity platform for reference generation and analysis. *Nature Protocols* **8**, 1494-1512.

Hikasa, H. and Sokol, S. Y. (2013). Wnt signaling in vertebrate axis specification. *Cold Spring Harb Perspect Biol* **5**, a007955.

Hill, C., Jain, A., Takemoto, H., Silver, M. D., Nagesh, S. V. S., Ionita, C. N., Bednarek, D. R. and Rudin, S. (2012). A histological comparison of the original and regenerated tail in the green anole, Anolis carolinensis. *Anat Rec (Hoboken)* **295**, 1609-1619.

Holzman, M. A., Bergmann, J. M., Feldman, M., Landry-Truchon, K., Jeannotte, L. and Mansfield, J. H. (2018). HOXA5 protein expression and genetic fate mapping show lineage restriction in the developing musculoskeletal system. *Int J Dev Biol* **62**, 785-796.

Hu, X., Li, J., Fu, M., Zhao, X. and Wang, W. (2021). The JAK/STAT signaling pathway: from bench to clinic. *Signal Transduct Target Ther* **6**, 402.

Hutchins, E. D., Markov, G. J., Eckalbar, W. L., George, R. M., King, J. M., Tokuyama, M. A., Geiger, L. A., Emmert, N., Ammar, M. J., Allen, A. N., et al. (2014). Transcriptomic Analysis of Tail Regeneration in the Lizard Anolis carolinensis Reveals Activation of Conserved Vertebrate Developmental and Repair Mechanisms. **9**.

Kageyama, R., Niwa, Y., Isomura, A., González, A. and Harima, Y. (2012). Oscillatory gene expression and somitogenesis.

Kawanishi, C. Y., Hartig, P., Bobseine, K. L., Schmid, J., Cardon, M., Massenburg, G. and Chernoff, N. (2003). Axial skeletal and Hox expression domain alterations induced by retinoic acid, valproic acid, and bromoxynil during murine development. *J Biochem.Mol.Toxicol.* **17**, 346-356.

Komiya, Y. and Habas, R. (2008). Wnt signal transduction pathways. *Organogenesis* **4**, 68-75.

Koseki, H., Wallin, J., Wilting, J., Mizutani, Y., Kispert, A., Ebensperger, C., Herrmann, B. G., Christ, B. and Balling, R. (1993). A role for Pax-1 as a mediator of notochordal signals during the dorsoventral specification of vertebrae. *Development* **119**, 649-660.

Kragl, M., Knapp, D., Nacu, E., Khattak, S., Maden, M., Epperlein, H. H. and Tanaka, E. M. (2009). Cells keep a memory of their tissue origin during axolotl limb regeneration. *Nature* **460**, 60-65.

Krogh, A., Larsson, B., von Heijne, G. and Sonnhammer, E. L. L. (2001). Predicting transmembrane protein topology with a hidden markov model: application to complete genomes11Edited by F. Cohen. *Journal of Molecular Biology* **305**, 567-580.

Kutmon, M., van Iersel, M. P., Bohler, A., Kelder, T., Nunes, N., Pico, A. R. and Evelo, C. T. (2015). PathVisio 3: an extendable pathway analysis toolbox. *PLoS Comput Biol* **11**, e1004085.

Laplace-Builhé, B., Barthelaix, A., Assou, S., Bohaud, C., Pratlong, M., Severac, D., Tejedor, G., Luz-Crawford, P., Nguyen-Chi, M., Mathieu, M., et al. (2021). NRG1/ErbB signalling controls the dialogue between macrophages and neural crest-derived cells during zebrafish fin regeneration. *Nature Communications* **12**, 6336.

Lewis, J., Hanisch, A. and Holder, M. (2009). Notch signaling, the segmentation clock, and the patterning of vertebrate somites. *Journal of Biology* **8**, 44.

Liu, T., Zhang, L., Joo, D. and Sun, S. C. (2017). NF-kappaB signaling in inflammation. *Signal Transduct Target Ther* **2**, 17023-.

Londono, R., Tighe, S., Milnes, B., DeMoya, C., Quijano, L. M., Hudnall, M. L., Nguyen, J., Tran, E., Badylak, S. and Lozito, T. P. (2020). Single cell sequencing analysis of lizard phagocytic cell populations and their role in tail regeneration. *Journal of Immunology and Regenerative Medicine* **8**, 100029-100029.

Lozito, T. P. and Tuan, R. S. (2015). Lizard tail regeneration: Regulation of two distinct cartilage regions by Indian hedgehog. *Developmental Biology* **399**, 249-262.
---- (2016). Lizard tail skeletal regeneration combines aspects of fracture healing and blastema-based regeneration. *Development (Cambridge)* **143**, 2946-2957.
Manni, M., Berkeley, M. R., Seppey, M., Simao, F. A. and Zdobnov, E. M. (2021a). BUSCO Update: Novel and Streamlined Workflows along with Broader and Deeper Phylogenetic Coverage for Scoring of Eukaryotic, Prokaryotic, and Viral Genomes. *Mol Biol Evol* **38**, 4647-4654.
Manni, M., Berkeley, M. R., Seppey, M. and Zdobnov, E. M. (2021b). BUSCO: Assessing Genomic Data Quality and Beyond. *Current Protocols* **1**, e323.
McCusker, C., Bryant, S. V. and Gardiner, D. M. (2015). The axolotl limb blastema: cellular and molecular mechanisms driving blastema formation and limb regeneration in tetrapods. *Regeneration* **2**, 54-71.
McGinnis, W. and Krumlauf, R. (1992). Homeobox genes and axial patterning. *Cell* **68**, 283-302.
McLean, K. E. and Vickaryous, M. K. (2011). A novel amniote model of epimorphic regeneration: the leopard gecko, Eublepharis macularius. *BMC Developmental Biology* **11**, 50-50.
Mescher, A. L., Neff, A. W. and King, M. W. (2015). Inflammation and immunity in organ regeneration. *Developmental and Comparative Immunology*.
Mishra, R., Sehring, I., Cederlund, M., Mulaw, M. and Weidinger, G. (2020). NF-kappaB Signaling Negatively Regulates Osteoblast Dedifferentiation during Zebrafish Bone Regeneration. *Dev Cell* **52**, 167-182 e167.
Muneoka, K. and Bryant, S. V. (1982). Evidence that patterning mechanisms in developing and regenerating limbs are the same. *Nature* **298**, 369-371.
---- (1984). Cellular contribution to supernumerary limbs resulting from the interaction between developing and regenerating tissues in the axolotl. *Dev.Biol.* **105**, 179-187.
Nagumantri, S. P., Banu, S. and Idris, M. M. (2021). Transcriptomic and proteomic analysis of Hemidactylus frenatus during initial stages of tail regeneration. *Scientific Reports* **11**.
Noro, M., Uejima, A., Abe, G., Manabe, M. and Tamura, K. (2009). Normal developmental stages of the Madagascar ground gecko Paroedura pictus with special reference to limb morphogenesis. *Dev Dyn* **238**, 100-109.
Oishi, Y. and Manabe, I. (2018). Macrophages in inflammation, repair and regeneration. *Int Immunol* **30**, 511-528.
Okubo, Y., Sugawara, T., Abe-Koduka, N., Kanno, J., Kimura, A. and Saga, Y. (2012). Lfng regulates the synchronized oscillation of the mouse segmentation clock via trans-repression of Notch signalling. *Nature Communications* **3**, 1141.
Oviedo, N. J. and Beane, W. S. (2009). Regeneration: The origin of cancer or a possible cure? *Seminars in Cell & Developmental Biology* **20**, 557-564.
Patro, R., Duggal, G., Love, M. I., Irizarry, R. A. and Kingsford, C. (2017). Salmon provides fast and bias-aware quantification of transcript expression. *Nature Methods* **14**, 417-419.
Pfefferli, C. and Jazwinska, A. (2015). The art of fin regeneration in zebrafish. *Regeneration (Oxf)* **2**, 72-83.
Potter, S. C., Luciani, A., Eddy, S. R., Park, Y., Lopez, R. and Finn, R. D. (2018). HMMER web server: 2018 update. *Nucleic Acids Research* **46**, W200-W204.
Price, F. D., von Maltzahn, J., Bentzinger, C. F., Dumont, N. A., Yin, H., Chang, N. C., Wilson, D. H., Frenette, J. and Rudnicki, M. A. (2014). Inhibition of JAK-STAT signaling stimulates adult satellite cell function. *Nat Med* **20**, 1174-1181.
Randal Voss, S., Murrugarra, D., Jensen, T. B. and Monaghan, J. R. (2018). Transcriptional correlates of proximal-distal identify and regeneration timing in axolotl limbs. *Comparative Biochemistry and Physiology Part - C: Toxicology and Pharmacology* **208**, 53-63.

Ricci, L. and Srivastava, M. (2018). Wound-induced cell proliferation during animal regeneration. *Wiley Interdisciplinary Reviews: Developmental Biology* **7**, 1-17.

Ritchie, M. E., Phipson, B., Wu, D., Hu, Y., Law, C. W., Shi, W. and Smyth, G. K. (2015). limma powers differential expression analyses for RNA-sequencing and microarray studies. *Nucleic Acids Research* **43**, e47-e47.

Russell, A. P., Lynn, S. E., Powell, G. L. and Cottle, A. (2015). The regenerated tail of juvenile leopard geckos (Gekkota: Eublepharidae: Eublepharis macularius) preferentially stores more fat than the original. *Zoology* **118**, 183-191.

Rux, D. R. and Wellik, D. M. (2017). Hox genes in the adult skeleton: Novel functions beyond embryonic development. *Developmental Dynamics* **246**, 310-317.

Sarig, R. and Tzahor, E. (2017). The cancer paradigms of mammalian regeneration: Can mammals regenerate as amphibians? *Carcinogenesis* **38**, 359-366.

Simkin, J., Gawriluk, T. R., Gensel, J. C. and Seifert, A. W. (2017). Macrophages are necessary for epimorphic regeneration in African spiny mice. *eLife* **6**, e24623.

Spitz, F., Gonzalez, F., Peichel, C., Vogt, T. F., Duboule, D. and Zákány, J. (2001). Large scale transgenic and cluster deletion analysis of the HoxD complex separate an ancestral regulatory module from evolutionary innovations. *Genes Dev.* **15**, 2209-2214.

Stocum, D. L. (2006). An Overview of Regenerative Biology and Medicine.

Subramanian, A., Tamayo, P., Mootha, V. K., Mukherjee, S., Ebert, B. L., Gillette, M. A., Paulovich, A., Pomeroy, S. L., Golub, T. R., Lander, E. S. and Mesirov, J. P. (2005). Gene set enrichment analysis: A knowledge-based approach for interpreting genome-wide expression profiles. *Proceedings of the National Academy of Sciences* **102**, 15545-15550.

Tanaka, E. and Reddien, P. W. (2011). The cellular basis for animal regeneration Sources of new cells in animal regeneration. *Dev Cell* **21**, 172-185.

Thummel, R., Ju, M., Sarras, M. P., Jr. and Godwin, A. R. (2007). Both Hoxc13 orthologs are functionally important for zebrafish tail fin regeneration. *Dev Genes Evol* **217**, 413-420.

Tierney, M. T., Aydogdu, T., Sala, D., Malecova, B., Gatto, S., Puri, P. L., Latella, L. and Sacco, A. (2014). STAT3 signaling controls satellite cell expansion and skeletal muscle repair. *Nat Med* **20**, 1182-1186.

Tsai, S. L., Baselga-Garriga, C. and Melton, D. A. (2019). Blastemal progenitors modulate immune signaling during early limb regeneration. *Development (Cambridge)* **146**.

van den Akker, E., Fromental-Ramain, C., de Graaff, W., Le Mouellic, H., Brulet, P., Chambon, P. and Deschamps, J. (2001). Axial skeletal patterning in mice lacking all paralogous group 8 Hox genes. *Development* **128**, 1911-1921.

Varjosalo, M. and Taipale, J. (2008). Hedgehog: Functions and mechanisms. *Genes and Development* **22**, 2454-2472.

Vitulo, N., Dalla Valle, L., Skobo, T., Valle, G. and Alibardi, L. (2017). Transcriptome analysis of the regenerating tail vs. the scarring limb in lizard reveals pathways leading to successful vs. unsuccessful organ regeneration in amniotes. *Developmental Dynamics* **246**, 116-134.

Vonk, A. C., Zhao, X., Pan, Z., Hudnall, M. L., Oakes, C. G., Lopez, G. A., Hasel-Kolossa, S. C., Kuncz, A. W. C., Sengelmann, S. B., Gamble, D. J. and Lozito, T. P. (2023). Single-cell analysis of lizard blastema fibroblasts reveals phagocyte-dependent activation of Hedgehog-responsive chondrogenesis. *Nat Commun* **14**, 4489.

Wang, J., Etheridge, L. and Wynshaw-Boris, A. (2007). The Wnt-signaling pathways in mammalian patterning and morphogenesis. In *Advances in Developmental Biology*, pp. 111-158: Elsevier.

Wouter, M., Tobias, G., Francisco, F., Tom, D., Sofia-Christina, P., Marko, P., Vijayishwer Singh, J., Yuka, T.-S., Tzi-Yang, L., Thomas, K., et al. (2024). Somite-independent regeneration of the axolotl primary body axis. *bioRxiv*, 2024.2001.2031.577464.

Wu, T., Hu, E., Xu, S., Chen, M., Guo, P., Dai, Z., Feng, T., Zhou, L., Tang, W., Zhan, L., et al. (2021). clusterProfiler 4.0: A universal enrichment tool for interpreting omics data. *The Innovation* **2**, 100141.

Wynn, T. A. and Vannella, K. M. (2016). Macrophages in tissue repair, regeneration, and fibrosis. *Immunity* **44**, 450-462.

Zaret, K. S. (2002). Regulatory phases of early liver development: paradigms of organogenesis. *Nature Reviews Genetics* **3**, 499-512.

Zhao, A., Qin, H. and Fu, X. (2016). What Determines the Regenerative Capacity in Animals? *BioScience* **66**, 735-746.

Supplementary Information

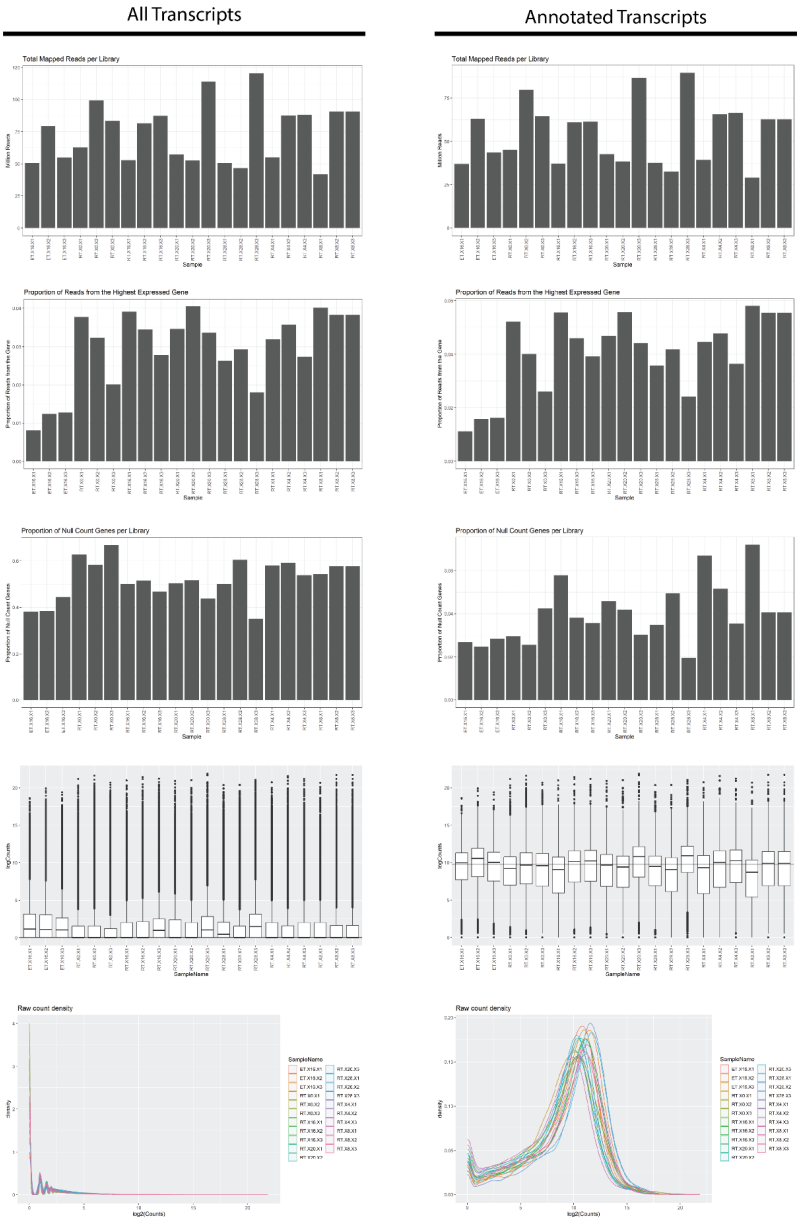

Figure S 3-1. **Quality control results of transcriptome analysis in this chapter.** Note that using only annotated transcript for further analysis give more distinguishable sample comparison.

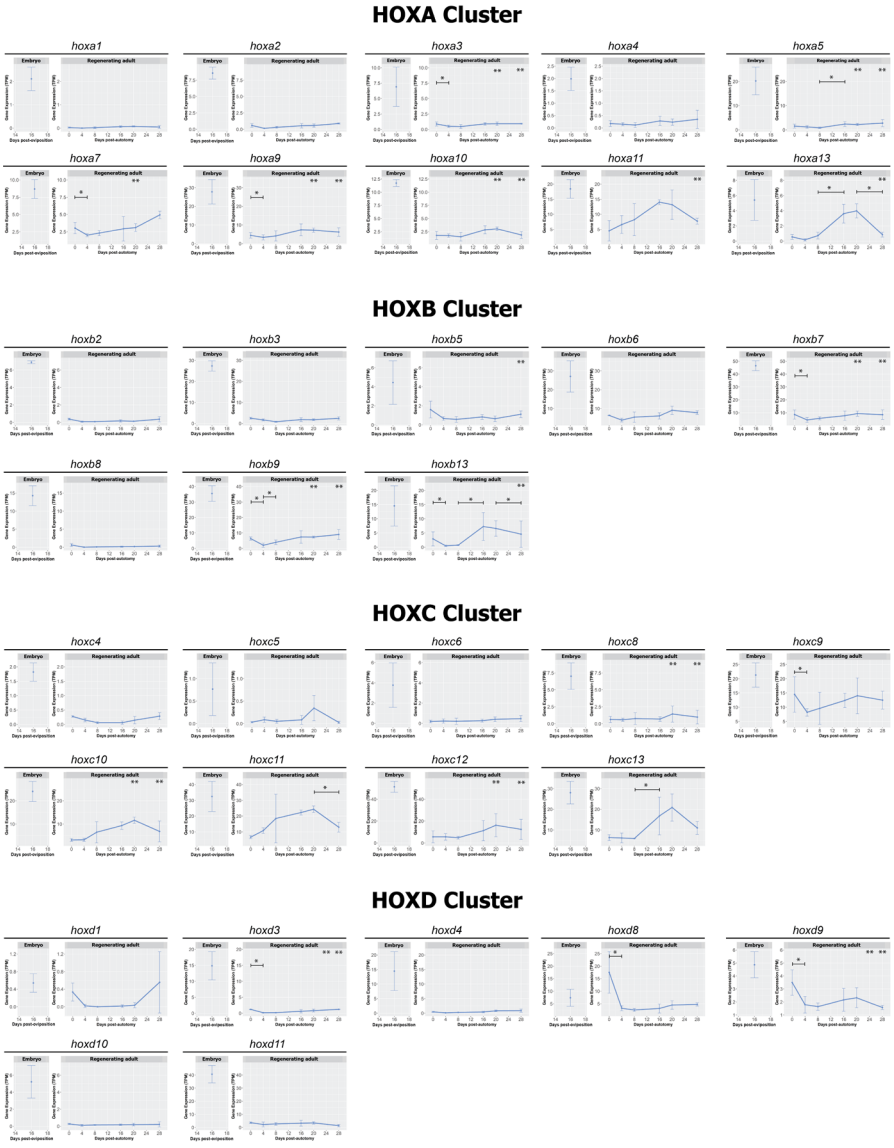

Figure S 3-2**. The transcriptome profiles of HOX genes in the embryonic and the regenerating tail of tokay gecko (*G. gecko*).**

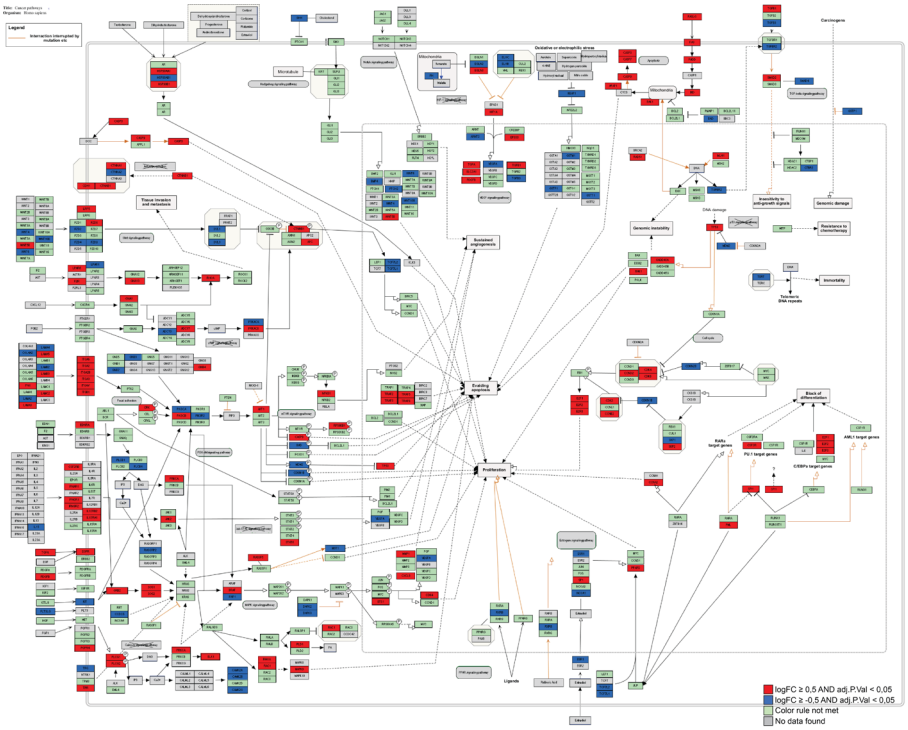

Figure S 3-3. **Pathway visualization of Cancer pathways in the 4 dpa regenerating tail of the tokay gecko**. The pathway visualization was made using Pathvisio based on differential gene expression in the 4 dpa *vs*. 0 dpa comparison.

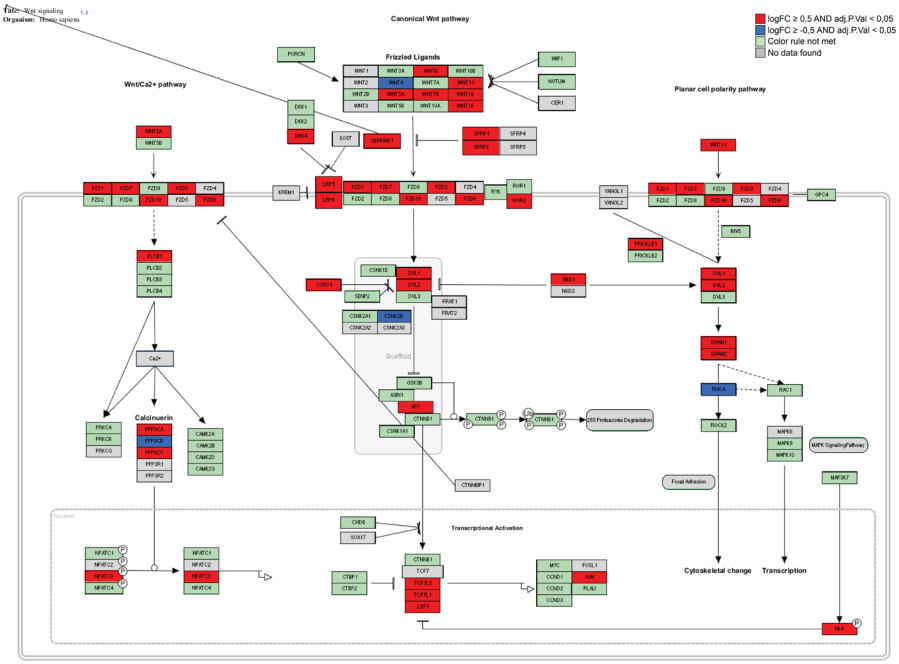

Figure S 3-4. **Pathway visualization of Wnt signaling pathways in the 16 dpa regenerating tail of the tokay gecko.** The pathway visualization was made using Pathvisio based on differential gene expression in the 16 dpa *vs.* 8 dpa comparison.

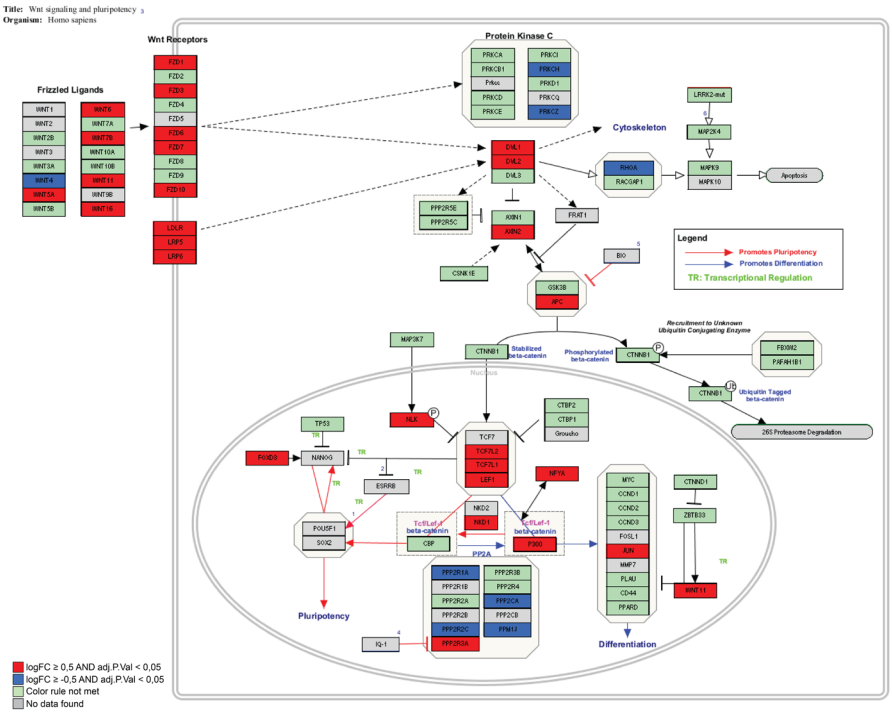

Figure S 3-5. **Pathway visualization of Wnt signaling and pluripotency pathways in the 16 dpa regenerating tail of the tokay gecko.** The pathway visualization was made using Pathvisio based on differential gene expression in the 16 dpa *vs.* 8 dpa comparison.

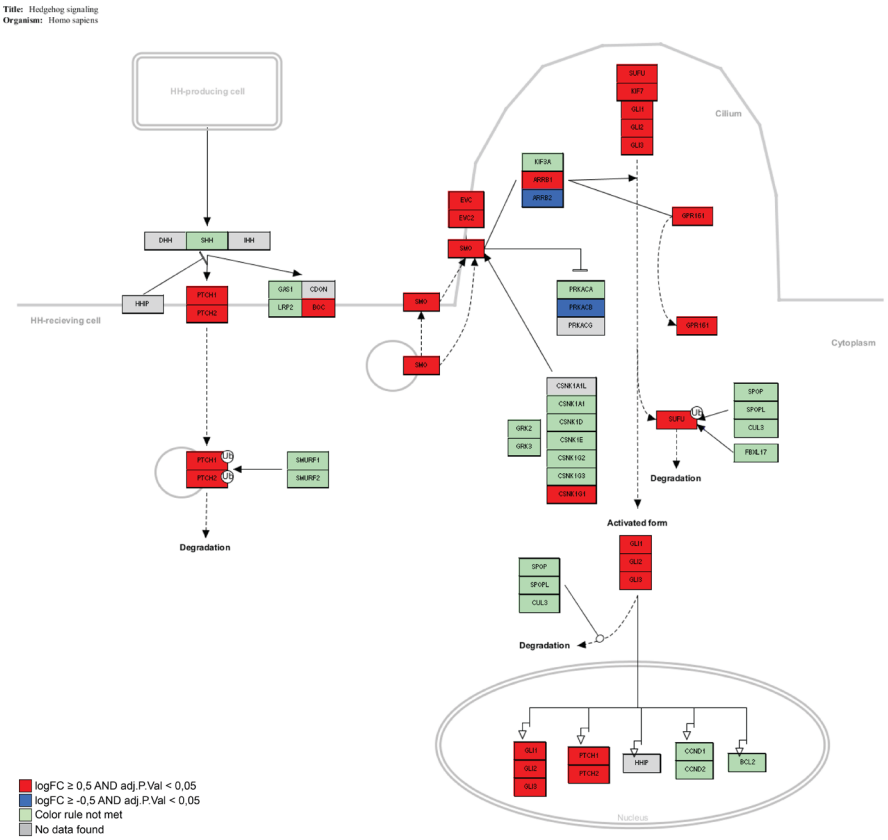

Figure S 3-6. **Pathway visualization of hedgehog signaling pathways in the 16 dpa regenerating tail of the tokay gecko**. The pathway visualization was made using Pathvisio based on differential gene expression in the 16 dpa *vs.* 8 dpa comparison.

Chapter 4. Single Cell Sequence Analysis of Tokay Gecko Tail Regeneration

Luthfi Nurhidayat[1,2], Vladimir Benes[3], Herman P. Spaink[1], Michael K. Richardson[1]

1. Institute of Biology Leiden, Leiden University, Sylvius Laboratory, Sylviusweg 72, 2333 BE, Leiden, The Netherlands.
2. Faculty of Biology, Universitas Gadjah Mada, Jalan Teknika Selatan Sekip Utara, 55281, Yogyakarta, Indonesia
3. Genomics Core Facility, European Molecular Biology Laboratory Heidelberg, Meyerhofstraße 1, 69117 Heidelberg, Germany

---

This chapter is part of: Nurhidayat, L., Benes, V., Blom, S., Gomes, I., Firdausi, N., de Bakker, M.A.G., Spaink, H.P., Richardson. M.K. Tokay gecko tail regeneration involves temporally collinear expression of HOXC genes and early expression of satellite cell markers. *BMC Biology*. Under revision. (2024).

Abstract

Regeneration is the replacement of missing or lost tissue with a functional copy. The capacity for regeneration in different species is influenced by various factors including the characteristics of the stem cells involved. In axolotl limb and zebrafish caudal fin regeneration, there is activation of developmental patterning genes in the regeneration blastema (cell mass). The properties of the blastema are in some respects similar to an embryonic limb bud or tailbud. In this study, we examined whether the tail regeneration blastema in the adult tokay gecko involves similar cell populations and programming as in embryonic tail development. We used single-cell mRNA sequencing of the regeneration blastemata of the adult tokay gecko tail (16, 20, 24 and 28 days post-autotomy) and compared it with the embryonic tailbud (3 and 7 days post-oviposition). Our analysis reveals differences in the cell populations of the regeneration blastema and the embryonic tailbud/tail. The regeneration blastema is dominated by fibroblasts from 16 days post-amputation onwards, whereas the tailbud shows a substantial population of pluripotent stem cells. In the regeneration blastema, RNA velocity analysis estimated that stromal cells (resident stem cells) and fibroblasts were the initial state, while the terminal states predominantly developed within their own lineages. Notably, keratinocytes only developed from their own cluster. By contrast, in the embryonic tailbud/tail, we estimated mesenchymal cells to be the initial state, with high probabilities of becoming chondrocytes and myocytes, medium-to-low probabilities of becoming endothelial cells, and very low probabilities of becoming nerve cells. In summary, our findings suggest that gecko tail regeneration predominantly relies on the activation of resident stem cells in the uninjured tissue, rather than on dedifferentiation. This contrasts with the blastema-based regeneration in the zebrafish and many urodeles, and is more similar to regeneration in mammals, both of which primarily involve activation of resident stem cells.

Introduction

Regeneration is the replacement of missing or lost tissue with a functional copy. It is important as a one of the survival strategies used by animals to deal with injuries (Bely and Nyberg, 2010; Gurtner et al., 2008). It is seen at various levels of biological organization, ranging from the cell to the whole body, and can be induced at different stages of the lifecycle (Bely and Nyberg, 2010). It involves a program of cell-proliferation, pattern formation and differentiation after injury (Ricci and Srivastava, 2018; Tanaka and Reddien, 2011).

It is important to study the similarities and differences in regeneration in different species because, for example, it may help us understand why mammals, including humans, have such a limited regeneration capacity (Alibardi, 2010; Daponte et al., 2021; Zhao et al., 2016). Indeed, one goal of regeneration research is to translate this knowledge to regenerative medicine (Ahmed et al., 2014; Oviedo and Beane, 2009; Stocum, 2006).

Regeneration is dependent on stem cells (Poss, 2010; Ricci and Srivastava, 2018; Tanaka and Reddien, 2011). Species differences in the availability or source of stem cells might partly explain the differing regenerative capacity of different species (Tanaka and Reddien, 2011; Zhao et al., 2016). Other factors possible influencing regeneration capacity include the characteristics of the stem cells involved, the potential for dedifferentiation and transdifferentiation, the expression patterns of genes associated with regeneration, the presence of epigenetic regulators, and immune system responses (Zhao et al., 2016).

Regeneration in the vertebrates is more limited compared to that of invertebrates such as *Hydra* and planarians. In humans, for example, the capacity for true regeneration is limited to the fingertips, and then only takes place when the nail bed is preserved (Gang and Lenghi, 1982; Narayanan, 2015; Tang et al., 2014). The liver in humans and other mammals can restore lost parts, but some researchers regard this as physiological size regulation rather than true regeneration (Michalopoulos, 2007; Wang et al., 2019b). Some vertebrates, however, do show an impressive capacity for regenerations. These include teleosts such as the zebrafish (Pfefferli and Jazwinska, 2015), Lissamphibia such as salamanders (Joven et al., 2019) and the axolotl, (Polikarpova et al., 2022) and Squamata such as lizards (Alibardi, 2014; Alibardi, 2018; Li et al., 2015)

Interestingly, in the axolotl limb (Gardiner et al., 1995; Gerber et al., 2018; Kragl et al., 2009; Muneoka and Bryant, 1982; Muneoka and Bryant, 1984) and the zebrafish caudal fin (Pfefferli and Jazwinska, 2015), regeneration bears a number of similarities to the embryonic development of those same structures. For example, an entire suite of

developmental patterning genes is activated in the regeneration blastema (Blum and Begemann, 2012; Gerber et al., 2018; Pfefferli and Jazwinska, 2015; Sinclair et al., 2021). Furthermore, the tissue organization of the blastema is similar to an embryonic limb bud or tailbud. Thus, the early blastema is small, and is composed of a mass of undifferentiated cells capped by a wound epithelium. This is similar to the embryonic limb bud in which there is a 'progress zone' of undifferentiated mesenchymal cells capped by an apical ectodermal ridge according to some models (Tickle, 2015; Vargesson, 2020). The embryonic tailbud has a simlar structure (Goldman et al., 2000). In the green anole, some developmental pathways are re-activated during tail regeneration, but are not expressed in a growth zone. Rather, they are distributed throughout the blastema (Hutchins et al., 2014). Furthermore, the regeneration blastema in lizards is relatively large compared to that in the axolotl and zebrafish.

In this thesis, we have studied the tokay gecko (*Gekko gecko*). This is one of many lizard species which shows caudal autotomy. This process is the spontaneous shedding of the tail when the animal is attacked by a predator. The tail fragment may continue to twitch after it is shed, distracting the predator and allowing the gecko to escape (Rumping and Jayne, 1996). After the tail has been shed by autotomy, the tail undergoes regeneration.

The normal (unregenerated) tail of the tokay gecko consists of structures including the spinal cord, caudal vertebrae, blood vessels, skeletal muscles, connective tissue and adipose tissue, all covered by the epidermis. By contrast, the regenerated lizard tail (RLT) is a non-identical, but functional, replica of the original (Alibardi, 2014; McLean and Vickaryous, 2011). The differences found in the RLT compared with the original tail are: (1) the axial skeleton is replaced by a continuous cartilage tube; (2) there is a lack of true tendons, presumably due to the lack of vertebrae for them to attach to; (3) the spinal cord is replaced by the ependymal cells and their covering of meninges; (4) the pattern of scales (scalation) is slightly different and the scales are smaller (Higham et al., 2013; Nurhidayat et al., 2020a; Nurhidayat et al., 2020b).

In this chapter, we have examined the question of whether the tail regeneration blastema in the adult tokay gecko contains a similar cell population as the embryonic tailbud. We examine this question using single cell RNA sequencing (scRNA-seq). We apply RNA velocity analysis to the data in order to estimate the cell fate probabilities.

Material and Methods

Ethics statement

The tokay gecko (*Gekko gecko*) is listed as 'least concern' in the International Union for Conservation of Nature *Red List* (IUCN, https://www.iucnredlist.org/species/195309/2378260) and also listed in Appendix II in

the Convention on International Trade in Endangered Species of Wild Fauna and Flora (CITES; https://cites.org/eng/taxonomy/term/3919). In Indonesia, the tokay gecko is not a protected species. All animals were collected in Yogyakarta, Indonesia under a license issued by the Ministry of Environment and Forestry, the Republic of Indonesia (permit number SK.83/KSDAE/SET/KSA.2/5/2021 signed on 7 May 2021) and a recommendation letter issued by The Indonesian Institute of Sciences (Lembaga Ilmu Pengetahuan Indonesia/LIPI; Recommendation Number: B- 2158 /IV/KS.01.04/3/2021 signed on 19 March 2021). The transport of samples from Indonesia to the Netherlands was conducted under CITES permit numbers 05717/IV/SATS-LN/2021 and 09160/IV/SATS-LN/2022 issued by the Ministry of Environment and Forestry, the Republic of Indonesia.

All experimental and surgical procedures needed for samples collection were carried out at Faculty of Biology, Universitas Gadjah Mada, Yogyakarta, Indonesia with the approval from The Ethical Committee of the Integrated Laboratory for Research and Testing (Laboratorium Penelitian dan Pengujian Terpadu/LPPT) Universitas Gadjah Mada (Ethical Clearance number: 00014/04/LPPT/IV/2021 signed on 30 April 2021).

Experimentation and sample collection

Regenerated tail samples

Twenty-one adult tokay geckos were anaesthetized with intramuscular ketamine injection (50–75 mg/Kg body weight) administered in the thigh prior to the autotomy procedure. Autotomy was performed by gently restraining the gecko manually, while leaving the tail accessible. Using the thumb and index finger, a firm pinch was applied to the required autotomous region (every segment after the 5th caudal vertebra) of the tail causing the gecko to spontaneously shed its tail. The wound was painted with Betadine® iodine antiseptic solution but no dressing was applied. After the autotomy procedure was performed, the geckos were allowed to regenerate a new tail. The geckos were distributed into experimental groups based on the number of days post-autotomy, each consisting of three geckos. After ketamine anesthesia, the tails of geckos in each group were re-autotomized 2 cm cranially from the previous autotomy site at 16, 20, 24, and 28 days post-autotomy (dpa). The regenerated tail samples were washed and further handled in phosphate-buffered saline (PBS, 4 °C) and subsequently processed with tissue dissociation protocols.

Embryo samples

Eighteen adult tokay geckos were grouped and bred as described above. The terraria were checked daily for the presence of gecko eggs. The eggs were left in the terrarium for the required number of days of incubation at ambient temperature (which in Yogyakarta ranged from 24–26 °C). The embryos were then harvested at 3 days post-oviposition (dpo) for the tailbud, and 7 dpo for the embryonic tail (we refer to the later

sample as embryonic tail because it was more extensive than the tailbud alone). The tailbuds and embryonic tail were then cut off and transferred to cold PBS and subsequently processed for tissue dissociation (see below).

Tissue dissociation and ACME Fixation

Samples were cut into pieces and were transferred into 15 mL tubes containing cold 1% trypsin (Sigma Aldrich®; T7409) 1mM EDTA (380 mg/L) in Hanks' Balanced Salt solution (Sigma Aldrich®; H9394), which was without magnesium and calcium, with phenol red. Samples were then incubated for 90–120 min on a shaker at 200 rpm with trituration every 30 minutes. The samples were then centrifuged at 440 RCF (relative centrifugal force) which equates to 16 radian/minute, at 4 °C for 5 minutes and the supernatant was then carefully discarded. Acetic-methanol (ACME) solution was made according to (Garcia-Castro et al., 2021). ACME solution without methanol (8.5 mL) was added to the tube. After 20 min incubation, 1.5 mL of methanol was then added to each tube and incubated for another 20 min. The dissociated tissue of all samples was then strained through a 70 µm Corning® cell strainer (cat. 431751). The cell suspensions were then centrifuged at 440 RCF at 4 °C for 5 min and the supernatant was then discarded. Bovine serum albumin (BSA; 1% in PBS) was added to resuspend and wash the cells and they were subsequently recentrifuged at 440 RCF at 4 °C for 5 min. One and a half mL of 1% BSA in PBS was then added to resuspend the cells. About 100 µL of dimethyl sulfoxide (DMSO) was added to each tube containing the cell suspension, and the tubes then snap-frozen with liquid nitrogen. They were then stored at −80 °C until being shipped on dry ice.

Single-cell RNA sequencing Analysis

The single-cell library preparation was done by the European Molecular Biology Laboratory (EMBL) in Heidelberg, Germany using 10X genomics v3 (28bp). The sequencing was done using Illumina NextSeq 2000 with a read length of 2×50 bp.

Gene expression data were obtained using Cell Ranger v. 6.1.2 pipelines (https://www.10xgenomics.com/support/software/cell-ranger/latest) carried out within the computing resources of the Academic Leiden Interdisciplinary Cluster Environment (ALICE) of Leiden University. The genome of Townsend's least gecko *Sphaerodactylus townsendi* (GCF_021028975.2) was used as a custom genome reference by utilizing 'cellranger mkref' pipeline. The transcript quantification and gene expression data matrix were produced by using 'cellranger count' pipeline.

Seurat5 v. 5.0.0 (https://satijalab.org/seurat/articles/install.html) was used to analyze the scRNA-seq sample datasets, including standard quality control and pre-processing, data integration applying the reciprocal principle component analysis (RPCA) approach, data normalization, linear dimensional reduction, cells clustering, non-linear

dimensional reduction, differential gene expression (marker genes determination), and cell type assignment (Hao et al., 2024). Cell type assignment was done manually by curating the cell type prediction results with the clustermole package (https://igordot.github.io/clustermole/) and SCtype pipeline (Ianevski et al., 2022). RNA velocity was determined using Velocyto and analyzed with Cellrank (Lange et al., 2022).

Results

Different cell populations in the regeneration blastema and embryonic the tailbud

To test the hypothesis that adult regeneration is based on the reactivation of embryonic developmental pathways, we compared cell populations in the regenerating and embryonic tails. We used single-cell RNA sequencing (scRNA-seq) on the following tissue samples: embryonic tailbud/tail (3 dpo and 7 dpo), and regenerating tail blastemata (16, 20, 24 and 28 dpa; (Figure 4-1A; all samples *N*=1). Note that we sampled the whole regeneration blastema (Figure 4-1A). After data preprocessing, data integration, cell clustering and semi-automatic cell type assignment, we identified 13 cell clusters (Figure 4-1B) based on the differential expression of the panel of genes shown in Figure 4-2.

Interestingly, the embryonic tailbud/tail did not, for the most part, cluster with the regenerating tail blastema, even though there are some common cell clusters (Figure 4-1C). These common clusters shared by both the tailbud/tail and the blastema were chondrocytes, endothelial cells, erythroid cells and myocytes. Cell clusters unique to the embryonic tailbud/tail samples were tailbud mesenchymal cells, neuroblast, neurons and mesenchymal stem cells. Clusters unique to the regeneration blastema, on the other hand, were fibroblasts, keratinocytes, stromal cells, macrophages and myoblasts. Note that we have named the pluripotent stem cell cluster in the embryonic tailbud/tail as ‘tailbud mesenchymal cells’ at 3 dpo and as ‘mesenchymal stem cells’ at 7 dpo.

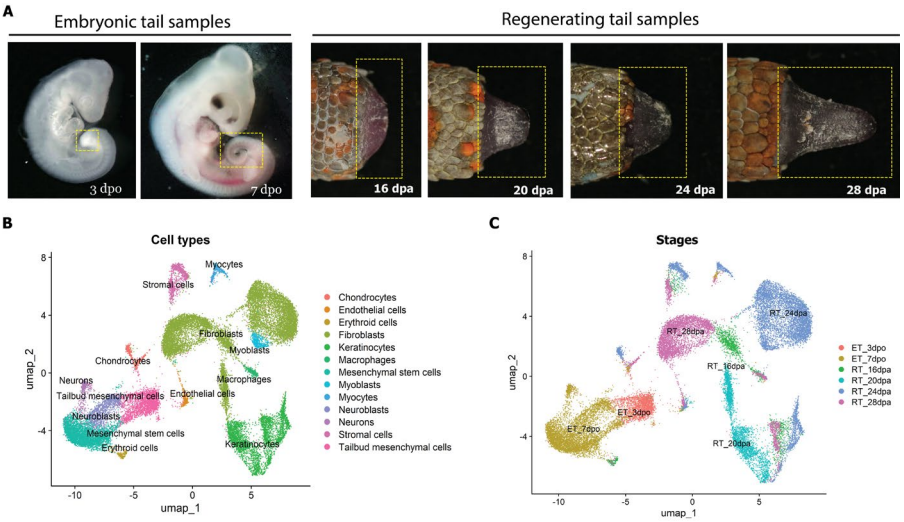

Figure 4-1. **Different cell populations in the regeneration blastema and embryonic the tailbud.** (A) Samples used for single-cell RNA sequencing (area boxed with yellow dashes). (B) UMAP plot showing cells in the regeneration blastema and embryonic the tailbud clustered by cell type. (C) UMAP plot of cells in the regeneration blastema and embryonic tailbud clustered by stages. For the panel of genes used for determining the cell types, see Figure 4-2.

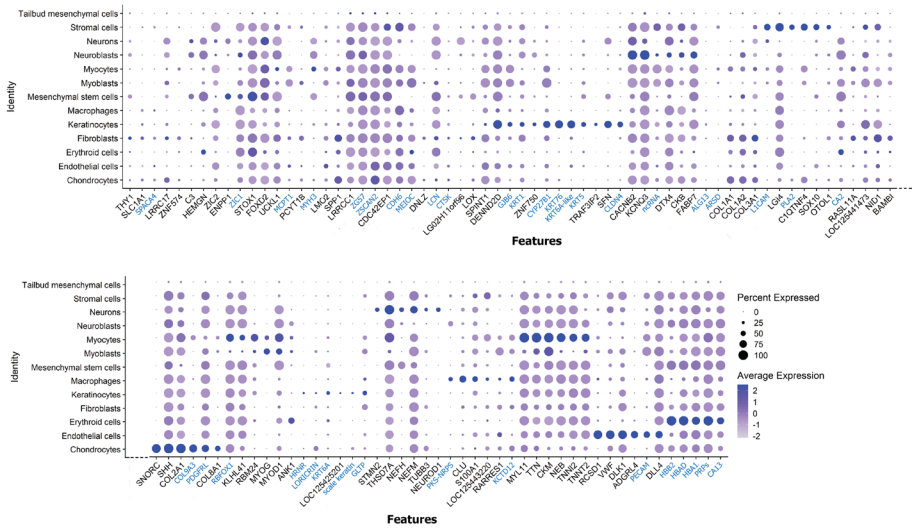

Figure 4-2. **Genes making up the expression profiles of the different cell types in Figure 4-1B and C.** The gene symbols highlighted in blue represent human gene orthologs identified based on gene descriptions from the *Sphaerodactylus townsendi* genome. The mapping of gene symbols and corresponding gene identifiers in *Sphaerodactylus townsendi* genome is provided in the Table S 4-1.

Blastema is lineage-restricted

We estimated the terminal state, and cell fate probability, of cell clusters using Velocyto and Cellrank. In the embryonic tailbud/tail, mesenchymal cells were identified as the initial state (Figure 4-3A). They have a high probability of becoming (as terminal states) chondrocytes and myocytes (Figure 4-3B and C), a medium-to-low probability of becoming endothelial cells (Figure 4-3D), and a very low probability of becoming nerve cells (Figure 4-3E). In the regeneration blastema, we estimated stromal cells (resident stem cells in mesenchymal lineages) and fibroblasts to be the initial state (Figure 4-4A). However, the terminal states in the tail regeneration blastema predominantly develop within their own lineage (Figure 4-4B–F). Notably, keratinocytes develop only from the keratinocyte cell cluster (Figure 4-4E).

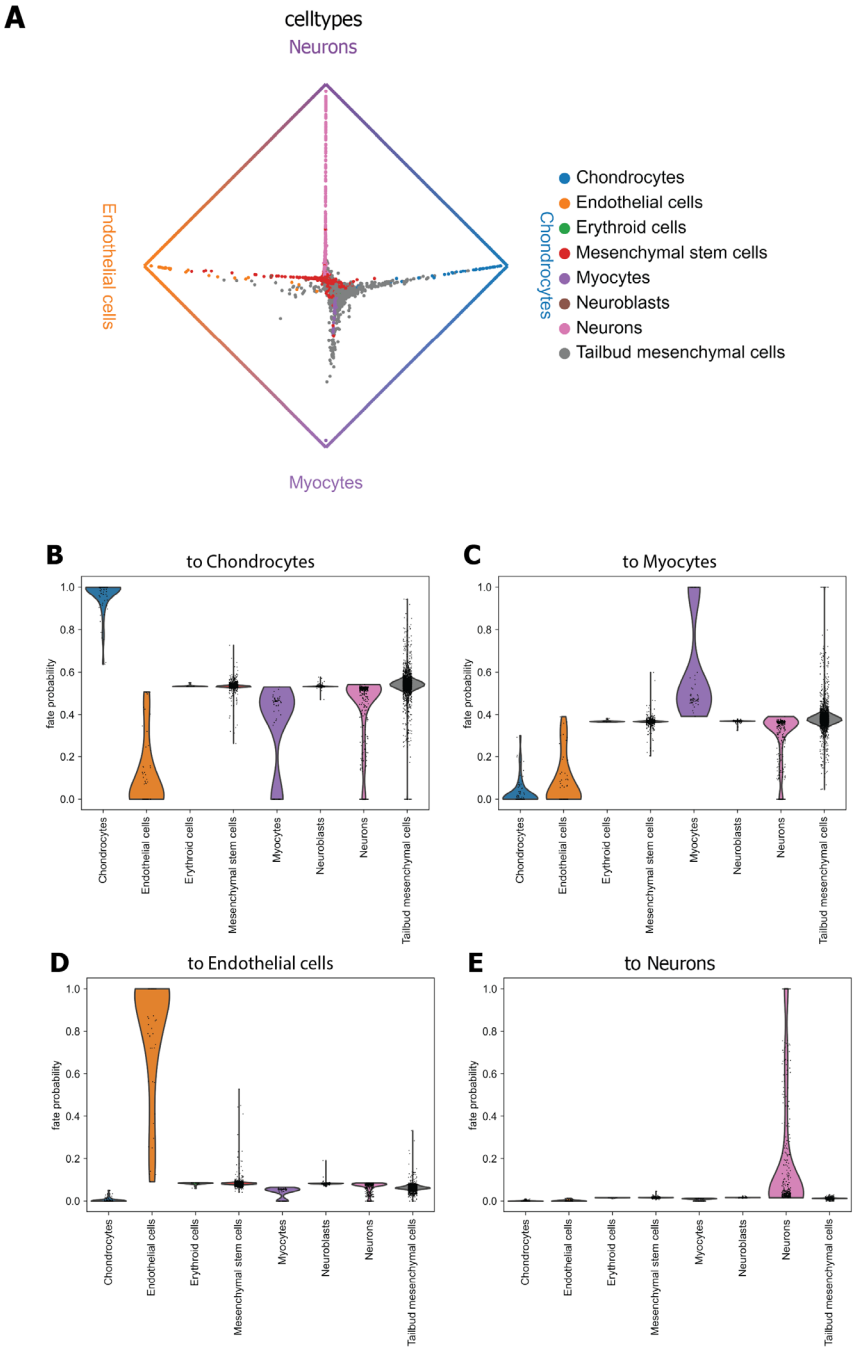

Figure 4-3. **Cell fate probability estimation for the embryonic tailbud and tail.** (A) fate probabilities of merged [embryonic tailbud + embryonic tail] cell clusters towards estimated terminal states. (B–E) fate commitment of each cell cluster in the merged [embryonic tailbud + embryonic tail] data towards terminal states.

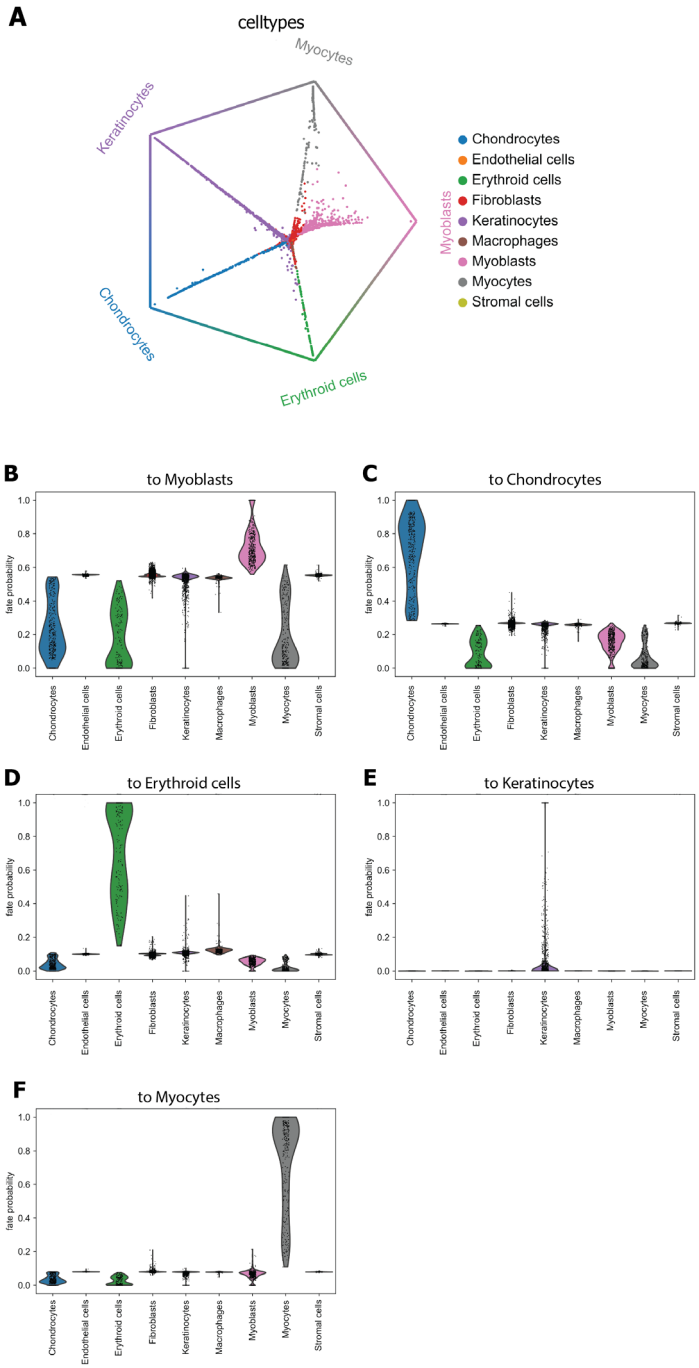

Figure 4-4. **Cell fate probability estimation of tail regeneration blastema.** (A) fate probabilities of tail regeneration blastema cell clusters towards estimated terminal states. (B–F) fate commitment of each cell cluster in the tail regeneration blastema towards terminal states.

We explored these results further (in the blastema only) using pseudotime estimation with Cellrank (Figure 4-5A). In this analysis, keratinocytes were the earliest of all cell clusters followed by endothelial cells and fibroblasts (Figure 4-5A). We then subset the cell clusters of mesenchymal lineages since our previous cell fate probability analysis showed that the keratinocytes only develop from their own cell cluster. We found that the stromal cells were the earliest among the mesenchymal lineages, followed by fibroblasts and chondrocytes (Figure 4-5B).

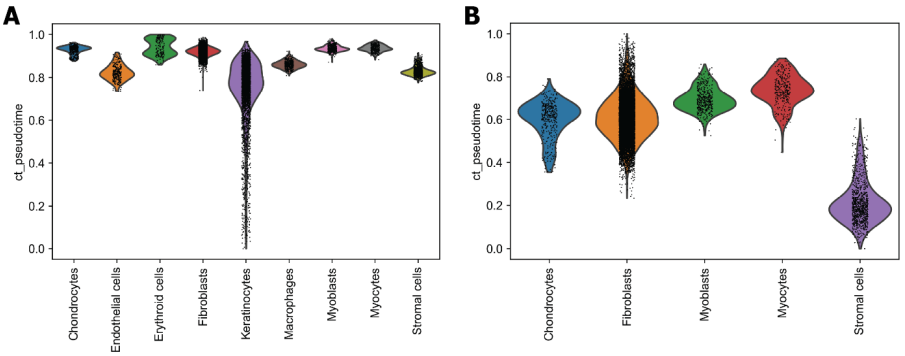

Figure 4-5. **Pseudotime analysis of tail regeneration blastema.** (A) distribution of pseudotime values of all cell clusters of the tail regeneration blastema. (B) distribution of pseudotime values of mesenchymal lineage cell clusters of the tail regeneration blastema.

Discussion

In this chapter, we compared the adult tail regeneration blastema with embryonic tailbud and embryonic tail samples in the tokay gecko using single cell RNA sequencing (scRNA-seq). We wanted to examine whether regeneration in the blastema on the one hand, and normal development in the embryonic tailbud/tail on the other, involve similar cell populations and their lineage restriction. Our analysis does reveal some differences in the cell populations in tail regeneration vs. tail development. Thus, the regeneration blastema is dominated from 16 dpa onwards by fibroblasts. By contrast, the embryonic tailbud/tail shows a substantial population of pluripotent stem cells, which we classify these cells as 'tailbud mesenchymal cells' at 3 dpo and as 'mesenchymal stem cells' at 7 dpo.

Blastema formation is a key feature of epimorphic regeneration, which is the type of regeneration seen in salamanders and zebrafish (Joven et al., 2019; Lee et al., 2009; McCusker et al., 2015). The regeneration blastema consists of proliferative, undifferentiated cells that give rise to the regenerated structure (Seifert and Muneoka, 2018). In axolotl limb regeneration the blastema, at least in some respects, recapitulates embryonic limb bud development at certain stages. For example, in the axolotl limb, the

mid-late regeneration blastema shows similar cell clusters to the embryonic tailbud (Gerber et al., 2018). In zebrafish tail regeneration, the blastema cells also share developmental signatures with the embryonic tailbud (Blum and Begemann, 2012; Pfefferli and Jazwinska, 2015; Sinclair et al., 2021) .

Interestingly, our single cell data analysis in this chapter shows that the majority of clusters are not shared between the tokay gecko regeneration blastema on the one hand, and its embryonic tailbud/tail bud on the other. The regeneration blastema in the tokay gecko is predominantly composed of fibroblasts and does not exhibit a distinct pluripotent stem cell population. A transcriptomic study of tail regeneration in the green anole (a lizard) also found that the blastema formed is not similar to the typical blastema of the axolotl and zebrafish. For example, the green anole blastema is highly vascular, unlike the axolotl and zebrafish blastema. Our histological findings confirm this for the tokay gecko (See Chapter 2). They further suggest that the green anole tail regeneration is more likely to involve tissue-specific regeneration through stem/progenitor populations (Hutchins et al., 2014). Our data in Chapter 2 found that the no apical growth zone in the tokay gecko regeneration blastema. This suggests that the regenerative process in the lizard may involve distinct mechanisms compared to the blastema-based regeneration seen in zebrafish and salamanders (Hutchins et al., 2014).

Cellular dedifferentiation and transdifferentiation are hypothesized to be the key mechanisms underlying regeneration in vertebrates and other animals (Jopling et al., 2011). Dedifferentiation involves a change in cell state of a terminally differentiated, quiescent cell into a pluripotent, undifferentiated cell capable of proliferation (Yao and Wang, 2020). Transdifferentiation by contrast is when a terminally differentiated cell transforms into a terminally differentiated cell from a different lineage; this sometimes involves an intermediate stage where the differentiated cell first reverts to a stem cell like state (regression; (Debuysschere et al., 2024; Jopling et al., 2011). Transdifferentiation and dedifferentiation are both thought to occur in the formation of the regeneration blastema in teleost (Knopf et al., 2011; Sousa et al., 2011) and urodele models (Echeverri et al., 2001; Stocum, 2017; Tanaka and Reddien, 2011; Tsonis et al., 1995). Transdifferentiation between muscle and cartilage may occur in tail regeneration in the Mourning Gecko (Londono et al., 2017). One exception among the urodeles to the patterns outlined above is limb regeneration in the Eastern Newt *Notophthalmus viridescens* which requires the dedifferentiation of myotubes, whereas myogenesis during limb regeneration in axolotls relies on the activation of resident stem cells (Sandoval-Guzman et al., 2014).

Regeneration of the tokay gecko tail may rely on the activation of resident stem cells, rather than the dedifferentiation seen in some urodeles and in zebrafish. This has also been suggested for regeneration in other lizard species (Hutchins et al., 2014; Londono et al., 2018). We found no common pool of mesenchymal precursors in the

tokay gecko regeneration blastema. Instead, the terminal states develop mostly from their own resident stem cells. Resident stem cells (stromal cells) are a population of stem cells in adult mesenchymal tissues that sometimes contribute to cancer progression (Zhao et al., 2023). The activation of resident stem cells has been proposed as a key mechanism underlying the regeneration of complex body structures in amniotes (Hutchins et al., 2014; Johnson et al., 2020; Kierdorf et al., 2009; Lehoczky et al., 2011; Wang et al., 2019a) and myogenesis during limb regeneration in the axolotl (Sandoval-Guzman et al., 2014).

Furthermore, we find that the development of keratinocytes is different from that of mesenchymal cell clusters. This difference makes it unlikely, we believe, that the epidermis contributes in any way to the blastema (for example by epithelial-mesenchymal transition). We found no evidence of transdifferentiation and dedifferentiation in the tokay gecko regeneration blastema. Instead, our data support a model in which the tail regeneration blastema in the tokay gecko is composed of multiple stem cells that were already committed to a particular lineage at the start of regeneration. A prime candidate for these stem cells are resident stem cells from the uninjured stump tissue. Regeneration in mammals, such regeneration of the rodent digit tip (Johnson et al., 2020; Lehoczky et al., 2011) and regeneration of deer antlers (Qin et al., 2023; Wang et al., 2019a), also relies on resident stem cells that were already committed to a particular lineage.

Axolotl limb development involves a major component of dedifferentiation supplemented by the activation of resident stem cells. Thus, in the axolotl limb a major source of to muscle and cartilage in the blastema is dedifferentiation of fibroconnective tissue of the stump (Gerber et al., 2018). However, (Sandoval-Guzman et al., 2014) have suggested that muscles in the regenerating axolotl limb may originate from resident stem cells. Our pseudotime analysis suggests that the cluster ‘stromal cells’ has a significant role in initiating blastema formation (followed later in this role by fibroblasts and other cell types). And, although axolotls and geckos both need resident stem cells from existing mature tissue to form a blastema, we did not find evidence of dedifferentiation in the tokay gecko, although it has been reported during tail regeneration in the Mourning Gecko *Lepidodactylus lugubris* (Londono et al., 2017).

In conclusion, our findings indicate that tokay gecko tail regeneration predominantly relies on the activation of tissue-resident stem/progenitor cells, rather than the formation of a blastema formed by dedifferentiation. This contrasts with the blastema-based regeneration observed in amphibians such as urodele and teleost model species. Instead, the regenerative process in lizards is more akin to the mechanisms found in mammals, which primarily involve the utilization of resident stem cell populations.

References

Ahmed, N., Iu, J., Brown, C. E., Taylor, D. W. and Kandel, R. A. (2014). Serum- and growth-factor-free three-dimensional culture system supports cartilage tissue formation by promoting collagen synthesis via sox9– col2a1 interaction. *Tissue Engineering Part A* **20**, 2224-2233.

Alibardi, L. (2010). Morphological and cellular aspects of tail and limb regeneration in lizards. A model system with implications for tissue regeneration in mammals. *Advances in anatomy, embryology, and cell biology* **207**, iii, v-x, 1-109.

---- (2014). Histochemical, Biochemical and Cell Biological aspects of tail regeneration in lizard, an amniote model for studies on tissue regeneration. *Progress in Histochemistry and Cytochemistry* **48**, 143-244.

---- (2018). Perspective: Appendage regeneration in amphibians and some reptiles derived from specific evolutionary histories. *Journal of Experimental Zoology Part B: Molecular and Developmental Evolution* **330**, 396-405.

Bely, A. E. and Nyberg, K. G. (2010). Evolution of animal regeneration: re-emergence of a field. *Trends in Ecology and Evolution* **25**, 161-170.

Blum, N. and Begemann, G. (2012). Retinoic acid signaling controls the formation, proliferation and survival of the blastema during adult zebrafish fin regeneration. *Development* **139**, 107-116.

Daponte, V., Tylzanowski, P. and Forlino, A. (2021). Appendage Regeneration in Vertebrates: What Makes This Possible? *Cells* **10**.

Debuysschere, C., Nekoua, M. P., Alidjinou, E. K. and Hober, D. (2024). The relationship between SARS-CoV-2 infection and type 1 diabetes mellitus. *Nature Reviews Endocrinology*.

Echeverri, K., Clarke, J. D. and Tanaka, E. M. (2001). In vivo imaging indicates muscle fiber dedifferentiation is a major contributor to the regenerating tail blastema. *Developmental biology* **236**, 151-164.

Gang, R. K. and Lenghi, M. (1982). Conservative management of guillotine amputations of finger tips - Another application of zinc oxide tape. *Chirurgia Plastica* **7**, 75-81.

Garcia-Castro, H., Kenny, N. J., Iglesias, M., Alvarez-Campos, P., Mason, V., Elek, A., Schonauer, A., Sleight, V. A., Neiro, J., Aboobaker, A., et al. (2021). ACME dissociation: a versatile cell fixation-dissociation method for single-cell transcriptomics. *Genome Biol* **22**, 89.

Gardiner, D. M., Blumberg, B., Komine, Y. and Bryant, S. V. (1995). Regulation of HoxA expression in developing and regenerating axolotl limbs. *Development* **121**, 1731-1741.

Gerber, T., Murawala, P., Knapp, D., Masselink, W., Schuez, M., Hermann, S., Gac-Santel, M., Nowoshilow, S., Kageyama, J., Khattak, S., et al. (2018). Single-cell analysis uncovers convergence of cell identities during axolotl limb regeneration. *Science* **362**.

Goldman, D. C., Martin, G. R. and Tam, P. P. (2000). Fate and function of the ventral ectodermal ridge during mouse tail development. *Development* **127**, 2113-2123.

Gurtner, G. C., Werner, S., Barrandon, Y. and Longaker, M. T. (2008). Wound repair and regeneration. *Nature* **453**, 314-321.

Hao, Y., Stuart, T., Kowalski, M. H., Choudhary, S., Hoffman, P., Hartman, A., Srivastava, A., Molla, G., Madad, S., Fernandez-Granda, C. and Satija, R. (2024). Dictionary learning for integrative, multimodal and scalable single-cell analysis. *Nature Biotechnology* **42**, 293-304.

Higham, T. E., Russell, A. P. and Zani, P. a. (2013). Integrative biology of tail autotomy in lizards. *Physiological and biochemical zoology* **86**, 603-610.

Hutchins, E. D., Markov, G. J., Eckalbar, W. L., George, R. M., King, J. M., Tokuyama, M. A., Geiger, L. A., Emmert, N., Ammar, M. J., Allen, A. N., et al. (2014). Transcriptomic

analysis of tail regeneration in the lizard Anolis carolinensis reveals activation of conserved vertebrate developmental and repair mechanisms. *PLoS ONE* **9**.

Ianevski, A., Giri, A. K. and Aittokallio, T. (2022). Fully-automated and ultra-fast cell-type identification using specific marker combinations from single-cell transcriptomic data. *Nature Communications* **13**, 1246.

Johnson, G. L., Masias, E. J. and Lehoczky, J. A. (2020). Cellular heterogeneity and lineage restriction during mouse digit tip regeneration at single-cell resolution. *Developmental Cell* **52**, 525-540.e525.

Jopling, C., Boue, S. and Izpisua Belmonte, J. C. (2011). Dedifferentiation, transdifferentiation and reprogramming: three routes to regeneration. *Nat Rev Mol Cell Biol* **12**, 79-89.

Joven, A., Elewa, A. and Simon, A. (2019). Model systems for regeneration: salamanders. *Development* **146**, dev167700.

Kierdorf, U., Li, C. and Price, J. S. (2009). Improbable appendages: Deer antler renewal as a unique case of mammalian regeneration. *Seminars in Cell and Developmental Biology* **20**, 535-542.

Knopf, F., Hammond, C., Chekuru, A., Kurth, T., Hans, S., Weber, C. W., Mahatma, G., Fisher, S., Brand, M., Schulte-Merker, S. and Weidinger, G. (2011). Bone regenerates via dedifferentiation of osteoblasts in the zebrafish fin. *Developmental Cell* **20**, 713-724.

Kragl, M., Knapp, D., Nacu, E., Khattak, S., Maden, M., Epperlein, H. H. and Tanaka, E. M. (2009). Cells keep a memory of their tissue origin during axolotl limb regeneration. *Nature* **460**, 60-65.

Lange, M., Bergen, V., Klein, M., Setty, M., Reuter, B., Bakhti, M., Lickert, H., Ansari, M., Schniering, J., Schiller, H. B., et al. (2022). CellRank for directed single-cell fate mapping. *Nature Methods* **19**, 159-170.

Lee, Y., Hami, D., De Val, S., Kagermeier-Schenk, B., Wills, A. A., Black, B. L., Weidinger, G. and Poss, K. D. (2009). Maintenance of blastemal proliferation by functionally diverse epidermis in regenerating zebrafish fins. *Dev Biol* **331**, 270-280.

Lehoczky, J. A., Robert, B. and Tabin, C. J. (2011). Mouse digit tip regeneration is mediated by fate-restricted progenitor cells. *Proc Natl Acad Sci U S A* **108**, 20609-20614.

Li, Q., Yang, H. and Zhong, T. P. (2015). Regeneration across metazoan phylogeny: lessons from model organisms. *Journal of genetics and genomics = Yi chuan xue bao* **42**, 57-70.

Londono, R., Sun, A. X., Tuan, R. S. and Lozito, T. P. (2018). Tissue Repair and Epimorphic Regeneration: An Overview. *Curr Pathobiol Rep* **6**, 61-69.

Londono, R., Wenzhong, W., Wang, B., Tuan, R. S. and Lozito, T. P. (2017). Cartilage and Muscle Cell Fate and Origins during Lizard Tail Regeneration. *Frontiers in Bioengineering and Biotechnology* **5**, 1-9.

McCusker, C., Bryant, S. V. and Gardiner, D. M. (2015). The axolotl limb blastema: cellular and molecular mechanisms driving blastema formation and limb regeneration in tetrapods. *Regeneration* **2**, 54-71.

McLean, K. E. and Vickaryous, M. K. (2011). A novel amniote model of epimorphic regeneration: the leopard gecko, Eublepharis macularius. *BMC Developmental Biology* **11**, 50-50.

Michalopoulos, G. K. (2007). Liver regeneration. *Journal of Cellular Physiology* **213**, 286-300.

Muneoka, K. and Bryant, S. V. (1982). Evidence that patterning mechanisms in developing and regenerating limbs are the same. *Nature* **298**, 369-371.

---- (1984). Cellular contribution to supernumerary limbs resulting from the interaction between developing and regenerating tissues in the axolotl. *Dev.Biol.* **105**, 179-187.

Narayanan, A. (2015). Biochips & Tissue Chips The Initiation and Progression of Tail Regeneration in Northern House Gecko Hemidactylus Flaviviridis at Role of Fibroblast Growth Factor 2. *Biochip & Tissue Chip* **5**, 1-7.

Nurhidayat, L., Devi, N. A. and Fadhillah, D. (2020a). Histological structure of nerve fiber and blood vessels in regenerated tail of Tokay gecko (Gekko gecko (Linnaeus, 1758). In *THE*

6TH INTERNATIONAL CONFERENCE ON BIOLOGICAL SCIENCE ICBS 2019: "Biodiversity as a Cornerstone for Embracing Future Humanity".

Nurhidayat, L., Pratama, D. K., Devi, N. A. and Rohmah, Z. (2020b). The development of integument and muscle in regenerated tail of Tokay gecko (Gekko gecko Linnaeus, 1758). In *THE 6TH INTERNATIONAL CONFERENCE ON BIOLOGICAL SCIENCE ICBS 2019: "Biodiversity as a Cornerstone for Embracing Future Humanity"*.

Oviedo, N. J. and Beane, W. S. (2009). Regeneration: The origin of cancer or a possible cure? *Seminars in Cell & Developmental Biology* **20**, 557-564.

Pfefferli, C. and Jazwinska, A. (2015). The art of fin regeneration in zebrafish. *Regeneration (Oxf)* **2**, 72-83.

Polikarpova, A., Ellinghaus, A., Schmidt-Bleek, O., Grosser, L., Bucher, C. H., Duda, G. N., Tanaka, E. M. and Schmidt-Bleek, K. (2022). The specialist in regeneration-the Axolotl-a suitable model to study bone healing? *NPJ Regen Med* **7**, 35.

Poss, K. D. (2010). Advances in understanding tissue regenerative capacity and mechanisms in animals. *Nature Reviews Genetics* **11**, 710-722.

Qin, T., Zhang, G., Zheng, Y., Li, S., Yuan, Y., Li, Q., Hu, M., Si, H., Wei, G., Gao, X., et al. (2023). A population of stem cells with strong regenerative potential discovered in deer antlers. *Science* **379**, 840-847.

Ricci, L. and Srivastava, M. (2018). Wound-induced cell proliferation during animal regeneration. *Wiley Interdisciplinary Reviews: Developmental Biology* **7**, 1-17.

Rumping, J. M. and Jayne, B. C. (1996). Muscle activity in autotomized tails of a lizard (Gekko gecko): a naturally occurring spinal preparation. *Journal of comparative physiology. A, Sensory, neural, and behavioral physiology* **179**, 525-538.

Sandoval-Guzman, T., Wang, H., Khattak, S., Schuez, M., Roensch, K., Nacu, E., Tazaki, A., Joven, A., Tanaka, E. M. and Simon, A. (2014). Fundamental differences in dedifferentiation and stem cell recruitment during skeletal muscle regeneration in two salamander species. *Cell Stem Cell* **14**, 174-187.

Seifert, A. W. and Muneoka, K. (2018). The blastema and epimorphic regeneration in mammals. *Journal of Developmental Biology* **433**, 190-199.

Sinclair, J. W., Hoying, D. R., Bresciani, E., Nogare, D. D., Needle, C. D., Berger, A., Wu, W., Bishop, K., Elkahloun, A. G., Chitnis, A., et al. (2021). The Warburg effect is necessary to promote glycosylation in the blastema during zebrafish tail regeneration. *NPJ Regen Med* **6**, 55.

Sousa, S., Afonso, N., Bensimon-Brito, A., Fonseca, M., Simões, M., Leon, J., Roehl, H., Cancela, M. L. and Jacinto, A. (2011). Differentiated skeletal cells contribute to blastema formation during zebrafish fin regeneration. *Development* **138**, 3897-3905.

Stocum, D. L. (2006). An Overview of Regenerative Biology and Medicine.

Stocum, D. L. (2017). Mechanisms of urodele limb regeneration. *Regeneration (Oxf)* **4**, 159-200.

Tanaka, E. and Reddien, P. W. (2011). The cellular basis for animal regeneration Sources of new cells in animal regeneration. *Dev Cell* **21**, 172-185.

Tang, J. B., Elliot, D., Adani, R., Saint-Cyr, M. and Stang, F. (2014). Repair and reconstruction of thumb and finger tip injuries: A global view. *Clinics in Plastic Surgery* **41**, 325-359.

Tickle, C. (2015). How the embryo makes a limb: determination, polarity and identity. *J Anat* **227**, 418-430.

Tsonis, P. A., Washabaugh, C. H. and Del Rio-Tsonis, K. (1995). Transdifferentiation as a basis for amphibian limb regeneration. *Seminars in Cell Biology* **6**, 127-135.

Vargesson, N. (2020). Positional Information-A concept underpinning our understanding of developmental biology. *Dev Dyn* **249**, 298-312.

Wang, D., Berg, D., Ba, H., Sun, H., Wang, Z. and Li, C. (2019a). Deer antler stem cells are a novel type of cells that sustain full regeneration of a mammalian organ-deer antler. *Cell Death Dis* **10**, 443.

Wang, S., Zhang, C., Hasson, D., Desai, A., SenBanerjee, S., Magnani, E., Ukomadu, C., Lujambio, A., Bernstein, E. and Sadler, K. C. (2019b). Epigenetic compensation promotes liver regeneration. *Developmental Cell* **50**, 43-56.e46.

Yao, Y. and Wang, C. (2020). Dedifferentiation: inspiration for devising engineering strategies for regenerative medicine. *npj Regenerative Medicine* **5**, 14.

Zhao, A., Qin, H. and Fu, X. (2016). What Determines the Regenerative Capacity in Animals? *BioScience* **66**, 735-746.

Zhao, Y., Shen, M., Wu, L., Yang, H., Yao, Y., Yang, Q., Du, J., Liu, L., Li, Y. and Bai, Y. (2023). Stromal cells in the tumor microenvironment: accomplices of tumor progression? *Cell Death & Disease* **14**, 587.

Supplementary Information

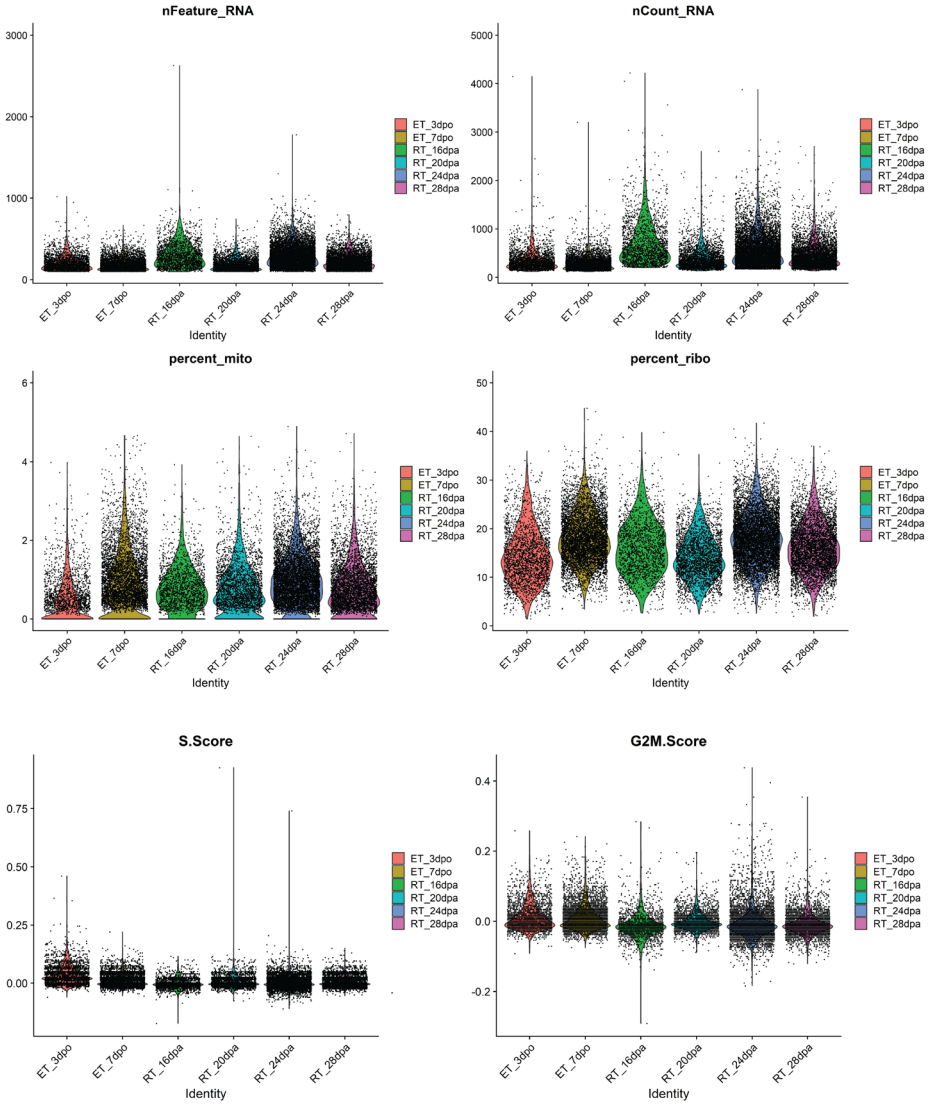

Figure S 4-1. **Quality Control assessment of single cell data used in this chapter.**

Table S 4-1. **The mapping of gene symbols and corresponding gene identifiers in *Sphaerodactylus townsendi* genome**.

No.	Gene symbol	Gene Identifier	Gene description
1.	SPACA4	LOC125430222	sperm acrosome membrane-associated protein 4-like
2.	CDH6	LOC125439157	cadherin-6
3.	LCN	LOC125442120	lipocalin-like
4.	ZIC1	LOC125437433	zinc finger protein ZIC 1 (ZIC 1)
5.	CA13	LOC125438970	carbonic anhydrase 13-like
6.	CA2	LOC125438766	carbonic anhydrase 2-like
7.	HBA1	LOC125431165	hemoglobin subunit alpha-A (HBA1)
8.	ZG57	LOC125428732	gastrula zinc finger protein XlCGF57.1-like
9.	PRPs	LOC125435388	PRPs-basic proline-rich protein (PRPs)
10.	ZSCAN2	LOC125428616	ZSCAN2-zinc finger and SCAN domain-containing protein 2-like
11.	MCPT1	LOC125433220	MCPT1-mast cell protease 1A
12.	MYH3	LOC125429055	MYH3-myosin-3
13.	RBFOX1	LOC125445098	RBFOX1 RNA binding fox-1 homolog 1
14.	KCTD12	LOC125442777	BTB/POZ domain-containing protein KCTD12
15.	MEIOC	LOC125440652	MEIOC-meiosis-specific coiled-coil domain-containing protein MEIOC
16.	PDGFRL	LOC125428064	PDGFRL-platelet-derived growth factor receptor-like protein
17.	CTSK	LOC125444042	cathepsin K-like
18.	GJB6	LOC125432195	GJB6-gap junction beta-6 protein-like
19.	KRT76	LOC125427915	KRT76-keratin, type II cytoskeletal 60 kDa, component III
20.	KRT1	LOC125427914	KRT1-keratin, type II cytoskeletal 1
21.	KRT6A	LOC125429328	KRT6A-keratin, type II cytoskeletal 6A
22.	GLTP	LOC125442796	GLTP glycolipid transfer protein
23.	CYP27B1	LOC125427926	Cyp27b1-25-hydroxyvitamin D-1 alpha hydroxylase, mitochondrial
24.	KRT6A-like	LOC125429093	keratin, type II cytoskeletal 6A-like
25.	KRT5	LOC125429094	KRT5-keratin, type II cytoskeletal 5
26.	LOC125441473	LOC125441473	uncharacterized LOC125441473
27.	ncRNA	LOC125444722	ncRNA
28.	ALG13	LOC125442804	ALG13-UDP-N-acetylglucosamine transferase subunit ALG13 homolog
29.	ARSD	LOC125431876	arylsulfatase D-like
30.	L1CAM	LOC125428002	L1CAM-neural cell adhesion molecule L1
31.	PLA2	LOC125438409	phospholipase A2 inhibitor alpha-like protein
32.	COL9A3	LOC125433411	COL9A3-collagen alpha-3(IX) chain gene
33.	LORICRIN	LOC125439757	loricrin-like
34.	HRNR	LOC125432313	hornerin-like
35.	LOC125425201	LOC125425201	uncharacterized LOC125425201
36.	scale keratin	LOC125439306	scale keratin-like
37.	PKS-NRPS	LOC125440523	hybrid PKS-NRPS synthetase fsa1-like
38.	PECAM	LOC125430216	PECAM-platelet endothelial cell adhesion molecule-like
39.	HBB2	LOC125430938	HBB2-hemoglobin subunit beta-2-like
40.	HBAD	LOC125431166	HBAD-hemoglobin subunit alpha-D-like
41.	CLDN4	LOC125444890	CLDN4-claudin-4
42.	LOC125443220	LOC125443220	5-hydroxyisourate hydrolase-like (Transthyretin)

Chapter 5. *In Situ* Hybridization Study of Gene Expression in Tokay Gecko Tail Regeneration

Luthfi Nurhidayat[1,2], Sira Blom[1], Christina Noordermeer[1], Inês Gomes[1], Nisrina Firdausi[1], Ismail Shaleh[1], Merijn A.G de Bakker[1], Michael K. Richardson[1*]

1. Institute of Biology Leiden, Leiden University, Sylvius Laboratory, Sylviusweg 72, 2333 BE, Leiden, The Netherlands.
2. Faculty of Biology, Universitas Gadjah Mada, Jalan Teknika Selatan Sekip Utara, 55281, Yogyakarta, Indonesia

---

This chapter is part of: Nurhidayat, L., Benes, V., Blom, S., Gomes, I., Firdausi, N., de Bakker, M.A.G., Spaink, H.P., Richardson. M.K. Tokay gecko tail regeneration involves temporally collinear expression of HOXC genes and early expression of satellite cell markers. *BMC Biology*. Under revision. (2024).

Abstract

Lizards (including geckos) can regenerate their tail after shedding it (autotomy). Lizards show the 'epimorphic' type of regeneration which does not involve reorganization of the uninjured part (as in morphallaxis) but instead show regeneration from an outgrowth of stem cells organized into a compact mass or blastema. Lizard tail regeneration involves multiple types of histogenesis: replacement of vertebrae with cartilage (chondrogenesis), formation of new vasculature (angiogenesis), new muscle development (myogenesis), adipose tissue regeneration (adipogenesis), and innervation by axons (axonogenesis). In this chapter, we examined the spatial and temporal expression of genes involved in histogenesis and tissue patterning during tokay gecko tail regeneration. We performed *in situ* hybridization on sections of tails at 4, 8, 16, 20, 24, 28, and 49 days post-autotomy. The results showed that the regenerating tail of the tokay gecko expressed relatively few axonogenesis genes. Moreover, we found the unique expression pattern of cartilage and skeletal muscle development in the regenerating tail. In addition, we also found temporally collinear expression of posterior HOXC genes in the regenerating tail. These results are consistent with a model in which the regeneration of the tail in the tokay gecko involves an early activation of a stem cell population, likely comprising satellite cells and fibroblasts, that retain positional information from the original tail. This positional memory allows the regeneration of a replacement tail that is consistent with the axial level of autotomy. This likely contrasts with regeneration in the axolotl and zebrafish where a new positional coordinate system is established *de novo*, as seen in normal development.

Introduction

Regeneration is the ability of organisms to replace their damaged cells, tissue or organ with a new functional one. Lizards (including geckos) show remarkable tail regeneration after undergoing autotomy. Autotomy is the self-defense mechanism in which a lizard can shed part of its tail to distract predators (Congdon et al., 1974). This mechanism is morphologically adapted with the presence of bone fracture planes and autotomy septa along the tail tissues that make it easier for the tail to be shed (Lozito and Tuan, 2017).

Tail regeneration in lizards is of the 'epimorphic' type of regeneration because it does not involve reorganization of the uninjured part (as in morphallaxis) but instead involves regeneration from an outgrowth from stem cells organized into a compact mass or blastema (Lozito et al., 2016). The process of tail regeneration in lizards consist of the following conserved major stages (Alibardi, 2014; Lozito and Tuan, 2017; McLean and Vickaryous, 2011): (1) degeneration (wound healing); (2) proliferation (blastema formation); (3) differentiation (tail elongation); and (4) maturation. Note that these stages are also described as including the formation of an apical ectodermal cap over the blastema, but we have not found such a structure in this thesis (see Chapter 2).

These stages involve the replacement of lost vertebrae with a cartilage tube (chondrogenesis), formation of new vasculature (angiogenesis), new muscle development (myogenesis), adipose tissue regeneration (adipogenesis), and innervation by axons (axonogenesis). In geckos, tail regeneration results in a new tail structure that lacks vertebrae and true tendons (Lozito and Tuan, 2017). Instead, the unsegmented cartilage tube is formed to functionally replace the vertebrae by chondrogenesis as response to hedgehog signaling (Alibardi, 2010; Londono et al., 2017; McLean and Vickaryous, 2011). Furthermore, the spinal cord is replaced by an ependymal tube growing inside the lumen of the cartilage tube (Alibardi, 2010; Londono et al., 2017; McLean and Vickaryous, 2011). The ependymal tube is thought to be derived from the epithelial lining of the central canal of the uninjured spinal cord (Alibardi, 2014; Alibardi, 2015; Lozito and Tuan, 2015; Lozito and Tuan, 2016). The regenerating tail is innervated by nerve fibers that enter from the dorsal root ganglia located in the normal (uninjured) tail (Cristino et al., 2000; McLean and Vickaryous, 2011; Tokuyama et al., 2018).

Finally, the skeletal muscle in the regenerated tail is arranged in a ring and not in four blocks as it was in the original (Alibardi, 2010; Londono et al., 2017; McLean and Vickaryous, 2011). The regeneration of muscle in lizard tails begins with the aggregation and differentiation of blastema cells into individual myoblasts (Lozito and Tuan, 2017). Investigations of the regenerating tails of the green anole and the Common Garden Skink have demonstrated that these myoblasts then fuse into bundles of myotubes (Alibardi, 1995). Additionally, the non-fusing cells present among the myotubes

contribute to the formation of the connective tissue myosepta (Alibardi, 1995). However, the mechanism of segmentation of muscle without somite formation in lizard tail regeneration remains unclear. It is interesting to ask whether *lfng* and *hes7* are involved in muscle segmentation or not, because they are known to be involved in somite segmentation in the embryo (Bessho et al., 2001; Chen et al., 2005; Kageyama et al., 2012; Okubo et al., 2012)

These features indicate that the regeneration process only partially replicates the embryonic development of the tail, and likely relies on distinct mechanisms to redevelop the lost structures. Therefore, in this chapter, we have analyzed the spatial and temporal expression of genes involved in axonogenesis, chondrogenesis, myogenesis, segmentation and tissue patterning during tokay gecko tail regeneration using *in situ* hybridization on tissue sections.

Material and Methods

Ethics statement

The tokay gecko (*Gekko gecko*) is listed as 'least concern' in the International Union for Conservation of Nature *Red List* (IUCN, https://www.iucnredlist.org/species/195309/2378260) and also listed in Appendix II in the Convention on International Trade in Endangered Species of Wild Fauna and Flora (CITES; https://cites.org/eng/taxonomy/term/3919). In Indonesia, the tokay gecko is not a protected species. All animals were collected in Yogyakarta, Indonesia under a license issued by the Ministry of Environment and Forestry, the Republic of Indonesia (permit number SK.83/KSDAE/SET/KSA.2/5/2021 signed on 7 May 2021) and a recommendation letter issued by The Indonesian Institute of Sciences (Lembaga Ilmu Pengetahuan Indonesia/LIPI; Recommendation Number: B- 2158 /IV/KS.01.04/3/2021 signed on 19 March 2021). The transport of samples from Indonesia to the Netherlands was conducted under CITES permit numbers 05717/IV/SATS-LN/2021 and 09160/IV/SATS-LN/2022 issued by the Ministry of Environment and Forestry, the Republic of Indonesia.

All experimental and surgical procedures needed for samples collection were done at Faculty of Biology, Universitas Gadjah Mada, Yogyakarta, Indonesia with the approval from The Ethical Committee of the Integrated Laboratory for Research and Testing (Laboratorium Penelitian dan Pengujian Terpadu/LPPT) Universitas Gadjah Mada (Ethical Clearance number: 00014/04/LPPT/IV/2021 signed on 30 April 2021).

Experimentation and samples collection

Twenty-one adult tokay geckos were anaesthetized with intramuscular ketamine injection (50–75 mg/Kg body weight) administered in the thigh prior to the autotomy procedure. Autotomy was performed by gently restraining the gecko manually, while

leaving the tail accessible. Using the thumb and index finger, a firm pinch was applied to the required autotomous region (every segment after the 5th caudal vertebra) of the tail causing the gecko to spontaneously shed its tail. The wound was painted with Betadine® iodine antiseptic solution but no dressing was applied. After the autotomy procedure was performed, the geckos were allowed to regenerate a new tail. The geckos were distributed into experimental groups based on the number of days post-autotomy, each consisting of three geckos. After ketamine-anesthesia, the tails of geckos in each group were re-autotomized 2 cm cranially from the previous autotomy site at 0, 4, 8, 16, 20, 24, 28, and 49 days post-autotomy (dpa). The regenerated tail samples were washed and further handled in phosphate-buffered saline (PBS, 4 °C) and subsequently fixed with cold 4% paraformaldehyde (pFA) in PBS.

Probe synthesis

In this project, all gene names follow the style and nomenclature of the NCBI database for *Podarcis muralis* (Common Wall Lizard). There was no published annotated genome sequence available for the tokay gecko (*Gekko gecko*) at the time. The predicted regions of the *Gekko gecko* genome for the genes were aligned using the NCBI nucleotides database, to find orthologues in other lizard genomes. Primers were designed based on the conserved regions of the aligned sequences using BLASTn. Using these primers (approximately 800 bp in length), each gene of interest was amplified using the PCR from Gekko gecko cDNA (Supplementary protocol).

The amplicons were cloned into a plasmid (*Escherichia coli* vector pCR™II-TOPO™) following the TOPO™ cloning reaction protocol (Invitrogen, Carlsbad). The bacterial clones were subsequently sequenced (BaseClear B.V., the Netherlands). Probe synthesis was carried by labelling antisense RNA probes with dioxygenin-11-UTP (Roche) according to the manufacturer's protocols.

Histology and in situ hybridization

The regenerating tail blastema samples were rinsed in RNAse-free PBS and fixed in cold 4% paraformaldehyde in PBS. The fixed samples were decalcified by soaking them in Osteosoft® (Sigma-Aldrich) for 3–5 d. The decalcified samples were then dehydrated with a graded concentration series of methanol starting from methanol 70%, 80%, 90%, 100% for 2 x 30 min. The samples were cleared 3 x 1 h (Neo-Clear®, Merck-Millipore). The samples were infiltrated 2 x 1 h molten paraffin (62 °C) and 1 x 8–18 h. The samples were finally embedded with fresh molten paraffin and solidified at room temperature.

The paraffin blocks were then sectioned longitudinally at 6–8 µm on a rotary microtome. The sections were mounted on poly-L-lysine coated slides and left overnight at 37 °C. Alternating sections were taken for *in situ* hybridization or histological staining, respectively. For *in situ* hybridization we based our protocol on those in (Acloque et al.,

2008). The sections were deparaffinized with xylene 3 x 7 min and rehydrated using a graded ethanol series (100% 3 x 2 min; 90%, 80%, 70% for 1 min each). After that, pre-treatment was performed using PBST (phosphate buffered saline with triton) 3 x 5 min, proteinase K (10 ng/ml) 10 min, PBST 3 x 5 min, 4% paraformaldehyde (pFA) 10 min, and PBST 2 x 5 min. Then, the sections were covered with pre-hybridization mix (without probe) for ≥1 h at 60 °C, and incubated with probe mix (1000-1500 ng/mL) at 60 °C overnight with a cover slip. Next day, the sections were washed using washing solution A (2 x SSC (standard sodium citrate) 0.1% CHAPS (3-[(3-cholamidopropyl) dimethylammonium]-1-propanesulfonate), 50% formamide) 3 x 30 min and TBST ([tris (hydroxymethyl)aminomethane] buffered saline with triton) 3 x 10 min. Anti-DIG-AP detection was carried out using 10% sheep serum in TBS (tris buffered saline) for 1 h and continued with anti-DIG-AP (1:1000 concentration) in 10% sheep serum in TBST at 4 °C overnight. Finally, the sections were covered with TBST 3 x 10 min and NTT (NaCl tris buffer with tween) pH 9.5 3 x 10 min. Staining was conducted using BM purple (Roche) and was checked regularly under the microscope for up to two days. When the desired, degree of color was achieved, the staining was stopped. The samples were then dehydrated by quickly dipping in graded ethanols (70%, 80%, 90%, 3 x 100%), and coverslip using Eukit®.

Results

At 8 dpa, there were scattered mesenchymal cells beneath the wound epithelium and most of these cells were *col1a2* expressing (Figure 5-1A, B, C). Together with this mesenchymal tissue we observed structures that resembled adult skeletal muscle (arrowhead in Figure 5-1B, C). By 16–20 dpa, *col1a2* was widely expressed in the blastema, except in developing muscle and cartilage (Figure 5-1, D–I). At 24 dpa, *col1a2* became expressed in the myosepta (Figure 5-1 K, L). We found no expression of *col1a2* in the uninjured (adult) tail (Figure 5-1A, D, G, J, M).

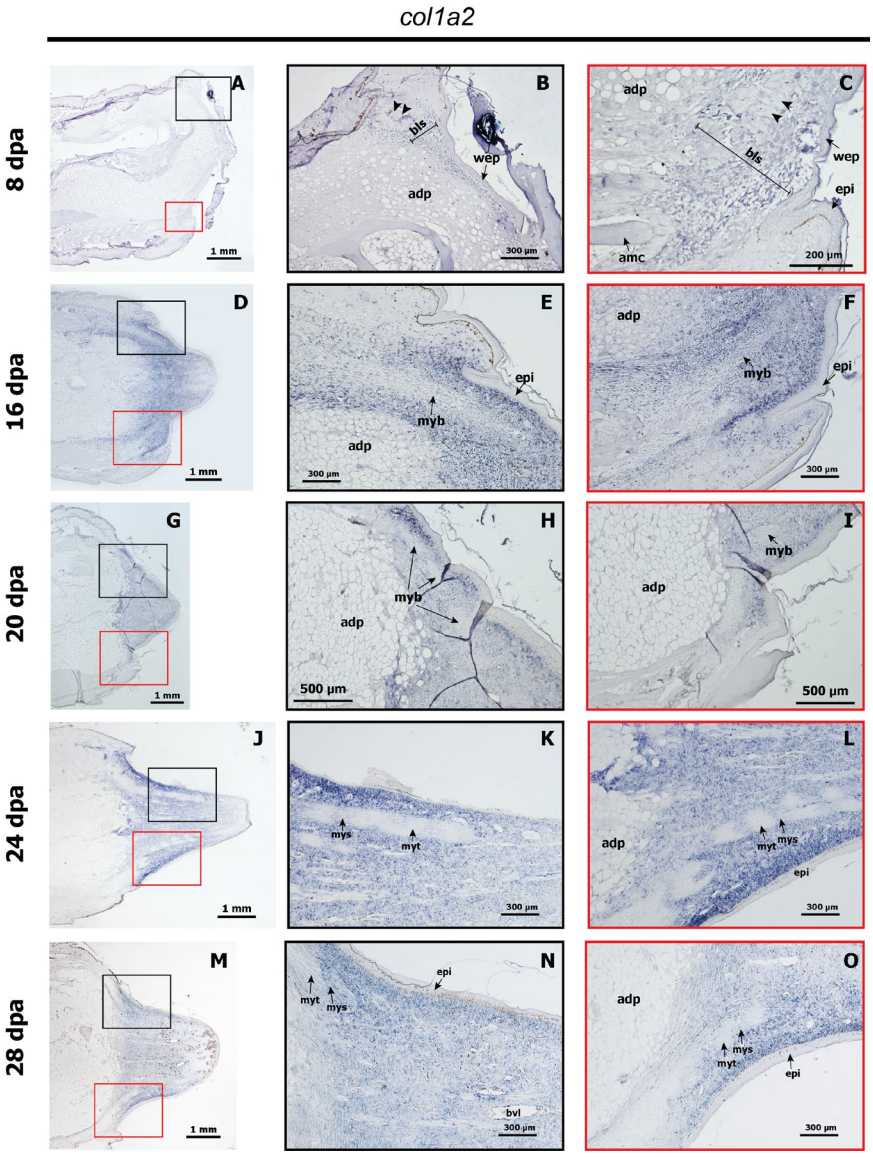

Figure 5-1. **Expression of *col1a2* is specific to developing connective tissue in the tokay gecko regeneration blastema.** Note that *col1a2* is expressed in the blastema but not at all in the original tail tissue. *Key*: adp, adipose tissue; amc, adult muscle cells; bls, blastema; bvl, blood vessel; ct, cartilage tube; ep, epidermis; ery, erythrocytes; leu, leukocytes; pbl, pre-blastema; myb, myoblast; mys, myoseptum; myt, myotubes; nvf, nerve fiber; wep, wound epithelium.

The regenerating tail expressed relatively few genes involved in axon development (axonogenesis)

The regenerated gecko tail has only an ependymal tube in place of a spinal cord. In order to understand why development of the nervous system is so limited in the regenerated, we studied the expression of eight axonogenesis-related genes, namely: *ngf*, *unc5a*, *nefh*, *notch3*, *efna*, *ntf3*, *gap43*, and *sema3a* (Figure S 5-2). This should also help us determine whether axonogenesis in the regenerating tail makes use of the same genes that are deployed in normal embryonic development.

We found that only three of these axonogenesis genes, *unc5a*, *nefh*, and *notch3*, were expressed in the regenerating tail blastema (Figure 5-2). At 20 dpa, there was slight expression of *unc5a* and *nefh* in the myotubes of the regenerating tail (Figure 5-2C, F). There was no expression of *notch3* at this stage (Figure S 5-2 E, F). At 28 dpa, *unc5a* and *nefh* showed clear expression in the developing skeletal muscle myotubes (Figure 5-2I, L). Moreover, *notch3* was weakly expressed in myotubes in the proximal part of the blastema, at this stage (Figure 5-2O). In addition, expression of *unc5a* and *nefh* was detected in cell bodies in the dorsal root ganglia (DRG) of the original (uninjured) tail at 20 and 28 dpa (Figure 5-2B, E, H, K). Even though the other genes (*ngf*, *efna*, *ntf3*, *gap43*, and *sema3a)* were not expressed in the blastema, we know that the probe worked because these genes were expressed strongly in the dorsal root ganglia and dermis of the uninjured tail, in the same histological sections (Figure S 5-2).

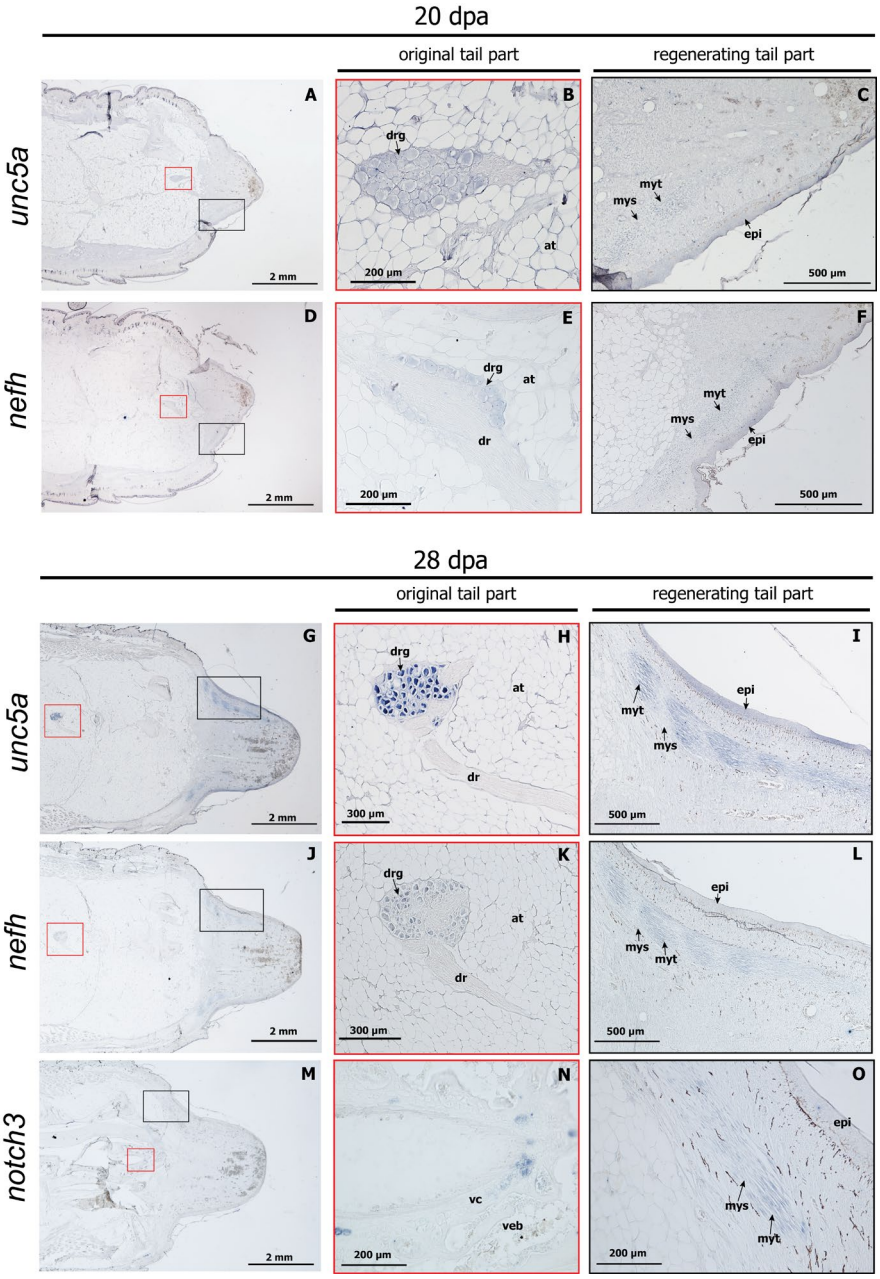

Figure 5-2. **The regenerating tail expresses relatively few genes involved in axon development (axonogenesis)**. (A) The expression of *unc5a* and *nefh* in 20 dpa regenerating tail. In situ hybridization on tissue sections. (B) The expression of *unc5a*, *nefh*, and *notch3* in 28 dpa regenerating tail. Key: at, adipose tissue; dr, dorsal root; drg, dorsal root ganglia, epi, epidermis; myt, myotube; mys, myoseptum.

Chondrogenesis in the regenerating tail is uncoupled from segmentation

The absence of vertebrae in the regenerated tail is a major unexplained phenomenon. One possible explanation could be that genes normally associated with chondrogenesis in embryonic development of the vertebrae, are not expressed in the regenerating tail. In this section we examine this hypothesis by looking at the expression of the chondrogenesis-related genes *sox9*, *wnt5a*, *wnt3*, *bmp1* and *bmp3*. Using *in situ* hybridization on tissue sections, we find *sox9* expression in the cartilage tube from 20–49 dpa, and in myotubes at 20 dpa only (Figure 5-3). *Wnt5a* was expressed in the cartilage tube, myotubes and dermis at the 20 and 49 dpa (Figure 5-4A, B, C). *Wnt3* was expressed in myotubes, the pre-cartilaginous cartilage tube, and epidermis at 20 and 30 dpa (Figure 5-4D–I). By 49 dpa the cartilage tube showed strong expression of *bmp3* in its proximal part; expression of *bmp3* in the myotubes was weak by this stage (Figure 5-5A, B, C). *Col2a1*, a cartilage marker, was expressed specifically in the cartilage tube at 24 dpa (Figure 5-5D, E).

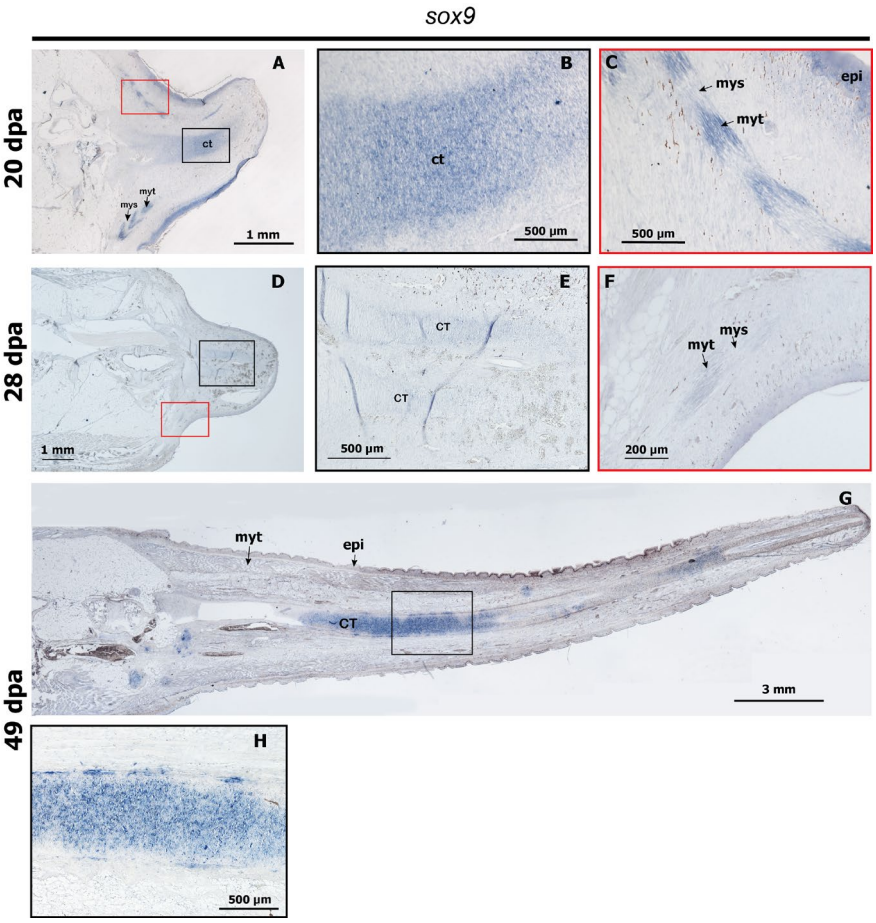

Figure 5-3. **Expression of *sox9* in the regenerating tail of tokay gecko**. *Key*: epi, epidermis; ct, cartilage tube; myt, myotube; mys, myoseptum.

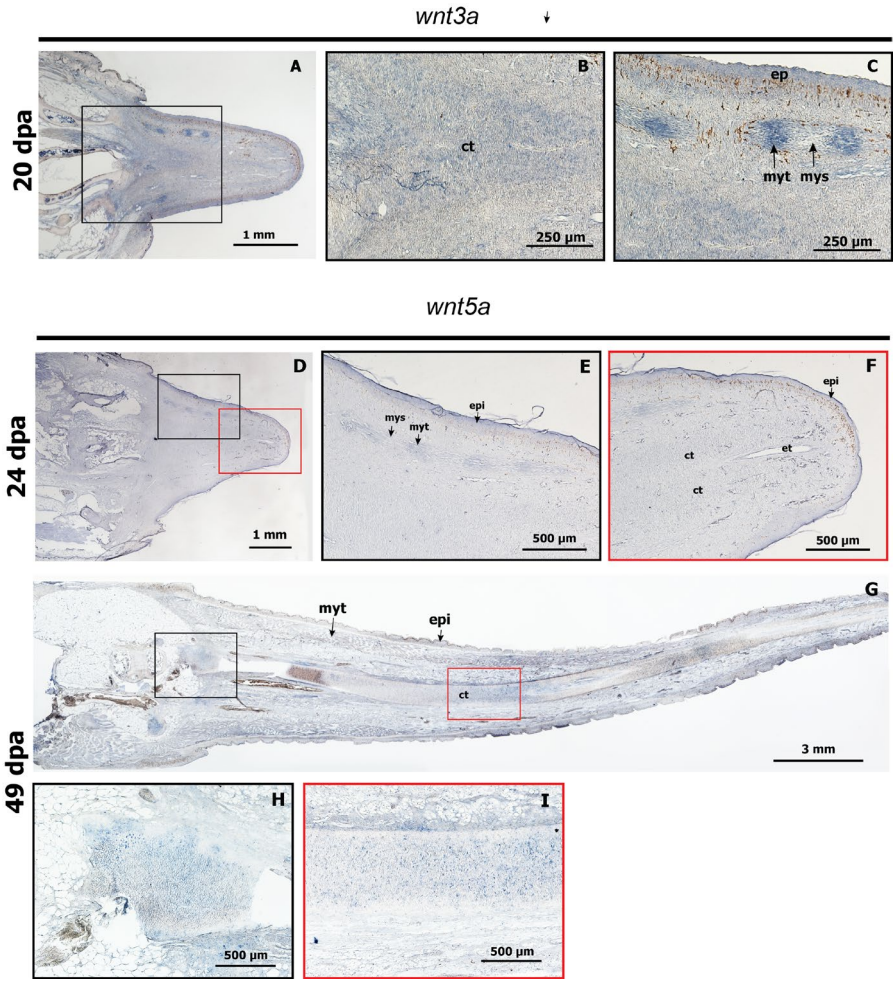

Figure 5-4. **Expression of *wnt3* and *wnt5a* in the regenerating tail**. *Key:* epi, epidermis; ct, cartilage tube; myt, myotube; mys, myoseptum.

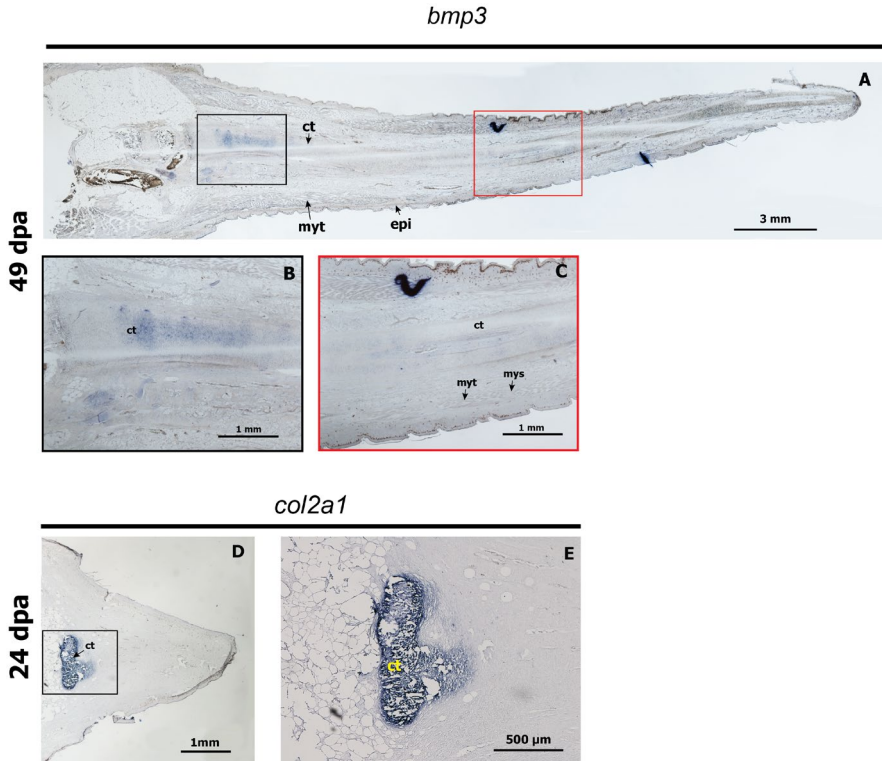

Figure 5-5. **Expression of *bmp3 col2a1* in the regenerating tail**. *Key*: epi, epidermis; ct, cartilage tube; myt, myotube; mys, myoseptum.

Tail regeneration in the tokay gecko involves a unique pattern of skeletal muscle development

The skeletal muscles of the regenerating tail are formed segmentally, as a longitudinal series of myomeres separated by fibro-connective tissue myosepta. We wanted to examine whether muscle development in the regenerating tail resembles muscle development in the embryo. To do this, we looked at the expression of genes related to muscle development, namely: *pax3*, *pax7*, *myod1*, *myog*, *ckm*, and *tnc*. We also hypothesized that the segmentation of regenerating muscles was based on the activity of genes that are normally involved in embryonic somite segmentation. Therefore, we also looked at the expression of *lfng* and *hes7*, which are known to be involved in somite segmentation. We also looked at paralogs of *hes7*, namely: *hes1*, *hes2*, *hes5*, and *hes6*, to see if they have acquired a function in regeneration (by neofunctionalization, for example).

We found expression of *pax3*, *pax7* and *myod1* in some of the mesenchymal cells under the wound epidermis (i.e. the newly-formed blastema), at 8 dpa (Figure 5-6). At 16 dpa these three genes are expressed in cells that appear to be forming myoblast

clusters (as indicated by their *myod1* expression) (Figure 5-7). These clusters are present in regions of the blastema that lack *col1a2* expression (Figure 5-1E, F). The expression of *myog, ckm* and *tnc* is first seen in myotubes at 24 dpa (Figure 5-8). Myotubes at this stage, like the myoblasts before them, lack *col1a2* expression; however, *col1a2* was expressed in the connective tissue myosepta (Figure 5-1K, L). Furthermore, *lfng* was expressed in myoblasts at 16 and 20 dpa, and in myotubes at 24 and 28 dpa (Figure 5-9). *Hes2* was expressed in myotubes and blood cells at 24 and 28 dpa (Figure 5-9). We found no expression of *hes6* in the regenerating tail (Figure S 5-3).

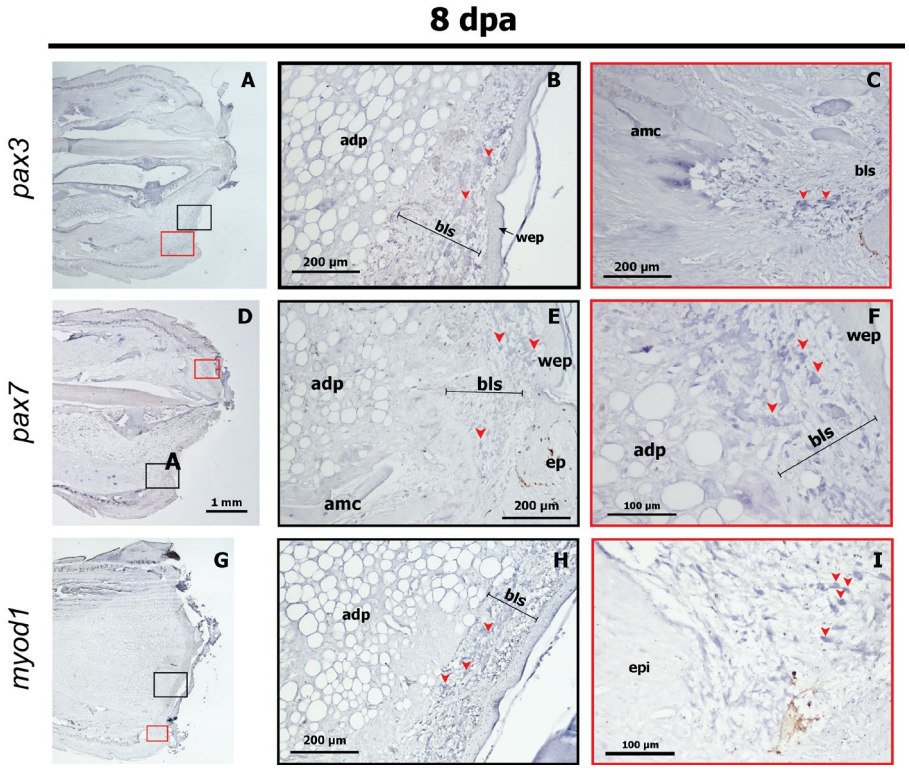

Figure 5-6. **Expression of *pax3*, *pax7* and *myod1* at 8 dpa in the regenerating tail**. *Key*: adp, adipose tissue; amc, adult muscle cells; bls, blastema; wep, wound epithelium.

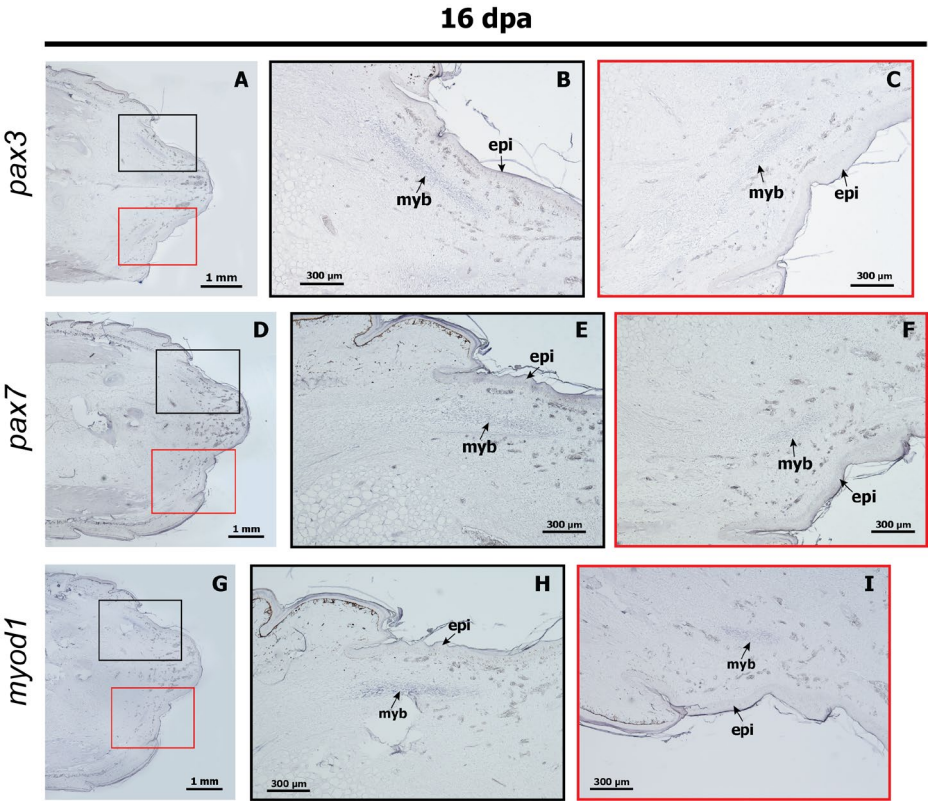

Figure 5-7. **Expression of pax3, pax7 and myod1 at 16 dpa in the regenerating tail**. *Key*: epi, epidermis; myb, myoblast.

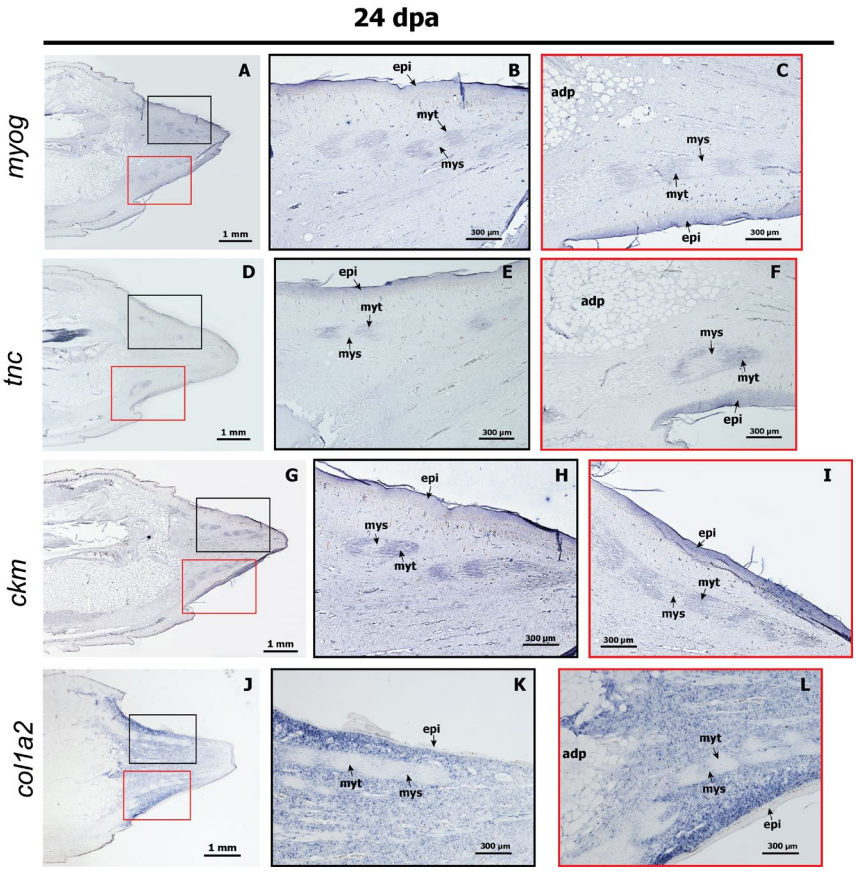

Figure 5-8. **Expression of *myog*, *tnc*, and *ckm*, at 24 dpa in the regenerating tail**. *Key*: myt, myotube; mys, myoseptum.

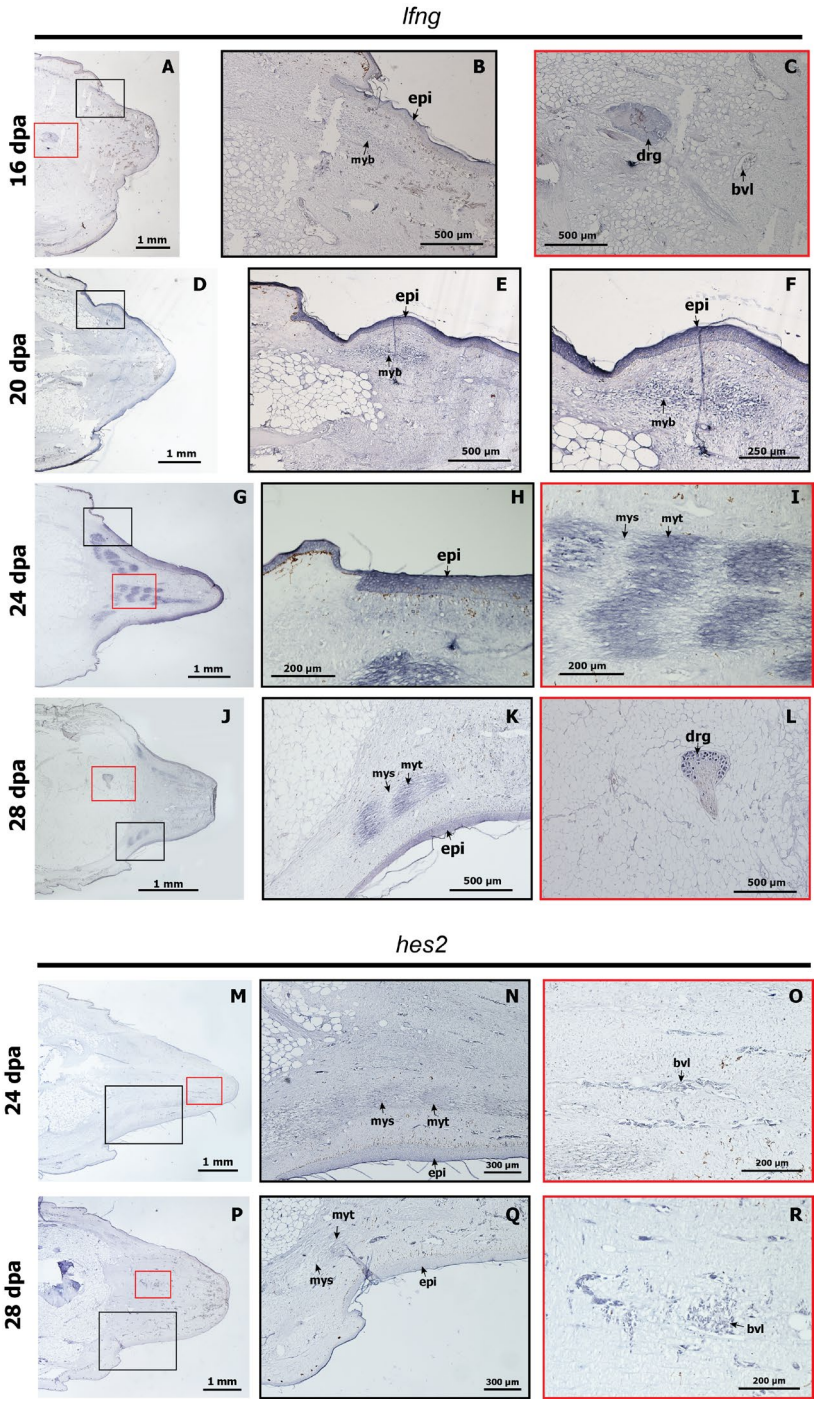

Figure 5-9. **Expression of *Ifng* and *hes2* in the regenerating tail**. *Key*: bvl, blood vessel; drg, dorsal root ganglion; myt, myotube; mys, myoseptum.

Posterior HOXC genes show temporally colinear expression during regeneration

To examine the expression of the posterior HOXC genes (*hoxc10–13*), we used *in situ* hybridization on tissue sections. We found that these genes are all expressed in the developing skeletal muscles and the wound epithelium of the regenerating tail (Figure 5-10). However, these genes differed in the timing of their expression. Thus, at 16 dpa, weak expression of *hoxc10* was observed in the wound epithelium, and in scattered mesenchymal cells, which we believe to be putative muscle progenitor cells (myoblasts) because of their expression of myod1 (see previous section above) and their peripheral location in the proximal region of the blastema (Figure 5-10A, Figure S 5-1). There was no expression of *hoxc11–13* genes at this stage (Figure 5-10E, I, M).

At 20 dpa, we observed expression of *hoxc10–12* in both the wound epithelium, and in the myotubes of developing muscles, but not the myosepta, thereby forming a metameric pattern (Figure 5-10B, F, and J). *Hoxc13* was not expressed at this stage (Figure 5-10N). At 24 dpa, all posterior HOXC genes are expressed in the wound epithelium and in newly-formed skeletal myotubes with myosepta (Figure 5-10C, G, K, O). *Hoxc13* expression at this stage was relatively weak (Figure 5-10O). At 28 dpa, only *hoxc12* and *hoxc13* expression can still be observed in the wound epithelium and regenerating muscles (Figure 5-10L, P). However, at this stage, *hoxc10*, *hoxc11* and *hox13* are no longer expressed (Figure 5-10D, H).

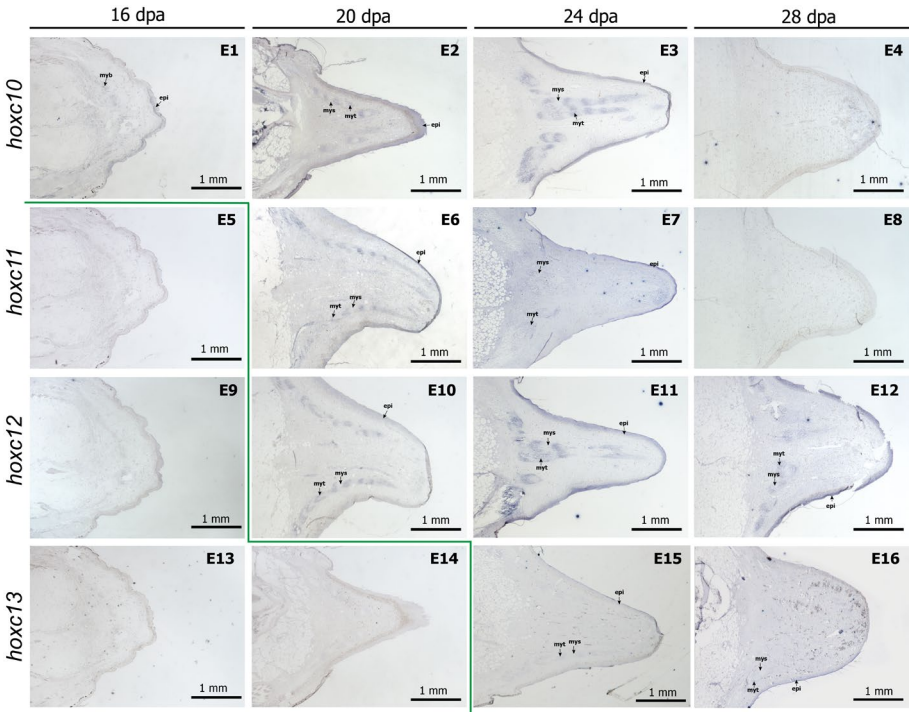

Figure 5-10. **Temporal collinearity in expression of caudal HOXC genes during tail regeneration**. *In situ* hybridization on tissue sections. For high magnification views of these sections, see Figure S 5-1. *Key*: myb, myoblast; myt, myotube; mys, myoseptum; epi, epidermis.

Discussion

In this chapter, we examined the expression of genes involved in axonogenesis, chondrogenesis, myogenesis, segmentation, and tissue patterning during tokay gecko tail regeneration. The results revealed unique gene expression patterns associated with the histogenesis of the regenerating tail. Furthermore, the findings indicated the activation of stem cells residing within the tissues of the original tail, which we suggest utilizing their existing positional memory to guide the regeneration process.

As we have found in Chapter 3 with our transcriptomics study, the regenerating tail of the tokay gecko seems to implement an atypical pattern of gene regulation for tissue development. For example, in this chapter, we find that only three out of eight examined axonogenesis-related genes were expressed in the regenerating gecko tail. These three genes (*unc5a*, *nefh*, and *notch3*) were all expressed in differentiating myotubes at 28 dpa. It is likely that this expression corresponds to the formation of motor end plates because it is known from studies on tail regeneration in other lizard species that the myomeres become innervated by axons that grow into the blastema

from the uninjured stump (Alibardi, 2021; Tokuyama et al., 2018). *Unc5a* orchestrates axonal repulsion, outgrowth, and branching initiated by Netrin-1 (Tokuyama et al., 2018). It is possible that *unc5a* expression in the regenerating myotubes activates axonal branching as growth cones reach the myotubes, and that it also influences the site of formation of neuromuscular junctions (Tokuyama et al., 2018). *Nefh* encodes the neurofilament heavy chain subunit (Elder et al., 1998). In our study, *nefh* is expressed in myoblasts at 20 dpa, and in differentiated myotubes at 28 dpa. On the other hand, we find expression of *notch3*, known for inhibiting the differentiation of neural stem cells, in muscle progenitors at 28 dpa. This indicates a probable role for *notch3* in maintaining the development of regenerating muscle tissue, consistent with prior findings (Kitamoto and Hanaoka, 2010).

In addition, we also found robust expression of *nefh* and another axonogenesis-related gene *gap43* in the dorsal root ganglia (DRGs) of the uninjured part of the tail. This supports the notion (Alibardi, 2021; Lozito and Tuan, 2017) that the uninjured DRGs are the source of axons that innervate the regenerating tail blastema. DRGs proximal to the autotomy plane are known to exhibit hypertrophy and heightened amino acid uptake following autotomy (Geuna et al., 1998). Consistent with this, increased *gap43* expression in DRGs has been observed in rats following nerve injury (Li et al., 2015), and GAP43 protein was detected in the regenerating lizard tail (Alibardi, 2021). Our data also implicate the involvement of axonal pathfinding receptor genes, particularly *unc5a*, in sensory axonogenesis, especially in axons elongated from DRGs of 28-dpa gecko regenerating tails. Our finding of robust expression of *unc5a* in DRGs is consistent with its role in the axonogenesis of sensory neurons during lizard tail regeneration (Alibardi, 2021).

In Chapter 3, we found that the GO term 'cartilage development' was enriched at 16 dpa. However, in this chapter, we find that early cartilage histogenesis did not begin until 20 dpa, when the *sox9*$^{+}$ pre-cartilage precursor of the cartilage tube was first seen. This precursor had the form of a pre-cartilage condensation. In general, pre-cartilage condensations consist of chondroprogenitor cells which differentiate into chondroblasts, secrete extracellular matrix and ultimately develop into mature cartilage cells or chondrocytes (Song and Park, 2020). These processes culminate in the formation of the first hyaline cartilage in the proximal part of the tail by 49 dpa. The cartilage tube continues to differentiate after the skin and muscles have matured, consistent with findings in other lizard species (Alibardi, 2014; McLean and Vickaryous, 2011).

Sox9 is expressed not only in the pre-cartilage condensations at 20 dpa but is also strongly expressed in the cartilage tube at 49 dpa. This is consistent with a role of *sox9* in chondroblast differentiation, a process that may be co-activated by *sox5* and *sox6* (Kozhemyakina et al., 2015). *Sox9* may also inhibit bone differentiation (Dy et al., 2012) which is interesting because the cartilage tube is still un-ossified at oldest stage we

examined (49 dpa). *Bmp3* is also thought to suppress osteoblast differentiation and inhibit ossification (Daluiski et al., 2001; Kokabu et al., 2011) and was also expressed at 49 dpa. *Wnt3* was expressed in the distal part of the regenerating cartilage tube, consistent with a known role in chondrocyte differentiation (Green et al., 2015). *Wnt5a* was expressed in the pre-cartilage condensations and in myoblasts, consistent with its multiple roles in lizard tail regeneration (Hutchins et al., 2014). Our findings align with studies emphasizing the importance of Wnt pathways in tissue patterning and differentiation during development and regeneration (Klaus and Birchmeier, 2008; Nusse and Clevers, 2017).

We found that the reactivation of resident stem cells may underlie myogenesis during tail regeneration, as it does in axolotl limb regeneration (Sandoval-Guzman et al., 2014). The maturation of skeletal muscle becomes apparent at 24 dpa with the appearance of myotubes expressing *myog, tnc* and *ckm*. There are two existing hypotheses of myogenesis in tetrapod tail and limb regeneration. One postulates the dedifferentiation of mature skeletal muscle fibers in the uninjured stump tissue (Echeverri et al., 2001; Slack, 2006). The other postulates the activation of resident stem cells (Rodrigues et al., 2012; Sandoval-Guzmán et al., 2014; Slack, 2006). For example, limb regeneration in newts requires the dedifferentiation of myotubes, but myogenesis during limb regeneration in axolotls relies on the activation of resident stem cells (Sandoval-Guzman et al., 2014).

The results show that the expression of the muscle lineage markers *pax3*, *pax7* and *myod1* began at 8 dpa. It is possible, therefore, that myogenesis during gecko tail regeneration involves an early activation of satellite cells (muscle resident stem cells). Our reasoning is that *pax7* and *myod1* are co-expressed during satellite cell activation (Zammit et al., 2006). Based on previous studies (Alibardi, 2014; Wosczyna and Rando, 2018), and on our data in this chapter, it is likely that cells that express *pax3*, *pax7* and *myod1* will aggregate and differentiate into mononuclear myoblasts at 16 dpa. The early expression of *pax3* and *pax7* is also seen in the regenerating tail blastema of the green anole lizard *Anolis carolinensis* (Hutchins et al., 2014) and Schlegel's Japanese Gecko, *Gekko japonicus* (Liu et al., 2021).

The fact that the skeletal muscle in the regenerated lizard is arranged into segments (bundles of myotubes separated by myosepta) raises the question of whether regeneration involves a re-activation of embryonic segmentation genes. Such genes could included *lfng* and *hes7* which are necessary for somitogenesis in the embryo (Bessho et al., 2001; Kageyama et al., 2012). Our results suggest that only *lfng* is expressed in the muscle lineage of the regenerating gecko tail. *Lfng* is a modulator of the Notch signaling pathway (Mugisha et al., 2022), and this pathway is recognized for its function in promoting the self-renewal of satellite cells through direct modulation of *pax7* (Wen et al., 2012).

Among the Hes genes, only *hes2* was expressed in gecko tail regenerates, in the skeletal muscle and haemopoietic lineages. And even *hes2* is unlikely to be involved in muscle segmentation because we only find it expressed at 24 dpa, after the muscles have already segmented. Our suggestion, of a lack of Hes gene involvement in muscle segmentation in the regenerating gecko tail, is consistent with a study on axolotl tail regeneration (Wouter et al., 2024). That study found evidence that *lfng*$^{+}$ multipotent stem cells (which they called 'asomitic' stem cells) give rise to segmented structures during regeneration without the involvement of *hes7* (Wouter et al., 2024). We suggest that muscle segmentation in the regenerating tokay gecko tail relies on positional memory in satellite cells, which 'remember' the segmental pattern of the original muscle. This hypothesis is supported by a study of mouse cell lines, showing that satellite cells have positional memory regulated by *hoxa10* (Yoshioka et al., 2021). In summary, there is evidence supporting our resident stem-cell hypothesis in muscle regeneration in the tokay gecko tail.

In relation to the concept of positional memory, we also found interesting results on posterior HOXC gene expression. These genes are member of the HOX family that may encode anatomical positional memory or cellular identity (Steens and Klein, 2022; Yoshioka et al., 2021). During embryonic development, HOX gene expression is both spatially and temporally collinear (Mallo and Alonso, 2013; Woltering et al., 2009), meaning that HOX genes become transcriptionally active along the body axis, and over developmental time, in a sequence reflecting their position along the chromosome. However, our results indicate that the posterior HOXC genes (*hoxc10–13*) show temporal collinearity, but not spatial collinearity, in the regenerating tail.

Hox genes are known to be important in regeneration. In caudal fin regeneration in the zebrafish, for example, *hoxc13a* and *hoxc13b* are expressed early and distally in the blastema (Thummel et al., 2007). It would be interesting to know whether HOXC expression patterns in the regenerating tail are determined by existing positional information in the intact tail, before it was shed. This could arise, for example, if there is differential expression of hox genes along the normal tail. It would also explain why the regenerating gecko tail replaces a similar number of muscle segments that were present before the tail was amputated. This is also the case in the axolotl limb, which regenerates only those limb parts appropriate to the proximodistal level of the amputation plane (Pescitelli and Stocum, 1980). A similar situation is seen with the zebrafish caudal fin regeneration in which only the appropriate missing parts are replaced (Uemoto et al., 2020).

In mammals, at least some HOX genes are expressed in the adult, often in the same position-specific pattern or 'hox code' that they showed during embryonic development (Hubert and Wellik, 2023; Leucht et al., 2008; Rux et al., 2016). Furthermore, fibroblasts from adult humans (Chang et al., 2002) and skeletal muscle

from adult mice (Yoshioka et al., 2021) have 'positional memory' that reflects their anatomical location. Together, these findings may shed light on tail regeneration in the gecko. Thus, it is possible that resident stem cells at the autotomy site may have some kind of positional memory. Consistent with this idea, our data also indicate that resident stem cells might be the main precursor cell population in the regenerating tail. Our single cell analysis (Chapter 4) confirmed this.

These and other data suggest a model in which resident stem cells, in this case satellite cells, at the amputation plane use their positional memory to regenerate an appropriate number of muscle segments. Furthermore, we suggest that resident stem cells do this without generating *de novo* a system of positional information as is the case in normal development (of the embryonic limb bud or tailbud, for example). We suggest this because the gecko regeneration blastema has properties very different from a classical developmental field, in which positional values are specified *de novo*. Finally, we suggest that the late expression of *hoxc13* that we observed here represents the finalization of the patterning process in gecko tail regeneration, since it is known that *hoxc13* is essential for terminating normal tail development in the embryo (Aires et al., 2019).

In summary, this chapter provides evidence that the regeneration of the tail in the tokay gecko involves an early activation of a stem cell population, likely comprising satellite cells and fibroblasts, that retain positional memory from the original tail. This positional memory allows the regeneration of an appropriate tail replacement, without the regenerative blastema establishing a new positional coordinate system *de novo* as seen in normal development.

References

Acloque, H., Wilkinson, D. G. and Nieto, M. A. (2008). Chapter 9 In Situ Hybridization Analysis of Chick Embryos in Whole-Mount and Tissue Sections. *Methods in Cell Biology* **87**, 169-185.

Aires, R., de Lemos, L., Nóvoa, A., Jurberg, A. D., Mascrez, B., Duboule, D. and Mallo, M. (2019). Tail bud progenitor activity relies on a network comprising gdf11, lin28, and hox13 genes. *Developmental Cell* **48**, 383-395.e388.

Alibardi, L. (1995). Muscle differentiation and morphogenesis in the regenerating tail of lizards. *J Anat* **186 (Pt 1)**, 143-151.

Alibardi, L. (2010). Morphological and cellular aspects of tail and limb regeneration in lizards. A model system with implications for tissue regeneration in mammals. *Advances in anatomy, embryology, and cell biology* **207**, iii, v-x, 1-109.

---- (2014). Histochemical, Biochemical and Cell Biological aspects of tail regeneration in lizard, an amniote model for studies on tissue regeneration. *Progress in Histochemistry and Cytochemistry* **48**, 143-244.

---- (2015). Original and regenerating lizard tail cartilage contain putative resident stem / progenitor cells. *Micron* **78**, 10-18.

Alibardi, L. (2021). Spinal ganglia and peripheral nerves innervating the regenerating tail and muscles of lizards. *J Morphol* **282**, 1731-1744.

Bessho, Y., Sakata, R., Komatsu, S., Shiota, K., Yamada, S. and Kageyama, R. (2001). Dynamic expression and essential functions of Hes7 in somite segmentation. *Genes Dev* **15**, 2642-2647.

Chang, H. Y., Chi, J. T., Dudoit, S., Bondre, C., van de Rijn, M., Botstein, D. and Brown, P. O. (2002). Diversity, topographic differentiation, and positional memory in human fibroblasts. *Proc Natl Acad Sci U S A* **99**, 12877-12882.

Chen, J., Kang, L. and Zhang, N. (2005). Negative feedback loop formed by Lunatic fringe and Hes7 controls their oscillatory expression during somitogenesis. *genesis* **43**, 196-204.

Congdon, J. D., Vitt, L. J. and King, W. W. (1974). Geckos: adaptive significance and energetics of tail autotomy. *Science (New York, N.Y.)* **184**, 1379-1380.

Cristino, L., Pica, A., Corte, F. D. and Bentivoglio, M. (2000). Plastic changes and nitric oxide synthase induction in neurons which innervate the regenerated tail of the lizard Gekko gecko II. The response of dorsal root ganglion cells to tail amputation and regeneration. *Brain Research* **871**, 83-93.

Daluiski, A., Engstrand, T., Bahamonde, M. E., Gamer, L. W., Agius, E., Stevenson, S. L., Cox, K., Rosen, V. and Lyons, K. M. (2001). Bone morphogenetic protein-3 is a negative regulator of bone density. *Nature Genetics* **27**, 84-88.

Dy, P., Wang, W., Bhattaram, P., Wang, Q., Wang, L., Ballock, R. T. and Lefebvre, V. (2012). Sox9 Directs Hypertrophic Maturation and Blocks Osteoblast Differentiation of Growth Plate Chondrocytes. *Developmental Cell* **22**, 597-609.

Echeverri, K., Clarke, J. D. and Tanaka, E. M. (2001). In vivo imaging indicates muscle fiber dedifferentiation is a major contributor to the regenerating tail blastema. *Developmental biology* **236**, 151-164.

Elder, G. A., Friedrich, V. L., Jr., Kang, C., Bosco, P., Gourov, A., Tu, P. H., Zhang, B., Lee, V. M. and Lazzarini, R. A. (1998). Requirement of heavy neurofilament subunit in the development of axons with large calibers. *J Cell Biol* **143**, 195-205.

Geuna, S., Borrione, P., Poncino, A. and Giacobini-Robecchi, M. G. (1998). Morphological and morphometrical changes in dorsal root ganglion neurons innervating the regenerated lizard tail. *International journal of developmental neuroscience : the official journal of the International Society for Developmental Neuroscience* **16**, 85-95.

Green, J. D., Tollemar, V., Dougherty, M., Yan, Z., Yin, L., Ye, J., Collier, Z., Mohammed, M. K., Haydon, R. C., Luu, H. H., et al. (2015). Multifaceted signaling regulators of chondrogenesis: Implications in cartilage regeneration and tissue engineering.

Hubert, K. A. and Wellik, D. M. (2023). Hox genes in development and beyond. *Development* **150**.

Hutchins, E. D., Markov, G. J., Eckalbar, W. L., George, R. M., King, J. M., Tokuyama, M. A., Geiger, L. A., Emmert, N., Ammar, M. J., Allen, A. N., et al. (2014). Transcriptomic Analysis of Tail Regeneration in the Lizard Anolis carolinensis Reveals Activation of Conserved Vertebrate Developmental and Repair Mechanisms. **9**.

Kageyama, R., Niwa, Y., Isomura, A., González, A. and Harima, Y. (2012). Oscillatory gene expression and somitogenesis.

Kitamoto, T. and Hanaoka, K. (2010). Notch3 Null Mutation in Mice Causes Muscle Hyperplasia by Repetitive Muscle Regeneration. *Stem Cells* **28**, 2205-2216.

Klaus, A. and Birchmeier, W. (2008). Wnt signalling and its impact on development and cancer. *Nature Reviews Cancer* **8**, 387-398.

Kokabu, S., Gamer, L., Cox, K., Lowery, J., Tsuji, K., Raz, R., Economides, A., Katagiri, T. and Rosen, V. (2011). BMP3 Suppresses Osteoblast Differentiation of Bone Marrow Stromal Cells via Interaction with Acvr2b. *Molecular Endocrinology* **26**, 87-94.

Kozhemyakina, E., Lassar, A. B. and Zelzer, E. (2015). A pathway to bone: signaling molecules and transcription factors involved in chondrocyte development and maturation. *Development* **142**, 817-831.

Leucht, P., Kim, J. B., Amasha, R., James, A. W., Girod, S. and Helms, J. A. (2008). Embryonic origin and Hox status determine progenitor cell fate during adult bone regeneration. *Development* **135**, 2845-2854.

Li, Q., Yang, H. and Zhong, T. P. (2015). Regeneration across metazoan phylogeny: lessons from model organisms. *J Genet Genomics* **42**, 57-70.

Liu, Z., Huang, S., Xu, M., Zhang, W., Guan, T., Wang, Q., Liu, M., Yao, J. and Liu, Y. (2021). The vascularization, innervation and myogenesis of early regenerated tail in Gekko japonicus. *Journal of Molecular Histology* **52**, 1189-1204.

Londono, R., Wenzhong, W., Wang, B., Tuan, R. S. and Lozito, T. P. (2017). Cartilage and Muscle Cell Fate and Origins during Lizard Tail Regeneration. *Frontiers in Bioengineering and Biotechnology* **5**, 1-9.

Lozito, T. P. and Tuan, R. S. (2015). Lizard tail regeneration: Regulation of two distinct cartilage regions by Indian hedgehog. *Developmental Biology* **399**, 249-262.

---- (2016). Lizard tail skeletal regeneration combines aspects of fracture healing and blastema-based regeneration. *Development* **143**, 2946-2957.

---- (2017). Lizard tail regeneration as an instructive model of enhanced healing capabilities in an adult amniote. *Connective Tissue Research* **58**, 145-154.

Lozito, T. P., Tuan, R. S., Alibardi, L., Bai, X., Wang, Y., Man, L., Zhang, Q., Sun, C., Hu, W., Liu, Y., et al. (2016). Lizard tail skeletal regeneration combines aspects of fracture healing and blastema-based regeneration. *Development (Cambridge, England)* **143**, 2946-2957.

Mallo, M. and Alonso, C. R. (2013). The regulation of Hox gene expression during animal development. *Development* **140**, 3951-3963.

McLean, K. E. and Vickaryous, M. K. (2011). A novel amniote model of epimorphic regeneration: the leopard gecko, Eublepharis macularius. *BMC Developmental Biology* **11**, 50-50.

Mugisha, S., Di, X., Disoma, C., Jiang, H. and Zhang, S. (2022). Fringe family genes and their modulation of Notch signaling in cancer. *Biochim Biophys Acta Rev Cancer* **1877**, 188746.

Nusse, R. and Clevers, H. (2017). Wnt/β-Catenin Signaling, Disease, and Emerging Therapeutic Modalities. *Cell* **169**, 985-999.

Okubo, Y., Sugawara, T., Abe-Koduka, N., Kanno, J., Kimura, A. and Saga, Y. (2012). Lfng regulates the synchronized oscillation of the mouse segmentation clock via trans-repression of Notch signalling. *Nature Communications* **3**, 1141.

Pescitelli, M. J., Jr. and Stocum, D. L. (1980). The origin of skeletal structures during intercalary regeneration of larval Ambystoma limbs. *Dev Biol* **79**, 255-275.

Rodrigues, A. M. C., Christen, B., Martí, M. and Izpisúa Belmonte, J. C. (2012). Skeletal muscle regeneration in Xenopus tadpoles and zebrafish larvae. *BMC Developmental Biology* **12**, 9.

Rux, D. R., Song, J. Y., Swinehart, I. T., Pineault, K. M., Schlientz, A. J., Trulik, K. G., Goldstein, S. A., Kozloff, K. M., Lucas, D. and Wellik, D. M. (2016). Regionally restricted hox function in adult bone marrow multipotent mesenchymal stem/stromal cells. *Dev Cell* **39**, 653-666.

Sandoval-Guzman, T., Wang, H., Khattak, S., Schuez, M., Roensch, K., Nacu, E., Tazaki, A., Joven, A., Tanaka, E. M. and Simon, A. (2014). Fundamental differences in dedifferentiation and stem cell recruitment during skeletal muscle regeneration in two salamander species. *Cell Stem Cell* **14**, 174-187.

Sandoval-Guzmán, T., Wang, H., Khattak, S., Schuez, M., Roensch, K., Nacu, E., Tazaki, A., Joven, A., Tanaka, Elly M. and Simon, A. (2014). Fundamental Differences in

Dedifferentiation and Stem Cell Recruitment during Skeletal Muscle Regeneration in Two Salamander Species. *Cell Stem Cell* **14**, 174-187.

Slack, J. M. W. (2006). Amphibian muscle regeneration – dedifferentiation or satellite cells? *Trends in Cell Biology* **16**, 273-275.

Song, H. and Park, K.-H. (2020). Regulation and function of SOX9 during cartilage development and regeneration. *Seminars in Cancer Biology* **67**, 12-23.

Steens, J. and Klein, D. (2022). HOX genes in stem cells: Maintaining cellular identity and regulation of differentiation. *Front Cell Dev Biol* **10**, 1002909.

Thummel, R., Ju, M., Sarras, M. P., Jr. and Godwin, A. R. (2007). Both Hoxc13 orthologs are functionally important for zebrafish tail fin regeneration. *Dev Genes Evol* **217**, 413-420.

Tokuyama, M. A., Xu, C., Fisher, R. E., Wilson-Rawls, J., Kusumi, K. and Newbern, J. M. (2018). Developmental and adult-specific processes contribute to de novo neuromuscular regeneration in the lizard tail. *Developmental Biology* **433**, 287-296.

Uemoto, T., Abe, G. and Tamura, K. (2020). Regrowth of zebrafish caudal fin regeneration is determined by the amputated length. *Scientific reports* **10**, 649.

Wen, Y., Bi, P., Liu, W., Asakura, A., Keller, C. and Kuang, S. (2012). Constitutive Notch Activation Upregulates Pax7 and Promotes the Self-Renewal of Skeletal Muscle Satellite Cells. *Molecular and Cellular Biology* **32**, 2300-2311.

Woltering, J. M., Vonk, F. J., Müller, H., Bardine, N., Tuduce, I. L., de Bakker, M. A. G., Knöchel, W., Sirbu, I. O., Durston, A. J. and Richardson, M. K. (2009). Axial patterning in snakes and caecilians: Evidence for an alternative interpretation of the Hox code. *Developmental Biology* **332**, 82-89.

Wosczyna, M. N. and Rando, T. A. (2018). A Muscle Stem Cell Support Group: Coordinated Cellular Responses in Muscle Regeneration. *Developmental Cell* **46**, 135-143.

Wouter, M., Tobias, G., Francisco, F., Tom, D., Sofia-Christina, P., Marko, P., Vijayishwer Singh, J., Yuka, T.-S., Tzi-Yang, L., Thomas, K., et al. (2024). Somite-independent regeneration of the axolotl primary body axis. *bioRxiv*, 2024.2001.2031.577464.

Yoshioka, K., Nagahisa, H., Miura, F., Araki, H., Kamei, Y., Kitajima, Y., Seko, D., Nogami, J., Tsuchiya, Y., Okazaki, N., et al. (2021). Hoxa10 mediates positional memory to govern stem cell function in adult skeletal muscle. *Science Advances* **7**, eabd7924.

Zammit, P. S., Relaix, F., Nagata, Y., Ruiz, A. P., Collins, C. A., Partridge, T. A. and Beauchamp, J. R. (2006). Pax7 and myogenic progression in skeletal muscle satellite cells. *J Cell Sci* **119**, 1824-1832.

Supplementary Information

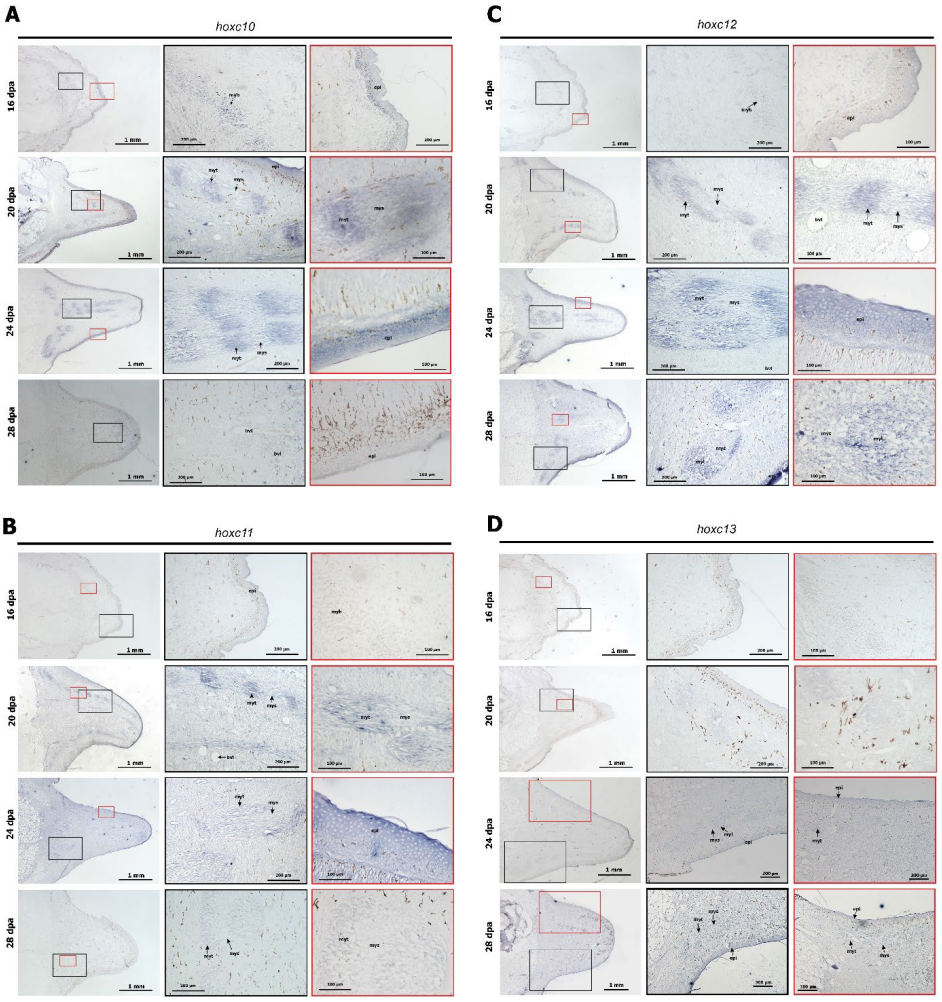

Figure S 5-1. **The expression of posterior HOXC genes in regenerating tail of tokay gecko (*G. gecko*).** (A) Detail expression of *hoxc10* in 16, 20, 24, and 28 dpa of regenerating tail. Key: bvl, blood vessel; ep, epidermis; myb, myoblast; mys, myoseptum; myt, myotubes. (B) Detail expression of *hoxc11* in 16, 20, 24, and 28 dpa of regenerating tail. (C) Detail expression of *hoxc12* in 16, 20, 24, and 28 dpa of regenerating tail. (D) Detail expression of *hoxc13* in 16, 20, 24, and 28 dpa of regenerating tail.

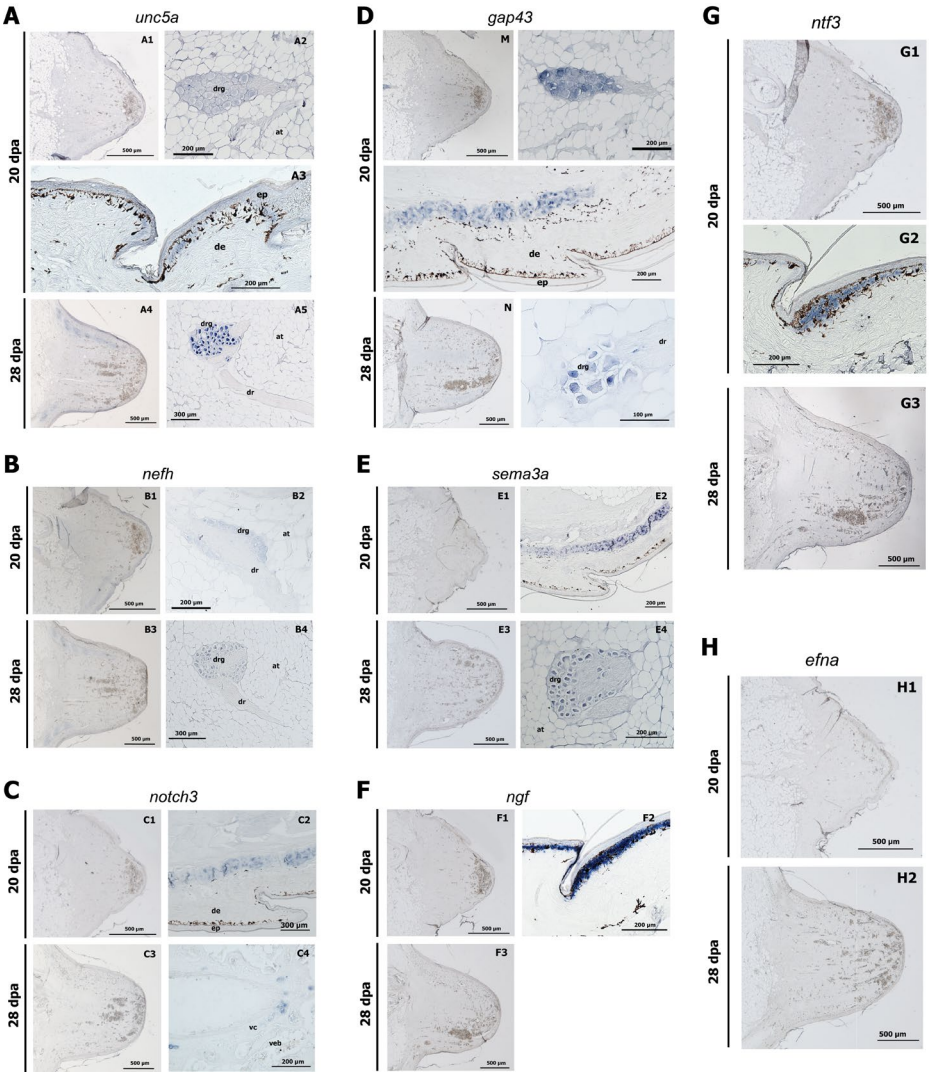

Figure S 5-2. **The expression of axonogenesis genes in the regenerating tail of tokay gecko (G. *gecko*).** (A) Detail expression of *unc5a* in the regenerating tail. Key: at, adipose tissue; bvl, blood vessel; de, dermis; dr, dorsal root nerve; drg, dorsal root ganglia; ep, epidermis. (B) Detail expression of *nefh* in the regenerating tail**.** (C) Detail expression of notch3 in the regenerating tail. (D) Detail expression of gap43 in the regenerating tail. (E) Detail expression of *sema3a* in the regenerating tail. (F) Detail expression of *ngf* in the regenerating tail. (G) Detail expression of *ntf3* in the regenerating tail. (H) Detail expression of *efna* in the regenerating tail.

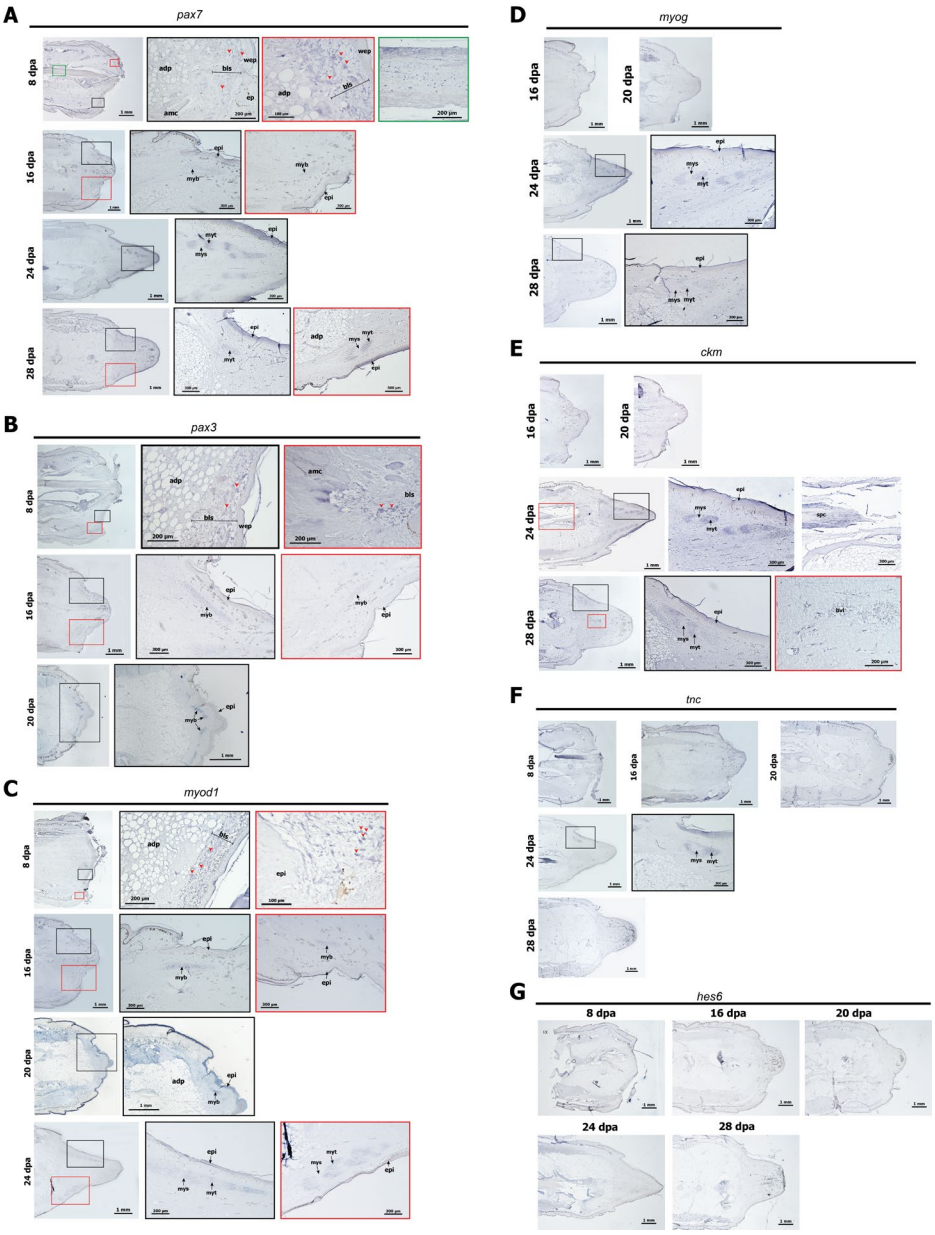

Figure S 5-3. **The expression of muscle genes in regenerating tail of tokay gecko (G. *gecko*)**. (A) Detail expression of *pax7* in regenerating tail. adp, adipose tissue; amc, adult muscle cells; bls, preblastema; ep, epidermis; myb, myoblast; mys, myoseptum; myt, myotubes; wep, wound epithelium. (B) Detail expression of *pax3* in the regenerating tail. (C) Detail expression of *myod1* in the regenerating tail. (D) Detail expression of *myog* in the regenerating tail. (E) Detail expression of *ckm* in the regenerating tail. (F) Detail expression of *tnc* in the regenerating tail. (G) Detail expression of *hes6* in the regenerating tail.

Chapter 6. A High-Quality Genome of The Tokay Gecko (*Gekko gecko*)

Luthfi Nurhidayat[1,2], Vladimir Benes[3], Herman P. Spaink[1], Michael K. Richardson[1]

1. Institute of Biology Leiden, Leiden University, Sylvius Laboratory, Sylviusweg 72, 2333 BE, Leiden, The Netherlands.
2. Faculty of Biology, Universitas Gadjah Mada, Jalan Teknika Selatan Sekip Utara, 55281, Yogyakarta, Indonesia
3. Genomics Core Facility, European Molecular Biology Laboratory Heidelberg, Meyerhofstraße 1, 69117 Heidelberg, Germany

---

Manuscript in preparation.

Abstract

The tokay gecko is an ideal model organism for studying regeneration biology, as it can regenerate its tail, which is a complex structure. Sequencing of the tokay gecko genome holds great potential for advancing research on regeneration, including therapeutic applications, and on other biological research that uses the tokay gecko as a model. In this chapter, we describe a high-quality, scaffold-level genome assembly for the tokay gecko using a hybrid approach combining Illumina and Nanopore sequencing. The assembly has 4,208 scaffolds with an N50 of 190.8 Mbp and L50 of 6, and it reaches 94.8% completeness of BUSCO genes. By integrating two annotation pipelines, BRAKER2 and funannotate, we identified 27,350 genes with 172,817 distinct exons and 30,229 predicted transcripts. As a reference, we also asked Ensembl run our genome assembly through their genebuild pipeline. This predicted 22,009 genes with 35,820 transcripts built from 232,387 exons. Our preliminary synteny analysis showed the tokay gecko assembly is comparable in completeness and contiguity to chromosome-level assemblies of both Townsend's least gecko *Sphaerodactylus townsendi* and the leopard gecko *Eublepharis macularius*. In summary, we were able to produce a high-quality, scaffold-level genome assembly with relatively high-quality annotation. This genome annotation needs some improvements, including reducing fragmentation and duplications.

Introduction

The tokay gecko (*Gekko gecko*) is a lizard belonging to the Gekkonidae, and known for its distinctive appearance with vibrant blue-gray skin covered with orange or red spots (Kongbuntad et al., 2016). Native to Southeast Asia and the Western Pacific, tokay geckos are nocturnal and arboreal, and are commonly found in urban areas, forests, and agricultural lands (Das, 2015). They exhibit territorial behavior and possess adhesive toe pads that enable them to climb vertical surfaces with ease (Cobos and Higham, 2022).

One of the most remarkable features of tokay geckos and some other lizards is their ability to undergo tail autotomy, the voluntary shedding of their tails as a defense mechanism against predators (Rumping and Jayne, 1996). Upon autotomy, the detached tail continues to wriggle, diverting the predator's attention while the gecko escapes. Following tail loss, tokay geckos can regenerate a functional tail, complete with bone, muscle, skin, and nerves. This process involves the formation of a specialized structure called the blastema, which gives rise to the replacement tail unlike axolotls which can regenerate their limbs and tails (Franklin et al., 2017; McCusker et al., 2015; McHedlishvili et al., 2012; Polikarpova et al., 2022), lizards only regenerate their tails (Alibardi, 2019; Lozito and Tuan, 2017). Humans and other mammals have a much more limited regeneration capacity. As an amniote, geckos are closer phylogenetically to mammals than are axolotls and as this thesis argues, may be a better model for human translation research in regeneration biology.

By investigating the cellular and molecular processes involved in tail regeneration, researchers can uncover key mechanisms that drive tissue regeneration in vertebrates. Additionally, tokay geckos have a number of advantages as experimental animals. The tokay gecko has an excellent adaptation to the urban environment as shown by the low genetic diversity in Indonesia despite the geographic isolation of the islands (Kadafi et al., 2024). This means they are relatively easy to maintain in laboratory settings, making them accessible for experimental studies. They also have a larger body size compared to the other lizards, which in our experience makes it easier to sample tissues and perform experiments. Furthermore, they have the advantage of being are oviparous (egg-laying) with the freshly-laid egg containing a very early stage of embryo. Finally, they are able to regenerate multiple times throughout their lifespan.

Several lizard genomes have been sequenced and their implications for regeneration research explored. For instance, a study of Schlegel's Japanese Gecko (*Gekko japonicus*) genome, a species closely related to the tokay gecko, described the evolution of gene families potentially involved in tail regeneration (Liu et al., 2015). Additionally, those genome data have provided insights into the evolution of adhesive toe pads, and the sex determination mechanisms (Liu et al., 2015). In addition, the lizard genomes give a perspective on evolutionary aspect of high-altitude adaptation in lizards

(Li et al., 2023), population structure (Davalos-Dehullu et al., 2023), chromosome transition (Pinto et al., 2022), and asymmetric fates of duplicated genes (Hara et al., 2018).

Genome sequencing of the tokay gecko holds immense potential for advancing research on regeneration and other biological processes. It may also provide valuable insights into the genetic basis of regeneration. Thus, by identifying genes and regulatory elements associated with tail regeneration, researchers can unravel the molecular pathways underlying this phenomenon. Furthermore, genome sequencing facilitates comparative genomics studies, allowing researchers to understand the evolution of geckos, as well as the conservation and divergence of regenerative mechanisms across species. Ultimately, a fully annotated genome of the tokay gecko will serve as a foundation for future studies aiming to translate them to therapeutic applications in humans and other organisms.

Materials and Methods

Ethics statement

The tokay gecko (*Gekko gecko*) is listed as 'least concern' in the International Union for Conservation of Nature *Red List* (IUCN, https://www.iucnredlist.org/species/195309/2378260) and also listed in Appendix II in the Convention on International Trade in Endangered Species of Wild Fauna and Flora (CITES; https://cites.org/eng/taxonomy/term/3919). In Indonesia, the tokay gecko is not a protected species. All animals were collected in Yogyakarta, Indonesia under a license issued by the Ministry of Environment and Forestry, the Republic of Indonesia (permit number SK.83/KSDAE/SET/KSA.2/5/2021 signed on 7 May 2021) and a recommendation letter issued by The Indonesian Institute of Sciences (Lembaga Ilmu Pengetahuan Indonesia/LIPI; Recommendation Number: B- 2158 /IV/KS.01.04/3/2021 signed on 19 March 2021). The transport of samples from Indonesia to the Netherlands was conducted under CITES permit numbers 05717/IV/SATS-LN/2021 and 09160/IV/SATS-LN/2022 issued by the Ministry of Environment and Forestry, the Republic of Indonesia.

All experimental and surgical procedures needed for samples collection were done at Faculty of Biology, Universitas Gadjah Mada, Yogyakarta, Indonesia with the approval from The Ethical Committee of the Integrated Laboratory for Research and Testing (Laboratorium Penelitian dan Pengujian Terpadu/LPPT) Universitas Gadjah Mada (Ethical Clearance number: 00014/04/LPPT/IV/2021 signed on 30 April 2021). Tail autotomy was performed under ketamine anesthesia.

Animal collection and maintenance

Thirty-nine adult tokay geckos were captured in the vicinity of the Faculty of Biology, Universitas Gadjah Mada, Yogyakarta, Indonesia. They were acclimatized for two weeks,

two males with one female, in a stainless-steel terrarium and fed various species of live crickets and sometimes cockroaches, twice a day. They were maintained at ambient temperature and sprayed once a day with water. The geckos were also basked under natural sunlight once every two days for 1 h in the period 09:00–11:00. Twenty-one were used for the harvesting of regeneration blastemas under anesthesia. Of these, three were euthanized for the harvesting of internal organs. The remaining 18 geckos were bred to produce eggs for embryo sampling.

Experimentation and sample collection

Regenerated tail samples

Twenty-one adult tokay geckos were anaesthetized with intramuscular ketamine injection (50–75 mg/Kg body weight) administered in the thigh prior to the autotomy procedure. Autotomy was performed by gently restraining the gecko manually, while leaving the tail accessible. Using the thumb and index finger, a firm pinch was applied to the required autotomous region (every segment after the 5th caudal vertebra) of the tail causing the gecko to spontaneously shed its tail. The wound was painted with Betadine® iodine antiseptic solution but no dressing was applied. After the autotomy procedure was performed, the geckos were allowed to regenerate a new tail. The geckos were distributed into experimental groups based on the number of days post-autotomy, each consisting of three geckos. After ketamine-anesthesia, the tails of geckos in each group were re-autotomized 2 cm cranially from the previous autotomy site at 4 and 16 dpa (days post-autotomy). The regenerated tail samples were rinsed and further handled in phosphate-buffered saline (PBS, 4 °C) and subsequently fixed with cold RNA*later*® stabilization solution (Invitrogen).

Embryo samples

Eighteen adult tokay geckos were grouped and bred as described above. The terraria were checked daily for the presence of gecko eggs. The eggs were left in the terrarium for the required number of days of incubation at ambient temperature. The whole embryo stage 16 dpo (days post-oviposition) and embryonic tail of 22 dpo were harvested into cold PBS and subsequently fixed with RNA*later*® (4 °C).

Organ samples

Three adult tokay geckos were euthanized by an overdose of intramuscular ketamine (150 mg/Kg body weight, intramuscular injection). They were then dissected to harvest organs, namely: pancreas, hearth, muscle, brain, skin, kidney, liver and lung. These eight organ samples were cut up in cold PBS (phosphate-buffered saline) and stored at 4 °C in RNA*later*® stabilization solution (Invitrogen).

RNA extraction and sequencing

RNA isolation and cleaning

The tissues and organs used for RNA sequencing were pancreas, heart, muscle, brain, skin, kidney, liver, lung, whole embryo (16 dpo), embryonic tail (22 dpo), and regenerating tail (4 dpa and 16 dpa). The samples were taken from RNA*later*® solution with sterile forceps and rinsed with sterile PBS. They were then put in 1.5 mL Eppendorf tubes together with 1 mL Trizol and two steel balls (⌀ 4 mm). The tubes were then shaken with a TissueLyser II (Qiagen) at 30/s for 1–2 min. The resulting tissue homogenates were triturated with a hypodermic needle (21G = 0.8mm) attached to a 1 mL syringe until no tissue clumps were visible. The homogenates were then incubated for 30 min and subsequently centrifuged for 10 min at 12,000 RCF (relative centrifugal force).

The supernatants were transferred into new tubes and 0.2 mL of chloroform added to each. The mixture in the tubes were incubated for 2 to 3 min after 11 s of vigorous hand shaking and then centrifuged for 15 min at 16,000 RCF. The colorless aqueous phase of each mixture was transferred to a fresh tube, and 0.7 mL of propan-2-ol (isopropyl alcohol, isopropanol) added to each tube. After leaving for 10 min at room temperature, the samples were centrifuged at 16,000 RCF for 15 min. The supernatants were discarded, and the RNA pellet washed with 1 mL of 75% ethanol. The pellet with 75% ethanol was centrifuged again for 5 min at 7,500 RCF. The supernatants were discarded, and the RNA pellets allowed to dry for 5–10 min. The dry RNA pellets were dissolved in 50 µL of RNase-free water and incubated at 55° C for 10 min. The total RNA of each sample was then cleaned with Qiagen RNeasy Mini Kit (Cat. No. 74104) according to the manufacturer's protocols.

RNA sequencing

Library preparation and transcriptome sequencing were done by the European Molecular Biology Laboratory (EMBL), Heidelberg, Germany. The sequencing platform used was Illumina NextSeq 2000 with a read length of 2×100 bp. The RNA sequencing results were used to assist genome annotation.

Genomic DNA extraction and sequencing

We combined two sequencing technologies: Illumina sequencing technology for short reads and Oxford Nanopore technology for long reads. This hybrid approach was in order to get an optimal quality of assembly considering the lower sequencing errors of Illumina, and the longer reads, that facilitate assembly, of Oxford Nanopore (Sović et al., 2016; Utturkar et al., 2014). Each technology requires a different genomic DNA extraction protocol.

Genomic DNA extraction for Illumina sequencing

We used liver and brain tissue samples for Illumina (short read) sequencing. The samples were taken from RNA*later*® solution using sterile forceps and weighed and rinsed in sterile PBS. They were then put in 1.5 mL Eppendorf tubes and genomic DNA extracted and purified using The Wizard® Genomic DNA Purification Kit (Promega, A1120). Chilled nuclei lysis solution (200 µL) was added to the sample tubes and the mixture homogenized using a plastic microtube pestle until tissue clumps were no longer visible. Another 400 µl of chilled nuclei lysis solution was added to the tubes and the samples were homogenized again by trituration with a 23 G needle fitted to a 1 ml syringe. The homogenates were then incubated at 65 °C for 30 min. RNase from the kit was added to the homogenate (3 µL per tube), and the mixture incubated at 37°C for 15–30 min before cooling to room temperature. Next, protein precipitation solution (200 µL) was added, and the solution vortexed and chilled on ice for 5 min. The mixture was then centrifuged at 13,000–16,000 × g for 4 min. The supernatant was transferred to a fresh tube containing 600 µL isopropanol, gently mixed by inversion, and centrifuged again at 13,000–16,000 × g for 1 min. The supernatant was removed, 70% ethanol (600µl) was subsequently added, and the tube was centrifuged again at 13,000–16,000 × g for 1 min. The ethanol was removed, and the pellet was air-dried for 15 min. Finally, the DNA was rehydrated in 100 µL of DNA rehydration solution for 1 h at 65 °C or overnight at 4 °C.

Genomic DNA extraction for Oxford Nanopore sequencing

We used brain, pancreas and heart tissue samples for Oxford Nanopore (long read) sequencing. The samples were taken from RNA*later*® solution with sterile forceps, and weighed, then rinsed with sterile PBS. These samples were then put in 1.5 mL Eppendorf tubes and subsequently proceeded to high molecular weight (HMW) DNA extraction protocols using Monarch® HMW DNA Extraction Kit for tissue (New England Biolabs, cat. NEB T3060). Lysis master mix (300 µl, consisting of 30 parts tissue lysis buffer: 1 part proteinase K) and the sample were homogenized using a clean plastic microtube pestle until all clumps disappeared. Another 300 µl of the lysis master mix was added to the tubes containing the homogenized samples and they were mixed by trituration with wide bore 200 µL micropipette tip with a wide bore to avoid shearing. The mixture was incubated at 56 °C for 45 min with agitation. Then, 10 µL of RNase A from the Monarch® kit was added and mixed by inverting 5–10 ×. Incubation for 10 min at 56 °C with agitation. The heat block in a thermal mixer was changed to accommodate a 2 ml tube, and preheated to 56 °C. Next, 300 µL of protein separation solution was added and mixed by inversion for 1 min. Centrifugation for 10 min at 16,000 × g was conducted. Using a 1000 µL wide-bore micropipette tip (see above), the upper phase containing the DNA was transferred to a labeled Monarch® 2 mL tube.

Two DNA capture beads from the Monarch® kit were added to each sample. Then, 550 µL of isopropanol was added, and the tubes placed on a vertical rotating mixer at 10 rpm for 5 min to allow DNA to attach to the beads. Then, the liquid was removed from the tubes by pipetting, taking care to avoid dislodging any gDNA adhering to the capture beads. To optimize DNA solubility, care was taken not to let the bound DNA dry out on the beads during the following steps. gDNA wash buffer (500 µL) was added, the cap closed, and the tube inverted 2–3 × before removing the wash buffer by pipetting. This wash step was repeated, and the wash buffer was removed by pipetting. A labeled bead retainer was placed into a Monarch® Collection Tube II, and the beads were poured into the bead retainer before closing the cap. A pulse spin (≤ 1 s) in a benchtop minicentrifuge was performed to remove residual wash buffer from the beads. The bead retainer was separated from the collection tube, and the beads were poured into a new, labeled Monarch® 2 mL tube, while the used bead retainer was inserted into a labeled 1.5 mL microfuge tube. Immediately, 100 µL of elution buffer II was added to the glass beads, and the tube with the beads was incubated for 5 min at 56 °C in a thermal mixer with agitation (300 rpm). Ensuring the bead retainer was inserted into the 1.5 mL microfuge tube, the eluate and beads were poured into the bead retainer and the cap closed. Centrifugation for 30 s at 12,000 × g was conducted to separate the eluate from the beads, which were then discarded along with the retainer. The eluate was triturated 5–10 × with a wide bore pipette tip, to ensure that any visible DNA aggregates were dispersed.

Illumina sequencing

Genomic DNA extracted from the tokay gecko liver sample was used for short read library preparation and sequencing, which were done by Genomics Core Facility at EMBL. The sequencing platform used was Illumina NextSeq 400 with 40× coverage.

Oxford Nanopore sequencing

Genomic DNA extracted from the tokay gecko brain sample was used for long read library preparation and sequencing, which were done at Future Genomics Technologies, Leiden, the Netherlands. The ligation sequencing Kit 1D ligation SQK-LSK110 (Oxford Nanopore) was used for library preparation. The genome sequencing was done using FLO-PRO002 (PromethION; Oxford Nanopore Technology) combined with Guppy vs5.0.17 (Oxford Nanopore Technology) at high accuracy (minimum Q-score = 9). The genome was sequenced to give 25× coverage.

Genome assembly and annotation

Genome assembly

De novo contig assembly was performed by Future Genomics Technologies using Flye 2.9-b1768 and were then polished based on Illumina reads using Pilon v. 1.23. The

polished contigs were then scaffolded using RagTag v. 2.1.0 (Alonge et al., 2022) with the genome of Townsend's least gecko *Sphaerodactylus towsendi* (GCF_021028975.2) as a reference.

Genome annotations

Genome annotation was carried out within the computing resources from the Academic Leiden Interdisciplinary Cluster Environment (ALICE) provided by Leiden University. The genome assembly was soft-masked using RepeatMasker v. 4.1.4. (http://www.repeatmasker.org) before going through the genome annotation pipeline. Genome structural annotation (gene prediction) was done using the BRAKER2 pipeline (Bruna et al., 2021) with gene prediction tools GeneMark-ES/ET/EP/ETP (Brůna et al., 2020) and AUGUSTUS (Stanke et al., 2008), and with RNA-seq data as extrinsic evidence. The structural annotation result from the BRAKER2 pipeline was then functionally annotated using the 'funannotate annotate' command of the Funannotate pipeline (https://funannotate.readthedocs.io/en/latest/install.html). This pipeline utilizes InterProScan5 (Jones et al., 2014), Eggnog-Mapper (Cantalapiedra et al., 2021), SignalP 5.0 (Almagro Armenteros et al., 2019), TMHMM 2.0 (Krogh et al., 2001) to generate gene names and product descriptions from protein-coding models. The genome annotation was then evaluated using BUSCO analysis (Manni et al., 2021).

Ensembl also performed genome annotation of our tokay gecko genome using their in-house genome annotation pipeline Genebuild (https://www.ensembl.org/info/genome/genebuild/index.html).

Duplicate genes classification and Comparative genomics

The protein sequences in the tokay gecko genome predicted by Ensembl genebuild were aligned to eachother using BLAST+ v. 2.14.1 (https://blast.ncbi.nlm.nih.gov/doc/blast-help/downloadblastdata.html). The alignment results and the gff (general feature format) file containing gene position in the genome were then further analyzed using the 'Duplicate_gene_classifier' function of MCScanX (Wang et al., 2012) to identify gene duplications.

We then performed all-against-all alignment of coding sequences (CDS) of three gecko genomes: our tokay gecko (GCA_029375565.1), Townsend's least Gecko *Sphaerodactylus townsendi* (Genbank accession number GCA_021028975.2) and the leopard gecko *Eublepharis macularius* (GCA_028583425.1), using BLAST+ v. 2.14.1 (https://blast.ncbi.nlm.nih.gov/doc/blast-help/downloadblastdata.html). The alignment results were then concatenated into one file. The gff files were also concatenated. These files were then further analyzed using MCScanX (Wang et al., 2012) to detect gene synteny and collinearity. The results were then explored and visualize using SynVisio (Bandi et al., 2022)

Data Availability

The tokay gecko genome assembly was submitted to GenBank (https://www.ncbi.nlm.nih.gov/genbank/; accession number GCA_029375565.1). All raw sequencing data related to the assembly have been deposited in the NCBI database SRA (sequencing reads archive) under BioProject accession number PRJNA894965. The genome tokay gecko annotation done by Ensembl can be found in the Ensembl rapid-release page (https://rapid.ensembl.org/Gekko_gecko_GCA_029375565.1/Info/Index.)

Results

The Genome assembly of the tokay gecko shows high contiguity and completeness

By implementing a hybrid genome assembly method, using Illumina and Nanopore reads, we produced a complete, high quality, scaffold-level genome assembly of the tokay gecko. The assembly has 4,208 scaffolds with scaffold N50 and L50 of 190.8 MB and 6 respectively (Table 6-1). These scaffolds were constructed from 5,480 contigs with contig N50 and L50 of 10.8 Mbp and 69, respectively (Table 6-1). Furthermore, the genome assembly of the tokay gecko reached 94.8% of complete BUSCOs, of which 92.7% were complete and single-copy, and 2.1% were complete and duplicated (Table 6-1). The complete statistics of the tokay gecko genome assembly can be found in Table S 6-1.

We also examined the interspersed repeats and low complexity DNA sequences contained in the tokay gecko genome assembly (Table 6-2). The total genome consisted of 6.38% interspersed repeats, 0.38% small RNA, 1.18% simple repeats, and 0.25% low complexity repeats (Table 6-2). The total interspersed repeats were largely composed by retroelements (6.34% of the total assembly), especially L2/CR1/Rex (5.14%) from LINEs (Table 6-2). The complete repeat statistics of the tokay gecko genome assembly, including the number and the length occupied, can be found in Table S 6-2.

Table 6-1. **Summary of assembly statistics of the tokay gecko genome.**

Assembly Level	Scaffold
Number of scaffolds	4,208
Total scaffold length	2,741,107,181
Average scaffold length	651,403.80
Scaffold N50	190,862,615
Scaffold L50	6
Largest scaffold	341,137,916
Smallest scaffold	503
Number of contigs	5,480
Total contig length	2,740,979,981
Average contig length	500,178.83

Contig N50	10,858,724
Contig L50	69
Largest contig	78,618,297
Smallest contig	503
Number of gaps in scaffolds	1,272
Total gap length in scaffolds	127,200
Average gap length in scaffolds	100
GC content %	45.37
Complete BUSCOs	7,088 (94.8%)
Complete and single-copy BUSCOs	6,932 (92.7%)
Complete and duplicated BUSCOs	156 (2.1%)
Fragmented BUSCOs	78 (1.0%)
Missing BUSCOs	314 (4.2%)
Total BUSCO groups searched	7480

Table 6-2. **Repeat statistics of the tokay gecko genome**.

Total interspersed repeats (6.38%)	Retroelements	6.34%	SINEs:	0.98%		
			LINEs	5.14%	L2/CR1/Rex	5.14%
			LTR elements	0.22%	Gypsy/DIRS1	0.21%
					Retroviral	0.01%
	DNA transposons	0.04%	hobo-Activator	0.01%		
			Tourist/Harbinger	0.01%		
	Unclassified:	0.01%				
Small RNA	0.38%					
Simple repeats	1.18%					
Low complexity	0.25%					

Notes: Percentages are relative to the total genome sequence. We only used RepeatMasker combined with Dfam-Dfam_3.0 and RepBase-20181026 Databases for repeat identification. *De novo* transposable element (TE) family identification and modeling will be done in the future using Repeat Modeler; we therefore expect the repeat statistics to increase.

The genome of the tokay gecko is well annotated

We used a combination of the BRAKER2 and Funannotate pipelines for genome annotation because BRAKER2 pipeline alone does not support functional annotation, while Funannotate showed a low accuracy in predicting gene structure in gigabyte-sized genome. By combining these two pipelines, we identified 27,350 genes, 172,817 distinct exons and 30,229 predicted transcripts (Table 6-3). Our genome annotation reached 83.9% completed BUSCOs consisting of 77% Complete and single-copy BUSCOs and 11% complete and duplicated BUSCOs. We also asked Ensembl to run our assembly through their in-house genome annotation pipeline, genebuild. This annotation pipeline predicted 22,009 genes, 232,387 distinct exons and 35,820 transcripts. The Ensembl

annotation reached 95.8% completed BUSCOs of which 93.8% were complete and single-copy, and 2.0% were complete and duplicated.

Table 6-3. **Annotation statistics of the tokay gecko genome**.

Criterion	BRAKER2 + Funannotate	Ensembl genebuild
Max number of transcripts per gene	4	10
Mean exon size	226.1	278.5
Mean gene locus size (first to last exon)	31,439.6	53,792.3
Mean number of distinct exons per gene	6.3	10.6
Mean number of transcripts per gene	1.1	1.6
Mean transcript size (UTR, CDS)	1,385	2,667.1
Number of distinct exons	172,817	232,387
Number of genes	27,350	22,009
Number of genes with alternative transcript variants	15,718 (57.5%)	8,011 (36.4%)
Number of multi-exon genes	15,718 (57.5%)	21,171 (96.2%)
Number of predicted transcripts	30,229	35,820
Number of single-exon genes	11,632 (42.5%)	838 (3.8%)
Complete BUSCOs	6,283 (83.9%)	7,161 (95.8%)
Complete and single-copy BUSCOs	5,759 (77%)	7,014 (93.8%)
Complete and duplicated BUSCOs	824 (11%)	147 (2.0%)
Fragmented BUSCOs	89 (1.2%)	106 (1.4%)
Missing BUSCOs	808 (10.8%)	213 (2.8%)
Total BUSCO groups searched	7480	7480

Note: The lineage dataset for BUSCO analysis is sauropsida_odb10 (Creation date: 2024-01-08, number of genomes: 76, number of BUSCOs: 7480). BUSCO was run in euk_genome_met mode utilizing metaeuk gene predictor.

The Ensembl genebuild gave more complete annotations than our combined BRAKER2 and Funannotate analysis. Therefore, we used the Ensembl annotations to perform gene duplication classification in the tokay gecko genome. We found that most of the gene duplications (22,977 genes) are tandem duplications, followed in number by dispersed duplications (8,863 genes), proximal duplications (1,155 genes) and WGD (whole genome duplication) or segmental duplications (1,023 genes). We identified 1,802 singleton genes.

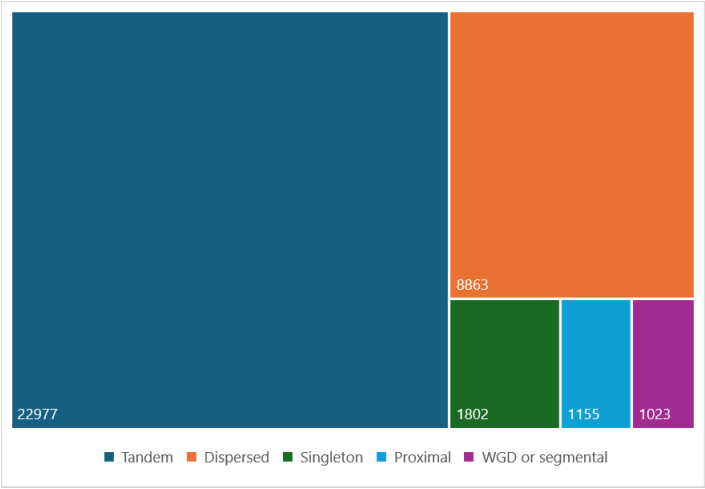

Figure 6-1. **Gene duplication classification in the tokay gecko genome.** Note that a gene can be classified into more than one gene duplication type.

Comparison of the tokay gecko with two other gecko genomes gives an estimate of their phylogenetic distances

We performed synteny analysis by comparing our scaffold-level tokay gecko genome assembly with the chromosome-level assemblies of Townsend's least gecko (Pinto et al., 2022) and the leopard gecko (Pinto et al., 2023). These three geckos belong to the same infraorder (Gekkota; see (Pyron et al., 2013)) but different families (Gekkonidae, Sphaerodactylidae, and Eublepharidae, respectively). We found that the tokay gecko genome assembly is comparable in completeness and contiguity to the those of the Townsend's least gecko and the leopard gecko (Figure 6-2). This is indicated by the extensive syntenic blocks shared between their genomes (Figure 6-2A, B, C). In a comparison of the genomes of the tokay gecko *vs*. the Townsend's least gecko (Figure 6-2B, C), we found that only a few macrosyntenic re-arrangements. By contrast, there were many macrosynteny (chromosomes) and microsynteny (gene clusters) inversions in the comparison of the leopard gecko *vs.* the other two (Figure 6-2A, D). We also found translocations in the comparison of the tokay gecko genome *vs*. the Townsend's least gecko genome (Figure 6-2B, C, D). However, the comparison of the tokay gecko *vs*. the leopard gecko genomes showed more translocations of synteny blocks than in the Townsend's least gecko *vs*. the leopard gecko comparison (Figure 6-2A).

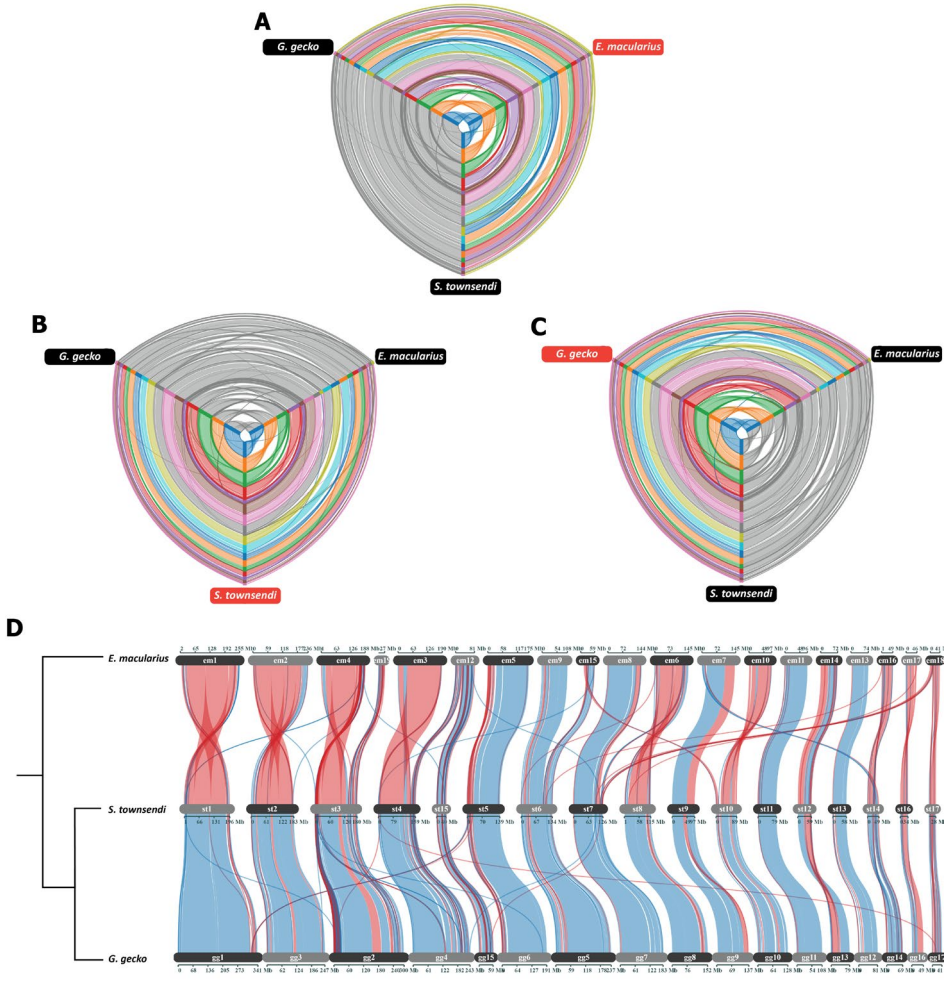

Figure 6-2. **Synteny analysis shows that the genome of the tokay gecko is phylogenetically closer to the Townsend's Least Gecko than the leopard gecko**. (A–C) Overview of synteny comparisons between the tokay gecko (*G. gecko*), the Townsend's least gecko (*S. townsendi*), and the leopard gecko (*E. macularius*). Each color represents one chromosome. (D) Alignment orientation of synteny block between three genomes. Blue color represents regular syntenic block links and red color represents reverse syntenic block links. The chromosomes were reordered for better visualization. The chromosome order in A–C and D is the same. The phylogenetic tree was adapted from (Pyron et al., 2013). *Key* to annotations in D*:* em1–em19, chromosomes of the leopard gecko (chromosome accession NC_072790.1–NC_072808.1); st1–st17, chromosomes of the Townsend's least gecko (chromosome accession NC_059425.1–NC_059441.1); gg1–gg17, chromosomes of the tokay gecko (chromosome accession JAPDNY010000001.1– JAPDNY010000017.1).

Discussion

In this chapter, we sequenced, assembled, and annotated the genome of the tokay gecko. Through the implementation of a hybrid genome assembly approach, that utilized both Illumina and Nanopore sequencing technologies, we were able to produce a high-quality, scaffold-level genome assembly. Our genome annotation was of relatively high-quality, despite specific areas (duplications, fragmentation, missing genes) that we plan to optimize in the future.

Our genome assembly has high contiguity and completeness and has a coverage of 40× (Illumina sequencing) and 24× coverage (Nanopore sequencing). Our assembly result is better than other lizard genomes that were sequenced by Illumina sequencing only but have higher coverage. For instance, the genome assembly of the Schlegel's Japanese gecko (GCA_001447785.1) that used Illumina sequencing and has a coverage of 95× (Liu et al., 2015) has a scaffold N50 of 707.7 kb and scaffold L50 of 963. The other example is the genome of the Madagascar ground gecko (*Paroedura picta*; GCA_003118565.2) which has 77.7× genome coverage, a scaffold N50 of 109 Mb and a scaffold L50 of 6 (Hara et al., 2018; Yamaguchi et al., 2021). These comparisons confirm that combining Illumina and Nanopore sequencing is a good option for providing a more contiguous and complete genome assembly than using Illumina sequencing alone, even if the latter produces a high genome coverage (as has also been argued for example by (Utturkar et al., 2014)).

The tokay gecko genome annotations produced using the BRAKER2 and Funannotate pipelines predicts more genes than the annotations from genebuild. However, the genebuild annotation result is more complete than the combined BRAKER2 + Funannotate annotations. This might be related to the genebuild pipeline utilizing more extensive and comprehensive data integration, including transcriptomic and proteomic data, according to their web notes (https://www.ensembl.org/info/genome/genebuild/index.html). This data integration produces better gene models for genome annotation in general (Prasad et al., 2017; Venturini et al., 2018). Moreover, genebuild has an advanced prediction algorithm, according to their website. Meanwhile, our BRAKER2 + Funannotate genome annotation used only our tokay gecko RNA-seq data (in this thesis) and UniProt (https://www.uniprot.org/) for the protein references. Genebuild, however, uses a larger number of reference databases (https://www.ensembl.org/info/genome/genebuild/annotation_sources.html). Finally, the BRAKER3 pipeline, an update of BRAKER2 pipeline that integrates both RNA-seq data and protein evidence, was not yet stable when we annotated the tokay gecko genome (Bruna et al., 2021; Gabriel et al., 2024). We should consider using BRAKER3 with more

optimal parameters, and re-training gene models, to achieve higher genome annotation completeness in the future.

The tokay gecko genome has a relatively high-quality annotation, especially the annotation done by Ensembl using genebuild. That Ensembl annotation is publicly available (see data availability in Materials and Methods, this chapter). Our tokay gecko genome annotations are even higher in term of the number of genes and BUSCO completeness, compared to the Schlegel's Japanese gecko (https://www.ncbi.nlm.nih.gov/datasets/genome/GCF_001447785.1) and the Townsend's least gecko genome annotations (https://www.ncbi.nlm.nih.gov/datasets/genome/GCF_021028975.2). In general, well-annotated genomes are the most useful for researchers studying molecular mechanisms in model species (Richards, 2015; Worley et al., 2017).

I have shown in this chapter that the tokay gecko genome can be used for chromosomal genome comparison with other genomes having a chromosome-level assembly, namely Townsend's least gecko (Pinto et al., 2022) and the leopard gecko (Pinto et al., 2023). This comparison showed that there are few chromosomal rearrangements, especially translocations, in the three genomes. The fact that I only identified a few chromosomal rearrangements indicates that the three species compared are separated by a relatively small phylogenetic distance (Bhutkar et al., 2008; Sankoff, 2003). Moreover, this comparison showed that the tokay gecko is closer, phylogenetically, to the Towsend least gecko than it is to the leopard gecko. This result is consistent with the squamate phylogeny of (Pyron et al., 2013) showing that the family Gekkonidae, which includes the tokay gecko, is closer to the Sphaerodactylidae, that includes Townsend's least gecko, than to the family Eublepharidae, that includes the leopard gecko.

In summary, this chapter covers the genome assembly and annotation of the tokay gecko. Through the hybrid assembly approach using Illumina and Nanopore sequencing, we produced a high-quality scaffold-level genome assembly for the tokay gecko. Moreover, the genome annotation showed relatively high completeness. Our tokay gecko genome will provide a valuable resource for biological research using the tokay gecko and other lizards as model species, especially in the field regenerative biology. It might also be interesting to do comparative genomic studies of the tokay gecko genome and the genomes of other squamates, since the preliminary genome comparison reported here showed promising results.

References

Alibardi, L. (2019). Review: The Regenerating Tail Blastema of Lizards as a Model to Study Organ Regeneration and Tumor Growth Regulation in Amniotes. *Anat Rec (Hoboken)* **302**, 1469-1490.

Almagro Armenteros, J. J., Tsirigos, K. D., Sønderby, C. K., Petersen, T. N., Winther, O., Brunak, S., von Heijne, G. and Nielsen, H. (2019). SignalP 5.0 improves signal peptide predictions using deep neural networks. *Nature Biotechnology* **37**, 420-423.

Alonge, M., Lebeigle, L., Kirsche, M., Jenike, K., Ou, S., Aganezov, S., Wang, X., Lippman, Z. B., Schatz, M. C. and Soyk, S. (2022). Automated assembly scaffolding using RagTag elevates a new tomato system for high-throughput genome editing. *Genome Biology* **23**, 258.

Bandi, V., Gutwin, C., Siri, J. N., Neufeld, E., Sharpe, A. and Parkin, I. (2022). Visualization Tools for Genomic Conservation. *Methods Mol Biol* **2443**, 285-308.

Bhutkar, A., Schaeffer, S. W., Russo, S. M., Xu, M., Smith, T. F. and Gelbart, W. M. (2008). Chromosomal Rearrangement Inferred From Comparisons of 12 Drosophila Genomes. *Genetics* **179**, 1657-1680.

Bruna, T., Hoff, K. J., Lomsadze, A., Stanke, M. and Borodovsky, M. (2021). BRAKER2: automatic eukaryotic genome annotation with GeneMark-EP+ and AUGUSTUS supported by a protein database. *NAR Genom Bioinform* **3**, lqaa108.

Brůna, T., Lomsadze, A. and Borodovsky, M. (2020). GeneMark-EP+: eukaryotic gene prediction with self-training in the space of genes and proteins. *NAR Genomics and Bioinformatics* **2**, lqaa026.

Cantalapiedra, C. P., Hernández-Plaza, A., Letunic, I., Bork, P. and Huerta-Cepas, J. (2021). eggNOG-mapper v2: Functional Annotation, Orthology Assignments, and Domain Prediction at the Metagenomic Scale. *Molecular Biology and Evolution* **38**, 5825-5829.

Cobos, A. J. and Higham, T. E. (2022). Growing up in a rough world: scaling of frictional adhesion and morphology of the Tokay gecko (Gekko gecko). *Beilstein J Nanotechnol* **13**, 1292-1302.

Das, I. (2015). A field guide to the reptiles of South-East Asia. pp. 375-375.

Davalos-Dehullu, E., Baty, S. M., Fisher, R. N., Scott, P. A., Dolby, G. A., Munguia-Vega, A. and Cortez, D. (2023). Chromosome-Level Genome Assembly of the Blacktail Brush Lizard, Urosaurus nigricaudus, Reveals Dosage Compensation in an Endemic Lizard. *Genome Biology and Evolution* **15**, evad210.

Franklin, B. M., Voss, S. R. and Osborn, J. L. (2017). Ion channel signaling influences cellular proliferation and phagocyte activity during axolotl tail regeneration. *Mechanisms of Development* **146**, 42-54.

Gabriel, L., Bruna, T., Hoff, K. J., Ebel, M., Lomsadze, A., Borodovsky, M. and Stanke, M. (2024). BRAKER3: Fully automated genome annotation using RNA-seq and protein evidence with GeneMark-ETP, AUGUSTUS, and TSEBRA. *Genome Res* **34**, 769-777.

Hara, Y., Takeuchi, M., Kageyama, Y., Tatsumi, K., Hibi, M., Kiyonari, H. and Kuraku, S. (2018). Madagascar ground gecko genome analysis characterizes asymmetric fates of duplicated genes. *BMC Biology* **16**, 1-19.

Jones, P., Binns, D., Chang, H.-Y., Fraser, M., Li, W., McAnulla, C., McWilliam, H., Maslen, J., Mitchell, A., Nuka, G., et al. (2014). InterProScan 5: genome-scale protein function classification. *Bioinformatics* **30**, 1236-1240.

Kadafi, A. M., Fauzi, M. A., Ardiantoro, A., Zakky, Q., Nugraha, F. A. D., Priambodo, B., Fahmi, M., Munir, M., , Riyanto, A. and Hamidy, A. (2024). Low genetic diversity of the Indonesian Tokay Gecko (Gekko gecko) (Reptilia: Gekkonidae): Introduce or Native? *Jurnal Biologi Indonesia* **20**, 63-75.

Kongbuntad, W., Tantrawatpan, C., Pilap, W., Jongsomchai, K., Chanaboon, T., Laotongsan, P., Petney, T. N. and Saijuntha, W. (2016). Genetic diversity of the red-spotted tokay gecko (Gekko gecko Linnaeus, 1758) (Squamata: Gekkonidae) in Southeast Asia determined with multilocus enzyme electrophoresis. *Journal of Asia-Pacific Biodiversity* **9**, 63-68.

Krogh, A., Larsson, B., von Heijne, G. and Sonnhammer, E. L. L. (2001). Predicting transmembrane protein topology with a hidden markov model: application to complete genomes11Edited by F. Cohen. *Journal of Molecular Biology* **305**, 567-580.

Li, W., Du, J., Yang, L., Liang, Q., Yang, M., Zhou, X. and Du, W. (2023). Chromosome-level genome assembly and population genomics of Mongolian racerunner (Eremias argus) provide insights into high-altitude adaptation in lizards. *BMC Biol* **21**, 40.

Liu, Y., Zhou, Q., Wang, Y., Luo, L., Yang, J., Yang, L., Liu, M., Li, Y., Qian, T., Zheng, Y., et al. (2015). Gekko japonicus genome reveals evolution of adhesive toe pads and tail regeneration. *Nature Communications* **6**, 1-11.

Lozito, T. P. and Tuan, R. S. (2017). Lizard tail regeneration as an instructive model of enhanced healing capabilities in an adult amniote. *Connective Tissue Research* **58**, 145-154.

Manni, M., Berkeley, M. R., Seppey, M. and Zdobnov, E. M. (2021). BUSCO: Assessing Genomic Data Quality and Beyond. *Current Protocols* **1**, e323.

McCusker, C., Bryant, S. V. and Gardiner, D. M. (2015). The axolotl limb blastema: cellular and molecular mechanisms driving blastema formation and limb regeneration in tetrapods. *Regeneration* **2**, 54-71.

McHedlishvili, L., Mazurov, V., Grassme, K. S., Goehler, K., Robl, B., Tazaki, A., Roensch, K., Duemmler, A. and Tanaka, E. M. (2012). Reconstitution of the central and peripheral nervous system during salamander tail regeneration. *Proceedings of the National Academy of Sciences of the United States of America* **109**.

Pinto, B. J., Gamble, T., Smith, C. H., Keating, S. E., Havird, J. C. and Chiari, Y. (2023). The revised reference genome of the leopard gecko (Eublepharis macularius) provides insight into the considerations of genome phasing and assembly. *bioRxiv*.

Pinto, B. J., Keating, S. E., Nielsen, S. V., Scantlebury, D. P., Daza, J. D. and Gamble, T. (2022). Chromosome-Level Genome Assembly Reveals Dynamic Sex Chromosomes in Neotropical Leaf-Litter Geckos (Sphaerodactylidae: Sphaerodactylus). *J Hered* **113**, 272-287.

Polikarpova, A., Ellinghaus, A., Schmidt-Bleek, O., Grosser, L., Bucher, C. H., Duda, G. N., Tanaka, E. M. and Schmidt-Bleek, K. (2022). The specialist in regeneration-the Axolotl-a suitable model to study bone healing? *NPJ Regen Med* **7**, 35.

Prasad, T. S., Mohanty, A. K., Kumar, M., Sreenivasamurthy, S. K., Dey, G., Nirujogi, R. S., Pinto, S. M., Madugundu, A. K., Patil, A. H., Advani, J., et al. (2017). Integrating transcriptomic and proteomic data for accurate assembly and annotation of genomes. *Genome Res* **27**, 133-144.

Pyron, R. A., Burbrink, F. T. and Wiens, J. J. (2013). A phylogeny and revised classification of Squamata, including 4161 species of lizards and snakes. *BMC Evolutionary Biology* **13**, 93.

Richards, S. (2015). It's more than stamp collecting: how genome sequencing can unify biological research. *Trends Genet* **31**, 411-421.

Rumping, J. M. and Jayne, B. C. (1996). Muscle activity in autotomized tails of a lizard (Gekko gecko): a naturally occurring spinal preparation. *Journal of comparative physiology. A, Sensory, neural, and behavioral physiology* **179**, 525-538.

Sankoff, D. (2003). Rearrangements and chromosomal evolution. *Current Opinion in Genetics & Development* **13**, 583-587.

Sović, I., Križanović, K., Skala, K. and Šikić, M. (2016). Evaluation of hybrid and non-hybrid methods for de novo assembly of nanopore reads. *Bioinformatics* **32**, 2582-2589.

Stanke, M., Diekhans, M., Baertsch, R. and Haussler, D. (2008). Using native and syntenically mapped cDNA alignments to improve de novo gene finding. *Bioinformatics* **24**, 637-644.

Utturkar, S. M., Klingeman, D. M., Land, M. L., Schadt, C. W., Doktycz, M. J., Pelletier, D. A. and Brown, S. D. (2014). Evaluation and validation of de novo and hybrid assembly techniques to derive high-quality genome sequences. *Bioinformatics* **30**, 2709-2716.

Venturini, L., Caim, S., Kaithakottil, G. G., Mapleson, D. L. and Swarbreck, D. (2018). Leveraging multiple transcriptome assembly methods for improved gene structure annotation. *GigaScience* **7**, giy093.

Wang, Y., Tang, H., Debarry, J. D., Tan, X., Li, J., Wang, X., Lee, T. H., Jin, H., Marler, B., Guo, H., et al. (2012). MCScanX: a toolkit for detection and evolutionary analysis of gene synteny and collinearity. *Nucleic Acids Res* **40**, e49.

Worley, K. C., Richards, S. and Rogers, J. (2017). The value of new genome references. *Experimental Cell Research* **358**, 433-438.

Yamaguchi, K., Kadota, M., Nishimura, O., Ohishi, Y., Naito, Y. and Kuraku, S. (2021). Technical considerations in Hi-C scaffolding and evaluation of chromosome-scale genome assemblies. *Mol Ecol* **30**, 5923-5934.

Supplementary Information

Table S 6-1. **Complete genome assembly statistics of the tokay gecko (*Gekko gecko*)**

# scaffolds	**4,208**
Total scaffold length	2,741,107,181
Average scaffold length	651,403.80
Scaffold N50	190,862,615
Scaffold auN	200,046,474.16
Scaffold L50	6
Scaffold NG50	341,137,916
Scaffold auNG	203,092,158,088.95
Scaffold LG50	1
Largest scaffold	341,137,916
Smallest scaffold	503
# contigs	5,480
Total contig length	2,740,979,981
Average contig length	500,178.83
Contig N50	10,858,724
Contig auN	15,243,932.67
Contig L50	69
Contig NG50	78,618,297
Contig auNG	15,475,301,583.67
Contig LG50	1
Largest contig	78,618,297
Smallest contig	503
# gaps in scaffolds	1,272
Total gap length in scaffolds	127,200
Average gap length in scaffolds	100
Gap N50 in scaffolds	100
Gap auN in scaffolds	100
Gap L50 in scaffolds	636
Largest gap in scaffolds	100
Smallest gap in scaffolds	100
Base composition (A:C:G:T)	A: 748,908,636 C: 621,741,100 G: 621,751,449 T: 748,578,796
GC content %	45.37
# soft-masked bases	1,164,152,571
# segments	5,480
Total segment length	2,740,979,981
Average segment length	500,178.83
# gaps	1,272
# paths	4,208
Scaffold N10	341,137,916
Scaffold N20	299,885,588
Scaffold N30	247,548,350
Scaffold N40	243,323,372
Scaffold N50	190,862,615
Scaffold N60	182,932,204
Scaffold N70	138,791,800
Scaffold N80	107,697,327
Scaffold N90	68,720,646
Scaffold N100	503
Scaffold L10	1
Scaffold L20	2
Scaffold L30	3
Scaffold L40	4
Scaffold L50	6
Scaffold L60	7
Scaffold L70	9
Scaffold L80	11
Scaffold L90	14
Scaffold L100	4,208
Scaffold NG10	341,137,916
Scaffold NG20	341,137,916
Scaffold NG30	341,137,916
Scaffold NG40	341,137,916
Scaffold NG50	341,137,916
Scaffold NG60	341,137,916
Scaffold NG70	341,137,916
Scaffold NG80	341,137,916
Scaffold NG90	341,137,916
Scaffold NG100	341,137,916
Scaffold LG10	1
Scaffold LG20	1
Scaffold LG30	1
Scaffold LG40	1
Scaffold LG50	1
Scaffold LG60	1
Scaffold LG70	1
Scaffold LG80	1
Scaffold LG90	1

Scaffold LG100	1
Contig N10	31,810,334
Contig N20	23,242,895
Contig N30	18,319,056
Contig N40	14,176,216
Contig N50	10,858,724
Contig N60	8,172,830
Contig N70	5,514,941
Contig N80	3,153,579
Contig N90	1,316,638
Contig N100	503
Contig L10	6
Contig L20	17
Contig L30	30
Contig L40	47
Contig L50	69
Contig L60	98
Contig L70	140
Contig L80	206
Contig L90	333
Contig L100	5,480
Contig NG10	78,618,297
Contig NG20	78,618,297
Contig NG30	78,618,297
Contig NG40	78,618,297
Contig NG50	78,618,297
Contig NG60	78,618,297
Contig NG70	78,618,297
Contig NG80	78,618,297
Contig NG90	78,618,297
Contig NG100	78,618,297

Contig LG10	1
Contig LG20	1
Contig LG30	1
Contig LG40	1
Contig LG50	1
Contig LG60	1
Contig LG70	1
Contig LG80	1
Contig LG90	1
Contig LG100	1
Gap N10	100
Gap N20	100
Gap N30	100
Gap N40	100
Gap N50	100
Gap N60	100
Gap N70	100
Gap N80	100
Gap N90	100
Gap N100	100
Gap L10	128
Gap L20	255
Gap L30	382
Gap L40	509
Gap L50	636
Gap L60	764
Gap L70	891
Gap L80	1,018
Gap L90	1,145
Gap L100	1,272

Table S 6-2. **Complete genome repeat statistics of the tokay gecko**.

		number of elements*	length occupied	percentage of sequence
Retroelements		**738,120**	**173,753,694 bp**	**6.34%**
	SINEs:	272,912	26,735,118 bp	0.98%
	Penelope	75	14,042 bp	0.00%
	LINEs:	453,890	141,006,990 bp	5.14%
	CRE/SLACS	0	0 bp	0.00%
	L2/CR1/Rex	453,784	140,986,049 bp	5.14%
	R1/LOA/Jockey	0	0 bp	0.00%
	R2/R4/NeSL	0	0 bp	0.00%
	RTE/Bov-B	0	0 bp	0.00%
	L1/CIN4	31	6,899 bp	0.00%
	LTR elements:	11,318	6,011,586 bp	0.22%
	BEL/Pao	0	0 bp	0.00%
	Ty1/Copia	0	0 bp	0.00%
	Gypsy/DIRS1	9,536	5,663,273 bp	0.21%
	Retroviral	1,720	338,909 bp	0.01%
DNA transposons		**10,622**	**970,491 bp**	**0.04%**
	hobo-Activator	2,535	250,048 bp	0.01%
	Tc1-IS630-Pogo	288	49,187 bp	0.00%
	En-Spm	0	0 bp	0.00%
	MuDR-IS905	0	0 bp	0.00%
	PiggyBac	0	0 bp	0.00%
	Tourist/Harbinger	2,796	190,934 bp	0.01%
	Other (Mirage, P-element, Transib)	0	0 bp	0.00%
Rolling-circles		**15**	**2,208 bp**	**0.00%**
Unclassified:		**1,327**	**205,026 bp**	**0.01%**
Total interspersed repeats:			**174,929,211 bp**	**6.38%**
Small RNA:		**152,557**	**10,439,824 bp**	**0.38%**
Satellites:		**521**	**26,033 bp**	**0.00%**
Simple repeats:		**701,504**	**32,228,786 bp**	**1.18%**
Low complexity:		**94,953**	**6,768,206 bp**	**0.25%**

* as stated in the software report, most repeats fragmented by insertions or deletions have been counted as one element. Runs of >=20 X/Ns in query were excluded in % calcs. The query species was assumed to be *Gallus gallus*. RepeatMasker Combined Database: Dfam-Dfam_3.0, RepBase-20181026. run with rmblastn version 2.9.0+

Chapter 7. Summary, Discussion and Perspective

Summary

Regeneration is the ability of an organism to restore damaged or lost tissue, without the production of scar tissue, and with the newly formed tissue able to replace the function of the lost tissue (Pirotte et al., 2016; Poss, 2010). Regeneration is important as one of the survival strategies used by animals to deal with injuries (Bely and Nyberg, 2010; Gurtner et al., 2008). Regeneration goes beyond wound healing or repair, in which the lost tissue is simply covered over by epithelium or replaced by scar tissue (as in mammals, for example). Regeneration can take place at various level of biological organization, from a cell to a whole body, and can initiated at a wide range of stages in an animal's lifecycle (Bely and Nyberg, 2010). It always involves cell proliferation and differentiation after injury (Ricci and Srivastava, 2018; Tanaka and Reddien, 2011). Therefore, it relies on a population of stem cells (Ricci and Srivastava, 2018; Tanaka and Reddien, 2011). The availability of stem cells in different animals may explain the widely differing regenerative capacity in different species.

Regeneration in the vertebrates is more limited compared to that of the invertebrates. In humans and mice, for example, the capacity for true regeneration is limited to the fingertips, provided (in humans) that the nail bed is preserved (Gang and Lenghi, 1982; Muneoka and Dawson, 2021; Narayanan, 2015; Tang et al., 2014). The liver in humans and other mammals can restore lost parts, but there are some researchers who describe this as physiological size regulation rather than true regeneration (Michalopoulos, 2007; Wang et al., 2019b). However, other vertebrates show impressive regeneration capacity. These include teleost such as the zebrafish (*Danio rerio*), lissamphibians such as salamanders (Urodeles) and squamates such as lizards, including geckos (Li et al., 2015). Those animals are commonly used as models for regeneration studies as they can provide insights not available from mammals which have such limited regeneration capacities (Kurup and Ramachandran, 2011; Song et al., 2010).

Lizards are well-known for the phenomenon of tail autotomy whereby the tail breaks off at pre-existing fracture planes when grabbed by a predator. Autotomy is intended to distract a predator because the broken-off tail fragment remains twitching on the ground for some time (Bae et al., 2014). Autotomy in lizards is generally accompanied by an ability to regenerate the lost piece of tail.

Tail regeneration in lizards result in the development of a new, complex structure (the replacement tail) from a group of proliferating cells on the tail stump called the

blastema. It is this blastema formation and differentiation, among other things, that make the lizard a useful model for studying tissue regeneration (Bely and Nyberg, 2010; Hill et al., 2012; Lozito and Tuan, 2015; Russell et al., 2015).

In this thesis, we use the tokay gecko (*Gekko gecko*) as a model species. The tokay gecko is a lizard, a member of the suborder Lacertilia, family Gekkonidae whose members are found from Northeast India to Southern China and throughout Southeast Asia (Das, 2015). The total body length (TL; snout to tip of tail) of the tokay gecko is around 35 cm and the snout-vent length (SVL) is around 18.5 cm (Cobos and Higham, 2022); it is the second largest living gecko after the New Caledonian gecko (*Rhacodactylus leachianus*) (Kongbuntad et al., 2016).

In **Chapter 1**, We have summarized the current literature about regeneration, especially in the vertebrates, and the importance of studying regeneration in different species. Moreover, we have explored in more depth tail regeneration in lizards. As amniotes, lizards are closer to mammals (including humans) than are the urodeles and teleost model species.

In **Chapter 2**, We have described the tissue structure of seven stages of the adult tokay gecko regenerating tail. We found that the process of tail regeneration in the tokay gecko, histologically, involves a series of well-defined phases that mirror those observed in other lizards, albeit with species-specific variations in timing and complexity. Additionally, we found that the blastema in the regenerating tail of the tokay gecko is heterogeneous even when it was still in pre-blastema tissue underneath the wound epithelium at 8 dpa (days post-autotomy). Finally, we find no histological evidence of an apical growth zone as seen in urodeles.

In **Chapter 3**, We describe a distinctive molecular signature at each stage of tail regeneration in the tokay gecko. There was early upregulation of immune-related genes in the wound healing phase, followed by the upregulation of a subset developmental genes in the blastema phase and upregulation of genes related with skeletal muscle maturation and functional development at differentiation phase. Moreover, we also found that transcriptome profile of regenerating tail, with respect to developmental patterning genes, is different compared to that of embryonic tail.

In **Chapter 4**, We show, using single cell mRNA sequencing, that the regeneration blastema, and the embryonic tailbud, in the tokay gecko have different cell clusters. In addition, by using bioinformatics approach, we also find that the terminal states cell clusters in the regenerated tail blastema predominantly develop from within their own lineage. This is different compared to the embryonic tailbud in which the precursor cell population is predominantly pluripotent stem cells.

In **Chapter 5**, We focused particularly on genes involved in axonogenesis, chondrogenesis, myogenesis and segmentation. We examine the candidate genes identified with bulk transcriptomics and single-cell mRNA sequencing for spatial expression in the tissue section of regenerating tail using *in situ* hybridization. The findings presented in this chapter suggest that the regeneration of the tokay gecko tail may involves the early activation of a stem cell population, likely consisting of satellite cells and fibroblasts, that retain positional memory from the original tail. This positional memory facilitates the regeneration of an appropriate tail replacement, without establishing *de novo* patterning, as observed in normal development.

In **Chapter 6**, we have provided a sufficient genome assembly and annotation of the tokay gecko to be used as a genome reference for a diverse range of biological research using the tokay gecko as a model organism, especially studies focusing on tissue regeneration.

In summary, our study suggests that tail regeneration in the tokay gecko utilizes distinct mechanisms compared to the blastema-based regeneration observed in salamanders and teleost fish. Furthermore, regeneration in this gecko is not simply a reactivation of developmental processes. Despite the having similar stages of regeneration to the axolotl and zebrafish (wound healing, blastema formation, differentiation, and maturation), tokay gecko tail regeneration differs in terms of blastema cell recruitment. Thus, it appears to be more reliant on the activation of lineage-restricted resident stem cells within the uninjured tail, rather than on generating stem cells through the dedifferentiation of mature tissues. This may explain why the regenerating tokay gecko tail re-activates only a subset of developmental genes — and even that is at a relatively late stage of the regenerative process (16 dpa), not earlier, as would be expected if the blastema were a developmental field. tokay gecko tail regeneration also appears to leverage the existing positional memory of the resident stem cells to rebuild the lost structure.

Our finding of a lineage-restricted, stem-cell based regeneration mechanism in reptiles could have translational applications in human regenerative medicine. Interestingly, some phenomena in mammalian regeneration, such as the regeneration of mouse digit tips (Johnson et al., 2020; Lehoczky et al., 2011) and deer antlers (Qin et al., 2023; Wang et al., 2019a), have also been found to depend on the activation of lineage-restricted stem cells. However, mammals have certain limitations as research models for regeneration, when compared with the tokay gecko. For example, in the mouse digit model, regeneration is restricted to a very limited area, and only occurs if the digit is amputated distal to the last interphalangeal joint (Borgens, 1982). And the deer antler model would be impractical in terms of expense, and only involves the

regeneration of bone tissue (Qin et al., 2023; Wang et al., 2019a). Therefore, the gecko becomes an attractive model for studying a type of regeneration, that we believe is shared with humans and other mammals, that is based on lineage-restricted resident stem cells.

Future investigations should functionally examine the molecular pathways, signaling cascades, and cellular dynamics governing the activation and differentiation of resident stem cell populations responsible for tokay gecko tail regeneration. This can be complemented by lineage-tracing studies to definitively identify and characterize the resident stem cells involved, confirming their role and determining their activation during regeneration. Additionally, further study of the mechanisms underlying positional memory in tokay gecko resident stem cells would provide valuable insights into how positional memory directs the regeneration process. These insights could potentially be leveraged to develop bioengineering techniques, such as supportive scaffolds, that can guide and facilitate regeneration, thereby translating research findings into medical applications.

Discussion and Perspective

Taken together, these findings support the concept of two major pathways of regeneration in vertebrates (Table 7-1). One is exemplified by caudal fin regeneration in zebrafish, and limb regeneration in axolotls (Cox, 1969; Hutchins et al., 2014). In this type of regeneration, we suggest, the blastemas are relatively small — of the order of 1 mm. This, according to Wolpert, is the size of a classic developmental field, such as an embryonic limb bud or tailbud, in which positional values are specified *de novo* (Wolpert, 1969). In this type of regeneration, and in a classical developmental field, development gene expression is early, distal and occurs in a small area. For example, in zebrafish tail regeneration there is an apical growth zone in which there is a distal-to-proximal gradient in differentiation (Pfefferli and Jazwinska, 2015), very much like a developmental field such as the progress zone of the embryonic limb bud (Tabin and Wolpert, 2007).

The other pathway of regeneration in vertebrates is quite different and is exemplified by tail regeneration in geckos (and other lizards). The regeneration blastema in lizards is much larger that a classical developmental field or regeneration blastema of zebrafish caudal fin (Pfefferli and Jazwinska, 2015) and axolotl limb (Gerber et al., 2018; Kragl et al., 2009). Developmental gene expression and proliferating cells in this system are ‘distributed’ through the blastema (Hutchins et al., 2014), and not restricted to a small, apical growth zone. However, in the tokay gecko, we find no such gradient of expression. Furthermore, we only find expression of developmental patterning genes in regenerating cartilage, muscle and skin. Moreover, the developmental genes are

activated relatively late in tokay gecko tail regeneration. We examined the blastema for evidence of a growth zone but found only *col1a2*$^{+}$ connective tissue cells under the wound epithelium, a finding inconsistent with a growth zone.

We suggest that the large size of the regeneration blastema in the tokay gecko tail might be related to the relatively large body size of this species (see above) compared to other lizards in which regeneration has been studied (e.g. *Anolis carolinensis* (Xu et al., 2020) , *Eublepharis macularius* (Delorme et al., 2012), *Lepidodactylus lugubris* (Vonk et al., 2023), *Hemidactylus frenatus* (Nagumantri et al., 2021), and *Podarcis muralis* (Alibardi, 2017)). Furthermore, we suggest that there is no *de novo* specification of positional information in the blastema of the tokay gecko. Rather, regeneration depends on pre-existing positional values. This hypothesis is supported by HOXC gene expression in the regenerating tail of the tokay gecko. HOX genes are transcription factors that play a key role in embryonic axial patterning (Di-Poi et al., 2010; Kawanishi et al., 2003; van den Akker et al., 2001) and, potentially, in adult tissue regeneration (Gersch et al., 2005; Rux and Wellik, 2017).

Table 7-1. **The tokay geckos and other lizards show a pattern of regeneration that is quite different from a classical developmental field**. Note that the blastemas of the regenerating caudal fin, and the regenerating limbs in the axolotl, are similar in properties and size to developmental fields of embryos. By contrast, the regenerating tail blastema of geckos and other lizards is quite different from a developmental field.

model system	width of bud or blastema *	main site of pattern specification	gradient of cell and tissue differentiation	stage** of expression of patterning genes	Ref.
Tokay gecko adult tail regeneration	3–5 mm	distributed	distributed	middle-late	this study; (Hutchins et al., 2014)
Tokay gecko embryo tailbud	200 µm	distal only	distal to proximal	early	this study
Zebrafish adult caudal fin regeneration ***	150–200 µm	distal only	distal to proximal	early	(Thummel et al., 2007)
Zebrafish tailbud	125 µm	distal only	distal to proximal	early	(Kimmel et al., 1995)
Axolotl adult limb regeneration	300 µm	distal only	distal to proximal	early	(Gerber et al., 2018)
Axolotl embryo limb bud (Stage 40)	150 µm	distal only	distal to proximal	early	(Bordzilovskaya et al., 1989)

* Our interpretation based on the scale indicated in Figures within the manuscript.

** relative to cell differentiation and tissue maturation events

*** We assume that the caudal fin has not a single large blastema, but multiple small blastemas, one at the tip of each ray.

Our data show that HOX gene expression exhibits temporal collinearity in the regenerating gecko tail, primarily at mid-stages of regeneration, and primarily in

myoblasts. This contrasts with the regenerating axolotl limb, where HOX expression may not be temporally or spatially collinear (Mallo and Alonso, 2013; Woltering et al., 2009). These observations suggests that HOX expression plays a role in gecko tail regeneration. One possible function is that the late-stage expression of *hoxc13* signals the end of pattern formation during tail regeneration, similar to its role in normal tail development (Aires et al., 2019). Another potential function is that HOX expression provides positional cues that guide the regeneration process, as seen in other vertebrate's models where only the appropriate missing parts are regenerated. For instance in axolotl limb regeneration (Otsuki and Tanaka, 2022; Pescitelli and Stocum, 1980) and zebrafish caudal fin regeneration (Isabella et al., 2021; Uemoto et al., 2020) only the lost parts are replaced.

The analysis of our single-cell mRNA sequencing and *in situ* hybridization data suggests that the tokay gecko regeneration blastema is derived from existing resident stem cells. For instance, early expression of the myogenic markers *pax3*, *pax7*, and *myod1* indicates an early activation of satellite cells in the regeneration blastema, and their possible contribution to myogenesis. While the Notch signaling modulator *lfng* is expressed in tokay gecko tail regeneration, the Hes genes associated with embryonic segmentation, such as *hes7*, do not appear to be expressed. This observation is consistent with evidence from axolotl tail regeneration that *lfng+* multipotent stem cells give rise to segmented structures during regeneration without the involvement of *hes7* (Wouter et al., 2024). We suggest that muscle segmentation in the blastema may rely on positional memory in satellite cells, which 'remember' the segmentation of the original muscle. This suggestion is supported by a study of mouse cell lines, showing the satellite cells have positional memory regulated by *hoxa10* (Yoshioka et al., 2021).

The details of cartilage patterning in the gecko tail also support the idea that there is no *de novo* patterning in the regenerating gecko tail, but rather a reliance on existing positional information. Our starting point for this argument is that the regenerated cartilage tube in the tokay gecko tail is unsegmented, whereas the skeletal muscle is segmented. This is quite different to axolotl tail regeneration, where *de novo* patterning generates both segmented vertebrae and segmented muscles (Wouter et al., 2024). The lack of segmentation of the cartilage tube in gecko might be caused by the absence of *pax1* expression. In embryonic tail development, *Pax1* is needed to mediate SHH signaling by the notochord, which induces sclerotome development (Wallin et al., 1994) and is also essential for further development of the vertebral column (Koseki et al., 1993). Of these two genes, only *Shh* and not *Pax1* is expressed in the ependymal lining of the cartilage tube in the regenerating tokay gecko tail (Lozito and Tuan, 2015). The fact that the regenerated muscles are segmented but the cartilage tube is not, suggests that their regeneration is uncoupled. Nonetheless, we suggest that both muscle and cartilage regeneration are both guided by Wnt signaling genes (*wnt3* and

wnt5a) because we find that both are expressed in cartilage and muscle in the regenerating tail.

Given these differences between the gecko tail regeneration blastema, and other developmental systems, it appears that tail regeneration in the lizards is an evolutionarily derived process not reported in other vertebrates. Our proposed model is that pattern formation in the blastema is based on the existing positional values of existing resident stem cell populations. This model is consistent with the finding that the cartilage tube in the regenerating lizard tail is derived from stromal cells resident in the vertebral periosteum (Lozito and Tuan, 2016); and with the finding that regenerating muscle might derive from stromal cells in muscle of the tail stump (Londono et al., 2017).

Studies on regeneration in other vertebrates have often been difficult to translate to human medicine because it apparently requires the reactivation of developmental-scale processes as well as pluripotent stem cells. The latter are lacking in adult humans. This thesis work shows that regeneration may take place in the tokay gecko using resident stem cells, and these cells are present in adult human tissues. Therefore, further translation studies in mammalian regeneration could be informed by the single-cell analyses and other data reported here. Another potential translational application of our data might be in cancer research. It has already been shown that regeneration shares many pathways with cancer (Alibardi, 2019; Greco et al., 2023). In this study, we also find several pathways involved in cancer are enriched in the regenerating tokay gecko tail, especially early stages (4 dpa). The potential links between regeneration and cancer are enigmatic and worth exploring in future studies.

This thesis has several limitations. It did not involve functional studies to experimentally validate the roles of the identified genes and pathways in the context of tokay gecko tail regeneration. While the bioinformatic analyses and *in situ* hybridization provided critical insights into spatial gene expression patterns, they did not establish direct causal relationships. Furthermore, the research did not involve lineage tracing (e.g. by cell labeling experiments), which could have tracked the origins, fates, and differentiation trajectories of individual cell populations throughout regeneration. Consequently, the correspondence between specific gene expression patterns and cell behaviors or tissue formation during regeneration remains unclear. To overcome these limitations, future studies could incorporate functional approaches, such as gene knockdown or overexpression experiments, in combination with lineage tracing techniques. This integrated approach would help validate the roles of key genes and provide a more comprehensive understanding of the cellular dynamics and molecular mechanisms underlying tail regeneration in geckos, ultimately strengthening the conclusions drawn from this thesis. Additionally, further investigation of the mechanisms governing positional memory in tokay gecko resident stem cells would yield valuable insights into how positional memory directs the regeneration process.

References

Aires, R., de Lemos, L., Nóvoa, A., Jurberg, A. D., Mascrez, B., Duboule, D. and Mallo, M. (2019). Tail bud progenitor activity relies on a network comprising gdf11, lin28, and hox13 genes. *Developmental Cell* **48**, 383-395.e388.

Alibardi, L. (2017). Wnt-1 immunodetection in the regenerating tail of lizard suggests it is involved in the proliferation and distal growth of the blastema. *Acta Histochemica* **119**, 211-219.

Alibardi, L. (2019). Review: The Regenerating Tail Blastema of Lizards as a Model to Study Organ Regeneration and Tumor Growth Regulation in Amniotes. *Anat Rec (Hoboken)* **302**, 1469-1490.

Bae, K. S., Kim, S. Y., Park, S. Y., Jeong, A. J., Lee, H. H., Lee, J., Cho, Y. S., Leem, S. H., Kang, T. H., Bae, K. H., et al. (2014). Identification of lactoferrin as a human dedifferentiation factor through the studies of reptile tissue regeneration mechanisms. *Journal of Microbiology and Biotechnology* **24**, 869-878.

Bely, A. E. and Nyberg, K. G. (2010). Evolution of animal regeneration: re-emergence of a field. *Trends in Ecology and Evolution* **25**, 161-170.

Bordzilovskaya, N. P., Dettlaff, T. A., Duhon, S. T. and Malacinski, G. M. (1989). Developmental-stage series of axolotl embryos. In *Developmental Biology of the Axolotl* (ed. J. B. A. a. G. M. Malacinski), pp. 201-219. New York: Oxford University Press.

Borgens, R. B. (1982). Mice Regrow the Tips of Their Foretoes. *Science* **217**, 747-750.

Cobos, A. J. and Higham, T. E. (2022). Growing up in a rough world: scaling of frictional adhesion and morphology of the Tokay gecko (Gekko gecko). *Beilstein J Nanotechnol* **13**, 1292-1302.

Cox, P. G. (1969). Some aspects of tail regeneration in the lizard, Anolis carolinensis. I. A description based on histology and autoradiography. *Journal of Experimental Zoology* **171**, 127-149.

Das, I. (2015). A field guide to the reptiles of South-East Asia. pp. 375-375.

Delorme, S. L., Lungu, I. M. and Vickaryous, M. K. (2012). Scar-Free Wound Healing and Regeneration Following Tail Loss in the Leopard Gecko, Eublepharis macularius. *Anatomical Record* **295**, 1575-1595.

Di-Poi, N., Montoya-Burgos, J. I., Miller, H., Pourquie, O., Milinkovitch, M. C. and Duboule, D. (2010). Changes in Hox genes' structure and function during the evolution of the squamate body plan. *Nature* **464**, 99-103.

Gang, R. K. and Lenghi, M. (1982). Conservative management of guillotine amputations of finger tips - Another application of zinc oxide tape. *Chirurgia Plastica* **7**, 75-81.

Gerber, T., Murawala, P., Knapp, D., Masselink, W., Schuez, M., Hermann, S., Gac-Santel, M., Nowoshilow, S., Kageyama, J., Khattak, S., et al. (2018). Single-cell analysis uncovers convergence of cell identities during axolotl limb regeneration. *Science* **362**.

Gersch, R. P., Lombardo, F., McGovern, S. C. and Hadjiargyrou, M. (2005). Reactivation of Hox gene expression during bone regeneration. *Journal of Orthopaedic Research* **23**, 882-890.

Greco, N., Onisto, M. and Alibardi, L. (2023). Protein extracts from regenerating lizard tail show an inhibitory effect on human cancer cells cultivated in-vitro. *Ann Anat* **250**, 152115.

Gurtner, G. C., Werner, S., Barrandon, Y. and Longaker, M. T. (2008). Wound repair and regeneration. *Nature* **453**, 314-321.

Hill, C., Jain, A., Takemoto, H., Silver, M. D., Nagesh, S. V. S., Ionita, C. N., Bednarek, D. R. and Rudin, S. (2012). A histological comparison of the original and regenerated tail in the green anole, Anolis carolinensis. *Anat Rec (Hoboken)* **295**, 1609-1619.

Hutchins, E. D., Markov, G. J., Eckalbar, W. L., George, R. M., King, J. M., Tokuyama, M. A., Geiger, L. A., Emmert, N., Ammar, M. J., Allen, A. N., et al. (2014). Transcriptomic

Analysis of Tail Regeneration in the Lizard Anolis carolinensis Reveals Activation of Conserved Vertebrate Developmental and Repair Mechanisms. *PLOS ONE* **9**, e105004.

Isabella, A. J., Stonick, J. A., Dubrulle, J. and Moens, C. B. (2021). Intrinsic positional memory guides target-specific axon regeneration in the zebrafish vagus nerve. *Development* **148**.

Johnson, G. L., Masias, E. J. and Lehoczky, J. A. (2020). Cellular heterogeneity and lineage restriction during mouse digit tip regeneration at single-cell resolution. *Developmental Cell* **52**, 525-540.e525.

Kawanishi, C. Y., Hartig, P., Bobseine, K. L., Schmid, J., Cardon, M., Massenburg, G. and Chernoff, N. (2003). Axial skeletal and Hox expression domain alterations induced by retinoic acid, valproic acid, and bromoxynil during murine development. *J Biochem.Mol.Toxicol.* **17**, 346-356.

Kimmel, C. B., Ballard, W. W., Kimmel, S. R., Ullmann, B. and Schilling, T. F. (1995). Stages of embryonic development of the zebrafish. *Developmental Dynamics* **203**, 253-310.

Kongbuntad, W., Tantrawatpan, C., Pilap, W., Jongsomchai, K., Chanaboon, T., Laotongsan, P., Petney, T. N. and Saijuntha, W. (2016). Genetic diversity of the red-spotted tokay gecko (Gekko gecko Linnaeus, 1758) (Squamata: Gekkonidae) in Southeast Asia determined with multilocus enzyme electrophoresis. *Journal of Asia-Pacific Biodiversity* **9**, 63-68.

Koseki, H., Wallin, J., Wilting, J., Mizutani, Y., Kispert, A., Ebensperger, C., Herrmann, B. G., Christ, B. and Balling, R. (1993). A role for Pax-1 as a mediator of notochordal signals during the dorsoventral specification of vertebrae. *Development* **119**, 649-660.

Kragl, M., Knapp, D., Nacu, E., Khattak, S., Maden, M., Epperlein, H. H. and Tanaka, E. M. (2009). Cells keep a memory of their tissue origin during axolotl limb regeneration. *Nature* **460**, 60-65.

Kurup, A. and Ramachandran, A. V. (2011). Exogenous NGF favors initiation of lizard tail regeneration while EGF and TGF- β truncate regenerative growth and commit to precocious muscle and cartilage differentiation. *journal of Developmental Biology and Tissue Engineering* **3**, 1-10.

Lehoczky, J. A., Robert, B. and Tabin, C. J. (2011). Mouse digit tip regeneration is mediated by fate-restricted progenitor cells. *Proc Natl Acad Sci U S A* **108**, 20609-20614.

Li, Q., Yang, H. and Zhong, T. P. (2015). Regeneration across metazoan phylogeny: lessons from model organisms. *Journal of genetics and genomics = Yi chuan xue bao* **42**, 57-70.

Londono, R., Wenzhong, W., Wang, B., Tuan, R. S. and Lozito, T. P. (2017). Cartilage and Muscle Cell Fate and Origins during Lizard Tail Regeneration. *Frontiers in Bioengineering and Biotechnology* **5**, 1-9.

Lozito, T. P. and Tuan, R. S. (2015). Lizard tail regeneration: Regulation of two distinct cartilage regions by Indian hedgehog. *Developmental Biology* **399**, 249-262.

---- (2016). Lizard tail skeletal regeneration combines aspects of fracture healing and blastema-based regeneration. *Development (Cambridge)* **143**, 2946-2957.

Mallo, M. and Alonso, C. R. (2013). The regulation of Hox gene expression during animal development. *Development* **140**, 3951-3963.

Michalopoulos, G. K. (2007). Liver regeneration. *Journal of Cellular Physiology* **213**, 286-300.

Muneoka, K. and Dawson, L. A. (2021). Evolution of epimorphosis in mammals. *J Exp Zool B Mol Dev Evol* **336**, 165-179.

Nagumantri, S. P., Banu, S. and Idris, M. M. (2021). Transcriptomic and proteomic analysis of Hemidactylus frenatus during initial stages of tail regeneration. *Scientific Reports* **11**.

Narayanan, A. (2015). Biochips & Tissue Chips The Initiation and Progression of Tail Regeneration in Northern House Gecko Hemidactylus Flaviviridis at Role of Fibroblast Growth Factor 2. *Biochip & Tissue Chip* **5**, 1-7.

Otsuki, L. and Tanaka, E. M. (2022). Positional Memory in Vertebrate Regeneration: A Century's Insights from the Salamander Limb. *Cold Spring Harb Perspect Biol* **14**.

Pescitelli, M. J., Jr. and Stocum, D. L. (1980). The origin of skeletal structures during intercalary regeneration of larval Ambystoma limbs. *Dev Biol* **79**, 255-275.

Pfefferli, C. and Jazwinska, A. (2015). The art of fin regeneration in zebrafish. *Regeneration (Oxf)* **2**, 72-83.

Pirotte, N., Leynen, N., Artois, T. and Smeets, K. (2016). Do you have the nerves to regenerate? The importance of neural signalling in the regeneration process. *Developmental Biology* **409**, 4-15.

Poss, K. D. (2010). Advances in understanding tissue regenerative capacity and mechanisms in animals. *Nature Reviews Genetics* **11**, 710-722.

Qin, T., Zhang, G., Zheng, Y., Li, S., Yuan, Y., Li, Q., Hu, M., Si, H., Wei, G., Gao, X., et al. (2023). A population of stem cells with strong regenerative potential discovered in deer antlers. *Science* **379**, 840-847.

Ricci, L. and Srivastava, M. (2018). Wound-induced cell proliferation during animal regeneration. *Wiley Interdisciplinary Reviews: Developmental Biology* **7**, 1-17.

Russell, A. P., Lynn, S. E., Powell, G. L. and Cottle, A. (2015). The regenerated tail of juvenile leopard geckos (Gekkota: Eublepharidae: Eublepharis macularius) preferentially stores more fat than the original. *Zoology* **118**, 183-191.

Rux, D. R. and Wellik, D. M. (2017). Hox genes in the adult skeleton: Novel functions beyond embryonic development. *Developmental Dynamics* **246**, 310-317.

Song, F., Li, B. and Stocum, D. L. (2010). Amphibians as research models for regenerative medicine. *Organogenesis* **6**, 141-150.

Tabin, C. and Wolpert, L. (2007). Rethinking the proximodistal axis of the vertebrate limb in the molecular era. *Genes Dev.* **21**, 1433-1442.

Tanaka, E. and Reddien, P. W. (2011). The cellular basis for animal regeneration Sources of new cells in animal regeneration. *Dev Cell* **21**, 172-185.

Tang, J. B., Elliot, D., Adani, R., Saint-Cyr, M. and Stang, F. (2014). Repair and reconstruction of thumb and finger tip injuries: A global view. *Clinics in Plastic Surgery* **41**, 325-359.

Thummel, R., Ju, M., Sarras, M. P., Jr. and Godwin, A. R. (2007). Both Hoxc13 orthologs are functionally important for zebrafish tail fin regeneration. *Dev Genes Evol* **217**, 413-420.

Uemoto, T., Abe, G. and Tamura, K. (2020). Regrowth of zebrafish caudal fin regeneration is determined by the amputated length. *Scientific Reports* **10**, 1-11.

van den Akker, E., Fromental-Ramain, C., de Graaff, W., Le Mouellic, H., Brulet, P., Chambon, P. and Deschamps, J. (2001). Axial skeletal patterning in mice lacking all paralogous group 8 Hox genes. *Development* **128**, 1911-1921.

Vonk, A. C., Zhao, X., Pan, Z., Hudnall, M. L., Oakes, C. G., Lopez, G. A., Hasel-Kolossa, S. C., Kuncz, A. W. C., Sengelmann, S. B., Gamble, D. J. and Lozito, T. P. (2023). Single-cell analysis of lizard blastema fibroblasts reveals phagocyte-dependent activation of Hedgehog-responsive chondrogenesis. *Nature Communications* **14**, 4489.

Wallin, J., Wilting, J., Koseki, H., Fritsch, R., Christ, B. and Balling, R. (1994). The role of Pax-1 in axial skeleton development. *Development* **120**, 1109-1121.

Wang, D., Berg, D., Ba, H., Sun, H., Wang, Z. and Li, C. (2019a). Deer antler stem cells are a novel type of cells that sustain full regeneration of a mammalian organ-deer antler. *Cell Death Dis* **10**, 443.

Wang, S., Zhang, C., Hasson, D., Desai, A., SenBanerjee, S., Magnani, E., Ukomadu, C., Lujambio, A., Bernstein, E. and Sadler, K. C. (2019b). Epigenetic compensation promotes liver regeneration. *Developmental Cell* **50**, 43-56.e46.

Wolpert, L. (1969). Positional information and the spatial pattern of cellular differentiation. *Journal of Theoretical Biology* **25**, 1-47.

Woltering, J. M., Vonk, F. J., Müller, H., Bardine, N., Tuduce, I. L., de Bakker, M. A. G., Knöchel, W., Sirbu, I. O., Durston, A. J. and Richardson, M. K. (2009). Axial patterning in snakes and caecilians: Evidence for an alternative interpretation of the Hox code. *Developmental Biology* **332**, 82-89.

Wouter, M., Tobias, G., Francisco, F., Tom, D., Sofia-Christina, P., Marko, P., Vijayishwer Singh, J., Yuka, T.-S., Tzi-Yang, L., Thomas, K., et al. (2024). Somite-independent regeneration of the axolotl primary body axis. *bioRxiv*, 2024.2001.2031.577464.

Xu, C., Hutchins, E. D., Tokuyama, M. A., Wilson-Rawls, J. and Kusumi, K. (2020). Transcriptional analysis of scar-free wound healing during early stages of tail regeneration in the green anole lizard, Anolis carolinensis. *Journal of Immunology and Regenerative Medicine* **7**, 100025-100025.

Yoshioka, K., Nagahisa, H., Miura, F., Araki, H., Kamei, Y., Kitajima, Y., Seko, D., Nogami, J., Tsuchiya, Y., Okazaki, N., et al. (2021). Hoxa10 mediates positional memory to govern stem cell function in adult skeletal muscle. *Science Advances* **7**, eabd7924.

Nederlandse samenvatting

Regeneratie is het vermogen van een organisme om beschadigd of verloren weefsel te herstellen zonder de productie van littekenweefsel, waarbij het nieuwgevormde weefsel de functie van het verloren weefsel vervangt (Pirotte et al., 2016; Poss, 2010). Regeneratie is belangrijk als een van de overlevingsstrategieën die dieren gebruiken om met verwondingen om te gaan (Bely en Nyberg, 2010; Gurtner et al., 2008). Regeneratie gaat verder dan wondgenezing of reparatie, waarbij het verloren weefsel eenvoudig wordt bedekt door epitheel of vervangen door littekenweefsel (zoals bij zoogdieren bijvoorbeeld). Regeneratie kan plaatsvinden op verschillende biologische organisatieniveaus, van cel tot volledig lichaam, en kan op verschillende stadia in de levenscyclus van een dier worden geïnitieerd (Bely en Nyberg, 2010). Het omvat altijd celproliferatie en differentiatie na een verwonding en is daarom afhankelijk van de aanwezige populatie stamcellen (Ricci en Srivastava, 2018; Tanaka en Reddien, 2011). De beschikbaarheid van stamcellen in verschillende dieren kan het verschil in regeneratief vermogen tussen soorten verklaren.

Regeneratie bij gewervelde dieren is beperkter vergeleken met ongewervelden. Bij mensen en muizen, bijvoorbeeld, is de capaciteit voor echte regeneratie beperkt tot de vingertoppen, mits (bij mensen) het nagelbed behouden is (Gang en Lenghi, 1982; Muneoka en Dawson, 2021; Narayanan, 2015; Tang et al., 2014). De lever bij mensen en andere zoogdieren kan verloren delen herstellen, maar sommige onderzoekers beschrijven dit als een regulatie van de fysiologische grootte in plaats van echte regeneratie (Michalopoulos, 2007; Wang et al., 2019b). Andere gewervelde dieren vertonen echter indrukwekkende regeneratieve capaciteiten. Waaronder Teleostei (beenvissen) zoals de zebravis (*Danio rerio*), Lissamphibia zoals salamanders (Urodela) en Squamata zoals hagedissen, gekko's inbegrepen (Li et al., 2015). Deze dieren worden vaak gebruikt als modellen voor regeneratiestudies omdat ze inzichten bieden die niet beschikbaar zijn bij zoogdieren met hun beperkte regeneratie vermogen (Kurup en Ramachandran, 2011; Song et al., 2010).

Hagedissen staan bekend om het fenomeen van staart-autotomie, waarbij de staart afbreekt langs bestaande breukvlakken wanneer het gegrepen wordt door een roofdier. Autotomie is bedoeld om een roofdier af te leiden, omdat het afgebroken staartfragment enige tijd op de grond blijft trillen (Bae et al., 2014). Autotomie bij hagedissen gaat over het algemeen gepaard met het vermogen om het verloren stuk staart te regenereren.

De staartregeneratie van hagedissen resulteert in de ontwikkeling van een nieuwe, complexe structuur (de vervangende staart) vanuit een groep prolifererende cellen op de staartstomp, het blastema. Het is onder andere de vorming en differentiatie

van het blastema die de hagedis een nuttig model maakt voor het bestuderen van weefselregeneratie (Bely en Nyberg, 2010; Hill et al., 2012; Lozito en Tuan, 2015; Russell et al., 2015).

In dit proefschrift gebruiken we de tokay gekko (*Gekko gecko*) als modelsoort. De tokay gekko is een hagedis, lid van de suborde Lacertilia, familie Gekkonidae. De tokay gekko komt voot van noordoostelijk India tot zuidelijk China en in heel Zuidoost-Azië (Das, 2015). De totale lichaamslengte (TL; snuit tot het puntje van de staart) van de tokay gekko is ongeveer 35 cm en de snuit-vent lengte (SVL) is ongeveer 18,5 cm (Cobos en Higham, 2022); het is de op een na grootste levende gekko na de Nieuw-Caledonische gekko (Rhacodactylus leachianus) (Kongbuntad et al., 2016).

In **Hoofdstuk 1** hebben we de huidige literatuur over regeneratie, vooral bij gewervelden, en het belang van het bestuderen van regeneratie in verschillende soorten samengevat. Bovendien hebben we de staartregeneratie bij hagedissen dieper onderzocht. Als amnioten staan hagedissen dichter bij zoogdieren (inclusief mensen) dan de Urodela en Teleostei modelsoorten.

In **Hoofdstuk 2** beschrijven we de weefselstructuur van zeven stadia van de regenererende staart van de volwassen tokay gekko. We ontdekten dat het proces van staartregeneratie bij de tokay gekko histologisch gezien een reeks goed gedefinieerde fasen omvat die overeenkomen met die waargenomen bij andere hagedissen, hoewel er soortspecifieke variaties in timing en complexiteit zijn. Daarnaast ontdekten we dat het blastema in de regenererende staart van de tokay gekko heterogeen is, zelfs toen het nog in het pre-blastema weefsel onder het wondepitheel zat op 8 dpa (dagen na autotomie). Ten slotte vonden we geen histologisch bewijs van een apicale groeizone zoals gezien bij Urodela.

In **Hoofdstuk 3** beschrijven we een onderscheidend moleculair kenmerk in elk stadium van de staartregeneratie bij de tokay gekko. Er was een vroege verhoging van het aantal immuun-gerelateerde genen in de wondgenezingsfase, gevolgd door de verhoging van een subset ontwikkelingsgenen in de blastema fase en de verhoging van genen die verband houden met skeletspier maturatie en functionele ontwikkeling in de differentiatiefase. Bovendien vonden we dat het transcriptoom-profiel van de regenererende staart-blastema, met betrekking tot ontwikkelingspatroongenen, verschilt van dat van de embryonale staart.

In **Hoofdstuk 4** tonen we, met behulp van single-cell mRNA-sequencing, aan dat het regenererende staart-blastema en de embryonale staartknop bij de tokay gekko bestaat uit verschillende celclusters. Daarnaast ontdekten we, door gebruik te maken van een bioinformatica, dat de terminale toestanden in het geregenereerde staart-blastema

voornamelijk ontwikkelen vanuit hun eigen cellijn. Dit verschilt van de embryonale staartknop, waarin de voorloperpopulatie voornamelijk pluripotente stamcellen betreft.

In **Hoofdstuk 5** we richtten ons met name op genen die betrokken zijn bij axonogenese, chondrogenese, myogenese en segmentatie. Wij identificeerde de kandidaatgenen met bulktranscriptomics en single-cell mRNA-sequencing en met in situ hybridisatie hun ruimtelijke expressie in de weefselsecties van de regenererende staart. De bevindingen in dit hoofdstuk suggereren dat de regeneratie van de tokay gekko staart de vroege activering van een stamcelpopulatie omvat, waarschijnlijk bestaand uit satellietcellen en fibroblasten, die het positionele geheugen behouden van de oorspronkelijke staart. Dit positionele geheugen vergemakkelijkt de regeneratie van een passende staartvervanging, zonder nieuwe patroonvorming zoals waargenomen bij normale ontwikkeling.

In **Hoofdstuk 6** leveren we een genoomassemblage en annotatie van de tokay gekko, die kan worden gebruikt als een genoomreferentie voor een breed scala aan biologisch onderzoek met de tokay gekko als modelorganisme, met name studies gericht op weefselregeneratie.

Samenvattend suggereert onze studie dat staartregeneratie bij de tokay gekko gebruikmaakt van duidelijk ander mechanismen dan de blastema-gebaseerde regeneratie die wordt waargenomen bij salamanders en beenvissen. Bovendien is regeneratie bij deze gekko niet simpelweg een re-activatie van ontwikkelingsprocessen. Ondanks dat de regeneratiestadia vergelijkbaar zijn met die van de axolotl en zebravis (wondgenezing, blastemavorming, differentiatie en maturatie), verschilt de tokay gekko staartregeneratie in celrekrutering voor de blastema. Het lijkt meer afhankelijk te zijn van de activering van lijngebonden, residente stamcellen van de onbeschadigde staart, in plaats van het genereren van stamcellen door de-differentiatie van volwassen cellen. Dit zou kunnen verklaren waarom de regenererende tokay gekko staart slechts een subset van ontwikkelingsgenen heractiveert — en dat zelfs relatief laat in het regeneratie proces doet (16 dpa), niet eerder, zoals verwacht zou worden als het blastema een ontwikkelingsveld was. Tokay gekko staartregeneratie lijkt ook gebruik te maken van het bestaande positionele geheugen van de resdinte stamcellen om de verloren structuur te herbouwen.

Onze bevinding van een stamcelgebaseerd regeneratiemechanisme, beperkt tot bepaalde cellijnen bij reptielen, zou toepassingen kunnen hebben in de menselijke regeneratieve geneeskunde. Interessant genoeg zijn enkele fenomenen in zoogdierregeneratie, zoals de regeneratie van muisvingertopjes (Johnson et al., 2020; Lehoczky et al., 2011) en hertengeweien (Qin et al., 2023; Wang et al., 2019a), ook

afhankelijk van de activering van cellijn gebonden stamcellen. Zoogdieren hebben echter bepaalde beperkingen als onderzoeksmodellen voor regeneratie, vergeleken met de tokay gekko. In het muisvingermodel is regeneratie bijvoorbeeld beperkt tot een zeer klein gebied en vindt het alleen plaats als de vinger wordt geamputeerd distaal van het laatste interphalangeale gewricht (Borgens, 1982). En het hertengeweimodel zou onpraktisch zijn qua kosten en betreft alleen de regeneratie van botweefsel (Qin et al., 2023; Wang et al., 2019a). Daarom wordt de gekko een aantrekkelijk model voor het bestuderen van een type regeneratie, waarvan wij geloven dat het gedeeld wordt met mensen en andere zoogdieren, dat gebaseerd is op cellijn gebonden, residente stamcellen.

Toekomstig onderzoek zou de moleculaire routes, signaalcascades en cellulaire dynamiek die de activering en differentiatie van de residente stamcelpopulaties verantwoordelijk voor tokay gekko staartregeneratie beheersen moeten analyseren . Dit kan worden aangevuld met lijntraceringsstudies om de betrokken residente stamcellen definitief te identificeren en te karakteriseren, hun rol te bevestigen en hun activering tijdens regeneratie te bepalen. Bovendien zou verder onderzoek naar de mechanismen die ten grondslag liggen aan het positionele geheugen in tokay gekko residente stamcellen waardevolle inzichten kunnen bieden in hoe positioneel geheugen het regeneratieproces stuurt. Deze inzichten zouden mogelijk kunnen worden benut om bio-engineeringstechnieken te ontwikkelen, zoals ondersteunende scaffolds, die regeneratie kunnen begeleiden en vergemakkelijken, waardoor onderzoeksbevindingen naar medische toepassingen kunnen worden vertaald.

Curriculum vitae

Luthfi Nurhidayat was born on November 14, 1987, in Sragen, Central Java, Indonesia. After completing his secondary education at State Senior High School in Gemolong, Sragen Regency, he pursued both his bachelor's (2005–2010) and master's (2010–2012) degrees at the Faculty of Biology, Universitas Gadjah Mada, Yogyakarta. For his bachelor's thesis, he conducted research at the Laboratory of Animal Structure and Development on the topic, *Cranial Muscle and Skeleton Structure and Head Movement Pattern of* Malayemys subtrijuga *(Schlegel & Müller, 1844) and* Cuora amboinensis *(Daudin, 1802),* under the supervision of Zuliyati Rohmah, M.Si., Ph.D. Eng. Luthfi continued his research on turtle anatomy at the same laboratory for his master's thesis, titled *Structural and Functional Adaptation of* Amyda cartilaginea *(Boddaert, 1770) and* Cuora amboinensis *(Daudin, 1802) to the Aquatic Environment,* under the supervision of Prof. Dr. Nyoman Puniawati Soesilo, S.U.

After earning his master's degree, Luthfi joined the Animal Structure and Development Laboratory as a research and academic assistant. In 2014, he was appointed as a lecturer and researcher at the same laboratory. As a lecturer, he taught various undergraduate courses, including Animal Structure and Development, Animal Anatomy, Animal Pathoanatomy, Animal Microtechnique, Animal Embryology, and Animal Histology. His research focused on the structure and function of reptiles and amphibians, as well as on histopathology.

In September 2020, Luthfi began his Ph.D. studies at the Institute of Biology Leiden, Leiden University, The Netherlands, with a scholarship from LPDP (Indonesia Endowment Fund for Education). These studies form the basis of this Ph.D studies and focused ontail regeneration in the adult Tokay Gecko (*Gekko gecko*) and comparing it with embryonic tail development. He combined bulk transcriptomics, single-cell sequencing, and an extensive panel of *in situ* hybridization experiments on tissue sections to characterize tail regeneration in the Tokay Gecko. Additionally, he conducted whole-genome sequencing and analysis of the Tokay Gecko as part of his doctoral research. His work was selected for a talk at the International Society for Regenerative Biology Inaugural Meeting held in Vienna from September 3–6, 2023. The results of his research at Leiden University are presented in this thesis.

List of Publications

Nuriliani A., **Nurhidayat L.**, Fatmasari H., Afina D., Alamsyah F., Taruno W. P., & Pratiwi R. (2024). Non-Contact Electric Field May Induced Higher CD4, CD8, Caspase-8, and Caspase-9 Protein Expression in Breast Tumor Tissue of Rats (*Rattus norvegicus* Berkenhout, 1769). *Malaysian Journal of Fundamental and Applied Sciences* **20**: 74-88

Alamsyah F., Firdausi N., Nugraheni S.E.D., Fadhlurrahman A.G., **Nurhidayat L.**, Pratiwi R. & Taruno W.P. (2023). Effects of non-contact electric fields on kidney and liver histology in tumour-induced rats. *F1000Research* **12**: 117.

Wang M., Rücklin M., Poelmann R.E., Mooij C.L. de, Fokkema M., Lamers G.E.M., Bakker M.A.G. de, Chin E., Bakos L.J., Marone F., Wisse B.J., Ruiter M.C. de, Cheng S., **Nurhidayat L.**, Vijver M.G. & Richardson M.K. (2023). Nanoplastics causes extensive congenital malformations during embryonic development by passively targeting neural crest cells. *Environment International* **173**: 107865.

Retnoaji B., **Nurhidayat L.**, Pratama S.F., Anshori K., Hananya A., Sofyantoro F. & Bessho Y. (2023). Embryonic development of Indonesian native fish yellow rasbora (*Rasbora lateristriata*). *Journal of King Saud University - Science* **35**: 102810.

Nuriliani A., Wulandari R., **Nurhidayat L.** 2022. Tongue Structure of *Rhinolophus pusillus* and *Miniopterus schreibersii*. *Acta Veterinaria Indonesiana* **10**: 211–21

Nurhidayat L., Fajar I., Yati A., Prinanda H.H., Irfan M., Afina D., Fadlurrahman A.G., Antara N.Y., Alamsyah F., Taruno W.P. & Pratiwi R. (2022). Evaluation of static electric field exposure on histopathological structure and function of kidney and liver in DMBA-Induced RAT (*Rattus norvegicus* Berkenhout, 1769). *Malaysian Journal of Fundamental and Applied Sciences* **18**: 703-713.

Alamsyah F., Pratiwi R., Firdausi N., Pello J.I.M., Nugraheni S.E.D., Fadhlurrahman A.G. **Nurhidayat L.** & Taruno W.P. (2021). Cytotoxic T cells response with decreased CD4/CD8 ratio during mammary tumors inhibition in rats induced by non-contact electric fields. *F1000Research* **10**: 35.

Nurhidayat L., Devi N.A. & Fadhillah D. (2020), Histological structure of nerve fiber and blood vessels in regenerated tail of Tokay gecko (*Gekko gecko* Linnaeus, 1758). Saragih H.T., Ilmi M., Nopitasari S., Audinah L., Widyasari A., Sari M.A., Masri M., Palilu P.T., Prabowo B.H., Soleha A., Solikhah A. & Fitriana N. (Eds.). AIP Conference Proceedings. THE 6TH INTERNATIONAL CONFERENCE ON BIOLOGICAL SCIENCE ICBS 2019: "Biodiversity as a Cornerstone for Embracing Future Humanity" 10 October 2019 - 11 October 2019 no. 2260: AIP Publishing. 030010.

Nurhidayat L., Kurniawan Pratama D., Devi N.A. & Rohmah Z. (2020). The development of integument and muscle in regenerated tail of Tokay gecko (*Gekko gecko* Linnaeus, 1758). Trisakti Saragih H., Ilmi M., Nopitasari S., Audinah L., Widyasari A., Arum Sari M., Masri M., Toban Palilu P., Prabowo B.P., Soleha S., Solikhah A. & Fitriana N. (Eds.). AIP Conference Proceedings. THE 6TH INTERNATIONAL CONFERENCE ON BIOLOGICAL SCIENCE ICBS 2019: "Biodiversity as a Cornerstone for Embracing Future Humanity" 10 October 2019 – 11 October 2019 no. 2260: AIP Publishing. 030009.

Nuriliani A., Lukmawati D., Aemeliya V.F. & **Nurhidayat L.** (2020). Histopathological effects of ethanolic extract of Gaharu's (*Aquilaria malaccensis* Lamk.) leaves on liver and kidney of mice (Mus musculus L.) infected by Plasmodium berghei. Trisakti Saragih H., Ilmi M., Nopitasari S., Audinah L., Widyasari A., Arum Sari M., Masri M., Palilu P.T., Prabowo B.H., Soleha S., Solikhah A. & Fitriana N. (Eds.). AIP Conference Proceedings . THE 6TH INTERNATIONAL CONFERENCE ON BIOLOGICAL SCIENCE ICBS 2019: "Biodiversity as a Cornerstone for Embracing Future Humanity" 10 October 2019 – 11 October 2019 no. 2260: AIP Publishing. 040008 .

Pratiwi R., Nyoman Y.A., Fadliansyah L.G., Ardiansyah S.A., **Nurhidayat L.**, Sholikhah E.N., Sunarti S., Widyarini S., Fadhlurrahman A.G., Fatmasari H., Tunjung W.A.S., Haryana S.M., Alamsyah F. & Taruno W.P. (2020). CCL2 and IL18 expressions may associate with the anti-proliferative effect of noncontact electro capacitive cancer therapy in vivo [version 2; peer review: 2 approved, 1 approved with reservations]. *F1000Research* **8**: 1770.

Nurhidayat L., Arfiani F.N., Retnoaji B. 2017. Indeks Gonadosomatik dan Struktur Histologis Gonad Ikan Uceng (*Nemacheilus fasciatus*, Valenciennes in Cuvier and Valenciennes, 1846). *Biosfera* **34**: 67-74

Nurhidayat L., Soesilo N. & Sarto M. (2016). Diving strategy of *Amyda cartilaginea* (Boddaert, 1770) and *Cuora amboinensis* (Daudin, 1802) in the perspective of respiratory structure and function. *AIP Conference Proceedings* **1744**: 020036.

Setiawan P.G.M., Tunjung W.A.S & **Nurhidayat L.** (2016). Effect of diazepam on kidney function and histological structure of white rat's kidney. *Berkala Penelitian Hayati = Journal of Biological Researches* **22**: 1-6.

Retnoaji B., Wulandari R., **Nurhidayat L.** & Daryono B. (2016). Osteogenesis study of hybrids of Indonesia's native chicken pelung (*Gallus gallus* domesticus) with broiler (*Gallus gallus* domesticus). *Asian Journal of Animal and Veterinary Advances* **11**: 498-504.

Rachman A., Sugiyanto J., **Nurhidayat L.**, Nuriliani A., Rofiqoh A.A., Hermawan A., Narulita R. 2014. Tipe Echolokasi serta Struktur Larynx pada Miniopterus dan Rhinolophus. *Biosfera* **31**: 85-98.